Small molecule inhibitors of Nicotinamide N-Methyltransferase (NNMT)

Gao, Y.

This work was supported by the grant (No. 201506270162) from China Scholarship Council (CSC) to Yongzhi Gao

The printing of this thesis was financially supported by Universiteit Leiden

Cover design: Xin Zhou

Printing: Proefschriftmaken; www.proefschriftmaken.nl

Small Molecule Inhibitors of Nicotinamide *N*-Methyltransferase (NNMT)

Proefschrift

ter verkrijging van
de graad van Doctor aan de Universiteit Leiden,
op gezag van Rector Magnificus Prof.dr.ir. H. Bijl,
volgens besluit van het College voor Promoties
te verdedigen op woensdag 29 september 2021
klokke 10:00 uur

door

Yongzhi Gao

geboren te Xishui, China

14 oktober 1985

Promotor:	Prof.dr. N.I. Martin
Copromotor:	Dr. M.J. van Haren

Promotiecommissie	Prof. dr. Roland Pieters
	Prof. dr. Mario van der Stelt
	Prof. dr. Laura Heitman
	Dr. Monique Mulder
	Dr. Seino Jongkees

No matter how old you may be at this moment, it's never too late to change your brain for the better.

Richard Restak

Table of contents

Chapter 1

Introduction: Nicotinamide *N*-methyltransferase (NNMT), an emerging therapeutic target

Parts of this chapter have been published in:
Gao Y.; Martin N.I., van Haren, M.J. (2021). Nicotinamide *N*-methyl transferase (NNMT): an emerging therapeutic target. *Drug Discov Today*. *In press*. DOI: 10.1016/j.drudis.2021.05.011

Abstract

Nicotinamide *N*-methyltransferase (NNMT) methylates nicotinamide (NA) to generate 1-methyl nicotinamide. Since its discovery 70 years ago, the appreciation of the role of NNMT in human health has evolved from serving only metabolic functions to also being a driving force in diseases, including a variety of cancers. Despite the increasing evidence indicating NNMT as a viable therapeutic target, the development of cell-active inhibitors against this enzyme is lacking. In this chapter, we provide an overview of the current status of NNMT inhibitor development, relevant *in vitro* and *in vivo* studies, and a discussion of the challenges faced in the development of NNMT inhibitors.

1. Introduction

Nicotinamide *N*-methyltransferase (NNMT) (EC 2.1.1.1) is a phase II metabolizing enzyme that belongs to the family of *S*-adenosyl-L-methionine (SAM)-dependent methyltransferases.[1] In 1951, NNMT was first partially purified from rat liver by Cantoni, who subsequently discovered the structure of cofactor SAM in 1952.[2,3] In the 1990s the human and mouse NNMT genes were cloned, revealing the highly conserved nature of NNMT in mammals, with human and mouse NNMT both containing 264 amino acid residues with 92% sequence similarity and 86% sequence identity.[4–6] The closest structural homologues of NNMT are the small molecule methyltransferases indolethylamine *N*-methyltransferase (INMT) and phenylethanolamine N-methyltransferase (PNMT) having 53% and 39% sequence identity to NNMT, respectively.[4,7] NNMT catalyses the methylation of nicotinamide (NA) and a variety of other pyridine containing compounds using the methyl donor SAM to generate *S*-adenosyl-L-homocysteine (SAH) and 1-methyl nicotinamide (MNA) or the corresponding pyridinium ion (Figure 1).[8,9]

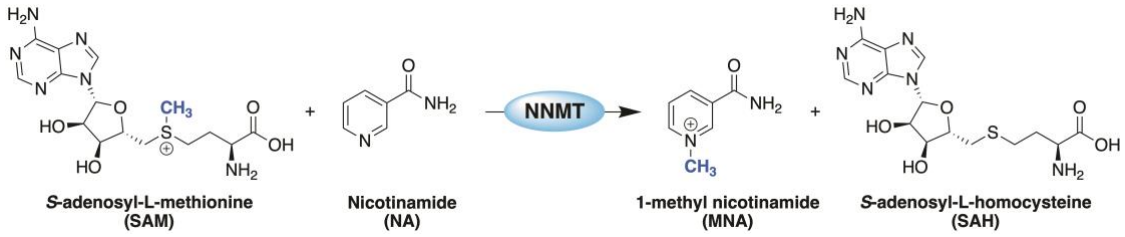

Figure 1. Nicotinamide N-methyltransferase (NNMT)-mediated methyl transfer from *S*-adenosyl-L-methionine (SAM) to nicotinamide (NA), forming 1-methylnicotinamide (MNA) and *S*-adenosyl-L-homocysteine (SAH).

The kinetics of NNMT appear to follow an ordered mechanism with SAM binding to NNMT before its pyridinyl substrate can bind. Subsequently, after the methyl transfer is completed, the methylated substrate leaves first after which SAH is released.[10] This mechanism is supported by Isothermal Titration Calorimetry data in which the binding affinity of NA could only be measured in the presence of SAH.[11] This finding suggests a significant conformational change of the enzyme upon cofactor binding, which has implications for the development of substrate competitive small molecule inhibitors of NNMT.

NNMT is found predominantly in the liver, but low levels of NNMT are also detected in most other organs.[4] It was originally thought that the primary roles of NNMT were centred around NA metabolism and detoxification of xenobiotic compounds.[12] However, more recent studies have provided evidence pointing towards a much broader function for NNMT in both healthy and disease states. NNMT is involved in the regulation of the cellular level of SAM as well as the

SAM/SAH ratio. Not only does NNMT consume SAM, but it also promotes SAM regeneration from homocysteine through interactions with betaine-homocysteine methyltransferase and methionine adenosyltransferase, both of which play key roles in the methionine cycle.[13] Furthermore, NNMT plays a critical part in NAD-dependent signalling and links the NAD^+ and methionine metabolism pathways through parallel depletion of NA and SAM.[14,15] Through these pathways, NNMT modulates energy expenditure in adipose tissue and controls glucose, cholesterol and triglyceride metabolism in hepatocytes through interaction with sirtuins.[16] Notably, in a *C. elegans* model, the activity of NNMT was found to extend lifespan by decreasing cellular SAM levels, producing a starvation signal and consequently inducing autophagy. Simultaneously, the MNA thereby formed is oxidized leading to the release of reactive oxygen species, thereby increasing stress resistance and promoting longevity.[17,18]

The elucidation of the various functions of NNMT demonstrates the complexity of the pathways in which the enzyme is involved. Not surprisingly, aberrant NNMT expression is observed in a wide range of disorders and diseases. Most pronounced in this regard is the overexpression of NNMT in a number of human cancers. Increased NNMT activity has been observed in bladder, breast, colorectal, gastric, hepatocellular, lung, oral, ovarian, pancreatic, and prostate cancer, as well as glioma, lymphoma, and insulinoma.[12,19,20] In these cancers, the overexpression of NNMT has been associated with tumour aggressiveness and shown to promote the migration, invasion, proliferation, and survival of cancer cells. At the cellular level, overexpression of NNMT facilitates epigenetic modifications by generating a metabolic methylation sink that boosts pro-tumorigenic gene products.[21] This finding was further substantiated by a recent proteomics-based study revealing NNMT to be a master metabolic regulator of cancer-associated fibroblasts (CAFs).[22] Expression of NNMT in CAFs leads to SAM depletion and decreased DNA and histone methylation levels, resulting in extensive gene expression changes in the tumour stroma, promoting cancer metastasis. A recent investigation also found that increases in MNA levels in the tumour microenvironment lead to the inhibition of T-cell functions resulting in their decreased killing capacity and increased tumour growth.[23] NNMT also interacts with oncogenic kinases, activated transducers and activators of transcription, and interleukins.[24,25] Given the absence of (cell-active) small molecule NNMT inhibitors, the role of NNMT is often studied through the use of RNA interference (siRNA or shRNA) to downregulate its expression.[24,26,27] This process occurs through inhibition of the translation of RNA to proteins in cells, resulting in lower NNMT levels, effectively mimicking inhibition of NNMT. Inhibition or down-regulation of NNMT decreases cell proliferation, reduces tumorigenicity in mice, and causes

tumour cell death via intrinsic apoptotic pathways, highlighting the potential of NNMT inhibitors as therapeutic agents.

A second disease area with increased interest in NNMT as a therapeutic target are metabolic disorders. Population studies have shown that serum MNA levels are positively correlated with obesity and diabetes.[28] In line with these findings, *Nnmt* knockdowns in mice were found to be protective against diet-induced obesity via increased energy expenditure.[29] In addition, glucose levels in *Nnmt*-knockdown mice were significantly reduced and insulin sensitivity increased.[30,31]

Aside from the clearly emerging roles in cancer and metabolic disease, links to aberrant NNMT expression have also been found in neurodegenerative diseases, including Alzheimer's disease, Parkinson's disease, Huntington's diseases and schizophrenia,[18,32–34] as well as functional disorders of the endothelium, such as thrombosis, high blood pressure, atherosclerosis, inflammation and pulmonary hypertension.[35]

The functions and mechanism of action of NNMT and its product MNA are not yet completely understood. The wide range of healthy and disease states in which NNMT is involved demonstrates the complexity of the role of this enzyme in human biology. To further elucidate the potential indications in which NNMT can be targeted to therapeutic benefit, potent, selective, and cell-permeable inhibitors are essential.

The first crystal structure demonstrating the active site interactions of NNMT with its substrate NA and cofactor analogue SAH was published in 2011 facilitating the development of rationally designed small molecule inhibitors of NNMT.[6] A second prerequisite for the development of inhibitors is the availability of a sensitive and specific assay for measuring NNMT activity. The first assays used for measuring NNMT activity involved the use of radiolabelled ^{3}H-methyl-SAM. In this approach NNMT activity is quantified based on the incorporation of radioactivity into the product MNA detected by scintillation counting. To avoid the use of radioactivity, a variety of alternative general methyltransferase assays as well as NNMT-specific assays have been developed, each with their own advantages and disadvantages. General methyltransferase assays that have been applied to the measurement of NNMT activity include enzyme-coupled reactions wherein the SAH by-product is subsequently detected by fluorescent or luminescent readout. Such approaches are technically straightforward and suitable for high-throughput screening (HTS). However, there are also disadvantages to this method. Firstly, the by-product SAH can be generated through degradation of SAM via either automethylation or chemical degradation pathways. Moreover, enzyme-coupled SAH detecting assays are unsuitable for use in cellular systems as the enzymes required are already present in cells, leading to interference and false positive results.[36] Another limitation of this assay is that it cannot distinguish the activity of different SAM-dependent

methyltransferases. It is therefore important that results obtained with SAH detecting are validated with an orthogonal, enzyme-specific assay.

A more specific assay for NNMT activity was developed by Sano and co-workers wherein the condensation of MNA with acetophenone results in the formation of fluorescent 2,7-naphthylpyridine analogues.[37,38] While this assay can be used in HTS, it involves significant sample workup, is an end-point assay, and, if used for inhibitor screening, also requires assessment of possible fluorescent interference by the inhibitors themselves. As an alternative, in 2016, our group reported an LCMS-based method for measuring the activity of NNMT through direct detection of MNA. The method can be used to quantify NNMT-mediated formation of MNA and a range of other positively charged, methylated pyridines with very high specificity and sensitivity.[9] While the method has a short run-time of less than 2 minutes, it is not directly suitable for HTS and is better suited for studying NNMT activity in complex mixtures and/or for validation of HTS hits. Recently, a complementary, non-coupled, real-time analytical assay for monitoring NNMT activity was reported by the Watowich group based on the fluorescent properties of 1-methylquinolinium (1-MQ).[39] This convenient method uses quinoline as an alternative substrate for NNMT instead of its primary substrate NA and relies on fluorescent detection of 1-MQ. While the method is compatible with HTS, care needs to be taken in accounting for the inherent fluorescent properties of the quinoline substrate.

In this chapter we provide a comprehensive summary of the NNMT inhibitors reported to date. The inhibition values and the analytical methods used to obtain them, are included in an overview table (Table 1) at the end of this review for ease of reference. In the subsequent sections, the following classes of NNMT inhibitors will be discussed: SAM competitive inhibitors of NNMT, nicotinamide competitive inhibitors, bisubstrate inhibitors, covalent inhibitors, and other NNMT inhibitors.

2. NNMT inhibitors

2.1 SAM Competitive Inhibitors

The by-product SAH (**1**, Figure 2), common to all SAM-dependent methyltransferases, is known as a feedback inhibitor and inhibits NNMT with an IC_{50} value of 35.3 μM.[40] SAH is only active in enzyme-based biochemical assays; it loses its activity in cellular assays were it is rapidly degraded by *S*-adenosyl-L-homocysteine hydrolase (SAHH) to adenosine and homocysteine. Another known general methyltransferase inhibitor is the natural product sinefungin (**2**, Figure 2), a SAM-mimicking methyltransferase inhibitor isolated from *Streptomyces*. Sinefungin is a moderate inhibitor of NNMT with an IC_{50} of 12.5 μM. Sinefungin has low cell membrane

permeability and exhibits severe toxicity in animal models, restricting its potential application as a therapeutic agent.[41] The moderate inhibitory activity of the SAM-mimics like SAH and sinefungin suggests that interactions in the SAM binding site alone are not sufficient for potent and selective inhibition of NNMT.

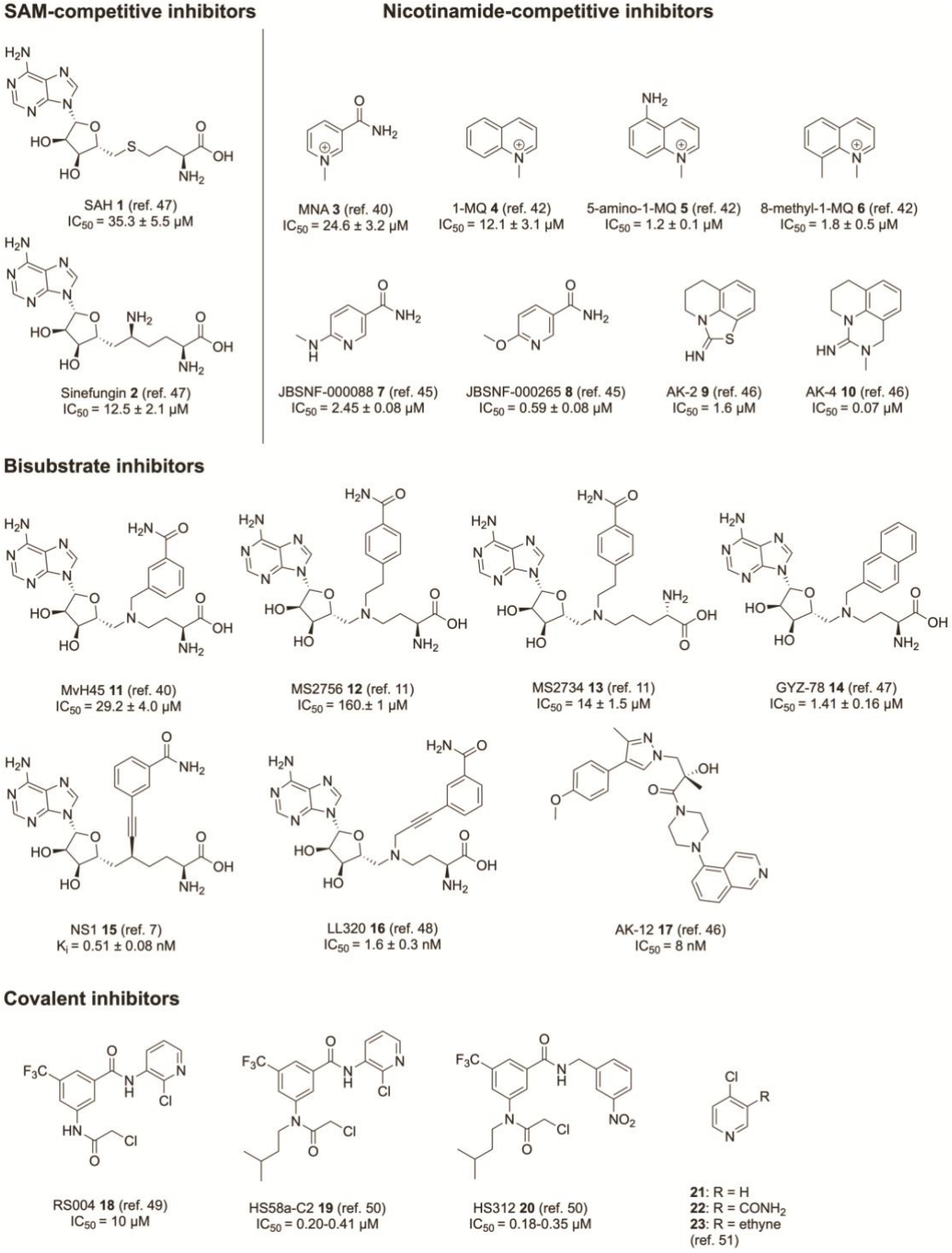

Figure 2. Overview of the chemical structures of nicotinamide N-methyltransferase (NNMT) inhibitors, including methyltransferase-specific inhibitors **1** and **2**,[47] nicotinamide-competitive inhibitors **3–10**,[40,42,45,46] bisubstrate inhibitors **11–17**,[7,11,40,46–48] and covalent inhibitors **18–23**.[49–51]

2.2 Nicotinamide Competitive Inhibitors

Inhibitors that compete with binding of the nicotinamide substrate have also been reported. As described above for the NNMT by-product SAH, the other enzymatic product, namely the methylated pyridine product MNA (**3**, Figure 2) is also a feedback inhibitor of NA methylation with comparable potency to that of SAH (IC_{50} = 24.6 μM). Similar levels of inhibition are observed for other *N*-methylated products formed from other substrate heterocycles including the *N*-methylated quinoline, 1-MQ (**4**, Figure 2) which exhibits an IC_{50} value of 12.1 μM. In a structure-activity relationship (SAR) study involving various methylated quinolines, both 5-amino-1-MQ (**5**, IC_{50} = 1.2 μM) and 8-methyl-1-MQ (**6**, IC_{50} = 1.8 μM) were shown to have improved inhibition compared with the parent compound.[42] Furthermore, in an aged mouse model, compound **5** was found to accelerate muscle regeneration, linking NNMT inhibition to functional improvements of aged skeletal muscles.[43] In addition, treatment of diet-induced obese (DIO) mice with compound **5** resulted in significantly reduced body weight and white adipose mass, decreased adipocyte size, and lowered plasma total cholesterol levels.[44]

In search of small molecule NNMT inhibitors for the treatment of metabolic disorders, an HTS screen was performed on over a million compounds.[45] The hit compound identified (JBSNF-000088, **7**, Figure 2) showed low micromolar activity against NNMT (IC_{50} = 2.4 μM), which was improved after a SAR study on this compound (JBSNF-000265, **8**, IC_{50} = 0.59 μM). Crystal structures show that compound **7** is methylated by NNMT in the nicotinamide binding site, which indicates the compounds are acting as slow turnover substrates. In high-fat DIO mice, compound **7** was able to reduce plasma levels of MNA, improve insulin sensitivity, normalize glucose tolerance, and reduce body weight.[30]

A recent publication from researchers at Sanofi reports the results of an HTS campaign in which tricyclic, nicotinamide competitive, inhibitors were identified (compound **9**, Figure 2).[46] After optimization, the most potent tricyclic inhibitor (compound **10**, Figure 2) was found to inhibit NNMT with an IC_{50} value of 0.07 μM. Co-crystallisation studies, requiring the addition of SAH, provide atomic level insight into the binding of these compounds in the nicotinamide binding pocket.

2.3 Bisubstrate Inhibitors

Based on the inhibitory activities of compounds that exclusively target either the SAM or NA binding pocket, it becomes apparent that targeting only one of these pockets may not be sufficient to achieve potent inhibition of NNMT. As an alternative, bisubstrate NNMT inhibitors have been

designed to simultaneously engage both of these binding pockets as a means of enhancing both inhibitor activity and selectivity. Our group described the first systematic approach towards the design of bisubstrate inhibitors of NNMT. From the SAR performed, it became clear that many of the functional groups present in SAM and NA are essential for binding and small alterations in the chemical structure of the bisubstrate compounds can have significant impact on their activity. The bisubstrate inhibitor MvH45 (**11**, Figure 2) linked a benzamide, mimicking NA, to an Aza-SAH moiety, mimicking SAM, resulting in moderate inhibition of NNMT (IC_{50} = 29.2 μM).[40] Building on this result, and based on the measured distance of 3.5 - 4.2 Å between the pyridinyl nitrogen atom of NA and the SAH sulphur atom as found in the NNMT crystal structure (PDB ID: 3ROD), Jin *et al*. extended the linker to the benzamide from one to two carbon atoms resulting in MS2756 (compound **12**, Figure 2) which exhibited a significantly reduced activity (IC_{50} = 160 μM). Interestingly, extension of the linker to the amino acid moiety by one carbon as in MS2734 (compound **13**, Figure 2), led to a restoration of inhibitory activity (IC_{50} = 14 μM).[11] Structural studies with compound **13** (PDB code: 6CHH) confirmed the hypothesized binding in the NNMT active site with the bisubstrate effectively recapitulating the majority of binding interactions present in the NNMT-NA-SAH ternary complex. An extensive selectivity screen on a panel of methyltransferases revealed additional activity against lysine methyltransferase DOT1L (IC_{50} = 1.3 μM) and arginine methyltransferase PRMT 7 (IC_{50} = 20 μM).

Optimization of the structural features of these bisubstrate inhibitors led us to pursue an SAR focusing on the amino acid and benzamide side-chains. From this work a naphthalene-containing compound (GYZ-78 (**14**), Figure 2) emerged with an IC_{50} of 1.4 μM. Modelling suggested that the compound benefits from additional π−π stacking interactions with several tyrosine residues in the NA binding pocket of the enzyme. No activity was found against representative members of the lysine methyltransferase (NSD2) or arginine methyltransferase (PRMT1) families and cellular data obtained for compound **14** showed a significant inhibitory effect on cell viability in HSC-2 oral cancer cells.[47] Shortly thereafter, the group of Shair found that a 2-carbon alkyne-linker provides for a superior mimicking of the orientation and distance between NA and SAM.[7] Applying an impressive multi-step stereo-controlled synthesis route, they also replaced the central nitrogen of the previous generation bisubstrate inhibitors with a carbon atom, to generate a set of highly potent NNMT inhibitors (K_i = 0.5 nM for compound NS1 **15**, Figure 2). A selectivity screen against a panel of methyltransferases, including closely related small molecule methyltransferases, revealed excellent selectivity. However, in cell-based assays, both **15** and its methyl ester prodrug only moderately decreased MNA levels in U2OS cells, most likely due to limited cell permeability. Following a similar strategy, Huang and co-workers found that the use of a three-carbon propargyl

linker to connect the central nitrogen of the first generation bisubstrate inhibitors (**11-14**) with the benzamide moiety also yielded very potent inhibitors.[48]. Among the compounds synthesized, LL320 (compound **16**, Figure 2) showed the highest activity with K_i values as low as 1.6 nM. Good selectivity was also observed against a panel of small molecule, lysine and arginine methyltransferases. As for the other SAM-based bisubstrate inhibitors of NNMT, however, both LL320 and its ethyl ester prodrug displayed poor cell permeability.

Notably, the recent HTS campaign reported by Sanofi identifying compounds **9** and **10**, also yielded compound **17** (IC_{50} = 8 nM, Figure 2) subsequently found to be a bisubstrate-like NNMT inhibitor.[46] Supported by structural insights, compound **17** represents an important step towards achieving inhibitors that less explicitly mimic the SAM and nicotinamide scaffolds. Notably, the carboxamide moiety present in nicotinamide and the amino acid side chain present in cofactor SAM are absent, while the adenosine moiety of SAM is effectively mimicked a piperazinyl-quinoline motif. While no cell-based or *in vivo* data were reported for these compounds, it will be interesting to see whether such NNMT inhibitors show improved activity in this regard.

2.4 Covalent Inhibitors

The active site of NNMT contains several non-essential cysteine residues, which can be explored as targets for covalent inhibition. The first covalent inhibitors of NNMT were identified by Cravatt and co-workers using SAH-based photoreactive probes, developed for chemical proteomic profiling of SAM-dependent methyltransferases.[49] Using these probes as a fluorescence polarization tool, an electrophilic fragment library was screened, identifying the chloroacetamide-containing covalent NNMT inhibitor RS004 (**18**, Figure 2) with a moderate IC_{50} value of 10 μM. The absence of activity against the C165A mutant of NNMT supports the interaction with a target cysteine. SAR studies on compound **18** yielded the more potent covalent NNMT inhibitors HS58a-C2 (**19**, IC_{50} = 200-410 nM, Figure 2) and HS312 (**20**, IC_{50} = 180-350 nM, Figure 2).[50] However, in cellular assays, these compounds did not show any appreciable inhibition of NNMT while interaction with other proteins was observed, contradicting the *in vitro* results. Following another approach, the Thompson group found 4-chloropyridine analogues (compounds **21-23**, Figure 2) to be substrates and inhibitors of NNMT.[51] Upon *N*-methylation of the pyridine analogue, the increased electrophilicity of the methylated pyridine promotes an aromatic nucleophilic substitution reaction by C159, a non-essential active site cysteine residue, resulting in covalent inhibition of NNMT. No IC_{50} or K_i values were given, but the K_M values of compounds **21-23** as substrates were stated as 22-44 μM. Covalency was confirmed by mass spectrometry, dialysis, and analysis of activity against C159A and/or C165A mutants of NNMT. Furthermore, in NNMT-

overexpressing HEK293T cells, the compounds showed inhibition of NNMT with EC_{50} values of 36-87 μM. In another study aimed at identifying covalent inhibitors, a library of mild electrophilic fragments was screened against a selection of cysteine-containing proteins. The screen identified several compounds that covalently labelled NNMT after incubation for 24 hours at 4°C at a concentration of 200 μM as determined by mass spectrometry.[52] However, in follow-up studies these hits did not show significant inhibition of NNMT at 200 μM.

2.5 Other NNMT Inhibitors

Another NNMT inhibitor of interest is the natural product Yuanhuadine (YD, **24**, Figure 3).[53] This compound is isolated from the flower bud of *Daphne genkwa*, which is used in traditional Chinese medicine. YD exhibits modest to potent growth inhibition of several tumour cell lines.[54–56] Lee and co-workers found that treatment of cancer cell lines with YD suppresses NNMT expression in non-small cell lung cancer (NSCLC) cells and biochemical assays indicate an IC_{50} value of 0.4 μM.[57] Docking studies suggest that YD binds in both nicotinamide and SAM binding pockets in the NNMT active site.

As another alternative source of NNMT inhibitors, our group recently applied an mRNA display technique wherein a large library of 10^{12} macrocyclic peptides was screened, resulting in a number of peptides that bind to NNMT.[58] Among the hits identified, several macrocyclic peptides were found to also potently inhibit NNMT with IC_{50} values as low as 229 nM (compound **26**, Figure 3). Interestingly, substrate competition experiments indicated that these cyclic peptide inhibitors are non-competitive with either SAM or NA, suggesting they may engage with and inhibit NNMT via an allosteric binding site. During preparation of this review article, a patent was disclosed by Eli Lilly describing a novel class of pyrimidine-5-carboxamide compounds as inhibitors of NNMT, exemplified by compound **25** in Figure 3.[59] The compound showed potent inhibition of NNMT (IC_{50} = 74 nM) in a biochemical assay as well as a dose-dependent reduction of the formation of d_4-MNA in mice dosed with d_4-nicotinamide.

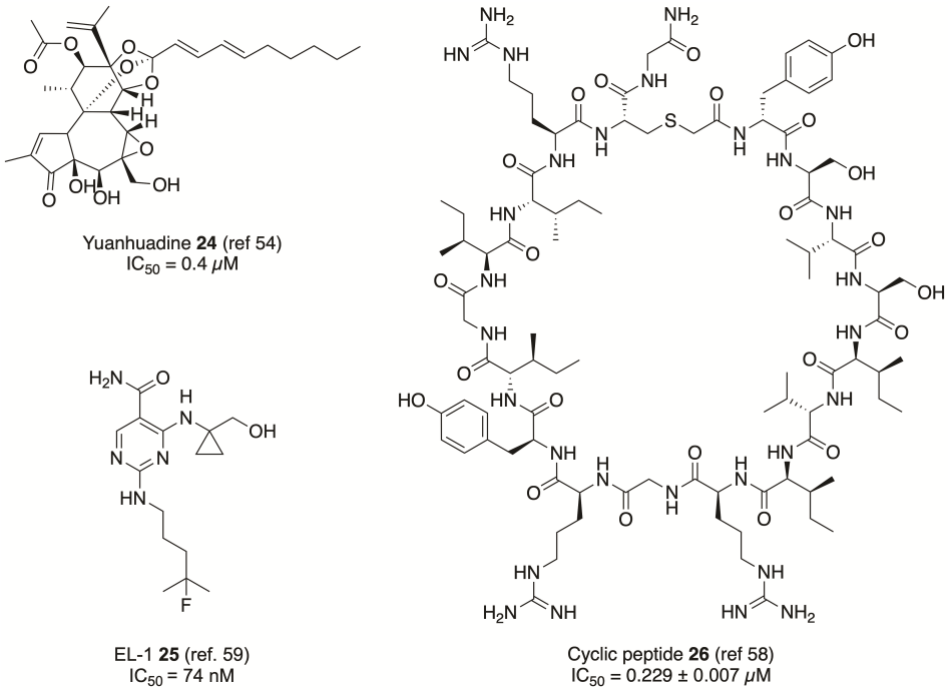

Figure 3. Chemical structures of the natural product Yuanhuadine (**24**),[54] Eli Lilly's pyrimidine 5-carboxamide compound **25**,[59] and macrocyclic peptide **26**,[58] which was found to be an allosteric inhibitor of nicotinamide N-methyltransferase (NNMT).

3. Conclusion

In this review, we present an overview of the current state of NNMT inhibitor development and highlight their advantages and drawbacks. While the search for effective NNMT inhibitors is still in its infancy, substantial progress has already been made in terms of potency and selectivity of small molecule inhibitors of NNMT. That said, the limited cellular and *in vivo* activity of these compounds speaks to the need to develop more drug-like inhibitors. The clinical importance of NNMT in a variety of diseases, including cancer and metabolic disorders, support NNMT as a viable therapeutic target. However, major challenges remain in developing NNMT inhibitors for clinical application. The SAR studies performed on bisubstrate inhibitors of NNMT reveal the importance of highly polar functional groups, including the adenosine and amino acid moieties of the SAM-mimetics. However, while these features are critical for activity, they are also detrimental to cell permeability. In order to establish the therapeutic viability of NNMT inhibition, the current set of NNMT inhibitors available needs to be expanded to provide more cell-permeable probe molecules. With such inhibitors in hand, it will be possible to more precisely assess the beneficial and detrimental effects, both acute and chronic, of NNMT inhibition in cellular systems and *in vivo* models.

Table 1. Overview of NNMT inhibitors with IC_{50} or K_i values, analytical methods used and results from *in vitro* and *in vivo* studies

No.	Name	IC_{50}	Analytical method	*In vitro*/*in vivo* results	Refs
1	SAH	35.3 ± 5.5 μM	LC-MS	N/A	47
2	Sinefungin	12.5 ± 2.1 μM	LC-MS	N/A	47
3	MNA	24.6 ± 3.2 μM	LC-MS	N/A	40
4	1-MQ	12.1 ± 3.1 μM	HPLC	No data	42
5	5-amino-1-MQ	1.2 ± 0.1 μM	HPLC	Accelerated muscle regeneration in aged mice; reduced body weight and white adipose tissue in diet-induced obese mice; treatment of human CAFs increased histone methylation and did not affect cell viability. Decreased tumour burden in mouse model of ovarian cancer metastasis, reduced tumour cell proliferation, and increased stromal H3K27 trimethylation	42–44
6	8-Methyl-1-MQ	1.8 ± 0.5 μM	HPLC	No data	42
7	JBSNF-000088	2.4 ± 0.1 μM	2,7-Naphthyridine fluorescence	Reduced body weight, improved insulin sensitivity, and restored glucose tolerance in mice with diet-induced obesity	30,45
8	JBSNF-000265	0.6 ± 0.1 μM	2,7-Naphthyridine fluorescence	No data	45
9	AK-2	1.6 μM	2,7-Naphthyridine fluorescence	No data	46
10	AK-4	0.07 μM	2,7-Naphthyridine fluorescence	No data	46
11	MvH45	29.2 ± 4.0 μM	LC-MS	No data	40
12	MS2756	160 ± 1 μM	SAHH-coupled fluorescence	K_D (ITC) of 42.8 ± 6.3 μM	11
13	MS2734	14 ± 1.5 μM	SAHH-coupled fluorescence	K_D (ITC) of 2.7 ± 0.2 μM	11
14	GYZ-78	1.4 ± 0.2 μM	LC-MS	K_D (ITC) of 5.6 ± 0.4 μM; reduced cell viability of HSC-2 oral cancer cell line	47
15	NS1	0.5 ± 0.1 nM(Ki)	Quinoline fluorescence	Moderately decreased MNA levels in U2OS osteosarcoma cells	7
16	LL320	1.6 ± 0.1 nM (Ki)	SAHH-coupled fluorescence	No Data	48
17	AK-12	0.008 μM	2,7-Naphthyridine fluorescence	No data	46
18	RS004	10.0 μM	ABPP probe/FP	No data	49
19	HS58A-C2	410/200 nM	ABPP probe/LC-MS	Good NNMT inhibition in lysates of human renal cell	50
20	HS312	350/180 nM	ABPP probe/LC-MS	carcinoma line 786O; however, despite cell permeability, no cellular NNMT inhibition reported	50
21–23	4-Chloropyridine analogs	N/A	MTase Glo/quinoline fluorescence	K_M values of 22–44 μM; inhibition of NNMT in HEK293T cells with EC_{50} values of 36–87 μM	51
24	Yuanhuadine	0.4 μM	SAHH-coupled fluorescence	Suppression of NNMT expression in NSCLC cells	57
25	EL-1	74 nM	LC-MS	Dose-dependent reduction of MNA in mice	59
26	Cyclic peptide	0.229 ± 0.007 μM	LC-MS	Noncompetitive inhibition indicated allosteric binding	58

4. Thesis Outline

The theme of this thesis is the development of small molecule inhibitors of NNMT with the aim of increasing their potency and selectivity. To this end, structural modifications were performed on a bisubstrate NNMT inhibitor previously identified in our group.[40] These investigations are described in **chapter 2**. A diverse library of inhibitors was prepared to probe the different regions of the enzyme's active site, revealing that incorporation of a naphthalene moiety intended to bind the hydrophobic nicotinamide binding pocket via π-π stacking interactions significantly increases the activity of the bisubstrate-like NNMT inhibitors. These findings were further supported by ITC binding assays as well as modeling studies. The most active NNMT inhibitor identified in the present study demonstrated a dose-dependent inhibitory effect on the cell proliferation of an HSC-2 oral cancer cell line.

To further increase the potency of NNMT inhibition, we next developed a series of compounds that depart from some of the conserved structural features found in the first generation bisubstrate inhibitors, specifically by introducing alternative electron-deficient aromatic groups to mimic the

nicotinamide moiety (**Chapter 3**). In addition, the identification of an optimal trans-alkene linker differs from the previously reported alkyl and alkynyl linkers used to connect the substrate and cofactor mimics in these inhibitors. The most potent NNMT inhibitor identified in our study exhibited an IC_{50} value of 3.7 nM placing it among the most active NNMT inhibitors reported to date. Complementary analytical techniques, modelling studies, and cell-based assays provide insight into these inhibitors' binding mode, affinity, and selectivity.

While our best compound showed potent NNMT inhibition in biochemical assay, it was lacking good cellular activity. In order to translate the observed potent affinity into strong cellular activity, a prodrug strategy was developed, which is described in **chapter 4**. The prodrug strategy focused on the temporary protection of the amine and carboxylic acid moieties of the highly polar amino acid side chain present in potent bisubstrate inhibitor. The modification of the carboxylic acid into a range of esters in the absence or presence of a trimethyllock (TML) protecting group at the amine group yielded a range of prodrugs. Based on good stability in buffers and the confirmed esterase-dependent conversion to the parent compound, the isopropyl ester was selected as the preferred acid prodrug. The isopropyl ester and isopropyl ester-TML prodrugs demonstrated improved cell permeability and translated into cellular activity.

In **chapter 5**, the most potent bisubstrate inhibitor described in chapter 3 was used as a scaffold to incorporate covalent warheads targeting cysteine and serine residues in the NNMT active site. While non-essential for catalytic activity, these residues are involved in substrate binding within the NNMT active site. Using a series of acrylamide and chloroacetamide containing compounds to target cysteine residues C159 and C165, as well as a series of sulfonyl fluoride and boronic acid containing compounds targeting serine residues S201 and S213, several compounds were identified with potent inhibitory activity against NNMT. Establishing the covalent nature of their interactions is part of an ongoing investigation.

Chapter 6 provides a summary of the results obtained in thesis chapters 1-5.

References

1. Martin JL, McMillan FM. SAM (dependent) I AM: the S-adenosylmethionine-dependent methyltransferase fold. Curr Opin Struct Biol. 2002;12(6):783-93.
2. Cantoni GL. Methylation of nicotinamide with soluble enzyme system from rat liver. J Biol Chem. 1951;189(1):203-16.
3. Cantoni GL. The nature of the active methyl donor formed enzymatically from L-methionine and adenosine triphosphate 1,2. J Am Chem Soc. 1952;74(11):2942-3.
4. Aksoy S, Szumlanski CL, Weinshilboum RM. Human liver nicotinamide N-methyltransferase. cDNA cloning, expression, and biochemical characterization. J Biol Chem. 1994;269(20):14835-40. http://www.ncbi.nlm.nih.gov/pubmed/8182091
5. Yan L, Otterness DM, Craddock TL, Weinshilboum RM. Mouse liver nicotinamide N-methyltransferase: CDNA cloning expression, and nucleotide sequence polymorphisms. Biochem Pharmacol. 1997;54(10):1139-49.
6. Peng Y, Sartini D, Pozzi V, Wilk D, Emanuelli M, Yee VC. Structural Basis of Substrate Recognition in Human Nicotinamide N -Methyltransferase. Biochemistry. 2011;50(36):7800-8.
7. Policarpo RL, Decultot L, May E, Kuzmič P, Carlson S, Huang D, et al. High-Affinity Alkynyl Bisubstrate Inhibitors of Nicotinamide N-Methyltransferase (NNMT). J Med Chem. 2019;62(21):9837-73.
8. Alston TA, Abeles RH. Substrate specificity of nicotinamide methyltransferase isolated from porcine liver. Arch Biochem Biophys. 1988;260(2):601-8.
9. van Haren MJ, Sastre Toraño J, Sartini D, Emanuelli M, Parsons RB, Martin NI. A Rapid and Efficient Assay for the Characterization of Substrates and Inhibitors of Nicotinamide N -Methyltransferase. Biochemistry. 2016;55(37):5307-15.
10. Loring HS, Thompson PR. Kinetic Mechanism of Nicotinamide N-Methyltransferase. Biochemistry. 2018;57(38):5524-32.
11. Babault N, Allali-Hassani A, Li F, Fan J, Yue A, Ju K, et al. Discovery of Bisubstrate Inhibitors of Nicotinamide N -Methyltransferase (NNMT). J Med Chem. 2018;61(4):1541-51.
12. Pissios P. Nicotinamide N -Methyltransferase: More Than a Vitamin B3 Clearance Enzyme. Trends Endocrinol Metab. 2017;28(5):340-53.
13. Hong S, Zhai B, Pissios P. Nicotinamide N-Methyltransferase Interacts with Enzymes of the Methionine Cycle and Regulates Methyl Donor Metabolism. Biochemistry. 2018;57(40):5775-9.

14. Komatsu M, Kanda T, Urai H, Kurokochi A, Kitahama R, Shigaki S, et al. NNMT activation can contribute to the development of fatty liver disease by modulating the NAD+ metabolism. Sci Rep. 2018;8(1):1-15.
15. Bockwoldt M, Houry D, Niere M, Gossmann TI, Reinartz I, Schug A. Identification of evolutionary and kinetic drivers of NAD-dependent signaling. Proc Natl Acad Sci U S A. 2019;116(32):15957-66.
16. Hong S, Moreno-Navarrete JM, Wei X, Kikukawa Y, Tzameli I, Prasad D, et al. Nicotinamide N-methyltransferase regulates hepatic nutrient metabolism through Sirt1 protein stabilization. Nat Med. 2015;21(8):887-94.
17. Schmeisser K, Mansfeld J, Kuhlow D, Weimer S, Priebe S, Heiland I, et al. Role of sirtuins in lifespan regulation is linked to methylation of nicotinamide. Nat Chem Biol. 2013;9(11):693-700.
18. Schmeisser K, Parker JA. Nicotinamide-N-methyltransferase controls behavior, neurodegeneration and lifespan by regulating neuronal autophagy. Ristow M, ed. PLOS Genet. 2018;14(9):e1007561.
19. Ramsden DB, Waring RH, Barlow DJ, Parsons RB. Nicotinamide N -Methyltransferase in Health and Cancer. Int J Tryptophan Res. 2017;10:117864691769173.
20. Lu XM, Long H. Nicotinamide N-methyltransferase as a potential marker for cancer. Neoplasma. 2018;65(05):656-63.
21. Ulanovskaya OA, Zuhl AM, Cravatt BF. NNMT promotes epigenetic remodeling in cancer by creating a metabolic methylation sink. Nat Chem Biol. 2013;9(5):300-6.
22. Eckert MA, Coscia F, Chryplewicz A, Chang JW, Hernandez KM, Pan S, et al. Proteomics reveals NNMT as a master metabolic regulator of cancer-associated fibroblasts. Nature. 2019;569(7758):723-8.
23. Kilgour MK, MacPherson S, Zacharias LG, Ellis AE, Sheldon RD, Liu EY, et al. 1-Methylnicotinamide is an immune regulatory metabolite in human ovarian cancer. Sci Adv. 2021;7(4):eabe1174.
24. Zhang J, Wang Y, Li G, Yu H, Xie X. Down-Regulation of Nicotinamide N-methyltransferase Induces Apoptosis in Human Breast Cancer Cells via the Mitochondria-Mediated Pathway. Filleur S, ed. PLoS One. 2014;9(2):e89202.
25. Palanichamy K, Kanji S, Gordon N, Thirumoorthy K, Jacob JR, Litzenberg KT, et al. NNMT Silencing Activates Tumor Suppressor PP2A, Inactivates Oncogenic STKs, and Inhibits Tumor Forming Ability. Clin Cancer Res. 2017;23(9):2325-34.
26. Giannatempo G, Santarelli A, Rocchetti R, Tomasetti M, Provinciali M, Emanuelli M, et al.

RNA-Mediated Gene Silencing of Nicotinamide N-Methyltransferase Is Associated with Decreased Tumorigenicity in Human Oral Carcinoma Cells. PLoS One. 2013;8(8):e71272.

27. Sartini D, Seta R, Pozzi V, Morganti S, Rubini C, Zizzi A, et al. Role of nicotinamide N-methyltransferase in non-small cell lung cancer: in vitro effect of shRNA-mediated gene silencing on tumourigenicity. Biol Chem. 2015;396(3):225-34.
28. Liu M, Li L, Chu J, Zhu B, Zhang Q, Yin X, et al. Serum N1-methylnicotinamide is associated with obesity and diabetes in Chinese. J Clin Endocrinol Metab. 2015;100(8):3112-7.
29. Kraus D, Yang Q, Kong D, Banks AS, Zhang L, Rodgers JT, et al. Nicotinamide N-methyltransferase knockdown protects against diet-induced obesity. Nature. 2014;508(7495):258-62.
30. Kannt A, Rajagopal S, Kadnur SV, Suresh J, Bhamidipati RK, Swaminathan S, et al. A small molecule inhibitor of Nicotinamide N-methyltransferase for the treatment of metabolic disorders. Sci Rep. 2018;8(1):3660.
31. Brachs S, Polack J, Brachs M, Jahn-Hofmann K, Elvert R, Pfenninger A, et al. Genetic Nicotinamide N-Methyltransferase (Nnmt) Deficiency in Male Mice Improves Insulin Sensitivity in Diet-Induced Obesity but Does Not Affect Glucose Tolerance. Diabetes. 2019;68(3):527-42.
32. Lautrup S, Sinclair DA, Mattson MP, Fang EF. NAD+ in Brain Aging and Neurodegenerative Disorders. Cell Metab. 2019;30(4):630-55.
33. Parsons RB, Smith SW, Waring RH, Williams AC, Ramsden DB. High expression of nicotinamide N-methyltransferase in patients with idiopathic Parkinson's disease. Neurosci Lett. 2003;342(1-2):13-6.
34. Kocinaj A, Chaudhury T, Uddin MS, Junaid RR, Ramsden DB, Hondhamuni G, et al. High Expression of Nicotinamide N-Methyltransferase in Patients with Sporadic Alzheimer's Disease. Mol Neurobiol. 2021;58(4):1769-81.
35. Fedorowicz A, Mateuszuk Ł, Kopec G, Skórka T, Kutryb-Zając B, Zakrzewska A, et al. Activation of the nicotinamide N-methyltransferase (NNMT)-1-methylnicotinamide (MNA) pathway in pulmonary hypertension. Respir Res. 2016;17(1):108.
36. Hsiao K, Zegzouti H, Goueli SA. Methyltransferase-Glo: a universal, bioluminescent and homogenous assay for monitoring all classes of methyltransferases. Epigenomics. 2016;8(3):321-39.
37. Sano A, Takimoto N, Takitani S. Fluorometric assay of nicotinamide methyltransferase with a new substrate, 4-methylnicotinamide. Chem Pharm Bull (Tokyo). 1989;37(12):3330-2.
38. Sano A, Endo N, Takitani S. Fluorometric Assay of Rat Tissue N-Methyltransferases with

Nicotinamide and Four Isomeric Methylnicotinamides. Chem Pharm Bull (Tokyo). 1992;40(1):153-6.

39. Neelakantan H, Vance V, Wang H-YL, McHardy SF, Watowich SJ. Noncoupled Fluorescent Assay for Direct Real-Time Monitoring of Nicotinamide N-Methyltransferase Activity. Biochemistry. 2017;56(6):824-32.
40. van Haren MJ, Taig R, Kuppens J, Sastre Toraño J, Moret EE, Parsons RB, et al. Inhibitors of nicotinamide N-methyltransferase designed to mimic the methylation reaction transition state. Org Biomol Chem. 2017;15(31):6656-67.
41. Zweygarth E, Schillinger D, Kaufmann W, Rottcher D. Evaluation of sinefungin for the treatment of Trypanosoma (Nannomonas) congolense infections in goats. Trop Med Parasitol. 1986;37(3):255-7.
42. Neelakantan H, Wang HY, Vance V, Hommel JD, McHardy SF, Watowich SJ. Structure-Activity Relationship for Small Molecule Inhibitors of Nicotinamide N-Methyltransferase. J Med Chem. 2017;60(12):5015-28.
43. Neelakantan H, Brightwell CR, Graber TG, Maroto R, Wang H-YL, McHardy SF, et al. Small molecule nicotinamide N-methyltransferase inhibitor activates senescent muscle stem cells and improves regenerative capacity of aged skeletal muscle. Biochem Pharmacol. 2019;163(January):481-92.
44. Neelakantan H, Vance V, Wetzel MD, Wang H-YL, McHardy SF, Finnerty CC, et al. Selective and membrane-permeable small molecule inhibitors of nicotinamide N-methyltransferase reverse high fat diet-induced obesity in mice. Biochem Pharmacol. 2018;147:141-52.
45. Ruf S, Hallur MS, Anchan NK, Swamy IN, Murugesan KR, Sarkar S, et al. Novel nicotinamide analog as inhibitor of nicotinamide N-methyltransferase. Bioorganic Med Chem Lett. 2018;28(5):922-5.
46. Kannt A, Rajagopal S, Hallur MS, Swamy I, Kristam R, Dhakshinamoorthy S, et al. Novel Inhibitors of Nicotinamide-N-Methyltransferase for the Treatment of Metabolic Disorders. Molecules. 2021;26(4):991.
47. Gao Y, van Haren MJ, Moret EE, Rood JJM, Sartini D, Salvucci A, et al. Bisubstrate Inhibitors of Nicotinamide N -Methyltransferase (NNMT) with Enhanced Activity. J Med Chem. 2019;62(14):6597-614.
48. Chen D, Li L, Diaz K, Iyamu ID, Yadav R, Noinaj N, et al. Novel Propargyl-Linked Bisubstrate Analogues as Tight-Binding Inhibitors for Nicotinamide N -Methyltransferase. J Med Chem. 2019;62(23):10783-97.

49. Horning BD, Suciu RM, Ghadiri DA, Ulanovskaya OA, Matthews ML, Lum KM, et al. Chemical Proteomic Profiling of Human Methyltransferases. J Am Chem Soc. 2016;138(40):13335-43.
50. Lee H-Y, Suciu RM, Horning BD, Vinogradova E V., Ulanovskaya OA, Cravatt BF. Covalent inhibitors of nicotinamide N-methyltransferase (NNMT) provide evidence for target engagement challenges in situ. Bioorg Med Chem Lett. 2018;28(16):2682-7.
51. Sen S, Mondal S, Zheng L, Salinger AJ, Fast W, Weerapana E, et al. Development of a Suicide Inhibition-Based Protein Labeling Strategy for Nicotinamide N-Methyltransferase. ACS Chem Biol. 2019;14(4):613-8.
52. Resnick E, Bradley A, Gan J, Douangamath A, Krojer T, Sethi R, et al. Rapid Covalent-Probe Discovery by Electrophile-Fragment Screening. J Am Chem Soc. 2019;141(22):8951-68.
53. Zhan ZJ, Fan CQ, Ding J, Yue JM. Novel diterpenoids with potent inhibitory activity against endothelium cell HMEC and cytotoxic activities from a well-known TCM plant Daphne genkwa. Bioorganic Med Chem. 2005;13(3):645-55.
54. He W, Cik M, Van Puyvelde L, Van Dun J, Appendino G, Lesage A, et al. Neurotrophic and antileukemic daphnane diterpenoids from Synaptolepis kirkii. Bioorganic Med Chem. 2002;10(10):3245-55.
55. Zhang S, Li X, Zhang F, Yang P, Gao X, Song Q. Preparation of yuanhuacine and relative daphne diterpene esters from Daphne genkwa and structure–activity relationship of potent inhibitory activity against DNA topoisomerase I. Bioorg Med Chem. 2006;14(11):3888-95.
56. Hong J-Y, Chung H-J, Lee H-J, Park HJ, Lee SK. Growth Inhibition of Human Lung Cancer Cells via Down-regulation of Epidermal Growth Factor Receptor Signaling by Yuanhuadine, a Daphnane Diterpene from Daphne genkwa. J Nat Prod. 2011;74(10):2102-8.
57. Bach D-H, Kim D, Bae SY, Kim WK, Hong J-Y, Lee H-J, et al. Targeting Nicotinamide N-Methyltransferase and miR-449a in EGFR-TKI-Resistant Non-Small-Cell Lung Cancer Cells. Mol Ther - Nucleic Acids. 2018;11(June):455-67.
58. van Haren MJ, Zhang Y, Buijs N, Thijssen V, Sartini D, Emanuelli M, et al. Macrocyclic Peptides as Allosteric Inhibitors of Nicotinamide N-Methyltransferase (NNMT). chemRxiv. Published online 2020:1-19.
59. Ruenoplaza G. Pyrimidine-5-carboxamide compound. 2020;48(51).

Chapter 2

Bisubstrate inhibitors of nicotinamide *N*-methyltransferase (NNMT) with enhanced activity

Parts of this chapter have been published in:

Gao, Y.; van Haren, M. J.; Moret, E. E.; Rood, J. J. M.; Sartini, D.; Salvucci, A.; Emanuelli, M.; Craveur, P.; Babault, N.; Jin, J.; Martin, N. I .（2019）. Bisubstrate Inhibitors of Nicotinamide *N*-Methyltransferase (NNMT) with Enhanced Activity. *J. Med. Chem*. 62, 6597−6614.

Abstract

Nicotinamide N-methyltransferase (NNMT) catalyzes the methylation of nicotinamide to form *N*- methylnicotinamide. Overexpression of NNMT is associated with a variety of diseases, including a number of cancers and metabolic disorders, suggesting a role for NNMT as a potential therapeutic target. By structural modification of a lead NNMT inhibitor previously developed in our group, we prepared a diverse library of inhibitors to probe the different regions of the enzyme's active site. This investigation revealed that incorporation of a naphthalene moiety, intended to bind the hydrophobic nicotinamide binding pocket via π–π stacking interactions, significantly increases the activity of bisubstrate-like NNMT inhibitors (IC_{50}1.41 μM). These findings are further supported by isothermal titration calorimetry binding assays as well as modeling studies. The most active NNMT inhibitor identified in the present study demonstrated a dose-dependent inhibitory effect on the cell proliferation of the HSC-2 human oral cancer cell line.

1. Introduction

Nicotinamide *N*-methyltransferase (NNMT) is an important metabolic enzyme that catalyzes the transfer of a methyl group from the co-factor *S*-adenosyl-L-methionine (SAM) onto its various substrates, most notably nicotinamide (NA) and other pyridines, to form 1-methyl-nicotinamide (MNA) or the corresponding pyridinium ions.[1–3] The past decade has seen a renewed interest in the biological function of NNMT in a range of human diseases. While it was previously assumed that NNMT's primary roles were limited to nicotinamide metabolism and xenobiotic detoxification of endogenous metabolites, broader roles for NNMT in human health and disease are becoming clearer.[4] NNMT has been found to be overexpressed in a variety of diseases, including metabolic disorders[5–7], cardiovascular disease[8,9], cancer[10–14] and Parkinson's disease[15,16]. In general, overexpression of NNMT has been linked to disease progression in the aforementioned afflictions, with the exception of its role in Parkinson's disease where NNMT seems to be neuroprotective.[17,18] Collectively, NNMT appears to play a unique role in the regulation of post-translational modifications and signal transduction, making it an attractive and viable therapeutic target.

Despite growing interest, few small-molecule NNMT inhibitors have been described to date. Among these structures, the product of the enzymatic reaction, MNA, is a known inhibitor of NNMT and has generally been used in biochemical activity assays.[19] Recently, Cravatt and coworkers reported chloroacetamide-based covalent NNMT inhibitors that react with cysteine C165 in the SAM-binding pocket of the enzyme.[20] Notably, Sanofi researchers also recently reported a series of nicotinamide analogues that inhibit NNMT activity, leading to decreased MNA production, stabilization of insulin levels, glucose regulation, and weight loss in mouse models of metabolic disorders.[21,22] In another approach, the group of Watowich focused on the development of inhibitors based on NNMT's alternative substrate quinoline. Their compounds showed improvement of symptoms in diet-induced obese mice.[23] Previous work in our group has focused on bisubstrate inhibitors designed to mimic the transition state of the methylation reaction catalyzed by NNMT with compound **1** (Figure 1) showing activity on par with the known general methyltransferase inhibitor sinefungin.[24]

Designing bisubstrate analogues as inhibitors is an established and effective strategy that has been applied to a range of methyltransferase enzymes including catechol *O*-methyltransferase (COMT),[25-26] histone lysine methyltransferases,[27] arginine methyltransferases,[28–30] and more recently nicotinamide *N*-methyltransferase.[24,31] A recently published co-crystal structure of a bisubstrate inhibitor bound to NNMT (PDB ID: 6CHH) clearly delineates key interactions with residues in the enzyme active site, providing valuable information for further optimization of

improved bisubstrate-like inhibitors.[31] The work here described builds on our previous findings for "trivalent" inhibitor **1**, which is assumed to simultaneously bind in the adenosine, amino acid, and nicotinamide binding pockets of the NNMT active site. Based upon insights provided by recent NNMT crystal structures, we have designed new inhibitors wherein the nicotinamide moiety is replaced by other aromatic substituents accompanied by variation in the length of the linker connecting the amino acid moiety. Based on the high conservation of the residues in the adenosine binding pocket, no changes were made to the adenosine group. A schematic overview of the design strategy is been presented in Figure 1.

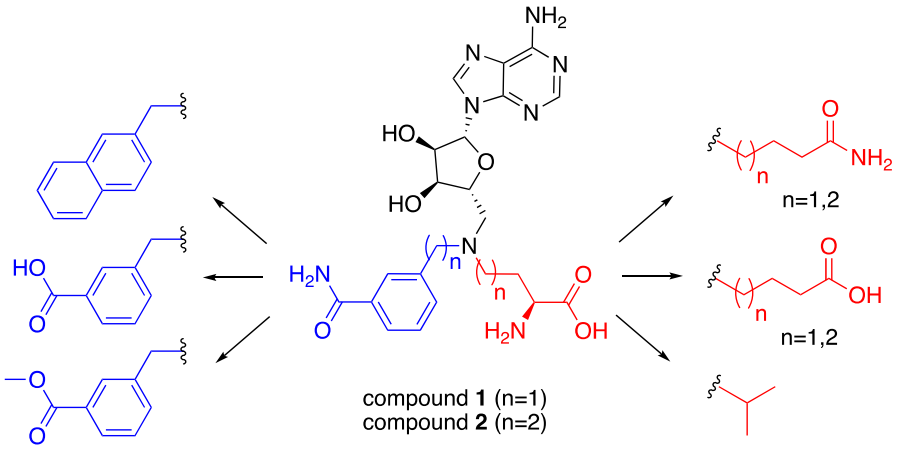

Figure 1. Schematic overview of the design strategy of the second generation of inhibitors based on trivalent bisubstrate compounds **1**[24] and **2**[31]

2. Results and discussion

Design: The ternary crystal structure of NNMT (PDB ID: 3ROD) reveals the interactions of nicotinamide and *S*-Adenosyl-L-homocysteine (SAH) with the active site residues.[32] The active site can be roughly divided into three binding regions for the adenosine group, the amino acid moiety, and the nicotinamide unit. The starting point was trivalent bisubstrate compound **1**, which was designed to bind all three binding regions. In order to find the optimal substitutions, a systematic approach was applied, where variations were made to the nicotinamide mimic on the one hand and the amino acid moiety on the other. The benzamide group, representing nicotinamide, was also replaced by methyl benzoate or benzoic acid moieties. Notably, the crystal structure of the NNMT–nicotinamide–SAH ternary complex reveals π-π stacking between tyrosine residue Y204 and the nicotinamide substrate.[32] We therefore also prepared an analogue bearing a naphthalene unit in the presumed nicotinamide position with the aim of introducing stronger π-π stacking with the tyrosine residues of the NNMT active site. We also explored variation of the amino acid moiety as part of our design strategy: in some analogues the amine of

the amino acid unit was omitted to reduce charge and in others the carboxylic acid replaced by the corresponding primary amide. In addition, variation in the length of the carbon chain linking the amino acid moiety was examined. Furthermore, inspired by the structure of histone methyltransferase DOTL1 inhibitor pinometostat,[33] we also investigated the incorporation of an isopropyl group to replace the amino acid moiety entirely.

Synthesis: Key aldehyde intermediates (compounds **6**, **8**, **9**, **16**, **17**, **22**, **23**, **27**, **28**) required for the synthesis of the various bisubstrate analogues pursued were prepared from commercially available materials, in good overall yields, as summarized in Scheme 1-3. The trivalent inhibitors were then prepared via a convenient double reductive amination strategy starting from the commercially available 2'-3'-*O*-isopropylidene-6-aminomethyl-adenosine starting material and the corresponding aldehydes (Scheme 4 and 5).

The preparation of aromatic aldehydes **6**, **8**, and **9** began with the selective mono-deprotection of dimethyl isophthalate using sodium hydroxide (Scheme 1).[34] Monomethyl isophthalate (**3**) was subsequently transformed into trityl-protected amide **4** using tritylamine via its acid chloride intermediate and reduced by diisobutylaluminum hydride (DIBAL-H) to give alcohol **5**. The alcohol was oxidized to aldehyde **6** using pyridinium dichromate (PDC). For aldehydes **8** and **9**, the carboxylic acid of **3** was selectively reduced using a mixture of sodium borohydride and boron trifluoride diethyl etherate.[35] The resulting alcohol (**7**) was oxidized using PDC to yield the corresponding aldehyde (**8**). Following hydrolysis of the methyl ester in **8** and subsequent conversion to the *tert*-butyl ester, aldehyde **9** was obtained.[36]

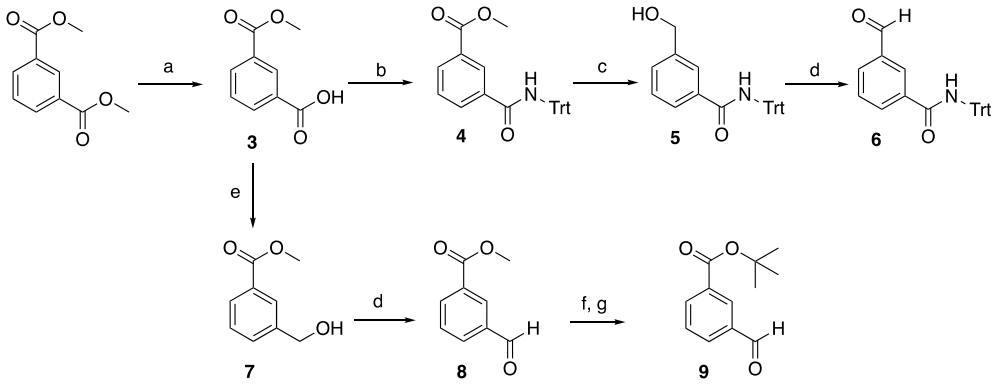

Scheme 1. Synthetic route for aldehydes **6**, **8** and **9**. Reagents and conditions: (a) NaOH, MeOH, rt, 16 h (95%); (b) i) $SOCl_2$, reflux, 2h, ii) tritylamine, CH_2Cl_2, 0°C-rt, 2 h (72%); (c) DIBAL-H, -78°C-rt, 2 h (85%); (d) PDC, CH_2Cl_2, rt, 2 h (53-64%); (e) $NaBH_4$, $BF_3{\cdot}Et_2O$, THF, 0°C-rt, 2 h (89%); (f) LiOH, THF/H_2O (2:1); (g) 2-tert-butyl-1,3-diisopropylisourea, CH_2Cl_2, tert-butanol (39% over 2 steps).

Aliphatic aldehydes **16** and **17** containing trityl-protected amide functionalities were prepared from succinimide and glutarimide respectively (Scheme 2). The cyclic amides were first trityl-protected and subsequently ring-opened using potassium hydroxide. Reduction to the corresponding alcohols and oxidization using PDC gave aldehydes **16** and **17**.[37,38] In analogous fashion, aldehydes **22** and **23**, both containing *tert*-buytl ester moieties, were prepared by ring opening of succinic or glutaric anhydride with *tert*-butyl alcohol to obtain mono-esters **18** and **19**.[39,40] The carboxylic acid functionalities were reduced to alcohols **20** and **21** and then oxidized using PDC to yield aldehydes **22** and **23**.

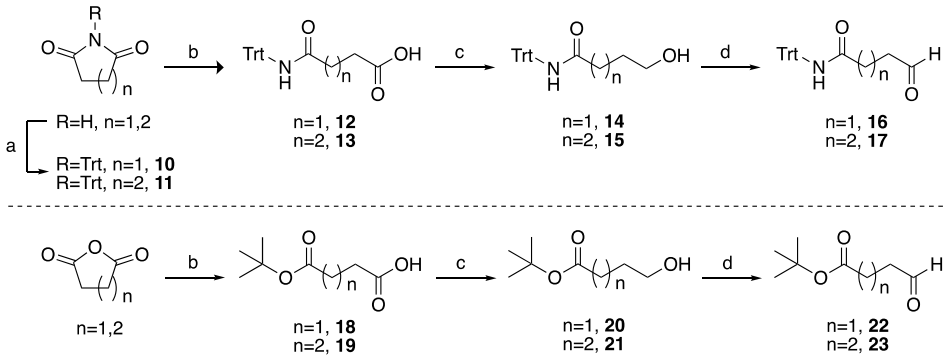

Scheme 2. Synthetic route for aldehydes **16**, **17**, **22** and **23**. Reagents and conditions: (a) TrtCl, CH_3CN, K_2CO_3, rt, 48 h (20-28%); (b) KOH, EtOH, reflux, overnight (37-93%) (c) $NaBH_4$, $BF_3{\cdot}Et_2O$, THF, 0°C-rt, 2 h (64-81%); (d) PDC, CH_2Cl_2, rt, 2 h (65-78%); (e) tert-butanol, DMAP, *N*-Hydroxysuccinimide, Et_3N, toluene, overnight (25-93%).

Aldehydes **27** and **28**, both containing protected amino acid functionalities, were prepared starting from the appropriately protected aspartic acid and glutamic acid building blocks (Scheme 3). Conversion of the side chain carboxylates to their corresponding Weinreb amides yielded intermediates **24** and **25**. Reduction of aspartate-derived **24** with DIBAL-H gave amino acid aldehyde **27** in high yield. For the preparation of aldehyde **28**, a similar route was followed with the addition of a second Boc-protection of intermediate **25** to avoid an intramolecular cyclization side reaction.[24,41]

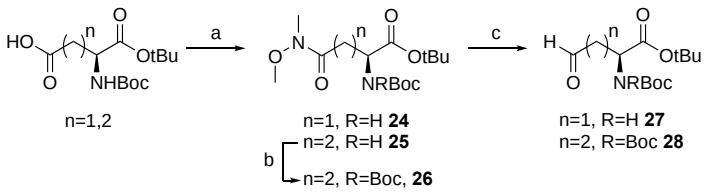

Scheme 3. Synthetic route for aldehydes **27** and **28**. Reagents and conditions: (a) $CH_3NHOCH_3{\cdot}HCl$, BOP, Et_3N, CH_2Cl_2, rt, 2 h (85-88%); (b) $(Boc)_2O$, Et_3N, DMAP, CH_2Cl_2 (94%); (c) DIBAL-H in hexanes (1 M), THF, -78°C, assumed quant.

With the necessary aldehyde building blocks in hand, assembly of the bisubstrate inhibitors was performed in each case starting from commercially available 2'-3'-*O*-isopropylidene-6-aminomethyl-adenosine (Scheme 4). Using a reliable reductive amination approach, aromatic aldehydes **6**, **8**, **9**, and commercially available 2-naphthaldehyde were each coupled to the protected adenosine species to yield intermediates **29-32.** These intermediates were next connected with aliphatic aldehydes **16**, **17**, **22**, **23**, **27, 28** or acetone via a second reductive amination step to give the corresponding protected tertiary amine intermediates **33-56 (Scheme 5)**. Global deprotection of the acid-labile protecting groups was carried out in CH_2Cl_2/TFA (1:1) with isopropylidene group cleavage facilitated by subsequent addition of water. The crude products were purified by preparative HPLC to yield bisubstrate analogues **1**, **57-61**.

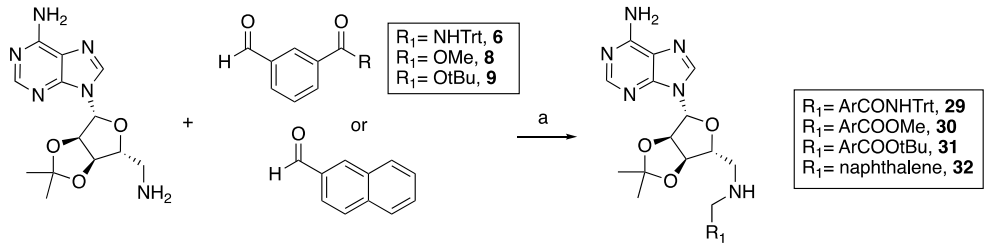

Scheme 4. Synthesis of intermediate compounds **29-32**. Reagents and conditions: (a) $NaBH(OAc)_3$, AcOH, DCE, rt, overnight (50-74%).

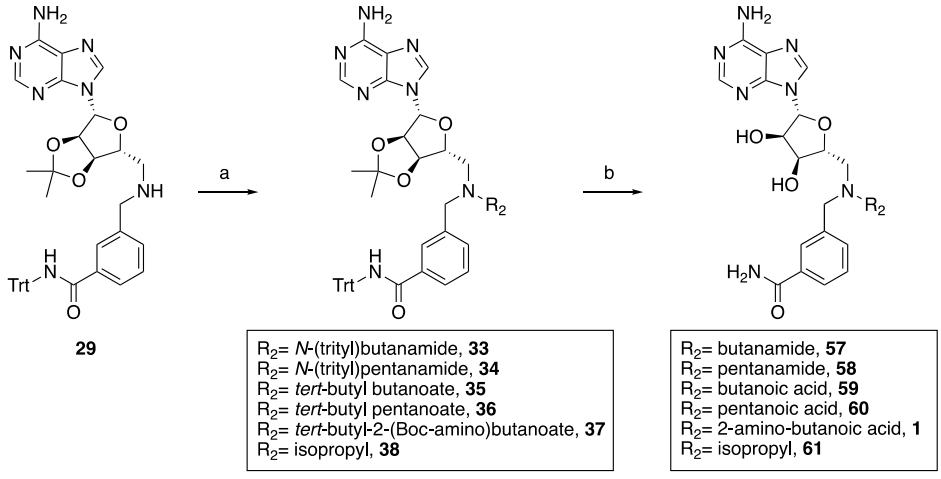

Scheme 5. Representative scheme for the synthesis of the final compounds, shown for compounds **1** and **57-61**. The same procedure was used starting from aldehydes **30-32** to form intermediate compounds **39-56** and **80** and final compounds **62-79** and **81** as detailed in the experimental section. Reagents and conditions: (a) aldehyde, $NaBH(OAc)_3$, AcOH, DCE, rt, overnight (49-77%); (b) i) TFA, CH_2Cl_2, rt, 2h, ii) H_2O, rt, 30 min (47-73%).

Inhibition Studies: The bisubstrate analogues were next tested for their NNMT inhibitory activity using a method recently developed in our group.[2] This assay employs Ultra High Performance (UHP) Hydrophilic Liquid Interaction Chromatography (HILIC) coupled to Quadrupole Time-Of-Flight Mass Spectrometry (QTOF-MS) to rapidly and efficiently assess NNMT inhibition by analysis of the formation of MNA. The NNMT inhibition of all compounds was initially screened at a fixed concentration of 250 μM for all of the compounds. In cases where at least 50% inhibition was detected at this concentration full inhibition curves were measured in triplicate to determine the corresponding IC_{50} values. As reference compounds, we included the well-established and general methyltransferase inhibitors sinefungin and SAH. In addition, we also synthesized two recently described NNMT inhibitors, compound **2** and 6-(methylamino)-nicotinamide, following the procedures described in the corresponding publications.[21,31] The structures of these reference compounds are provided in Figure 2.

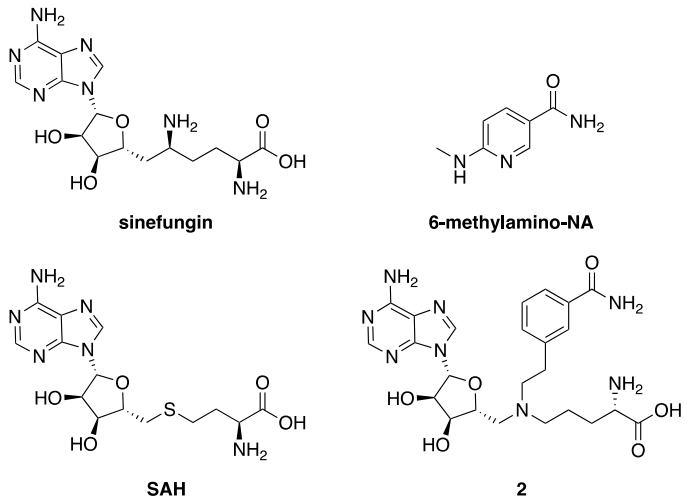

Figure 2. Chemical structures of the reference compounds used in NNMT inhibition studies

The results of the NNMT inhibition studies are summarized in Table 1 and clearly show that only minor adjustments to the functional groups found in the enzyme's natural substrates are tolerated. Among the compounds studied, the most potent inhibition was observed when the aliphatic moiety corresponded to the same length in the amino acid side chain as present in the methyl donor SAM. Notably, the preferred aromatic moiety was found to be the naphthalene group, an apparent confirmation of our hypothesis that increased π-π stacking can lead to enhanced binding in the nicotinamide pocket. The bisubstrate analogue containing both of these elements (compound **78**), displayed the highest inhibitory activity against NNMT with an IC_{50} of 1.41 μM. Interestingly, the amino acid and naphthyl moieties were also found to independently

enhance the activity of the other inhibitors prepared. In this way a suboptimal moiety at one position can be compensated – to an extent – by including either the SAM amino acid motif or the naphthalene unit at the other position. For example, bisubstrate analogues containing the benzamide, benzoic acid, or methyl benzoate groups only show inhibitory activity if they also contain the amino acid motif (compounds **1**, **2**, **66**, **72**) with IC_{50} values of 4.36-23.4 μM respectively. On the other hand, among the bisubstrate analogues lacking the amino acid motif, inclusion of the naphthalene moiety (compounds **74**-**79**) enhances NNMT inhibition albeit with moderate IC_{50} values in the range of 52.6-129.9 μM.

Table 1. Tabulated overview of the chemical structures and inhibition results of the final compounds and reference compounds

		IC_{50} values (μM)[a]			
Reference compounds		**Sinefungin**	**SAH**		**6-methylamino-nicotinamide**
IC_{50} (μM)		12.51 ± 2.11	35.30 ± 5.48		19.81 ± 2.50
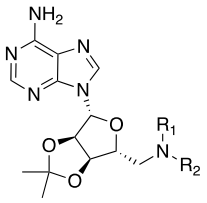		**R_1**			
		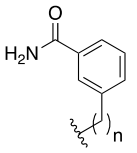	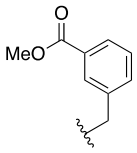	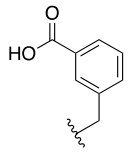	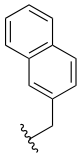
R_2	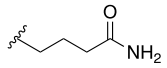	**57** (n=1): >250	**62**: >250	**68**: >250	**74**: 111.50 ± 28.79
	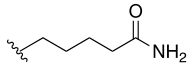	**58** (n=1): >250	**63**: >250	**69**: >250	**75**: 52.62 ± 9.08
	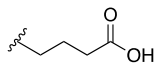	**59** (n=1): >250	**64**: >250	**70**: >250	**76**: >250
	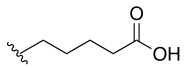	**60** (n=1): >250	**65**: >250	**71**: >250	**77**: >250
	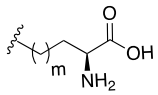	**1** (m=1, n=1): 14.90 ± 2.07 **2** (m=2, n=2): 4.36 ± 0.27	**66** (m=1, n=1): 17.45 ± 2.65	**72** (m=1, n=1): 23.41 ± 4.86	**78** (m=1, n=1): 1.41 ± 0.16 **81** (m=2, n=2): >250
		**61** (n=1): >250	**67**: >250	**73**: >250	**79**: 129.90 ± 14.80

[a]Assays performed in triplicate on at least six different inhibitor concentrations. Standard errors of the mean reported.

Other notable findings were the results obtained with the reference compounds. The general methyltransferase inhibitors sinefungin and SAH showed inhibitory activities in line with those previously reported.[24] Interestingly, the 6-methylamino-NA compound recently described by Sanofi to be a submicromolar inhibitor,[21] gave an IC_{50} of 19.8 μM in our assay. The recently published bisubstrate analogue **2** exhibited good activity (IC_{50} 4.4 μM) on par with published values.[31] Given the potent inhibition measured for both compound **2** and **78**, we also prepared and tested compound **81**, an analogue of **78** bearing the same naphthyl moiety but with the amino acid motif containing an additional methylene unit as in **2**. Somewhat surprisingly, this linker elongation resulted in a complete loss of inhibitory activity (IC_{50}>250 μM).

To gain insight into the selectivity of compound **78**, we also tested its activity against representative members of both the arginine and lysine families of methyltransferases, PRMT1 and NSD2 respectively. In both cases compound **78** was tested at a concentration of 50 μM and showed no significant inhibition (>50% of the enzyme's activity remained).

ITC binding studies: To further evaluate the binding interactions of the most active bisubstrate analogues with NNMT, isothermal titration calorimetry (ITC) studies were performed, Compounds, **1**, **66**, **72** and **78**, all containing the amino acid moiety but with varying aromatic substituents, were investigated. As illustrated in Figure 3, the dissociation constants (K_d) measured for these compounds track very well with the IC_{50} values measured in the in vitro assay. Compounds **1** and **66** display similar binding to NNMT with K_d values of 36 μM and 25 μM respectively while compound **72** binds less tightly with a K_d of 124 μM. In good agreement with the results of the inhibition assay, the most active inhibitor, compound **78**, also displayed the highest binding affinity for NNMT with a K_d of 5.6 μM. As expected, the inhibitors were each found to bind the enzyme with a 1:1 stoichiometry.

Modeling studies: To further investigate the way in which the inhibitors bind within the NNMT active site modeling studies were performed. Working from the available crystal structure of NNMT protein bounded to nicotinamide and SAH (PDB ID: 3ROD)[32], compounds **1**, **2**, **78**, and **81** were modeled in the binding pocket. In an attempt to explain the significant difference in activity of **78** and **81** additional molecular dynamic simulations were also performed for compounds **1**, **2**, **78** and **81**. While these simulations suggest differences in the binding interaction of the compounds, the calculated binding energies for each are all very similar. In terms of their active site orientations, compounds **1**, **2**, **78** and **81** are all predicted to position their three branches roughly in the same regions of the active site, however their orientations and interactions are quite different.

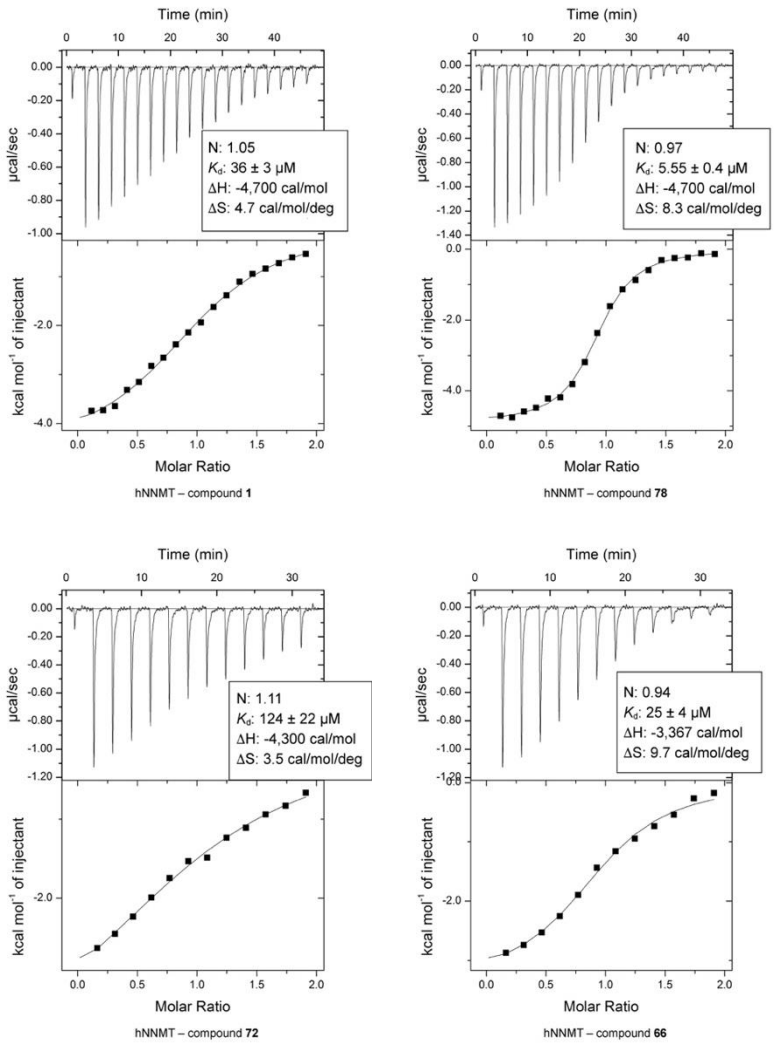

Figure 3. ITC isotherms and thermograms including thermodynamic binding parameters measured for compounds **1**, **66**, **72**, and **78** with hNNMT.

From the modeling data, two distinct features are apparent. First, when the chain linking the amino acid moiety is shorter (as in compounds **1** and **78**), the formation of an intramolecular hydrogen bond interaction was observed between the carboxylate of the amino acid moiety and the protonated tertiary amine (see Figure 4). This intramolecular interaction is highly stable for compound **78** and less stable for compound **1**. This additional interaction reduces the entropic energy of the ligand, thereby potentially stabilizing its binding, and re-orients the amino acid part in the pocket, preventing the polar interactions with neighboring residues (e.g. Y25, D61, Y69, and T163) observed when the chain is longer (as present in compounds **2** and **81**). This intramolecular hydrogen bond may explain the difference in activity observed between compounds **78** and **81**. The second distinct feature is the tyrosine rich environment around the naphthalene moiety of **78** compared to the nicotinamide unit of **1**. The orientation of the tyrosine

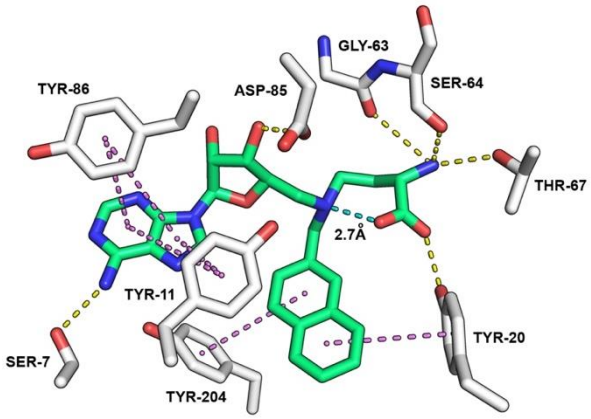

Figure 4. Modeling results for compound **78** in the NNMT active site (PDB ID: 3ROD). Molecular dynamics simulation indicates the presence of an intramolecular hydrogen bond (2.7Å, shown in cyan) specific to compound **78** (in green) that would be expected to reduce the entropic energy of the ligand and potentially stabilize binding to NNMT (in white). Proposed intermolecular hydrogen bond network (in yellow) and π-π stacking interactions with Tyr residues (in purple) stabilize compound **78** in the NNMT active site (hydrogens omitted for clarity).

residues surrounding this part of the molecule leads to π-π stacking interactions with the naphthalene and hint at an explanation for the strong inhibition and high affinity of compound **78** with NNMT protein (Figure 4).

Cell-based assays: To evaluate the cellular activity of the bisubstrate inhibitors, the compounds were tested for their effect on cell proliferation in the human oral cancer cell line HSC-2. We recently found that NNMT expression levels are high in this particular cell line and may contribute to its proliferation and tumorigenic capacity.[42] As shown in Figure 5, there were no significant differences in cell proliferation rate between HSC-2 cells treated with DMSO at 0.1% concentration and cells grown with culture medium only, at any time of each performed assay. Upon treatment with the NNMT inhibitors, cell proliferation was not significantly inhibited by compounds **1**, **2** and **81** (Figure 5). On the contrary, relative to the DMSO control, treatment with compound **78** led to a notable decrease in cell proliferation. In particular, cell proliferation was significantly ($p < 0.05$) inhibited by compound **78** at 10μM (20% reduction), 50 μM (21% reduction) and 100 μM (27% reduction) concentrations, 48 hours after treatment. Interestingly, at the longest 72-hour time-point taken, treatment with compound **78** lead to an even greater and significant ($p < 0.01$) decrease in cell proliferation (44% reduction), at the highest concentration (100 μM) (Figure 5).

We next investigated the effect of compound **78** on cellular NNMT activity by assessing its impact on MNA production in the same HSC-2 cell line. Cells were treated with 100 μM of **78**

and MNA levels determined after 0, 1, 2, and 3 days. Cells treated with compound 78 show a significant ($p < 0.01$) decrease in the levels of MNA (50% reduction) compared to controls after 48 hours. Interestingly, at 72 hours an increase in cellular MNA production was detected, however, the same effect was also observed in the DMSO control (but not in the untreated control) suggesting an effect attributable to longer-term DMSO exposure.

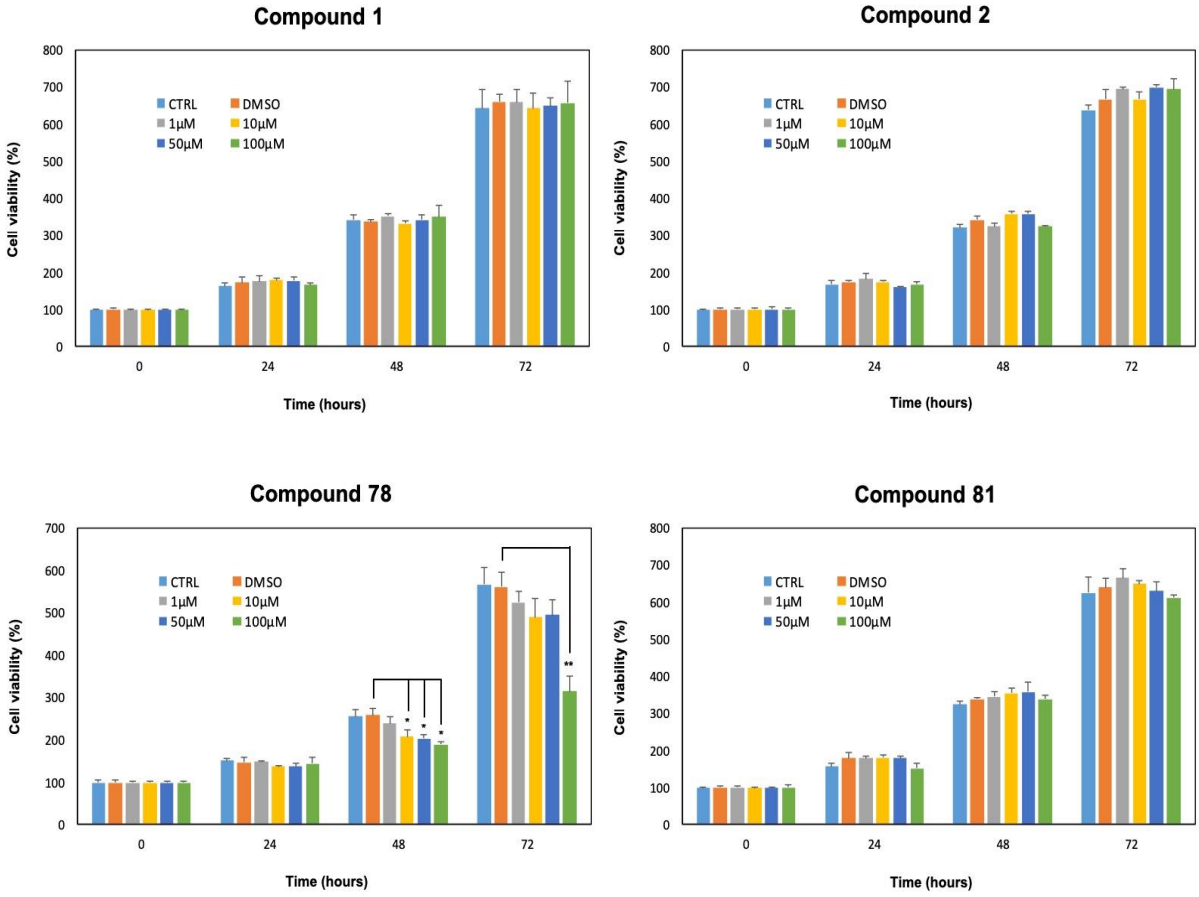

Figure 5. Results of the MTT cell viability assay on HSC-2 human oral cancer cells. Only compound **78** showed a significant effect on cell proliferation after 48 and 72 hours

3. Conclusion

Building from our earlier findings with first reported ternary bisubstrate NNMT inhibitor **1**,[24] we designed and prepared a focused library of novel inhibitors to provide new structure-activity insights. In doing so, various structural motifs were investigated for the ability to enhance inhibitor activity and binding within the NNMT active site. By probing the SAM and NA binding pockets with different spacers and functional groups, we found that the optimal ligands are the endogenous amino acid side-chain and the naphthalene moiety. Among the naphthalene-containing bisubstrate analogues prepared, compound **78** showed the most potent NNMT inhibition. In this way the activity of our initial NNMT inhibitor 1 (IC_{50} = 14.9 μM) was improved

10-fold with compound **78** displaying an IC_{50} value of 1.41 μM. Notably, using an assay designed to directly measure NNMT product formation, compound **78** was shown to be more potent than most other NNMT inhibitor reported to date. ITC-based binding studies provided additional insights in the affinity of the inhibitors for the enzyme with measured K_d value following a trend similar to that observed for the IC_{50} data obtained in the *in vitro* inhibition assays. From modeling studies, the improved activity of compound **78** can be rationalized by the apparent presence of an intramolecular hydrogen bonding interaction predisposing the compound to an active conformation with lower entropic cost. In addition, the modeling indicates that the naphthalene group in **78** is properly oriented so as to benefit from additional π-π stacking interactions with several tyrosine residues in the nicotinamide binding pocket of the enzyme. The cellular data obtained for compound **78** shows a significant inhibitory effect on cell proliferation in HSC-2 oral cancer cells. These promising results provide important new insights for the design and further optimization of potent NNMT inhibitors.

4. Experimental procedures

General Procedures: All reagents employed were of American Chemical Society (ACS) grade or finer and were used without further purification unless otherwise stated. For compound characterization, ^{1}H NMR spectra were recorded at 400 MHz with chemical shifts reported in parts per million (ppm) downfield relative to tetramethylsilane (TMS), H_2O (δ 4.79), $CHCl_3$ (7.26) or DMSO (δ 2.50). ^{1}H NMR data are reported in the following order: multiplicity (s, singlet; d, doublet; t, triplet; q, quartet and m, multiplet), coupling constant (*J*) in hertz (Hz) and the number of protons. Where appropriate, the multiplicity is preceded by br, indicating that the signal was broad. ^{13}C NMR spectra were recorded at 101 MHz with chemical shifts reported relative to $CDCl_3$ (δ 77.16), methanol (δ 49.00) or DMSO (δ 39.52). The ^{13}C NMR spectra of the compounds recorded in D_2O could not be referenced. High-resolution mass spectrometry (HRMS) analysis was performed using a Q-TOF instrument. Compounds **1**,[24] **2**,[31] **3**,[34] **7**,[34] **8**,[36] **9**,[37] **10**,[43] **12**,[38] **14**,[38] **16**,[44] **18**,[40] **19**,[40] **20**,[45] **21**,[46] **22**,[47] **23**,[40] **24**,[41] **25**,[41] **26**,[48] **27**,[41] **28**[48] were prepared as previously described and had NMR spectra and mass spectra consistent with the assigned structures. Purity was confirmed to be ≥ 95% by analytical RP-HPLC using a Phenomenex Kinetex C18 column (5 μm, 250 × 4.6 mm) eluted with a water–acetonitrile gradient moving from 0% to 100% CH_3CN (0.1% TFA) in 30 minutes. The compounds were purified via preparative HPLC using a Reprosil-Pur C18-AQ column (10 μm, 250 × 22 mm) eluted with a water–acetonitrile gradient moving from 0% to 50% CH_3CN (0.1% TFA) over 60 minutes at a flow rate of 12.0 ml min^{-1} with UV detection at 214 nm and 254 nm.

Methyl 3-(tritylcarbamoyl)benzoate (4). Mono-methylisophthalate **3** (0.98 g, 5.4 mmol) was refluxed in 10 mL $SOCl_2$ at 90 °C for about one hour (until the reaction mixture is a clear solution). The $SOCl_2$ was removed under reduced pressure and the acid chloride intermediate was redissolved in 15 mL dry CH_2Cl_2 and transferred to a cooled (ice-bath) solution of tritylamine (1.41 g, 5.4 mmol) and 2 mL triethylamine in 30 mL CH_2Cl_2. The reaction was stirred overnight under N_2 atmosphere, allowing the mixture to warm to room temperature. After the reaction was completed (monitored by TLC (petroleum ether / CH_2Cl_2= 1:1)), the reaction mixture was washed with water and brine and the organic phase dried over Na_2SO_4 and concentrated. The crude product was purified by column chromatography (petroleum ether / CH_2Cl_2= 2:1) to give compound **4** as a white powder (1.64 g, 72% yield). ^{1}H NMR (400 MHz, $CDCl_3$) δ 8.45 (t, *J* = 1.6 Hz, 1H), 8.18 (m, 1H), 8.03 (m, 1H), 7.53 (t, *J* = 7.8 Hz, 1H), 7.41 – 7.26 (m, 15H), 3.94 (s, 3H). ^{13}C NMR (101 MHz, $CDCl_3$) δ 166.3, 165.4, 144.5, 135.6, 132.5, 131.7, 130.6, 128.9, 128.7, 128.1, 128.1, 127.6, 127.2, 71.0, 52.4. HRMS (ESI): calculated for $C_{28}H_{23}NO_3$ $[M+Na]^+$ 444.1576, found 444.1581.

3-(Hydroxymethyl)-*N*-tritylbenzamide (5). Methyl 3-(tritylcarbamoyl)benzoate **4** (0.56 g, 1.33 mmol) was dissolved in dry CH_2Cl_2 (20 mL) under a N_2 atmosphere, the reaction solution was cooled down to -78 °C, and then diisobutylaluminum hydride (DIBAL-H) (5.5 mL, 1.0 M hexane solution) was added slowly. The reaction mixture was stirred at -78 °C for 2 hours. Saturated aq. NH_4Cl (50 mL) was added slowly to quench the reaction under -78 °C, followed by the addition of a saturated Rochelle salt solution (100 mL). The mixture was stirred at room temperature overnight, extracted with CH_2Cl_2 and the organic layers dried over Na_2SO_4 and concentrated under reduced pressure. The crude product was purified by column chromatography (CH_2Cl_2/EtOAc = 9:1) to obtain **5** as a white powder (0.44 g, 85% yield). ^{1}H NMR (400 MHz, DMSO-d_6) δ 8.92 (s, 1H), 7.78 (s, 1H), 7.75 – 7.71 (m, 1H), 7.47 (d, *J* = 7.8 Hz, 1H), 7.40 (t, *J* = 7.6 Hz, 1H), 7.36 – 7.18 (m, 15H), 5.26 (br, 1H), 4.54 (s, 2H). ^{13}C NMR (101 MHz, DMSO-d_6) δ 167.0, 145.3, 143.0, 135.5, 129.6, 128.9, 128.3, 127.9, 126.7, 126.5, 126.2, 79.6, 69.9, 69.9, 63.0. HRMS (ESI): calculated for $C_{27}H_{23}NO_2$ $[2M+Na]^+$ 809.3355, found 809.3359.

3-Formyl-*N*-tritylbenzamide (6). 3-(hydroxymethyl)-*N*-tritylbenzamide **5** (0.20 g, 0.51 mmol) and pyridinium dichromate (PDC) 0.23 g, 0.61 mmol) were placed in a 50 mL round bottom flask and 10 mL of dry CH_2Cl_2 was added under N_2 atmosphere at room temperature. The reaction was stirred till completion, as monitored by TLC (petroleum ether / CH_2Cl_2 = 5:1). The mixture was filtered and the organic layer was washed with brine, dried over anhydrous Na_2SO_4 and concentrated under reduced pressure. The resulting crude product was purified by

column chromatography (petroleum ether / CH_2Cl_2 = 9:1) to obtain **6** as a white powder (0.13 g, yield 64%). ^{1}H NMR (400 MHz, DMSO-d_6) δ 10.09 (s, 1H), 9.31 (s, 1H), 8.39 (s, 1H), 8.17 (d, *J* = 7.7 Hz, 1H), 8.06 (d, *J* = 7.7 Hz, 1H), 7.68 (t, *J* = 7.7 Hz, 1H), 7.41 – 7.17 (m, 15H). ^{13}C NMR (101 MHz, $CDCl_3$) δ 191.5, 165.1, 144.4, 136.5, 136.2, 133.0, 132.5, 129.5, 128.6, 128.5, 128.1, 127.7, 127.3, 77.2, 71.1. HRMS (ESI): calculated for $C_{27}H_{21}NO_2$ [2M+Na]$^+$ 805.3042, found 805.3047.

***N*-(triphenylmethyl)glutarimide (11).** Glutarimide (2.8 g, 25 mmol), triphenylchloromethane (7.4 g, 25 mmol), and potassium carbonate (3.7 g, 25 mmol) were added to 100 mL acetonitrile and the mixture was stirred at room temperature overnight. Saturated aqueous $NaHCO_3$ (50 mL) was added and the mixture was extracted with EtOAc. The combined organic layers were dried with anhydrous Na_2SO_4 and the solvent was removed under reduced pressure. The crude product was purified by column chromatography (petroleum ether / EtOAc = 4:1) to obtain **11** as a white powder (1.8 g, yield 20%). ^{1}H NMR (400 MHz, DMSO-d_6) δ 7.45 – 7.35 (m, 6H), 7.20 (t, *J* = 7.8 Hz, 6H), 7.08 (t, *J* = 7.3 Hz, 3H), 2.66 (t, *J* = 6.4 Hz, 4H), 2.01 (p, *J* = 6.5 Hz, 2H). ^{13}C NMR (101 MHz, $CDCl_3$) δ 172.4, 143.4, 128.5, 127.3, 125.9, 35.5, 16.7. HRMS (ESI): calculated for $C_{24}H_{21}NO_2$ [M+Na]$^+$ 378.1470, found 378.1493.

5-Oxo-5-(tritylamino)pentanoic acid (13). To 2.80 g of KOH dissolved in 50 ml of ethanol was added *N*-tritylglutarimide **11** (1.00 g, 2.8 mmol) and the mixture was refluxed for 48 hours. The mixture was then concentrated to dryness and redissolved in H_2O. Acidification of the basic solution with conc. HCl to pH=2 and filtration of the product gave compound **13** as a white powder (0.96 g, yield 91%). ^{1}H NMR (400 MHz, CD_3OD) δ 7.30 – 7.17 (m, 15H), 2.37 (t, *J* = 7.4 Hz, 2H), 2.25 (t, *J* = 7.4 Hz, 2H), 1.79-1.87 (m 2H). ^{13}C NMR (101 MHz, CD_3OD) δ 175.5, 173.3, 144.6, 128.6, 127.3, 127.2, 126.7, 126.3, 35.2, 32.6, 20.7. HRMS (ESI): calculated for $C_{24}H_{23}NO_3$ [M+Na]$^+$ 396.1576, found 396.1573.

5-Hydroxy-*N*-tritylpentanamide (15). To a solution of **13** (2.60 g, 6.96 mmol) in dry THF (60 mL) cooled to 0 °C was added $NaBH(OAc)_3$ (0.28 g, 7.3 mmol). The solution was stirred until evolution of H_2 stopped, and $BF_3.OEt_2$ (1.1 mL, 8.8 mmol) was added dropwise. The reaction was stirred at room temperature for 4 hours. The reaction was quenched by adding 50 mL H_2O at 0 °C. The mixture was extracted with EtOAc and the combined organic layers were washed with sat. aq. Na_2CO_3, brine and dried over Na_2SO_4. The crude product was purified by column chromatography (100% EtOAc) to give compound **15** as a white powder (1.60 g, 64% yield). ^{1}H NMR (400 MHz, $CDCl_3$) δ 7.22 – 6.74 (m, 15H), 6.36 (br, 1H), 3.29 – 3.19 (br, 2H), 2.01 (t, *J* = 7.2 Hz, 2H), 1.46 – 1.36 (m, 2H), 1.24 (m, 2H). ^{13}C NMR (101 MHz, $CDCl_3$) δ

171.9, 144.7, 128.6, 127.9, 127.0, 62.0, 37.0, 32.0, 21.4. HRMS (ESI): calculated for $C_{24}H_{25}NO_2$ $[M+Na]^+$ 382.1783, found 382.1783.

5-Oxo-*N*-tritylpentanamide (17). 5-hydroxy-*N*-tritylpentanamide **15** (1.30 g, 3.6 mmol) and PDC (2.00 g, 5.4 mmol) were dissolved in 50 mL of dry CH_2Cl_2 and stirred for 2 hours under N_2 atmosphere at room temperature. The mixture was filtered and the organic layer was washed with brine, dried over anhydrous Na_2SO_4 and concentrated under reduced pressure. The crude product was purified by column chromatography (100% CH_2Cl_2) to give compound **17** as an off-white powder (0.84 g, 65% yield). ^{1}H NMR (400 MHz, $CDCl_3$) δ 9.71 (s, 1H), 7.36 – 7.10 (m, 15H), 6.59 (s, 1H), 2.44 (t, *J* = 7.0 Hz, 2H), 2.32 (t, *J* = 7.2 Hz, 2H), 1.97 – 1.88 (m, 2H). ^{13}C NMR (101 MHz, $CDCl_3$) δ 202.0, 170.8, 144.6, 128.6, 127.9, 127.0, 70.5, 42.9, 36.1, 17.9. HRMS (ESI): calculated for $C_{24}H_{23}NO_2$ $[M+Na]^+$ 380.1626, found 380.1629.

3-(((((3a*R*,4*R*,6*R*,6a*R*)-6-(6-amino-9*H*-purin-9-yl)-2,2-dimethyltetrahydrofuro[3,4-d][1,3]-dioxol-4-yl)methyl)amino)methyl)-*N*-tritylbenzamide (29). 3-Formyl-*N*-tritylbenzamide **6** (1.22 g, 3.12 mmol), 2'-3'-*O*-isopropylidene-6-aminomethyl-adenosine (1.00 g, 3.43 mmol) and acetic acid (0.45 mL, 8 mmol) were dissolved in 1,2-dichloroethane (DCE, 50 mL) and stirred at room temperature under a N_2 atmosphere. After 3 hours, $NaBH(OAc)_3$ (1.09 g, 5.15 mmol) was added and the reaction mixture was stirred overnight at room temperature. The reaction was quenched by adding 1 N NaOH solution (50 mL), and the product was extracted with CH_2Cl_2. The combined organic layers were washed with brine and dried over Na_2SO_4. The solvent was evaporated and the crude product was purified by column chromatography (10% MeOH in CH_2Cl_2) to give compound 29 as a white powder (1.25 g, 59% yield). ^{1}H NMR (400 MHz, DMSO-d_6) δ 8.89 (s, 1H), 8.34 (s, 1H), 8.06 (s, 1H), 7.79 (s, 1H), 7.71 (d, *J* = 7.7 Hz, 1H), 7.43 (d, *J* = 7.7 Hz, 1H), 7.39 – 7.24 (m, 15H), 7.20 (m, 3H), 6.09 (d, *J* = 3.1 Hz, 1H), 5.76 (s, 1H), 5.46 (M, 1H), 5.00 (m, 1H), 4.28 – 4.23 (m, 1H), 3.73 (s, 2H), 2.75 - 2.66 (m, 2H), 1.54 (s, 3H), 1.31 (s, 3H). ^{13}C NMR (101 MHz, DMSO-d_6) δ 166.9, 156.5, 153.1, 149.3, 145.3, 140.4, 135.6, 128.9, 128.3, 127.9, 127.6, 126.7, 126.5, 119.7, 113.7, 89.7, 85.3, 83.1, 82.6, 69.9, 55.3, 53.0, 50.8, 27.5, 25.7. HRMS (ESI): calculated for $C_{40}H_{39}N_7O_4$ $[M+Na]^+$ 704.2961, found 704.2975.

Methyl-3-((((3a*R*,4*R*,6*R*,6a*R*)-6-(6-amino-9*H*-purin-9-yl)-2,2-dimethyltetrahydrofuro[3,4-d] [1,3]dioxol-4-yl)methyl)amino)benzoate (30). Following the procedure described for compound **29**, coupling methyl 3-formylbenzoate **8** (0.51 g, 3.12 mmol) and 2'-3'-*O*-isopropylidene-6-aminomethyl-adenosine (1.00 g, 3.43 mmol) afforded compound **30** as a white powder (0.92 g, 65% yield). ^{1}H NMR (400 MHz, $CDCl_3$) δ 8.08 (s, 1H), 7.92 (s, 1H), 7.90 – 7.83 (m, 2H), 7.44 (d, *J* = 7.6 Hz, 1H), 7.32 (t, *J* = 7.6 Hz, 1H), 6.37 (d, *J* = 5.7 Hz, 2H), 5.95 (d, *J* = 3.1 Hz, 1H), 5.45 (m, 1H), 5.04 (m, 1H), 4.40 – 4.34 (m, 1H), 3.86 (s, 3H), 3.79 (s, 2H), 2.90-

2.83 (m, 2H), 1.58 (s, 3H), 1.35 (s, 3H). ^{13}C NMR (101 MHz, $CDCl_3$) δ 167.1, 155.8, 155.8, 153.0, 149.2, 140.4, 140.4, 139.8, 132.6, 132.6, 130.1, 129.1, 129.1, 128.4, 128.4, 128.2, 120.2, 114.4, 91.0, 85.5, 83.2, 83.2, 82.2, 82.2, 53.3, 52.1, 52.1, 50.6, 27.3, 27.2, 25.4, 25.3. HRMS (ESI): calculated for $C_{22}H_{26}N_6O_5$ [M+H]$^+$ 455.2043, found 455.2050.

tert-Butyl-3-(((((3aR,4R,6R,6aR)-6-(6-amino-9H-purin-9-yl)-2,2-dimethyltetrahydrofuro[3,4-d][1,3]dioxol-4-yl)methyl)amino)methyl)benzoate (31). Following the procedure described for compound **29**, coupling *tert*-butyl 3-formylbenzoate **9** (0.64 g, 3.12 mmol) and 2'-3'-*O*-isopropylidene-6-aminomethyl-adenosine (1.00 g, 3.43 mmol) afforded compound **31** as a white powder (0.77 g, 50% yield). ^{1}H NMR (400 MHz, $CDCl_3$) δ 8.11 (s, 1H), 7.89 (s, 1H), 7.86-7.83 (m, 2H), 7.43 (d, *J* = 7.7 Hz, 1H), 7.31 (t, *J* = 7.6 Hz, 1H), 6.36 – 6.27 (m, 2H), 5.96 (d, *J* = 3.3 Hz, 1H), 5.46 (m, 1H), 5.04 (m, 1H), 4.38 (m, 1H), 3.80 (s, 2H), 2.94-2.81 (m, 2H), 1.58 (s, 3H), 1.55 (s, 9H), 1.36 (s, 3H). ^{13}C NMR (101 MHz, $CDCl_3$) δ 165.7, 155.8, 155.8, 153.0, 149.3, 140.2, 139.8, 132.0, 132.0, 129.0, 128.2, 128.1, 120.3, 114.5, 91.0, 85.4, 83.2, 82.2, 80.9, 53.4, 50.6, 28.1, 27.3, 25.4. HRMS (ESI): calculated for $C_{25}H_{32}N_6O_5$ [M+H]$^+$ 497.2512, found 497.2511.

9-((3a*R*,4*R*,6*R*,6a*R*)-2,2-dimethyl-6-(((naphthalen-2-ylmethyl)amino)methyl)tetrahydrofuro-[3,4-d][1,3]dioxol-4-yl)-9*H*-purin-6-amine (32). Following the procedure described for compound **29**, coupling 2-naphthaldehyde (0.49 g, 3.12 mmol) and 2'-3'-*O*-isopropylidene-6-aminomethyl-adenosine (1.00 g, 3.43 mmol) afforded compound **32** as a white powder (1.03 g, 74% yield). ^{1}H NMR (400 MHz, $CDCl_3$) δ 8.11 (s, 1H), 7.88 (s, 1H), 7.78 (m, 3H), 7.70 (s, 1H), 7.48 – 7.38 (m, 3H), 6.05 (s, 2H), 5.99 (d, *J* = 3.3 Hz, 1H), 5.48 (m, 1H), 5.06 (m, 1H), 4.45 – 4.39 (m, 1H), 3.95 (s, 2H), 3.01 – 2.87 (m, 2H), 2.33 (br, 2H), 1.61 (s, 3H), 1.38 (s, 3H). ^{13}C NMR (101 MHz, $CDCl_3$) δ 155.7, 153.0, 149.3, 139.9, 137.4, 133.3, 132.6, 128.0, 127.6 126.4, 126.4, 126.0, 125.5, 120.3, 114.5, 91.0, 85.6, 83.3, 82.3, 53.9, 50.7, 27.3, 25.4. HRMS (ESI): calculated for $C_{24}H_{26}N_6O_3$ [M+H]$^+$ 447.2145, found 447.2167.

3-(((((3a*R*,4*R*,6*R*,6a*R*)-6-(6-amino-9*H*-purin-9-yl)-2,2-dimethyltetrahydrofuro[3,4-d][1,3]-dioxol-4-yl)methyl)(4-oxo-4-(tritylamino)butyl)amino)methyl)-*N*-tritylbenzamide (33). Oxo-*N*-tritylbutanamide **16** (62 mg, 0.18 mmol), compound **29** (100 mg, 0.15 mmol) and AcOH (1 drop) were dissolved in 1,2-dichloroethane (DCE, 10 mL) and stirred at room temperature under a N_2 atmosphere. After 3 hours, $NaBH_4$ (49 mg, 0.23 mmol) was added and the reaction mixture was stirred overnight at room temperature. The reaction was quenched by adding 1 N NaOH (10 mL), and the product was extracted with CH_2Cl_2. The combined organic layers were washed with brine and dried over Na_2SO_4. The solvent was evaporated and the crude product was purified by

column chromatography (10% MeOH in CH_2Cl_2) to give compound **33** as a white powder (83 mg, 55% yield). ^{1}H NMR (400 MHz, $CDCl_3$) δ 8.15 (s, 1H), 7.69 (s, 1H), 7.67 (s, 1H), 7.53 (d, *J* = 7.1 Hz, 2H), 7.39 – 7.09 (m, 32H), 6.61 (s, 1H), 5.95 (d, *J* = 1.9 Hz, 1H), 5.65 (s, 2H), 5.36 (m, 1H), 4.89 (m, 1H), 4.40 – 4.34 (m, 1H), 3.56 (d, *J* = 3.4 Hz, 2H), 2.68 (d, *J* = 6.8 Hz, 2H), 2.46 (m, 2H), 2.26 (m, 2H), 1.81 – 1.69 (m, 2H), 1.52 (s, 3H), 1.30 (s, 3H). ^{13}C NMR (101 MHz, $CDCl_3$) δ 171.5, 166.7, 155.4, 152.9, 149.0, 144.8, 144.7, 140.0, 139.9, 135.3, 131.5, 128.8, 128.7, 128.0, 127.9, 127.0, 126.9, 125.3, 114.1, 90.8, 85.7, 83.8, 83.4, 70.7, 70.4, 58.6, 56.0, 53.5, 34.9, 27.0, 25.3, 22.7. HRMS (ESI): calculated for $C_{63}H_{60}N_8O_5$ $[M+H]^+$ 1009.4765, found 1009.4765.

3-(((((3a*R*,4*R*,6*R*,6a*R*)-6-(6-amino-9*H*-purin-9-yl)-2,2-dimethyltetrahydrofuro[3,4-d][1,3]dioxol-4-yl)methyl)(5-oxo-5-(tritylamino)pentyl)amino)methyl)-*N*-tritylbenzamide (34). Following the procedure described for compound **33**, coupling compound **29** (100 mg, 0.15 mmol) with 5-oxo-*N*-tritylpentanamide **17** (64 mg, 0.18 mmol) afforded compound **34** as a white powder (88 mg, 57% yield). ^{1}H NMR (400 MHz, $CDCl_3$) δ 8.16 (s, 1H), 7.67 (s, 2H), 7.57 (br, 1H), 7.52 (s, 1H), 7.41 – 7.13 (m, 32H), 6.62 (s, 1H), 5.96 (d, *J* = 1.8 Hz, 1H), 5.83 (br, 2H), 5.38 (m, 1H), 4.92 (m, 1H), 4.40 – 4.34 (m, 1H), 3.54 (s, 2H), 2.65 (d, *J* = 6.9 Hz, 2H), 2.46 – 2.38 (m, 2H), 2.13 (m, 2H), 1.56 (s, 3H), 1.42 – 1.33 (m, 2H), 1.30 (s, 3H). ^{13}C NMR (101 MHz, $CDCl_3$) δ 171.6, 166.6, 155.5, 152.9, 149.1, 144.8, 144.8, 140.3, 140.0, 135.2, 131.6, 128.8, 128.7, 128.2, 128.0, 127.9, 127.5, 127.0, 127.0, 125.4, 114.1, 90.9, 85.9, 83.8, 83.4, 77.3, 70.7, 70.4, 58.6, 56.1, 53.9, 37.1, 27.1, 26.3, 25.4, 23.1. HRMS (ESI): calculated for $C_{64}H_{62}N_8O_5$ $[M+H]^+$ 1023.4921, found 1023.4918.

***tert*-Butyl 4-((((3a*R*,4*R*,6*R*,6a*R*)-6-(6-amino-9*H*-purin-9-yl)-2,2-dimethyltetrahydrofuro-[3,4-d][1,3]dioxol-4-yl)methyl)(3-(tritylcarbamoyl)benzyl)amino)butanoate (35).** Following the procedure described for compound **33**, coupling *tert*-butyl 4-oxobutanoate **22** (29 mg, 0.18 mmol) and compound **29** (100 mg, 0.15 mmol) afforded compound 35 as a white powder (61 mg, 49% yield). ^{1}H NMR (400 MHz, $CDCl_3$) δ 8.16 (s, 1H), 7.70 (d, *J* = 5.8 Hz, 2H), 7.58 (d, *J* = 7.6 Hz, 2H), 7.38 – 7.15 (m, 17H), 5.97 (d, *J* = 2.0 Hz, 3H), 5.36 (m, 1H), 4.93 (m, 1H), 4.35 (m, 1H), 3.63 – 3.52 (m, 2H), 2.76 – 2.63 (m, 2H), 2.47 (t, *J* = 7.1 Hz, 2H), 2.23 – 2.12 (m, 2H), 1.75 – 1.65 (m, 2H), 1.55 (s, 3H), 1.36 (s, 9H), 1.29 (s, 3H). ^{13}C NMR (101 MHz, $CDCl_3$) δ 172.7, 166.7, 155.5, 152.9, 149.0, 144.8, 144.8, 140.0, 139.9, 131.6, 128.8, 128.7, 128.0, 128.0, 127.0, 125.5, 120.1, 90.8, 85.8, 83.9, 83.4, 80.1, 70.7, 61.9, 58.8, 55.9, 53.4, 33.0, 32.4, 28.0, 27.1, 25.3, 22.4. HRMS (ESI): calculated for $C_{48}H_{53}N_7O_6$ $[M+H]^+$ 824.4136, found 824.4142.

***tert*-Butyl-5-((((3a*R*,4*R*,6*R*,6a*R*)-6-(6-amino-9*H*-purin-9-yl)-2,2-dimethyltetrahydrofuro-[3,4-d][1,3]dioxol-4-yl)methyl)(3-(tritylcarbamoyl)benzyl)amino)pentanoate (36).** Following the

procedure described for compound **33**, coupling *tert*-butyl 5-oxopentanoate **23** (31 mg, 0.18 mmol) and compound **29** (100 mg, 0.15 mmol) afforded compound **36** as a white powder (67 mg, 53% yield). ^{1}H NMR (400 MHz, $CDCl_3$) δ 8.17 (s, 1H), 7.70 (d, *J* = 8.7 Hz, 2H), 7.58 (d, *J* = 7.8 Hz, 1H), 7.51 (s, 1H), 7.42 – 7.27 (m, 14H), 7.19 (t, *J* = 7.7 Hz, 1H), 5.98 (s, 1H), 5.72 (s, 2H), 5.38 (m, 1H), 4.94 (s, 1H), 4.40 – 4.33 (m, 1H), 3.57 (s, 2H), 2.70 – 2.65 (m, 2H), 2.47 (t, *J* = 7.0 Hz, 2H), 2.13 (t, *J* = 7.2 Hz, 2H), 1.57 (s, 3H), 1.52 – 1.45 (m, 2H), 1.41 (s, 9H), 1.32 (s, 3H). ^{13}C NMR (101 MHz, $CDCl_3$) δ 172.9, 166.6, 155.4, 152.9, 149.1, 144.8, 140.2, 139.9, 135.2, 131.6, 128.7, 128.2, 128.0, 127.4, 127.0, 125.4, 120.2, 114.1, 90.8, 85.8, 83.9, 83.4, 80.0, 70.7, 58.7, 56.0, 54.0, 35.2, 28.1, 27.1, 26.3, 25.3, 22.7. HRMS (ESI): calculated for $C_{49}H_{55}N_7O_5$ $[M+H]^+$ 838.4292, found 838.4298.

***tert*-Butyl-(S)-4-((((3a*R*,4*R*,6*R*,6a*R*)-6-(6-amino-9H-purin-9-yl)-2,2-dimethyltetrahydrofuro[3,4-d][1,3]dioxol-4-yl)methyl)(3-(tritylcarbamoyl)benzyl)amino)-2-((*tert*-butoxycarbonyl)amino)butanoate (37).** Following the procedure described for compound **33**, coupling *tert*-butyl (*R*)-2-((*tert*-butoxycarbonyl)amino)-4-oxobutanoate **27** (49 mg, 0.18 mmol) and compound **29** (100 mg, 0.15 mmol) afforded compound **37** as a white powder (94 mg, 67% yield). ^{1}H NMR (400 MHz, $CDCl_3$) δ 8.15 (s, 1H), 7.70 (m, 2H), 7.57 (d, *J* = 9.9 Hz, 2H), 7.41 – 7.14 (m, 15H), 5.98 (s, 1H), 5.59 (s, 2H), 5.37 (m, 2H), 4.91 (s, 1H), 4.36 (s, 1H), 4.17 (s, 1H), 3.62 (d, *J* = 13.8 Hz, 1H), 3.54 (d, *J* = 13.8 Hz, 1H), 2.76 – 2.48 (m, 4H), 1.99 (d, *J* = 6.2 Hz, 1H), 1.76 (br, 1H), 1.57 (s, 3H), 1.39 (m, 15H), 1.32 (s, 3H). ^{13}C NMR (101 MHz, $CDCl_3$) δ 171.6, 166.6, 155.4, 152.9, 149.0, 144.8, 140.0, 139.5, 135.4, 131.6, 128.8, 128.0, 127.0, 125.5, 114.2, 90.7, 85.6, 83.9, 83.4, 81.7, 79.4, 70.7, 58.9, 58.2, 55.9, 52.7, 50.9, 50.6, 36.5, 29.7, 28.3, 28.2, 28.0, 27.9, 27.1, 25.3. HRMS (ESI): calculated for $C_{53}H_{61}N_8O_8$ $[M+H]^+$ 939.4749, found 939.4784.

3-(((((3a*R*,4*R*,6*R*,6a*R*)-6-(6-amino-9*H*-purin-9-yl)-2,2-dimethyltetrahydrofuro[3,4-d][1,3]dioxol-4-yl)methyl)(*iso*propyl)amino)methyl)-*N*-tritylbenzamide (38). Following the procedure described for compound **33**, coupling 5 mL dry acetone (large excess) and compound **29** (100 mg, 0.15 mmol) afforded compound **38** as a white powder (68 mg, 63% yield). ^{1}H NMR (400 MHz, $CDCl_3$) δ 8.22 (s, 1H), 7.75 (s, 1H), 7.60 (d, *J* = 10.4 Hz, 2H), 7.49 – 7.40 (m, 2H), 7.33 – 7.21 (m, 15H), 5.91 (s, 1H), 5.34 (m, 2H), 4.92 – 4.87 (m, 1H), 4.23 (d, *J* = 3.2 Hz, 1H), 3.57 (s, 2H), 2.92 – 2.83 (m, 1H), 2.76 – 2.68 (m, 1H), 2.59 (m, 1H), 1.49 (s, 3H), 1.25 (s, 3H), 1.01 (d, *J* = 6.6 Hz, 3H), 0.90 (d, *J* = 6.6 Hz, 3H). ^{13}C NMR (101 MHz, $CDCl_3$) δ 166.7, 155.7, 152.9, 149.0, 144.8, 141.4, 139.9, 135.2, 131.4, 128.7, 128.3, 128.0, 127.1, 125.4, 120.2, 114.0, 90.9, 86.5, 83.7, 83.3, 70.7, 54.4, 51.8, 50.5, 27.1, 25.4, 18.7, 17.2. HRMS (ESI): calculated for $C_{43}H_{45}N_7O_4$ $[M+H]^+$ 724.3611, found 724.3618.

Methyl 3-(((((3a*R*,4*R*,6*R*,6a*R*)-6-(6-amino-9*H*-purin-9-yl)-2,2-dimethyltetrahydrofuro-[3,4-d][1,3]dioxol-4-yl)methyl)(4-oxo-4-(tritylamino)butyl)amino)methyl)benzoate (39). Following the procedure described for compound **33**, coupling 4-oxo-N-tritylbutanamide **16** (62 mg, 0.18 mmol) and compound **30** (68 mg, 0.15 mmol) afforded compound **39** as a white powder (63 mg, 54% yield). ^{1}H NMR (400 MHz, $CDCl_3$) δ 8.17 (s, 1H), 7.90 (s, 1H), 7.84 – 7.79 (m, 1H), 7.77 (s, 1H), 7.40 (d, *J* = 7.7 Hz, 1H), 7.31 – 7.08 (m, 17H), 6.60 (s, 1H), 5.97 (d, *J* = 2.2 Hz, 1H), 5.67 (s, 2H), 5.34 (m, 1H), 4.86 (m, 1H), 4.34 (m, 1H), 3.85 (s, 3H), 3.57 (m, 2H), 2.74 – 2.62 (m, 2H), 2.45 (t, *J* = 7.0 Hz, 2H), 2.31-2.16 (m, 2H), 1.75 (m, 2H), 1.53 (s, 3H), 1.32 (s, 3H). ^{13}C NMR (101 MHz, $CDCl_3$) δ 171.5, 167.0, 155.4, 153.0, 149.1, 144.7, 139.9, 139.6, 133.3, 129.9, 129.7, 128.7, 128.2, 128.1, 127.9, 127.0, 126.9, 120.2, 114.2, 90.8, 85.4, 83.7, 83.4, 70.4, 58.5, 55.7, 53.6, 52.1, 34.9, 27.0, 25.2, 22.7. HRMS (ESI): calculated for $C_{45}H_{48}N_7O_6$ $[M+H]^+$ 782.3666, found 782.3666.

Methyl 3-(((((3a*R*,4*R*,6*R*,6a*R*)-6-(6-amino-9*H*-purin-9-yl)-2,2-dimethyltetrahydrofuro-[3,4-d][1,3]dioxol-4-yl)methyl)(5-oxo-5-(tritylamino)pentyl)amino)methyl)benzoate (40). Following the procedure described for compound **33**, coupling 5-oxo-*N*-tritylpentanamide **17** (64 mg, 0.18 mmol) and compound **30** (68 mg, 0.15 mmol) afforded compound **40** as a white powder (67 mg, 53% yield). ^{1}H NMR (400 MHz, $CDCl_3$) δ 8.17 (s, 1H), 7.89 (s, 1H), 7.83 (d, *J* = 7.8 Hz, 1H), 7.76 (s, 1H), 7.44 (d, *J* = 7.6 Hz, 1H), 7.26-7.17 (m, 14H), 6.69 (s, 1H), 6.35 (br, 2H), 5.99 (d, *J* = 1.8 Hz, 1H), 5.39 (m, 1H), 4.90 (m, 1H), 4.36 (m, 1H), 3.83 (s, 3H), 3.62 – 3.48 (m, 2H), 2.65 (m, 2H), 2.41 (t, *J* = 6.9 Hz, 2H), 2.14 (p, *J* = 8.2 Hz, 2H), 1.56 (s, 3H), 1.33 (s, 3H). ^{13}C NMR (101 MHz, $CDCl_3$) δ 171.7, 167.1, 155.8, 152.9, 149.1, 144.8, 139.9, 139.8, 133.4, 129.9, 129.8, 128.7, 128.2, 128.2, 127.9, 126.9, 114.1, 90.8, 85.6, 83.7, 83.4, 70.4, 58.5, 55.8, 53.8, 52.1, 37.1, 27.1, 26.3, 25.3, 23.1. HRMS (ESI): calculated for $C_{46}H_{49}N_7O_6$ $[M+H]^+$ 796.3823, found 796.3814.

Methyl 3-(((((3a*R*,4*R*,6*R*,6a*R*)-6-(6-amino-9*H*-purin-9-yl)-2,2-dimethyltetrahydrofu ro-[3,4-d][1,3]dioxol-4-yl)methyl)(4-(*tert*-butoxy)-4-oxobutyl)amino)methyl)benzoate (41). Following the procedure described for compound **33**, coupling *tert*-butyl 4-oxobutanoate **22** (29 mg, 0.18 mmol) and compound **30** (68 mg, 0.15 mmol) afforded compound **41** as a white powder (65 mg, 73% yield). ^{1}H NMR (400 MHz, $CDCl_3$) δ 8.13 (s, 1H), 7.85 (s, 1H), 7.80 (d, *J* = 8.1 Hz, 2H), 7.41 (d, *J* = 7.6 Hz, 1H), 7.23 (t, *J* = 7.6 Hz, 1H), 6.47 (s, 2H), 5.98 (d, *J* = 1.9 Hz, 1H), 5.33 (d, *J* = 6.4 Hz, 1H), 4.87 (m, 1H), 4.30 (m, 1H), 3.84 (s, 3H), 3.61-3.48(m, 2H), 2.75 – 2.69 (m, 2H), 2.43 (m, 2H), 2.16-2.10 (m, 2H), 1.53 (s, 3H), 1.39 – 1.30 (m, 15H). ^{13}C NMR (101 MHz, $CDCl_3$) δ 172.8, 167.0, 155.8, 152.9, 148.9, 139.7, 139.6, 133.3, 129.9, 129.7, 128.2, 128.1, 120.0, 114.1, 114.1, 90.7, 85.4, 83.7, 83.3, 80.0, 61.6, 61.1, 58.6, 55.6, 53.4, 52.0,

32.9, 32.3, 28.0, 27.5, 27.0, 25.3, 22.3. HRMS (ESI): calculated for $C_{30}H_{40}N_6O_7$ $[M+H]^+$ 597.3037, found 597.3037.

Methyl 3-(((((3a*R*,4*R*,6*R*,6a*R*)-6-(6-amino-9*H*-purin-9-yl)-2,2-dimethyltetrahydrofuro-[3,4-d][1,3]dioxol-4-yl)methyl)(5-(*tert*-butoxy)-5-oxopentyl)amino)methyl)benzoate (42). Following the procedure described for compound **33**, coupling *tert*-butyl 5-oxopentanoate **23** (31 mg, 0.18 mmol) and compound **30** (68 mg, 0.15 mmol) afforded compound **42** as a white powder (56 mg, 61% yield). ^{1}H NMR (400 MHz, $CDCl_3$) δ 8.12 (s, 1H), 7.84 (s, 1H), 7.79 (d, *J* = 7.8 Hz, 2H), 7.39 (d, *J* = 7.5 Hz, 1H), 7.21 (t, *J* = 7.7 Hz, 1H), 6.52 (s, 2H), 5.97 (s, 1H), 5.36 – 5.30 (m, 1H), 4.86 (m, 1H), 4.33 – 4.26 (m, 1H), 3.82 (s, 3H), 3.58 (d, *J* = 13.8 Hz, 1H), 3.47 (d, *J* = 13.7 Hz, 1H), 2.69-2.56 (m, 2H), 2.43 – 2.35 (m, 2H), 2.07 (t, *J* = 6.8 Hz, 2H), 1.52 (s, 3H), 1.48 – 1.42 (m, 2H), 1.34 (s, 9H), 1.30 (s, 3H). ^{13}C NMR (101 MHz, $CDCl_3$) δ 172.8, 167.0, 155.8, 152.9, 149.0, 139.7, 139.7, 133.3, 129.9, 129.7, 128.2, 128.1, 128.1, 120.1, 114.1, 90.8, 85.5, 83.6, 83.5, 83.3, 79.9, 58.6, 55.6, 53.9, 52.0, 35.2, 28.0, 27.1, 26.2, 25.3, 22.7. HRMS (ESI): calculated for $C_{31}H_{42}N_6O_7$ $[M+H]^+$ 611.3193, found 611.3182.

Methyl 3-(((((3a*R*,4*R*,6*R*,6a*R*)-6-(6-amino-9*H*-purin-9-yl)-2,2-dimethyltetrahydrofuro-[3,4-d][1,3]dioxol-4-yl)methyl)((*S*)-4-(*tert*-butoxy)-2-((*tert*-butoxycarbonyl)amino)-4-oxobutyl)amino)methyl)benzoate (43). Following the procedure described for compound **33**, coupling *tert*-butyl (*R*)-2-((*tert*-butoxycarbonyl)amino)-4-oxobutanoate **27** (49 mg, 0.18 mmol) and compound **30** (68 mg, 0.15 mmol) afforded compound **43** as a white powder (62 mg, 58% yield). ^{1}H NMR (400 MHz, $CDCl_3$) δ 8.19 (s, 1H), 7.87 (d, *J* = 6.5 Hz, 2H), 7.82 (s, 1H), 7.48 (d, *J* = 7.7 Hz, 1H), 7.30 (t, *J* = 7.9 Hz, 1H), 6.01 (s, 1H), 5.73 (s, 2H), 5.38 (m, 2H), 4.89 (m, 1H), 4.35 (m, 1H), 4.20 – 4.11 (m, 1H), 3.90 (s, 3H), 3.71-3.52 (m, 2H), 2.78 (m, 1H), 2.65 (m, 2H), 2.51 (m, 1H), 1.96 (s, 2H), 1.76 (m, 1H), 1.59 (s, 3H), 1.40 (m, 18H), 1.37 (s, 3H). ^{13}C NMR (101 MHz, $CDCl_3$) δ 171.6, 167.0, 155.4, 155.4, 153.0, 149.1, 139.9, 139.2, 133.4, 130.0, 129.8, 128.4, 128.3, 120.3, 114.3, 90.7, 85.3, 83.8, 83.3, 81.7, 79.4, 58.6, 55.7, 52.7, 52.1, 50.5, 29.5, 28.3, 27.9, 27.1, 25.3. HRMS (ESI): calculated for $C_{35}H_{49}N_7O_9$ $[M+H]^+$ 712.3670, found 712.3682.

Methyl 3-(((((3a*R*,4*R*,6*R*,6a*R*)-6-(6-amino-9*H*-purin-9-yl)-2,2-dimethyltetrahydrofuro-[3,4-d][1,3]dioxol-4-yl)methyl)(*iso*propyl)amino)methyl)benzoate (44). Following the procedure described for compound **33**, coupling dry acetone (5 mL, large excess) and compound **30** (68 mg, 0.15 mmol) afforded compound **44** as a white powder (42 mg, 57% yield). ^{1}H NMR (400 MHz, $CDCl_3$) δ 8.22 (s, 1H), 7.94 (s, 1H), 7.84 (d, *J* = 7.7 Hz, 1H), 7.77 (s, 1H), 7.52 (d, *J* = 7.6 Hz, 1H), 7.29 (t, *J* = 7.7 Hz, 1H), 5.96 (d, *J* = 2.4 Hz, 2H), 5.36 (dd, *J* = 6.4, 2.4 Hz, 1H), 4.87 (dd, *J* = 6.4, 3.0 Hz, 1H), 4.26 – 4.20 (m, 1H), 3.88 (s, 3H), 3.62 (d, *J* = 14.2 Hz, 1H), 3.54 (d, *J* =

14.2 Hz, 1H), 2.88 (p, *J* = 6.6 Hz, 1H), 2.73-2.59(m, 2H), 1.53 (s, 3H), 1.33 (s, 3H). ^{13}C NMR (101 MHz, Chloroform-*d*) δ 167.1, 155.6, 152.9, 149.2, 141.0, 139.9, 133.2, 129.9, 129.6, 128.1, 128.1, 120.2, 114.0, 91.0, 86.1, 83.5, 83.2, 60.3, 54.3, 52.0, 51.4, 50.3, 27.1, 25.3, 21.0, 18.9, 16.8, 14.2. HRMS (ESI): calculated for $C_{35}H_{32}N_6O_5$ $[M+H]^+$ 497.2512, found 497.2510.

tert-Butyl 3-(((((3a*R*,4*R*,6*R*,6a*R*)-6-(6-amino-9*H*-purin-9-yl)-2,2-dimethyltetrahydrofuro-[3,4-d][1,3]dioxol-4-yl)methyl)(4-oxo-4-(tritylamino)butyl)amino)methyl)benzoate (45). Following the procedure described for compound **33**, coupling 4-oxo-*N*-tritylbutanamide **16** (62 mg, 0.18 mmol) and compound **31** (75 mg, 0.15 mmol) afforded compound **45** as a white powder (93 mg, 75% yield). ^{1}H NMR (400 MHz, $CDCl_3$) δ 8.23 (s, 1H), 7.90 (s, 1H), 7.84 – 7.79 (m, 2H), 7.43 (d, *J* = 7.6 Hz, 1H), 7.31 – 7.16 (m, 17H), 6.68 (s, 1H), 6.07 (s, 2H), 6.01 (d, *J* = 2.2 Hz, 1H), 5.39 (m, 1H), 4.89 (m, 1H), 4.37 (m, 1H), 3.66 (d, *J* = 13.9 Hz, 1H), 3.55 (d, *J* = 13.9 Hz, 1H), 2.76 (m, 1H), 2.66 (m, 1H), 2.47 (t, *J* = 6.8 Hz, 2H), 2.28 (m, 2H), 1.77 (m, 2H), 1.59 (s, 9H), 1.56 (s, 3H), 1.35 (s, 3H). ^{13}C NMR (101 MHz, $CDCl_3$) δ 171.6, 165.7, 155.6, 153.0, 149.1, 144.8, 139.7, 139.4, 132.8, 131.9, 129.6, 128.7, 128.1, 128.0, 127.9, 126.9, 120.2, 114.2, 90.8, 85.4, 83.6, 83.4, 80.9, 70.4, 58.6, 55.7, 53.6, 34.9, 28.2, 27.1, 25.3, 22.7. HRMS (ESI): calculated for $C_{49}H_{53}N_7O_6$ $[M+H]^+$ 824.4136, found 824.4123.

tert-Butyl-3-(((((3a*R*,4*R*,6*R*,6a*R*)-6-(6-amino-9*H*-purin-9-yl)-2,2-dimethyltetrahydrofuro-[3,4-d][1,3]dioxol-4-yl)methyl)(5-oxo-5-(tritylamino)pentyl)amino)methyl)benzoate (46). Following the procedure described for compound **33**, coupling 5-oxo-*N*-tritylpentanamide **17** (64 mg, 0.18 mmol) and compound **31** (75 mg, 0.15 mmol) afforded compound **46** as a white powder (97 mg, 77% yield). ^{1}H NMR (400 MHz, $CDCl_3$) δ 8.23 (d, *J* = 7.6 Hz, 1H), 7.90 (d, *J* = 9.6 Hz, 1H), 7.85 – 7.79 (m, 2H), 7.47 (d, *J* = 7.7 Hz, 1H), 7.32 – 7.15 (m, 16H), 6.71 (d, *J* = 8.4 Hz, 1H), 6.35 (d, *J* = 14.9 Hz, 2H), 6.03 (d, *J* = 2.1 Hz, 1H), 5.43 (m, 1H), 4.93 (m, 1H), 4.41-4.37 (m, 1H),, 3.65 (d, *J* = 13.8 Hz, 1H), 3.54 (d, *J* = 13.8 Hz, 1H), 2.75 -2.62 (m, 1H), 2.48 – 2.39 (m, 2H), 2.16 (t, *J* = 7.2 Hz, 2H), 1.59 (s, 12H), 1.45 – 1.37 (m, 2H), 1.36 (s, 3H). ^{13}C NMR (101 MHz, $CDCl_3$) δ 171.7, 165.8, 155.8, 153.0, 149.1, 144.8, 144.8, 139.9, 139.6, 132.9, 131.8, 129.7, 128.7, 128.2, 128.1, 128.0, 128.0, 127.9, 126.9, 120.2, 114.1, 90.9, 90.8, 85.6, 83.7, 83.6, 83.4, 80.9, 70.4, 58.6, 58.6, 55.7, 53.8, 53.6, 37.1, 34.9, 28.2, 27.1, 27.1, 26.3, 25.3, 25.3, 23.1, 22.7. HRMS (ESI): calculated for $C_{49}H_{55}N_7O_6$ $[M+H]^+$ 838.4292, found 838.4314.

tert-Butyl-3-(((((3a*R*,4*R*,6*R*,6a*R*)-6-(6-amino-9*H*-purin-9-yl)-2,2-dimethyltetrahydrofuro-[3,4-d][1,3]dioxol-4-yl)methyl)(4-(*tert*-butoxy)-4-oxobutyl)amino)methyl)benzoate (47). Following the procedure described for compound **33**, coupling *tert*-butyl 4-oxobutanoate **22** (29 mg, 0.18 mmol) and compound **31** (75 mg, 0.15 mmol) afforded compound **47** as a white powder (64 mg, 67% yield). ^{1}H NMR (400 MHz, $CDCl_3$) δ 8.21 (s, 1H), 7.86 – 7.77 (m, 3H), 7.42 (d, *J*

= 7.6 Hz, 1H), 7.26 (d, *J* = 7.7 Hz, 1H), 6.15 (s, 2H), 5.99 (d, *J* = 2.2 Hz, 1H), 5.36 (m, 1H), 4.88 (m, 1H), 4.32 (m, 1H), 3.65 (d, *J* = 13.8 Hz, 1H), 3.50 (d, *J* = 13.8 Hz, 1H), 2.78-2.73 (m, 1H), 2.64-2.59 (m,1H), 2.42 (m, 2H), 2.22 – 2.09 (m, 2H), 1.55 (s, 12H), 1.36 (s, 9H), 1.33 (s, 3H). ^{13}C NMR (101 MHz, $CDCl_3$) δ 172.8, 165.7, 155.7, 153.0, 149.1, 139.8, 139.5, 132.8, 131.8, 129.6, 128.1, 128.0, 120.2, 114.2, 90.8, 85.5, 83.7, 83.3, 80.8, 80.0, 58.7, 55.6, 53.4, 33.0, 28.2, 28.0, 27.1, 25.3, 22.4. HRMS (ESI): calculated for $C_{33}H_{46}N_6O_7$ $[M+H]^+$ 639.3506, found 639.3506.

tert-Butyl-3-(((((3a*R*,4*R*,6*R*,6a*R*)-6-(6-amino-9*H*-purin-9-yl)-2,2-dimethyltetrahydrofuro-[3,4-d][1,3]dioxol-4-yl)methyl)(5-(*tert*-butoxy)-5-oxopentyl)amino)methyl)benzoate (48). Following the procedure described for compound **33**, coupling *tert*-butyl 5-oxopentanoate **23** (31 mg, 0.18 mmol) and compound **31** (75 mg, 0.15 mmol) afforded compound **48** as a white powder (72 mg, 73% yield). ^{1}H NMR (400 MHz, $CDCl_3$) δ 8.20 (s, 1H), 7.84 – 7.77 (m, 3H), 7.42 (d, *J* = 7.6 Hz, 1H), 7.24 (t, *J* = 7.6 Hz, 1H), 6.19 (s, 2H), 5.99 (d, *J* = 2.2 Hz, 1H), 5.37 (m, 1H), 4.88 (m, 1H), 4.35 – 4.30 (m, 1H), 3.65 -3.48 1H), 2.71-2.59 (m, 1H), 2.46 – 2.38 (m, 2H), 2.10 (t, *J* = 7.1 Hz, 2H), 1.55 (s, 12H), 1.44 (m, 2H), 1.37 (s, 9H), 1.33 (s, 3H). ^{13}C NMR (101 MHz, $CDCl_3$) δ 172.9, 165.7, 155.7, 153.0, 149.1, 139.7, 139.5, 132.9, 131.8, 129.6, 128.0, 128.0, 120.2, 114.1, 90.8, 85.5, 83.6, 83.3, 80.8, 79.9, 58.7, 55.6, 53.9, 35.2, 28.2, 28.1, 27.1, 26.2, 25.3, 22.7. HRMS (ESI): calculated for $C_{34}H_{48}N_6O_7$ $[M+H]^+$ 653.3663, found 653.3669.

tert-Butyl-3-(((((3a*R*,4*R*,6*R*,6a*R*)-6-(6-amino-9*H*-purin-9-yl)-2,2-dimethyltetrahydrofuro-[3,4-d][1,3]dioxol-4-yl)methyl)((*S*)-4-(*tert*-butoxy)-3-((*tert*-butoxycarbonyl)amino)-4 oxobutyl)amino)methyl)benzoate (49). Following the procedure described for compound **33**, coupling *tert*-butyl (*R*)-2-((*tert*-butoxycarbonyl)amino)-4-oxobutanoate **27** (49 mg, 0.18 mmol) and compound **31** (75 mg, 0.15 mmol) afforded compound **49** as a white powder (85 mg, 75% yield). ^{1}H NMR (400 MHz, $CDCl_3$) δ 8.18 (s, 1H), 7.79 (d, *J* = 6.7 Hz, 3H), 7.44 (s, 1H), 7.28 – 7.23 (m, 1H), 6.20 (s, 2H), 5.99 (s, 1H), 5.50 – 5.43 (m, 1H), 5.34 (d, *J* = 5.6 Hz, 1H), 4.86 (m, 1H), 4.31 (m, 1H), 4.15 – 4.07 (m, 1H), 3.67 (br, 1H), 3.47 (br, 1H), 2.76 (br, 2H), 2.59 (m, 2H), 2.44 (m, 2H), 1.93 (m, 1H), 1.73 (m, 1H), 1.54 (s, 12H), 1.35 (m, 21H). ^{13}C NMR (101 MHz, $CDCl_3$) δ 171.6, 165.6, 155.7, 155.7, 155.3, 153.0, 149.1, 139.8, 139.0, 132.9, 131.8, 129.6, 128.2, 128.2, 120.2, 114.3, 90.6, 85.3, 83.7, 83.3, 81.6, 80.9, 79.3, 58.8, 55.7, 52.7, 50.5, 29.4, 28.3, 28.2, 27.9, 27.1, 25.4. HRMS (ESI): calculated for $C_{38}H_{55}N_7O_9$ $[M+H]^+$ 754.4140, found 754.4129.

tert-Butyl 3-(((((3a*R*,4*R*,6*R*,6a*R*)-6-(6-amino-9*H*-purin-9-yl)-2,2-dimethyltetrahydrofuro [3,4-d][1,3]dioxol-4-yl)methyl)(isopropyl)amino)methyl)benzoate (50). Following the procedure described for compound **33**, coupling 5 mL dry acetone (large excess) and compound **31** (75 mg,

0.15 mmol) afforded compound 50 as a white powder (85 mg, 79% yield). ^{1}H NMR (400 MHz, $CDCl_3$) δ 8.26 (s, 1H), 7.90 (s, 1H), 7.80 (m, 2H), 7.51 (d, *J* = 7.6 Hz, 1H), 7.28 (t, *J* = 7.7 Hz, 1H), 5.97 (d, *J* = 2.4 Hz, 1H), 5.92 (s, 2H), 5.37 (m, 1H), 4.86 (m, 1H), 4.26 – 4.20 (m, 1H), 3.64 (br, 1H), 3.54 (br, 1H), 2.87 (m, 1H), 2.73-2.56 (br, 2H), 1.57 (s, 9H), 1.53 (s, 3H), 1.33 (s, 3H), 1.03 (d, *J* = 6.6 Hz, 3H), 0.89 (d, *J* = 6.5 Hz, 3H). ^{13}C NMR (101 MHz, CDCl3-*d*) δ 165.8, 155.5, 153.0, 149.2, 140.8, 139.9, 132.7, 131.8, 129.4, 128.0, 127.9, 120.2, 114.0, 91.0, 86.1, 83.4, 83.2, 80.8, 54.5, 51.3, 50.4, 28.2, 27.1, 25.3, 19.0, 16.7. HRMS (ESI): calculated for $C_{28}H_{38}N_6O_5$ $[M+H]^+$ 539.2982, found 539.2982.

4-((((3a*R*,4*R*,6*R*,6a*R*)-6-(6-amino-9*H*-purin-9-yl)-2,2-dimethyltetrahydrofuro[3,4-d][1,3]dioxol-4-yl)methyl)(naphthalen-2-ylmethyl)amino)-*N*-tritylbutanamide (51). Following the procedure described for compound **33**, coupling 4-oxo-*N*-tritylbutanamide **16** (62 mg, 0.18 mmol) and compound **32** (67 mg, 0.15 mmol) afforded compound **51** as a white powder (85 mg, 73% yield). ^{1}H NMR (400 MHz, $CDCl_3$) δ 8.10 (s, 1H), 7.79 – 7.73 (m, 2H), 7.72 – 7.66 (m, 2H), 7.61 (s, 1H), 7.46 – 7.38 (m, 3H), 7.28 – 7.12 (m, 15H), 6.59 (s, 1H), 5.97 (d, *J* = 2.2 Hz, 1H), 5.81 (s, 2H), 5.30 (m, 1H), 4.83 (m, 1H), 4.38 (s, 1H), 3.77 (d, *J* = 13.7 Hz, 1H), 3.63 (d, *J* = 13.7 Hz, 1H), 2.78-2.64 (m, 2H), 2.51 (t, *J* = 6.9 Hz, 2H), 2.30 – 2.20 (m, 2H), 1.79 (m, 2H), 1.52 (s, 3H), 1.31 (s, 3H). ^{13}C NMR (101 MHz, $CDCl_3$) δ 171.6, 155.5, 153.0, 144.8, 139.7, 136.6, 133.2, 132.7, 128.7, 127.9, 127.8, 127.6, 127.6, 127.4, 127.2, 126.9, 126.0, 125.6, 114.2, 90.8, 85.4, 83.7, 83.4, 70.4, 59.1, 55.8, 53.8, 35.0, 27.0, 25.3, 22.8. HRMS (ESI): calculated for $C_{47}H_{47}N_7O_4$ $[M+H]^+$ 774.3768, found 774.3769.

5-((((3a*R*,4*R*,6*R*,6a*R*)-6-(6-amino-9H-purin-9-yl)-2,2-dimethyltetrahydrofuro[3,4-d][1,3]dioxol-4-yl)methyl)(naphthalen-2-ylmethyl)amino)-*N*-tritylpentanamide (52). Following the procedure described for compound **33**, coupling 5-oxo-*N*-tritylpentanamide **17** (64 mg, 0.18 mmol) and compound **32** (67 mg, 0.15 mmol) afforded compound **52** as a white powder (85 mg, 64% yield). ^{1}H NMR (400 MHz, $CDCl_3$) δ 8.12 (s, 1H), 7.84 – 7.55 (m, 5H), 7.42 (m, 3H), 7.28-7.16 (m, 14H), 6.57 (s, 1H), 5.98 (s, 1H), 5.76 (s, 2H), 5.35 (d, *J* = 6.3 Hz, 1H), 4.88 (d, *J* = 6.2 Hz, 1H), 4.39 (s, 1H), 3.75 (d, *J* = 13.6 Hz, 1H), 3.62 (d, *J* = 13.6 Hz, 1H), 2.77 – 2.62 (m, 2H), 2.52 – 2.37 (m, 2H), 2.16-2.09 (m, 2H), 1.56 (s, 3H), 1.45-1.38 (m, 2H), 1.32 (s, 3H). ^{13}C NMR (101 MHz, $CDCl_3$) δ 171.7, 155.4, 152.9, 149.2, 144.8, 139.9, 136.8, 133.2, 132.7, 128.7, 128.4, 127.9, 127.8, 127.6, 127.4, 127.2, 127.0, 125.9, 125.5, 120.2, 114.1, 90.9, 85.7, 83.7, 83.5, 70.4, 59.1, 55.8, 53.8, 37.2, 27.1, 26.3, 25.3, 23.2. HRMS (ESI): calculated for $C_{48}H_{49}N_7O_4$ $[M+H]^+$ 788.3924, found 788.3932.

***tert*-Butyl-4-((((3a*R*,4*R*,6*R*,6a*R*)-6-(6-amino-9*H*-purin-9-yl)-2,2-dimethyltetrahydrofuro-[3,4-d][1,3]dioxol-4-yl)methyl)(naphthalen-2-ylmethyl)amino)butanoate (53).** Following the

procedure described for compound **33**, coupling *tert*-butyl 4-oxobutanoate **22** (29 mg, 0.18 mmol) and compound **32** (67 mg, 0.15 mmol) afforded compound **53** as a white powder (67 mg, 76% yield). ^{1}H NMR (400 MHz, $CDCl_3$) δ 8.12 (s, 1H), 7.82 (s, 1H), 7.78 – 7.60 (m, 4H), 7.48 – 7.35 (m, 3H), 6.74 (s, 2H), 6.02 (s, 1H), 5.34 (m, 1H), 4.89 (m, 1H), 4.38 (m, 1H), 3.79 (d, *J* = 13.6 Hz, 1H), 3.60 (d, *J* = 13.6 Hz, 1H), 2.80 (m, 1H), 2.65 (m, 1H), 2.57-2.44 (m, 2H), 2.29-2.13 (m, 2H), 1.75 (p, *J* = 7.3 Hz, 2H), 1.57 (s, 3H), 1.40 – 1.08 (m, 12H). ^{13}C NMR (101 MHz, $CDCl_3$) δ 172.9, 156.0, 152.9, 152.9, 149.0, 139.6, 136.7, 133.2, 132.7, 127.8, 127.6, 127.3, 127.2, 125.9, 125.5, 120.1, 114.1, 90.8, 85.5, 83.7, 83.5, 80.0, 59.2, 55.7, 53.6, 33.0, 28.0, 27.5, 27.1, 25.4, 22.4. HRMS (ESI): calculated for $C_{32}H_{40}N_6O_5$ $[M+H]^+$ 589.3138, found 589.3143.

tert-Butyl-5-((((3a*R*,4*R*,6*R*,6a*R*)-6-(6-amino-9*H*-purin-9-yl)-2,2-dimethyltetrahydrofuro-[3,4-d][1,3]dioxol-4-yl)methyl)(naphthalen-2-ylmethyl)amino)pentanoate (54). Following the procedure described for compound **33**, coupling *tert*-butyl 5-oxopentanoate **23** (31 mg, 0.18 mmol) and compound **32** (67 mg, 0.15 mmol) afforded compound **54** as a white powder (62 mg, 69% yield). ^{1}H NMR (400 MHz, $CDCl_3$) δ 8.11 (s, 1H), 7.80 (d, *J* = 24.4 Hz, 2H), 7.73 (d, *J* = 8.4 Hz, 2H), 7.64 (s, 1H), 7.47 – 7.38 (m, 3H), 6.42 (s, 2H), 6.02 (s, 1H), 5.34 (d, *J* = 6.3 Hz, 1H), 4.90 (m, 1H), 4.42 – 4.36 (m, 1H), 3.80 (d, *J* = 13.6 Hz, 1H), 3.62 (d, *J* = 13.6 Hz, 1H), 2.77 (m, 1H), 2.70 – 2.62 (m, 1H), 2.54 (s, 2H), 2.15 (t, *J* = 6.7 Hz, 2H), 1.58 (s, 3H), 1.48 (d, *J* = 9.8 Hz, 2H), 1.41 (s, 9H), 1.35 (s, 3H). ^{13}C NMR (101 MHz, $CDCl_3$) δ 172.9, 155.8, 152.9, 149.1, 139.7, 136.8, 133.2, 132.7, 127.7, 127.6, 127.5, 127.3, 127.2, 125.9, 125.5, 120.2, 114.1, 90.9, 85.5, 83.7, 83.6, 83.4, 79.9, 59.1, 55.7, 54.1, 35.3, 28.1, 28.0, 27.1, 26.3, 25.3, 22.8. HRMS (ESI): calculated for $C_{33}H_{42}N_6O_5$ $[M+H]^+$ 603.3295, found 603.3311.

tert-Butyl-(*R*)-4-((((3a*R*,4*R*,6*R*,6a*R*)-6-(6-amino-9*H*-purin-9-yl)-2,2-dimethyltetrahydrofuro-[3,4-d][1,3]dioxol-4-yl)methyl)(naphthalen-2-ylmethyl)amino)-2-((*tert*-butoxycarbonyl)amino)butanoate (55). Following the procedure described for compound **33**, coupling *tert*-butyl (*R*)-2-((*tert*-butoxycarbonyl)amino)-4-oxobutanoate **27** (49 mg, 0.18 mmol) and compound **32** (67 mg, 0.15 mmol) afforded compound **55** as a white powder (72 mg, 68% yield). ^{1}H NMR (400 MHz, $CDCl_3$) δ 8.08 (s, 1H), 7.87 – 7.67 (m, 4H), 7.61 (s, 1H), 7.54-7.39 (m, 3H), 6.27 (d, *J* = 11.3 Hz, 2H), 6.00 (s, 1H), 5.71 – 5.61 (m, 1H), 5.30 (d, *J* = 5.1 Hz, 1H), 4.84 (m, 1H), 4.39 – 4.34 (m, 1H), 4.23 – 4.14 (m, 1H), 3.84 (d, *J* = 13.5 Hz, 1H), 3.59 (d, *J* = 13.5 Hz, 1H), 2.82 (br, 2H), 2.65 (br, 2H), 2.57-2.51 (m, 1H), 2.06 – 1.94 (m, 1H), 1.86 – 1.78 (m, 1H), 1.57 (s, 3H), 1.50-1.18 (m, 21H). ^{13}C NMR (101 MHz, $CDCl_3$) δ 171.7, 155.4, 152.9, 149.0, 139.7, 136.2, 133.2, 132.7, 127.9, 127.6, 127.6, 127.5, 127.2, 127.1, 125.9, 125.6, 120.1, 114.3, 90.7, 85.3, 83.7, 83.4, 81.6, 79.3, 59.2, 55.7, 52.9, 50.8, 29.4, 28.3, 27.9, 27.9, 27.1, 25.4. HRMS (ESI): calculated for $C_{33}H_{42}N_6O_5$ $[M+H]^+$ 704.3772, found 704.3777.

9-((3a*R*,4*R*,6*R*,6a*R*)-6-((*iso*propyl(naphthalen-2-ylmethyl)amino)methyl)-2,2-dimethyltetrahydrofuro[3,4-d][1,3]dioxol-4-yl)-9*H*-purin-6-amine (56). Following the procedure described for compound **33**, coupling 5 mL dry acetone (large excess) and compound **32** (67 mg, 0.15 mmol) afforded compound **56** as a white powder (35 mg, 48% yield). ^{1}H NMR (400 MHz, $CDCl_3$) δ 8.21 (s, 1H), 7.83 – 7.68 (m, 5H), 7.53 (m, 1H), 7.47 – 7.39 (m, 2H), 6.26 (s, 2H), 5.98 (d, *J* = 2.3 Hz, 1H), 5.32 (m, 1H), 4.85 (m, 1H), 4.32-4.27 (m, 1H), 3.79 (d, *J* = 13.9 Hz, 1H), 3.64 (d, *J* = 14.0 Hz, 1H), 3.00-2.93 (m, 1H), 2.78 (m 1H), 2.64 (m, 1H), 1.53 (s, 3H), 1.31 (s, 3H), 1.09 (d, *J* = 6.6 Hz, 3H), 0.95 (d, *J* = 6.6 Hz, 3H). ^{13}C NMR (101 MHz, $CDCl_3$) δ 155.7, 152.9, 149.1, 139.7, 138.0, 133.2, 132.7, 127.7, 127.6, 127.5, 127.2, 127.0, 125.9, 125.4, 120.2, 113.9, 91.1, 86.2, 83.5, 83.3, 77.3, 54.9, 51.4, 50.4, 27.0, 25.3, 19.2, 16.6. HRMS (ESI): calculated for $C_{27}H_{32}N_6O_3$ $[M+H]^+$ 489.2614, found 489.2611.

3-(((4-Amino-4-oxobutyl)(((2*R*,3*S*,4*R*,5*R*)-5-(6-amino-9*H*-purin-9-yl)-3,4-dihydroxytetrahydrofuran-2-yl)methyl)amino)methyl)benzamide (57). To a solution of compound **33** (100 mg, 0.098 mmol) in 5 mL CH_2Cl_2 was added 5 mL TFA and the mixture was stirred at room temperature. After 2 hours, 2 mL H_2O was added and the mixture was stirred for 1 hour at room temperature. The mixture was concentrated and the crude product was purified by preparative HPLC affording compound **57** as a white powder. ^{1}H NMR (400 MHz, D_2O) δ 8.46 – 8.06 (m, 2H), 7.87 – 7.26 (m, 4H), 6.08 (br, 1H), 4.75 – 4.36 (m, 4H), 4.27 (br, 1H), 3.84 – 3.27 (m, 4H), 2.38 (br, 2H), 2.10 (br, 2H). ^{13}C NMR (101 MHz, D_2O) δ 177.5, 162.8, 162.5, 149.6, 143.8, 134.8, 134.1, 132.7, 129.6, 129.1, 128.3, 118.9, 117.6, 114.7, 90.4, 77.7, 73.6, 71.5, 57.9, 54.8, 31.8, 19.0. HRMS (ESI): calculated for $C_{22}H_{28}N_8O_5$ $[M+H]^+$ 485.2261, found 485.2265.

3-(((5-Amino-5-oxopentyl)(((2*R*,3*S*,4*R*,5*R*)-5-(6-amino-9*H*-purin-9-yl)-3,4-dihydroxy-tetrahydrofuran-2-yl)methyl)amino)methyl)benzamide (58). Following the procedure described for compound **57**, compound **34** (50 mg, 0.049 mmol) was deprotected to obtain compound **58** as a white powder (16 mg, 56% yield). ^{1}H NMR (400 MHz, D_2O) δ 8.43 – 8.12 (m, 2H), 7.84 – 7.26 (m, 4H), 6.08 (br, 1H), 4.65 – 4.21 (m, 5H), 3.63-3.48 (m, 2H), 3.34 (br, 2H), 2.35 (br, 2H), 1.84 (br, 2H), 1.58 (br, 2H). ^{13}C NMR (101 MHz, D_2O) δ 177.6, 170.6, 162.8, 149.6, 147.3, 143.8, 134.8, 129.7, 129.6, 129.4, 129.1, 128.3, 117.6, 114.7, 90.5, 77.8, 77.4, 71.6, 71.4, 57.8, 54.6, 32.6, 22.4, 21.0. HRMS (ESI): calculated for $C_{23}H_{30}N_8O_5$ $[M+H]^+$ 499.2417, found 499.2420.

4-((((2*R*,3*S*,4*R*,5*R*)-5-(6-amino-9H-purin-9-yl)-3,4-dihydroxytetrahydrofuran-2-yl)methyl)(3-carbamoylbenzyl)amino)butanoic acid (59). Following the procedure described for compound **57**, compound **35** (50 mg, 0.060 mmol) was deprotected to obtain compound **59** as a

white powder (21 mg, 60% yield). ^{1}H NMR (400 MHz, D_2O) δ 8.38 – 8.06 (m, 2H), 7.71 – 7.26 (m, 4H), 6.05 (br, 1H), 4.64 – 4.21 (m, 5H), 3.53 (br, 2H), 3.35 (s, 2H), 2.41 (br, 2H), 2.02 (br, 2H). ^{13}C NMR (101 MHz, D_2O) δ 176.4, 170.5, 149.6, 147.3, 143.8, 134.8, 132.7, 129.6, 129.5, 128.3, 117.5, 114.6, 90.4, 77.7, 73.5, 71.4, 57.8, 52.8, 38.6, 30.2, 18.4. HRMS (ESI): calculated for $C_{22}H_{28}N_7O_6$ $[M+H]^+$ 486.2101, found 486.2103.

5-((((2*R*,3*S*,4*R*,5*R*)-5-(6-amino-9*H*-purin-9-yl)-3,4-dihydroxytetrahydrofuran-2-yl)methyl)(3-carbamoylbenzyl)amino)pentanoic acid (60). Following the procedure described for compound **57**, compound **36** (50 mg, 0.059 mmol) was deprotected to obtain compound **60** as a white powder (17 mg, 50% yield). ^{1}H NMR (400 MHz, D_2O) δ 8.29 (br, 2H), 7.84 – 7.58 (m, 3H), 7.46 (br, 1H), 6.13 (br, 1H), 4.70 – 4.33 (m, 5H), 3.66 (br, 2H), 3.48 – 3.31 (m, 2H), 2.42 (br, 2H), 1.88 (s, 2H), 1.65 (br, 2H). ^{13}C NMR (101 MHz, D_2O) δ 177.7, 170.8, 163.0, 150.5, 147.6, 145.1, 143.1, 134.5, 132.9, 129.7, 129.3, 128.4, 119.0, 117.7, 90.3, 77.7, 73.3, 32.8, 22.4, 21.0. HRMS (ESI): calculated for $C_{23}H_{30}N_7O_6$ $[M+H]^+$ 500.2258, found 500.2267.

3-(((((2*R*,3*S*,4*R*,5*R*)-5-(6-amino-9*H*-purin-9-yl)-3,4-dihydroxytetrahydrofuran-2-yl)methyl)(isopropyl)amino)methyl)benzamide (61). Following the procedure described for compound **57**, compound **38** (50 mg, 0.069 mmol) was deprotected to obtain compound **61** as a white powder (22 mg, 60% yield). ^{1}H NMR (400 MHz, Acetone-d_6) δ 8.48-8.39 (m, 2H), 8.26 (br, 1H), 7.94 (d, *J* = 7.8 Hz, 1H), 7.9-7.73 (m, 2H), 7.46 (m, 1H), 6.81 (br, 1H), 6.13 (d, *J* = 3.4 Hz, 1H), 4.74 (br, 2H), 4.65 (s, 1H), 4.53 (br, 1H), 4.46 (br, 1H), 3.93 – 3.69 (m, 3H), 3.31 (s, 1H), 1.49-1.45 (m, 6H). ^{13}C NMR (101 MHz, Acetone-d_6) δ 152.7, 148.4, 146.1, 142.5, 135.0, 134.0, 130.5, 130.2, 119.9, 90.6, 79.3, 73.5, 72.5, 55.6, 54.3, 54.0, 51.4, 16.6, 15.0. HRMS (ESI): calculated for $C_{21}H_{28}N_7O_4$ $[M+H]^+$ 442.2203, found 442.2203.

Methyl 3-(((4-amino-4-oxobutyl)(((2*R*,3*S*,4*R*,5*R*)-5-(6-amino-9*H*-purin-9-yl)-3,4-dihydroxytetrahydrofuran-2-yl)methyl)amino)methyl)benzoate (62). Following the procedure described for compound **57**, compound **39** (50 mg, 0.064 mmol) was deprotected to obtain compound **62** as a white powder (20 mg, 53% yield). ^{1}H NMR (400 MHz, D_2O) δ 8.38 – 7.98 (m, 2H), 7.88 – 7.50 (m, 3H), 7.35 (br, 1H), 6.05 (br, 1H), 4.64 – 4.32 (m, 4H), 4.20 (br, 1H), 3.78 (s, 3H), 3.55 (br, 1H), 3.47 – 3.30 (m, 2H), 2.39 (br, 2H), 2.08 (br, 2H). ^{13}C NMR (101 MHz, D_2O) δ 177.5, 167.3, 149.5, 147.2, 143.7, 143.6, 135.8, 134.6, 131.3, 130.7, 129.9, 129.8, 129.4, 129.1, 118.8, 90.6, 77.8, 77.4, 73.8, 73.1, 71.7, 71.4, 57.6, 56.9, 55.2, 54.8, 53.6, 52.7, 31.8, 19.0. HRMS (ESI): calculated for $C_{23}H_{29}N_7O_6$ $[M+H]^+$ 500.2258, found 500.2265.

Methyl 3-(((5-amino-5-oxopentyl)(((2*R*,3*S*,4*R*,5*R*)-5-(6-amino-9*H*-purin-9-yl)-3,4-dihydroxytetrahydrofuran-2-yl)methyl)amino)methyl)benzoate (63). Following the procedure described for compound **57**, compound **40** (50 mg, 0.063 mmol) was deprotected to obtain

compound **63** as a white powder (21 mg, 55% yield).^{1}H NMR (400 MHz, D_2O) δ 8.44 – 8.07 (m, 2H), 7.96 – 7.34 (m, 4H), 6.12 (br, 1H), 4.50 (br, 4H), 4.32 (s, 1H), 3.86 (s, 3H), 3.62 (br, 1H), 3.52 – 3.34 (m, 2H), 2.32 (br, 2H), 1.89 (br, 2H), 1.68 (br, 2H). ^{13}C NMR (101 MHz, D_2O) δ 178.7, 167.5, 162.6, 149.6, 143.8, 143.6, 135.9, 130.9, 130.0, 129.9, 129.5, 129.1, 117.6, 114.7, 111.8, 71.4, 52.7, 33.9, 22.4, 21.9. HRMS (ESI): calculated for $C_{24}H_{31}N_7O_6$ $[M+H]^+$ 514.2414, found 514.2415.

4-((((2*R*,3*S*,4*R*,5*R*)-5-(6-amino-9*H*-purin-9-yl)-3,4-dihydroxytetrahydrofuran-2-yl)methyl)(3-(methoxycarbonyl)benzyl)amino)butanoic acid (64). Following the procedure described for compound **57**, compound **41** (50 mg, 0.084 mmol) was deprotected to obtain compound **64** as a white powder (24 mg, 49% yield). ^{1}H NMR (400 MHz, D_2O) δ 8.29 (s, 1H), 8.11 (s, 1H), 7.94 – 7.64 (m, 4H), 7.45 (t, *J* = 7.9 Hz, 1H), 6.09 (s, 1H), 4.62 (br, 4H), 4.49 (br, 1H), 3.88 (s, 3H), 3.67 (br, 2H), 3.55-3.41 (m, 6.9 Hz, 3H), 2.53 (t, *J* = 6.4 Hz, 2H), 2.18 – 2.09 (m, 2H). ^{13}C NMR (101 MHz, D_2O) δ 176.8, 167.6, 150.3, 147.4, 144.8, 143.3, 130.1, 129.8, 129.5, 129.2, 90.5, 77.7, 71.6, 57.7, 52.8, 30.6, 18.5. HRMS (ESI): calculated for $C_{23}H_{28}N_6O_7$ $[M+H]^+$ 501.2098, found 501.2097.

5-((((2*R*,3*S*,4*R*,5*R*)-5-(6-amino-9*H*-purin-9-yl)-3,4-dihydroxytetrahydrofuran-2-yl)methyl)(3-(methoxycarbonyl)benzyl)amino)pentanoic acid (65). Following the procedure described for compound **57**, compound **42** (50 mg, 0.082 mmol) was deprotected to obtain compound **65** as a white powder (30 mg, 59% yield).^{1}H NMR (400 MHz, D_2O) δ 8.22 (br, 2H), 7.86 (br, 2H), 7.67 (br, 1H), 7.46 (br, 1H), 6.08 (br, 1H), 4.55 (br, 4H), 4.35 (br, 1H), 3.88 (s, 3H), 3.64 (br, 1H), 3.43 (br, 2H), 2.45 (br, 2H), 1.90 (br, 2H), 1.67 (br, 2H). ^{13}C NMR (101 MHz, D_2O) δ 178.1, 168.0, 150.3, 144.5, 143.8, 130.5, 130.2, 129.9, 129.6, 118.0, 115.1, 72.0, 53.1, 33.1, 23.6, 22.8, 21.4. HRMS (ESI): calculated for $C_{24}H_{30}N_6O_7$ $[M+H]^+$ 515.2254, found 515.2257.

(*S*)-2-Amino-4-((((2*R*,3*S*,4*R*,5*R*)-5-(6-amino-9*H*-purin-9-yl)-3,4-dihydroxytetrahydrofuran-2-yl)methyl)(3-(methoxycarbonyl)benzyl)amino)butanoic acid (66). Following the procedure described for compound **57**, compound **43** (50 mg, 0.070 mmol) was deprotected to obtain compound **66** as a white powder (26 mg, 60% yield).^{1}H NMR (400 MHz, D_2O) δ 8.24 (s, 1H), 8.01 (s, 1H), 7.72 (br, 1H), 7.64 (d, *J* = 7.8 Hz, 1H), 7.54 (d, *J* = 7.8 Hz, 1H), 7.31 (t, *J* = 7.8 Hz, 1H), 6.03 (s, 1H), 4.56 – 4.52 (m, 1H), 4.50 – 4.35 (m, 4H), 4.07 (m, 1H), 3.74 (s, 3H), 3.69 – 3.54 (m, 4H), 2.55-2.45 (m, 1H), 2.41-2.33 (m, 1H). ^{13}C NMR (101 MHz, D_2O) δ 170.8, 167.2, 162.7, 162.3, 149.5, 147.2, 143.6, 143.6, 131.0, 130.0, 129.5, 129.3, 129.1, 118.8, 117.6, 114.7, 90.8, 77.5, 73.5, 71.4, 53.9, 50.7, 24.4. HRMS (ESI): calculated for $C_{23}H_{29}N_7O_7$ $[M+H]^+$ 516.2207, found 516.2206.

Methyl 3-(((((2*R*,3*S*,4*R*,5*R*)-5-(6-amino-9*H*-purin-9-yl)-3,4-dihydroxytetrahydrofu ran-2-yl)methyl)(*iso*propyl)amino)methyl)benzoate (67). Following the procedure described for compound **57**, compound **44** (50 mg, 0.101 mmol) was deprotected to obtain compound **67** as a white powder (33 mg, 59% yield).^{1}H NMR (400 MHz, D_2O) δ 8.19 (d, *J* = 3.9 Hz, 1H), 7.99 – 7.54 (m, 4H), 7.29 (t, *J* = 7.6 Hz, 1H), 5.91 (s, 1H), 4.62 – 4.46 (m, 3H), 4.33 – 4.25 (m, 1H), 4.20 (br, 1H), 3.87 (s, 3H), 3.79-3.62 (m, 2H), 3.39 – 3.28 (m, 1H), 1.54 – 1.37 (m, 6H). ^{13}C NMR (101 MHz, D_2O) δ 167.6, 149.7, 147.3, 144.1, 143.3, 136.1, 131.3, 130.1, 129.7, 128.7, 118.7, 114.8, 90.6, 78.6, 73.6, 71.4, 58.7, 55.2, 52.7, 50.5, 16.2, 15.7. HRMS (ESI): calculated for $C_{22}H_{28}N_6O_5$ $[M+H]^+$ 457.2199, found 457.2196.

3-(((4-Amino-4-oxobutyl)(((2*R*,3*S*,4*R*,5*R*)-5-(6-amino-9*H*-purin-9-yl)-3,4-dihydroxytetrahydrofuran-2-yl)methyl)amino)methyl)benzoic acid (68). Following the procedure described for compound **57**, compound **45** (50 mg, 0.061 mmol) was deprotected to obtain compound **68** as a white powder (15 mg, 42% yield). ^{1}H NMR (400 MHz, D_2O) δ 8.21 (br, 2H), 7.86 (br, 2H), 7.65 (d, *J* = 7.6 Hz, 1H), 7.43 (br, 1H), 6.08 (br, 1H), 4.70 – 4.24 (m, 5H), 3.63 (br, 1H), 3.52 – 3.38 (m, 2H), 2.48 (br, 2H), 2.12 (br, 2H). ^{13}C NMR (101 MHz, D_2O) δ 177.5, 149.8, 147.4, 144.0, 143.6, 131.2, 130.3, 129.9, 129.1, 117.7, 114.8, 90.5, 77.7, 71.5, 31.8, 19.1. HRMS (ESI): calculated for $C_{22}H_{26}N_7O_6$ $[M+H]^+$ 486.2101, found 486.2089.

3-(((5-Amino-5-oxopentyl)(((2*R*,3*S*,4*R*,5*R*)-5-(6-amino-9*H*-purin-9-yl)-3,4-dihydroxytetrahydrofuran-2-yl)methyl)amino)methyl)benzoic acid (69). Following the procedure described for compound **57**, compound **46** (50 mg, 0.059 mmol) was deprotected to obtain compound **69** as a white powder (19 mg, 65 % yield). ^{1}H NMR (400 MHz, D_2O) δ 8.19 (br, 2H), 7.83(br, 2H), 7.63 (br, 1H), 7.40 (br, 1H), 6.03 (br, 1H), 4.58-4.41 (m, 4H), 4.31 (br, 1H), 3.63 (br, 1H), 3.42 (d, *J* = 7.8 Hz, 2H), 2.34 (br, 2H), 1.90 (br, 2H), 1.68 (br, 2H). ^{13}C NMR (101 MHz, D_2O) δ 178.7, 149.7, 143.9, 143.5, 130.3, 129.8, 129.8, 129.1, 120.6, 117.7, 114.8, 105.0, 77.9, 71.5, 33.9, 21.9. HRMS (ESI): calculated for $C_{23}H_{30}N_7O_6$ $[M+H]^+$ 500.2258, found 500.2253.

3-(((((2*R*,3*S*,4*R*,5*R*)-5-(6-amino-9*H*-purin-9-yl)-3,4-dihydroxytetrahydrofuran-2-yl)methyl)(3-carboxypropyl)amino)methyl)benzoic acid (70). Following the procedure described for compound **57**, compound **47** (50 mg, 0.078 mmol) was deprotected to obtain compound **70** as a white powder (21 mg, 46% yield). ^{1}H NMR (400 MHz, D_2O) δ 8.27 (s, 1H), 8.14 (s, 1H), 7.85 (br, 2H), 7.64 (d, *J* = 7.7 Hz, 1H), 7.49 – 7.35 (m, 1H), 6.08 (br, 1H), 4.55 (br, 5H), 3.65 (br, 1H), 3.48-3,43 (m, 2H), 2.52 (br, 2H), 2.13 (br, 2H). ^{13}C NMR (101 MHz, D_2O) δ 176.6, 168.8, 149.8, 147.4, 144.0, 143.5, 131.4, 130.4, 129.7, 129.1, 117.7, 114.8, 90.5, 77.7, 71.6, 30.4, 22.1, 18.5. HRMS (ESI): calculated for $C_{22}H_{27}N_6O_7$ $[M+H]^+$ 487.1941, found 487.1945.

3-(((((2*R*,3*S*,4*R*,5*R*)-5-(6-amino-9*H*-purin-9-yl)-3,4-dihydroxytetrahydrofuran-2-yl)methyl)(4-carboxybutyl)amino)methyl)benzoic acid (71). Following the procedure described for compound **57**, compound **48** (50 mg, 0.076 mmol) was deprotected to obtain compound **71** as a white powder (24 mg, 52% yield). ^{1}H NMR (400 MHz, D_2O) δ 8.20 (br, 2H), 7.83 (br, 2H), 7.63 (d, *J* = 7.5 Hz, 1H), 7.42 (br, 1H), 6.05 (br, 1H), 4.53 (br, 4H), 4.31 (br, 1H), 3.63 (br, 1H), 3.49 – 3.32 (m, 2H), 2.42 (br, 2H), 1.88 (br, 2H), 1.66 (br, 2H). ^{13}C NMR (101 MHz, D_2O) δ 177.7, 150.0, 144.3, 143.4, 131.4, 130.4, 130.1, 129.7, 129.1, 117.7, 114.8, 90.4, 77.7, 71.6, 32.7, 22.4, 21.0. HRMS (ESI): calculated for $C_{23}H_{29}N_6O_7$ $[M+H]^+$ 501.2098, found 501.2096.

3-((((*S*)-3-Amino-3-carboxypropyl)(((2*R*,3*S*,4*R*,5*R*)-5-(6-amino-9*H*-purin-9-yl)-3,4-dihydroxytetrahydrofuran-2-yl)methyl)amino)methyl)benzoic acid (72). Following the procedure described for compound **57**, compound **49** (50 mg, 0.066 mmol) was deprotected to obtain compound **72** as a white powder (24 mg, 61% yield). ^{1}H NMR (400 MHz, D_2O) δ 8.23 (bs, 1H), 8.06 (s, 1H), 7.76 (s, 1H), 7.69 (d, *J* = 7.6 Hz, 1H), 7.56 (d, *J* = 7.8 Hz, 1H), 7.33 (t, *J* = 7.8 Hz, 1H), 6.06 – 5.98 (m, 1H), 4.59 – 4.34 (m, 5H), 4.06 (m, 1H), 3.72 – 3.51 (m, 4H), 2.55 – 2.4m (m, 1H), 2.40-2.32 (m, 1H). ^{13}C NMR (101 MHz, D_2O) δ 171.0, 168.4, 162.8, 162.4, 149.5, 147.3, 143.7, 143.5, 131.3, 130.3, 129.7, 129.5, 129.1, 118.9, 117.6, 114.7, 90.6, 77.5, 73.5, 71.5, 50.9, 24.4. HRMS (ESI): calculated for $C_{22}H_{27}N_7O_7$ $[M+H]^+$ 502.2050, found 502.2048.

3-(((((2*R*,3*S*,4*R*,5*R*)-5-(6-amino-9*H*-purin-9-yl)-3,4-dihydroxytetrahydrofuran-2-yl)methyl)(isopropyl)amino)methyl)benzoic acid (73). Following the procedure described for compound **57**, compound **50** (50 mg, 0.093 mmol) was deprotected to obtain compound **73** as a white powder (27 mg, 54% yield). ^{1}H NMR (400 MHz, D_2O) δ 8.21 (s, 1H), 8.16 (s, 1H), 7.90 (s, 1H), 7.58 (m, 2H), 7.27 (t, *J* = 7.3 Hz, 1H), 5.89 (s, 1H), 4.55 (t, *J* = 10.4 Hz, 2H), 4.31 – 4.15 (m, 2H), 3.98 – 3.90 (m, 1H), 3.78 (br, 1H), 3.32 (br, 1H), 1.50 (m, 6H). ^{13}C NMR (101 MHz, D_2O) δ 215.3, 168.7, 149.9, 147.3, 144.4, 143.1, 136.1, 131.7, 129.9, 128.7, 118.7, 117.7, 114.8, 89.7, 78.5, 73.5, 71.4, 58.8, 55.3, 51.7, 30.1, 16.2, 15.7. HRMS (ESI): calculated for $C_{21}H_{26}N_6O_5$ $[M+H]^+$ 443.2043, found 443.2040.

4-((((2*R*,3*S*,4*R*,5*R*)-5-(6-amino-9*H*-purin-9-yl)-3,4-dihydroxytetrahydrofuran-2-yl)methyl)(naphthalen-2-ylmethyl)amino)butanamide (74). Following the procedure described for compound **57**, compound **51** (50 mg, 0.064 mmol) was deprotected to obtain compound **74** as a white powder (22 mg, 58% yield). ^{1}H NMR (400 MHz, D_2O) δ 8.11 (br, 1H), 7.57 – 7.25 (m, 4H), 7.09 (d, *J* = 8.0 Hz, 1H), 5.89 (br, 1H), 4.35 (br, 4H), 3.94 – 3.63 (m, 1H), 3.49 – 3.22 (m, 3H), 2.44 (br, 2H), 2.13 – 1.82 (br, 2H). ^{13}C NMR (101 MHz, D_2O) δ 177.5, 148.4, 146.0, 143.3, 142.3, 132.1, 131.6, 129.5, 128.0, 127.7, 127.2, 127.0, 126.8, 126.7, 125.1, 118.0, 90.6,

77.8, 74.1, 71.2, 58.0, 55.9, 54.9, 32.0, 19.0. HRMS (ESI): calculated for $C_{25}H_{29}N_7O_4$ $[M+H]^+$ 492.2359, found 492.2363.

5-((((2*R*,3*S*,4*R*,5*R*)-5-(6-amino-9*H*-purin-9-yl)-3,4-dihydroxytetrahydrofuran-2-yl)methyl)(naphthalen-2-ylmethyl)amino)pentanamide (75). Following the procedure described for compound 57, compound **52** (50 mg, 0.063 mmol) was deprotected to obtain compound **75** as a white powder (23 mg, 60% yield). ^{1}H NMR (400 MHz, D_2O) δ 8.11 (s, 1H), 7.72 – 7.61 (m, 2H), 7.55 – 7.48 (m, 2H), 7.46 – 7.39 (m, 1H), 7.37 – 7.15 (m, 2H), 5.89 (br, 1H), 4.66 – 4.48 (m, 2H), 4.42 – 4.11 (m, 3H), 3.61 – 3.33 (m, 4H), 2.43 – 2.27 (m, 2H), 1.89 (d, *J* = 9.8 Hz, 2H), 1.77 – 1.61 (m, 2H). ^{13}C NMR (101 MHz, D_2O) δ 178.8, 148.6, 146.3, 143.8, 143.4, 142.7, 142.2, 132.4, 131.8, 129.9, 128.2, 127.8, 127.4, 126.8, 125.1, 90.7, 78.1, 74.2, 71.3, 58.6, 57.8, 55.8, 54.6, 34.0, 22.5, 22.0. HRMS (ESI): calculated for $C_{26}H_{31}N_7O_4$ $[M+H]^+$ 506.2516, found 506.2520.

4-((((2*R*,3*S*,4*R*,5*R*)-5-(6-amino-9*H*-purin-9-yl)-3,4-dihydroxytetrahydrofuran-2-yl)methyl)(naphthalen-2-ylmethyl)amino)butanoic acid (76). Following the procedure described for compound **57**, compound **53** (50 mg, 0.085 mmol) was deprotected to obtain compound **76** as a white powder (30 mg, 60% yield). ^{1}H NMR (400 MHz, D_2O) δ 8.14 (br, 1H), 7.75 – 7.23 (m, 8H), 5.95 (br, 1H), 4.62 – 4.54 (m, 1H), 4.43 – 4.26 (m, 4H), 3.69 – 3.53 (m, 2H), 3.45 (m, 2H), 2.54 (t, *J* = 6.5 Hz, 2H), 2.19 – 2.04 (m, 2H). ^{13}C NMR (101 MHz, D_2O) δ 179.8, 179.8, 152.0, 149.1, 146.3, 145.7, 134.9, 134.4, 132.5, 130.6, 129.9, 129.8, 129.3, 121.0, 120.2, 117.3, 93.3, 80.2, 74.2, 60.8, 33.6, 21.4. HRMS (ESI): calculated for $C_{23}H_{30}N_8O_5$ $[M+H]^+$ 493.2199, found 493.2199.

5-((((2*R*,3*S*,4*R*,5*R*)-5-(6-amino-9*H*-purin-9-yl)-3,4-dihydroxytetrahydrofuran-2-yl)methyl)(naphthalen-2-ylmethyl)amino)pentanoic acid (77). Following the procedure described for compound **57**, compound **54** (50 mg, 0.083 mmol) was deprotected to obtain compound **77** as a white powder (31 mg, 61% yield). ^{1}H NMR (400 MHz, D_2O) δ 8.27 (br, 2H), 7.86 – 7.55 (m, 5H), 7.52 – 7.47 (m, 1H), 7.40 (d, *J* = 7.7 Hz, 1H), 5.95 (s, 1H), 4.66-4.40 (m, 4H), 4.31 (br, 1H), 3.70 – 3.43 (m, 4H), 2.50 (br, 2H), 1.97 (br, 2H), 1.80 – 1.67 (br, 2H). ^{13}C NMR (101 MHz, D_2O) δ 178.0, 163.0, 162.7, 149.5, 146.6, 143.8, 143.1, 132.4, 131.9, 130.0, 128.0, 127.3, 127.2, 126.8, 117.7, 38.6, 32.9, 21.2. HRMS (ESI): calculated for $C_{26}H_{28}N_6O_5$ $[M+H]^+$ 507.2356, found 507.2355.

(*S*)-2-Amino-4-((((2*R*,3*S*,4*R*,5*R*)-5-(6-amino-9*H*-purin-9-yl)-3,4-dihydroxytetrahydrofuran-2-yl)methyl)(naphthalen-2-ylmethyl)amino)butanoic acid (78). Following the procedure described for compound **57**, compound **55** (50 mg, 0.071 mmol) was deprotected to obtain compound **78** as a white powder (28 mg, 65% yield). ^{1}H NMR (400 MHz,

D_2O) δ 8.03 (bs, 2H), 7.54 – 6.97 (m, 7H), 5.83 (bs, 1H), 4.55 – 4.25 (m, 3H), 4.24 – 4.16 (m, 1H), 4.16 – 4.09 (m, 1H), 3.65 (s, 2H), 3.49 (s, 1H), 2.46 (br, 2H). ^{13}C NMR (101 MHz, D_2O) δ 170.8, 148.3, 146.0, 143.3, 142.2, 132.0, 131.5, 129.7, 127.1, 126.9, 126.6, 126.3, 118.2, 117.6, 114.7, 90.9, 77.5, 73.8, 71.4, 50.7, 24.5. HRMS (ESI): calculated for $C_{25}H_{29}N_7O_5$ $[M+H]^+$ 508.2308, found 508.2309.

(2*R*,3*R*,4*S*,5*R*)-2-(6-amino-9*H*-purin-9-yl)-5-((isopropyl(naphthalen-2-ylmethyl) amino)methyl) tetrahydrofuran-3,4-diol (79). Following the procedure described for compound **57**, compound **56** (50 mg, 0.102 mmol) was deprotected to obtain compound **79** as a white powder (36 mg, 65% yield).^{1}H NMR (400 MHz, D_2O) δ 7.86 (s, 1H), 7.64 – 7.47 (m, 2H), 7.42 – 7.10 (m, 6H), 5.58 (s, 1H), 4.41 – 4.35 (m, 1H), 4.29 (br, 1H), 4.16 – 4.04 (m, 2H), 3.92 (br, 1H), 3.80-3.73(m, 1H), 3.58 (br, 1H), 3.24 (m, 1H), 1.35 (m, 6H). ^{13}C NMR (101 MHz, D_2O) δ 148.7, 146.3, 143.6, 143.0, 142.6, 132.2, 131.7, 130.4, 128.3, 127.5, 127.4, 118.0, 90.0, 77.5, 73.9, 71.9, 59.1, 51.7, 49.6, 17.4, 15.9. HRMS (ESI): calculated for $C_{24}H_{28}N_6O_3$ $[M+H]^+$ 449.2301, found 449.2299.

tert-Butyl (*S*)-4-((((3a*R*,4*R*,6*R*,6a*R*)-6-(6-amino-9*H*-purin-9-yl)-2,2-dimethyltetrahydro-furo-[3,4-d][1,3]dioxol-4-yl)methyl)(naphthalen-2-ylmethyl)amino)-2-bis(*tert*-butoxycarbonyl)amino)pentanoate (80). Following the procedure described for compound **33**, *tert*-butyl (*R*)-2-((*tert*-butoxycarbonyl)amino)-5-oxopentanoate **28** (312 mg, 0.80 mmol) and compound 32 (300 mg, 0.67mmol) to obtain compound **80** as a white powder (319 mg, 58% yield). ^{1}H NMR (400 MHz, $CDCl_3$) δ 8.05 (s, 1H), 7.79 (s, 1H), 7.73 m, 1H), 7.68 (d, *J* = 8.6 Hz, 2H), 7.61 (s, 1H), 7.45 – 7.34 (m, 3H), 6.59 (s, 2H), 5.98 (d, *J* = 2.2 Hz, 1H), 5.27 (dd, *J* = 6.4, 2.2 Hz, 1H), 4.84 (dd, *J* = 6.4, 3.1 Hz, 1H), 4.69 (dd, *J* = 9.6, 5.2 Hz, 1H), 4.37 (m, 1H), 3.80 (br, 1H), 3.57 (br, 1H), 2.76 (m, 1H), 2.64 – 2.47 (m, 3H), 2.04 (m, 1H), 1.83 (m, 1H), 1.54 (s, 3H), 1.43 (s, 16H), 1.41 (s, 8H), 1.31 (s, 3H). ^{13}C NMR (101 MHz, $CDCl_3$) δ 155.9, 152.9, 152.5, 139.5, 127.7, 127.5, 127.3, 127.2, 125.8, 125.5, 90.8, 85.4, 83.6, 83.41, 82.6, 81.0, 59.0, 55.6, 54.0, 28.0, 27.1, 27.0, 25.3, 23.8. HRMS (ESI): calculated for $C_{43}H_{59}N_7O_9$ $[M+H]^+$ 818.4453, found 818.4458.

(*S*)-2-Amino-5-((((2*R*,3*S*,4*R*,5*R*)-5-(6-amino-9*H*-purin-9-yl)-3,4-dihydroxytetrahydrofuran-2-yl)methyl)(naphthalen-2-ylmethyl)amino)pentanoic acid (81). Following the procedure described for compound **57**, compound **80** (120 mg, 0.15 mmol) was deprotected to obtain compound **81** as a white powder (58 mg, 63% yield). ^{1}H NMR (600 MHz, D_2O) δ 8.14 (br, 1H), 7.69–6.93 (m, 8H), 5.93 (br, 1H), 4.59–4.43 (m, 2H), 4.27 (br, 2H), 4.15–3.73 (m, 2H), 3.47 (m, 4H), 2.16–1.90 (m, 4H). ^{13}C NMR (151 MHz, D_2O) δ 171.6, 162.9, 162.7, 148.6, 131.8 127.3, 127.1, 126.8, 119.2, 117.3, 115.3, 90.7, 78.0, 74.3, 71.3,

58.8, 52.3, 26.9, 19.4. HRMS (ESI): calculated for $C_{26}H_{31}N_7O_5$ $[M+H]^+$ 522.2465, found 522.2468.

Inhibition studies: Expression and purification of full-length wild type NNMT protein (NNMTwt) were performed as previously described.[32] The purity of the enzyme was confirmed using SDS-PAGE with Coomassie blue staining and NNMT identity was confirmed using SDS-PAGE and Western blotting. Catalytic activity of the recombinant protein was evaluated with 1 unit of enzyme activity representing the formation of 1 nmol of MNA per hour of incubation at 37 °C. The specific activity of the batch used in the inhibitory activity assays was 18,665 units per mg of protein at a protein concentration of 0.56 mg/mL. NNMT was used at a final concentration of 100 nM diluted in assay buffer (50 mM Tris buffer (pH 8.4) and 1 mM DTT). The compounds were dissolved in DMSO and diluted with water to concentrations ranging from 0.1 μM to 500 μM (DMSO was kept constant at 1.25% final concentration). The compounds were incubated with the enzyme for 10 minutes at 37 °C before initiating the reaction with a mixture of NA and AdoMet at their K_M values of 200 μM and 8.5 μM respectively. The formation of MNA was measured after 30 minutes at 37 °C. The reaction was quenched by addition of 15 μL sample to 70 μL acetonitrile containing 50 nM deutero-methylated nicotinamide as internal standard. The enzymatic activity assays were performed using UHP-HILIC-MS/MS as previously described with minor modifications.[24] The UHP-HILIC-MS/MS system consisted of a binary UHPLC system, consisting of two LC-30AD pumps, a SIL30-ACmp auto-sampler, a CTO-20AC column oven, and a DGU-20A5R degasser, (all from Shimadzu, 's-Hertogenbosch, The Netherlands). Isocratic elution was performed after 1 μL injections on a Waters Acquity BEH Amide HILIC column (3.0 x 100 mm, 1.7 μm particle size, Waters, Milford, USA), using water containing 300 μM formic acid and 550 μM NH_4OH (pH 9.2) at 40% v/v and acetonitrile at 60% v/v, with a run-time of 3 min. Calibration samples were prepared using 75 μL internal standard d_3-MNA at 50 nM in acetonitrile and 25 μL of an aqueous solution of reference standard MNA with concentrations ranging from 2500 nM to 1.221 nM. For detection, a Sciex QTRAP® 5500 triple quadrupole mass spectrometer, with Analyst 1.6.2, and MultiQuant 3.0.1 software (Sciex, Ontario, Canada) was used. Settings used for the ionization source were: curtain gas, 40 psi; collision gas, 'medium'; ionspray voltage, 5000 V; temperature, 600 °C; ion source gas 1, 60 psi; ion source gas 2, 80 psi. Dwell times were 10 msec, and entrance potential was set to 10 V; compound specific parameters can be found in Table 2. The whole eluate was transferred to the electrospray probe from 1.0 till 2.8 min using the MS diverter valve. Ratios of the sums of the MNA and d_3-MNA transitions were calculated and plotted versus concentration.

Table 2. Tuned MS/MS parameters for all quantified components.

Compound	Q1 (m/z)	Q3 (m/z)	DP	CE	CXP
MNA	137.101	94.0	136	27	12
		92.0	136	29	12
		78.0	136	35	10
MNA-d_3	140.128	97.1	121	29	12
		95.1	121	31	12
		78.0	121	35	10

The entrance potential was set at 10 V for all compounds, dwell-time was 10 msec. Q1: quadrupole 1, Q3: quadrupole 3, z: charge, DP: declustering potential, CE: collision energy, CXP: collision cell exit potential.

Isothermal Titration Calorimetry: Expression and purification of full-length wild type NNMT protein (NNMTwt) were performed as previously described.[31] Isothermal titration calorimetry (ITC) measurements were made at 25 °C on a MicroCal ITC200 Instrument (Malvern Instruments) with 2 μL injections. NNMTwt was diluted at 200 μM in ITC buffer (50 mM Tris (pH 8.0), 150 mM NaCl) supplemented with 4% DMSO. Compounds were dissolved in DMSO at 50 mM and diluted to 2 mM in ITC buffer with a final DMSO concentration of 4%. Binding constants were calculated by fitting the data using the ITC data analysis module in Origin 7.0 (OriginLab Corp.).

Modeling studies: Docking computations were performed using Autodock 4.2.[49] Compounds **1**, **2**, **78**, and **81** were docked into the catalytic pocket of the structure taken from PDB ID: 3ROD.[32] Four molecular dynamic simulations were performed with GROMACS 2018.2[50] using the AMBER03 force field[51]. Each structure was immersed in a cubic box using TIP3P water molecules[52] and neutralized with counter ions. A production step of 250 ns was carried out using the Parrinello-Rahman algorithm[53] for temperature and pressure control, with coupling constants of T=0.1 ps and P=2.0 ps, for compounds **1**, **2**, **81** and extended to 450 ns for compound **78**, in order to reach equilibrium of the system. Coordinates were saved every 200 ps and the protein/ligand binding energy was estimated using g_mmpbsa calculations[54,55] on the last 50 ns of each trajectory. The conformation of minimal energy in these 50 ns was extracted from the simulations and minimized in order to represent the interactions between the ligands and NNMT protein.

Enzyme assay for selectivity: Methyltransferase inhibition assays were performed as described[56] by using commercially available chemiluminescent assay kits for PRMT1 and NSD2

(purchased from BPS Bioscience). The enzymatic reactions were conducted in duplicate at room temperature for 1 h (PRMT1) or 2 h (NSD2) in substrate-coated well plates at a final reaction volume of 50 µL containing: the manufacturer's proprietary assay buffer, AdoMet (at a concentration of 5 times the respective Km value for each enzyme), the methyltransferase enzyme: PRMT1 (100 ng per reaction) and NSD2 (500 ng per reaction), and inhibitor **78**. Before addition of AdoMet, the enzyme was first incubated with the inhibitor for 15 min at room temperature. Positive controls were performed in the absence of inhibitor using water to keep the final volume consistent. Blanks and substrate controls were performed in the absence of the enzyme and AdoMet, respectively. Following the enzymatic reactions, 100 µL of primary antibody (recognizing the respective immobilized methylated product) was added to each well, and the plate was incubated at room temperature for an additional 1 h. Then, 100 µL of secondary horseradish peroxidase (HRP)-conjugated antibody was added to each well, and the plate was incubated at room temperature for additional 30 min. Finally, 100 µL of an HRP substrate mixture was added to the wells, and the luminescence was measured directly by using a standard microplate reader. The luminescence data were normalized with the positive controls defined as 100% activity and blank defined as 0%.

Cell culture and treatment with compounds: The HSC-2 human oral cancer cell line was purchased from the American Type Culture Collection (ATCC, Rockville, MD, USA), and cultured in DMEM/F12 medium, supplemented with 10% fetal bovine serum and 50 µg/ml gentamicin, at 37 °C in a humidified 5% CO_2 incubator. Compounds **1**, **2**, **78**, and **81** were tested for their inhibitory effect on cell proliferation of HSC-2 cells. Each compound was dissolved in DMSO at 100mM concentration. This stock solution was then diluted in culture medium to final concentration values ranging between 1 µM and 100 µM. For each sample, DMSO was kept constant at 0.1% final concentration.

The day before starting treatment, cells were seeded in 96-well plates, at a density of $1x10^3$ cells/well. Cells were allowed to attach overnight and then incubated with compounds at different final concentrations, or with DMSO only, for 24, 48 and 72 hours. All experiments were performed in triplicate.

MTT assay: Cell proliferation was determined using a colorimetric assay with 3-(4,5-dimethylthiazol-2-yl)-2,5-diphenyl tetrazolium bromide (MTT). The MTT assay measures the conversion of MTT to insoluble formazan by dehydrogenase enzymes of the intact mitochondria of living cells. HSC-2 cell proliferation was evaluated by measuring the conversion of the

tetrazolium salt MTT to formazan crystals upon treatment with compounds or DMSO only for 24, 48 and 72 hours. Briefly, cells were incubated for 2 hours at 37°C with 100 µl fresh culture medium containing 5 µl of MTT reagent (5mg/ml in PBS). The medium was removed and 200 µl isopropanol were added. The amount of formazan crystals formed correlated directly with the number of viable cells. The reaction product was quantified by measuring the absorbance at 540nm using an ELISA plate reader. Experiments were repeated three times. Results were expressed as percentage of the control (control equals 100% and corresponds to the absorbance value of each sample at time zero) and presented as mean values ± standard deviation of three independent experiments performed in triplicate. Data were analysed using GraphPad Prism software (GraphPad Software, San Diego, CA). Significant differences between groups were determined using the one-way analysis of variance (ANOVA). A p value <0.05 was considered as statistically significant.

Quantitative measurements of MNA levels in cultured cells: The analysis was performed as previously described[57] with minor modifications. Cellular MNA levels were determined using the same UHP-HILIC-MS/MS employed for the inhibition studies as described above. To determine the effect of compound **78** on NNMT activity in the HSC-2 oral cancer cell line used cells were treated with **78** at 100 µM (final DMSO content 0.1%) and incubated for 24, 48, or 72 hours. The day prior to starting treatment, cells were seeded in 6-well plates, at a density of $3x10^4$ cells/well. Cells were allowed to attach overnight and were then incubated with compound **78**. All experiments were performed in duplicate. Following treatment, medium was removed, and adherent cells were trypsinized and harvested by centrifugation at 1,000xg for 3 min at 4°C. Supernatant was then discarded and cell pellets were stored at -80 °C until further use. The extraction of MNA from the cell pellets was performed as previously described.[58] Briefly, 100 µL acetonitrile containing 50 nM d_3-MNA (as internal control) was added to the cell pellets and the cells were lysed for 20 minutes at room temperature with mild shaking. 50µL of purified water was added, followed by mixing and the resulting cell debris centrifuged for 10 minutes at 5,000 rpm. 100 µL of the resulting supernatant was then transferred to a 96-well plate and analysed for MNA content.

References

1. Alston TA, Abeles RH. Substrate specificity of nicotinamide methyltransferase isolated from porcine liver. Arch Biochem Biophys. 1988;260(2):601-8.
2. van Haren MJ, Sastre Toraño J, Sartini D, Emanuelli M, Parsons RB, Martin NI. A Rapid and Efficient Assay for the Characterization of Substrates and Inhibitors of Nicotinamide N -Methyltransferase. Biochemistry. 2016;55(37):5307-15.
3. Thomas MG, Sartini D, Emanuelli M, van Haren MJ, Martin NI, Mountford DM, et al. Nicotinamide N-methyltransferase catalyses the N-methylation of the endogenous -carboline norharman: evidence for a novel detoxification pathway. Biochem J. 2016;473(19):3253-67.
4. Pissios P. Nicotinamide N -Methyltransferase: More Than a Vitamin B3 Clearance Enzyme. Trends Endocrinol Metab. 2017;28(5):340-53.
5. Jung J, Kim LJY, Wang X, Wu Q, Sanvoranart T, Hubert CG, et al. Nicotinamide metabolism regulates glioblastoma stem cell maintenance. JCI Insight. 2017;2(10):1-23.
6. Kraus D, Yang Q, Kong D, Banks AS, Zhang L, Rodgers JT, et al. Nicotinamide N-methyltransferase knockdown protects against diet-induced obesity. Nature. 2014;508(7495):258-62.
7. ten Klooster JP, Sotiriou A, Boeren S, Vaessen S, Vervoort J, Pieters R. Type 2 diabetes-related proteins derived from an in vitro model of inflamed fat tissue. Arch Biochem Biophys. 2018;644(February):81-92.
8. Khalil EM, Mackie BD, Mao Y. Methyltransferases: Key Regulators in Cardiovascular Development and Disease. Ann Vasc Med Res. 2016;3(2):1032-9.
9. Fedorowicz A, Mateuszuk Ł, Kopec G, Skórka T, Kutryb-Zając B, Zakrzewska A, et al. Activation of the nicotinamide N-methyltransferase (NNMT)-1-methylnicotinamide (MNA) pathway in pulmonary hypertension. Respir Res. 2016;17(1):108.
10. Ulanovskaya OA, Zuhl AM, Cravatt BF. NNMT promotes epigenetic remodeling in cancer by creating a metabolic methylation sink. Nat Chem Biol. 2013;9(5):300-6.
11. Palanichamy K, Kanji S, Gordon N, Thirumoorthy K, Jacob JR, Litzenberg KT, et al. NNMT Silencing Activates Tumor Suppressor PP2A, Inactivates Oncogenic STKs, and Inhibits Tumor Forming Ability. Clin Cancer Res. 2017;23(9):2325-34.
12. Zhang J, Wang Y, Li G, Yu H, Xie X. Down-Regulation of Nicotinamide N-methyltransferase Induces Apoptosis in Human Breast Cancer Cells via the Mitochondria-Mediated Pathway. Filleur S, ed. PLoS One. 2014;9(2):e89202.
13. Sartini D, Muzzonigro G, Milanese G, Pierella F, Rossi V, Emanuelli M. Identification of

Nicotinamide N-Methyltransferase as a Novel Tumor Marker for Renal Clear Cell Carcinoma. J Urol. 2006;176(5):2248-54.

14. Sartini D, Santarelli A, Rossi V, Goteri G, Rubini C, Ciavarella D, et al. Nicotinamide N-Methyltransferase Upregulation Inversely Correlates with Lymph Node Metastasis in Oral Squamous Cell Carcinoma. Mol Med. 2007;13(7-8):415-21.
15. Parsons RB, Smith SW, Waring RH, Williams AC, Ramsden DB. High expression of nicotinamide N-methyltransferase in patients with idiopathic Parkinson's disease. Neurosci Lett. 2003;342(1-2):13-6.
16. Parsons RB, Smith M-L, Williams AC, Waring RH, Ramsden DB. Expression of Nicotinamide N-Methyltransferase (E.C. 2.1.1.1) in the Parkinsonian Brain. J Neuropathol Exp Neurol. 2002;61(2):111-24.
17. Thomas MG, Saldanha M, Mistry RJ, Dexter DT, Ramsden DB, Parsons RB. Nicotinamide N-methyltransferase expression in SH-SY5Y neuroblastoma and N27 mesencephalic neurones induces changes in cell morphology via ephrin-B2 and Akt signalling. Cell Death Dis. 2013;4(6):e669-e669.
18. van Haren MJ, Thomas MG, Sartini D, Barlow DJ, Ramsden DB, Emanuelli M, et al. The kinetic analysis of the N -methylation of 4-phenylpyridine by nicotinamide N -methyltransferase: Evidence for a novel mechanism of substrate inhibition. Int J Biochem Cell Biol. 2018;98(September 2017):127-36.
19. Aksoy S, Szumlanski CL, Weinshilboum RM. Human liver nicotinamide N-methyltransferase. cDNA cloning, expression, and biochemical characterization. J Biol Chem. 1994;269(20):14835-40. http://www.ncbi.nlm.nih.gov/pubmed/8182091
20. Horning BD, Suciu RM, Ghadiri DA, Ulanovskaya OA, Matthews ML, Lum KM, et al. Chemical Proteomic Profiling of Human Methyltransferases. J Am Chem Soc. 2016;138(40):13335-43.
21. Ruf S, Hallur MS, Anchan NK, Swamy IN, Murugesan KR, Sarkar S, et al. Novel nicotinamide analog as inhibitor of nicotinamide N-methyltransferase. Bioorganic Med Chem Lett. 2018;28(5):922-5.
22. Kannt A, Rajagopal S, Kadnur SV, Suresh J, Bhamidipati RK, Swaminathan S, et al. A small molecule inhibitor of Nicotinamide N-methyltransferase for the treatment of metabolic disorders. Sci Rep. 2018;8(1):3660.
23. Neelakantan H, Wang HY, Vance V, Hommel JD, McHardy SF, Watowich SJ. Structure-Activity Relationship for Small Molecule Inhibitors of Nicotinamide N-Methyltransferase. J Med Chem. 2017;60(12):5015-28.

24. van Haren MJ, Taig R, Kuppens J, Sastre Toraño J, Moret EE, Parsons RB, et al. Inhibitors of nicotinamide N-methyltransferase designed to mimic the methylation reaction transition state. Org Biomol Chem. 2017;15(31):6656-67.
25. Lerner C, Masjost B, Ruf A, Gramlich V, Jakob-Roetne R, Zürcher G, et al. Bisubstrate inhibitors for the enzyme catechol-O-methyltransferase (COMT): influence of inhibitor preorganisation and linker length between the two substrate moieties on binding affinity. Org Biomol Chem. 2003;1(1):42-9.
26. Paulini R, Trindler C, Lerner C, Brändli L, Schweizer WB, Jakob-Roetne R, et al. Bisubstrate Inhibitors of CatecholO-Methyltransferase (COMT): the Crucial Role of the Ribose Structural Unit for Inhibitor Binding Affinity. ChemMedChem. 2006;1(3):340-57.
27. Mori S, Iwase K, Iwanami N, Tanaka Y, Kagechika H, Hirano T. Development of novel bisubstrate-type inhibitors of histone methyltransferase SET7/9. Bioorg Med Chem. 2010;18(23):8158-66.
28. Dowden J, Hong W, Parry R V, Pike RA, Ward SG. Toward the development of potent and selective bisubstrate inhibitors of protein arginine methyltransferases. Bioorg Med Chem Lett. 2010;20(7):2103-5.
29. Van Haren M, Van Ufford LQ, Moret EE, Martin NI. Synthesis and evaluation of protein arginine N-methyltransferase inhibitors designed to simultaneously occupy both substrate binding sites. Org Biomol Chem. 2015;13(2).
30. van Haren MJ, Marechal N, Troffer-Charlier N, Cianciulli A, Sbardella G, Cavarelli J, et al. Transition state mimics are valuable mechanistic probes for structural studies with the arginine methyltransferase CARM1. Proc Natl Acad Sci. 2017;114(14):3625-30.
31. Babault N, Allali-Hassani A, Li F, Fan J, Yue A, Ju K, et al. Discovery of Bisubstrate Inhibitors of Nicotinamide N -Methyltransferase (NNMT). J Med Chem. 2018;61(4):1541-51.
32. Peng Y, Sartini D, Pozzi V, Wilk D, Emanuelli M, Yee VC. Structural Basis of Substrate Recognition in Human Nicotinamide N -Methyltransferase. Biochemistry. 2011;50(36):7800-8.
33. Waters NJ. Preclinical Pharmacokinetics and Pharmacodynamics of Pinometostat (EPZ-5676), a First-in-Class, Small Molecule S-Adenosyl Methionine Competitive Inhibitor of DOT1L. Eur J Drug Metab Pharmacokinet. 2017;42(6):891-901.
34. af Gennäs GB, Talman V, Aitio O, Ekokoski E, Finel M, Tuominen RK, et al. Design, Synthesis, and Biological Activity of Isophthalic Acid Derivatives Targeted to the C1 Domain of Protein Kinase C. J Med Chem. 2009;52(13):3969-81.

35. Cho SD, Park YD, Kim JJ, Falck JR, Yoon YJ. Facile Reduction of Carboxylic Acids, Esters, Acid Chlorides, Amides and Nitriles to Alcohols or Amines Using NaBH 4 /BF 3 ·Et 2 O. Bull Korean Chem Soc. 2004;25(3):407-9.
36. Maruoka H, Muto T, Tanaka T, Imajo S, Tomimori Y, Fukuda Y, et al. Development of 6-benzyl substituted 4-aminocarbonyl-1,4-diazepane-2,5-diones as orally active human chymase inhibitors. Bioorg Med Chem Lett. 2007;17(12):3435-9.
37. Pola Chemical Industries Inc.; Yokoyama, Kouji; Kimura, Makoto; Tamai, Masashi; Saitoh, Yuko; Kato, Tomomi; Ikeda Y. Melanin Production Inhibitor. :US Patent 8,846,012, September 30, 2014.
38. Schreiber KC, Fernandez VP. The Lithium Aluminum Hydride Reduction of Some N-Substituted Succinimides 1. J Org Chem. 1961;26(6):1744-7.
39. Colombo R, Mingozzi M, Belvisi L, Arosio D, Piarulli U, Carenini N, et al. Synthesis and Biological Evaluation (in Vitro and in Vivo) of Cyclic Arginine–Glycine–Aspartate (RGD) Peptidomimetic–Paclitaxel Conjugates Targeting Integrin α V β 3. J Med Chem. 2012;55(23):10460-74.
40. Chi Y, English EP, Pomerantz WC, Horne WS, Joyce LA, Alexander LR, et al. Practical Synthesis of Enantiomerically Pure β 2 -Amino Acids via Proline-Catalyzed Diastereoselective Aminomethylation of Aldehydes. J Am Chem Soc. 2007;129(18):6050-5.
41. Wernic D, DiMaio J, Adams J. Enantiospecific synthesis of L-.alpha.-aminosuberic acid. Synthetic applications in preparation of atrial natriuretic factor analogs. J Org Chem. 1989;54(17):4224-8.
42. Seta R, Mascitti M, Campagna R, Sartini D, Fumarola S, Santarelli A, et al. Overexpression of nicotinamide N-methyltransferase in HSC-2 OSCC cell line: effect on apoptosis and cell proliferation. Clin Oral Investig. 2019;23(2):829-38.
43. Myung-Hwa Kim, Kwangwoo Chun, Jae-Won, ChoiBo-Young Joe, Sang-Woo Park, Kwang Hee Kim, Byung-Kyu Oh J-HC. Tricyclic derivatives or pharmaceutically acceptable salts thereof, their preparations and pharmaceutical compositions containing them. :US Patent 2007/0179143 A1, August 2, 2007.
44. Ewa B, Maciej W, Marcin S, Grzegorz D, Michał Z, Jan P, et al. The development of first Staphylococcus aureus SplB protease inhibitors: Phosphonic analogues of glutamine. Bioorg Med Chem Lett. 2012;22(17):5574-8.
45. Chen S, Zhao X, Chen J, Chen J, Kuznetsova L, Wong SS, et al. Mechanism-Based Tumor-Targeting Drug Delivery System. Validation of Efficient Vitamin Receptor-Mediated

Endocytosis and Drug Release. Bioconjug Chem. 2010;21(5):979-87.

46. Berk SC, Kreutzer KA, Buchwald SL. A catalytic method for the reduction of esters to alcohols. J Am Chem Soc. 1991;113(13):5093-5.
47. Liu F, Zha H-Y, Yao Z-J. Synthesis of a New Conformation-Constrained L-Tyrosine Analogue as a Potential Scaffold for SH2 Domain Ligands. J Org Chem. 2003;68(17):6679-84.
48. Floyd N, Vijayakrishnan B, Koeppe JR, Davis BG. Thiyl Glycosylate of Olefinic Proteins: S-Linked Glycoconjugate Synthesis. Angew Chemie Int Ed. 2009;48(42):7798-802.
49. Morris GM, Huey R, Lindstrom W, Sanner MF, Belew RK, Goodsell DS, et al. AutoDock4 and AutoDockTools4: Automated docking with selective receptor flexibility. J Comput Chem. 2009;30(16):2785-91.
50. Abraham MJ, Murtola T, Schulz R, Páll S, Smith JC, Hess B, et al. GROMACS: High performance molecular simulations through multi-level parallelism from laptops to supercomputers. SoftwareX. 2015;1-2:19-25.
51. Ponder JW, Case DA. Force fields for protein simulations. Adv Protein Chem. 2003;66:27-85. http://www.ncbi.nlm.nih.gov/pubmed/14631816
52. Mahoney MW, Jorgensen WL. A five-site model for liquid water and the reproduction of the density anomaly by rigid, nonpolarizable potential functions. J Chem Phys. 2000;112(20):8910-22.
53. Parrinello M, Rahman A. Polymorphic transitions in single crystals: A new molecular dynamics method. J Appl Phys. 1981;52(12):7182-90.
54. Kumari R, Kumar R, Lynn A. g_mmpbsa —A GROMACS Tool for High-Throughput MM-PBSA Calculations. J Chem Inf Model. 2014;54(7):1951-62.
55. Baker NA, Sept D, Joseph S, Holst MJ, McCammon JA. Electrostatics of nanosystems: Application to microtubules and the ribosome. Proc Natl Acad Sci. 2001;98(18):10037-41.
56. Vedadi M, Barsyte-Lovejoy D, Liu F, Rival-Gervier S, Allali-Hassani A, Labrie V, et al. A chemical probe selectively inhibits G9a and GLP methyltransferase activity in cells. Nat Chem Biol. 2011;7(8):566-74.
57. Neelakantan H, Vance V, Wetzel MD, Wang HYL, McHardy SF, Finnerty CC, et al. Selective and membrane-permeable small molecule inhibitors of nicotinamide N-methyltransferase reverse high fat diet-induced obesity in mice. Biochem Pharmacol. 2018;147:141-52.
58. Policarpo RL, Decultot L, May E, Kuzmič P, Carlson S, Huang D, et al. High-Affinity Alkynyl Bisubstrate Inhibitors of Nicotinamide N -Methyltransferase (NNMT). J Med

Chem. 2019;62(21):9837-73.

Chapter 3

Potent inhibition of nicotinamide *N*-methyltransferase by alkene-linked bisubstrate mimics bearing electron-deficient aromatics

Parts of this chapter have been patented and submitted for publication in:
Netherlands Priority Patent Application No. N2027866; Title: Inhibitors of Nicotinamide N-Methyl Transferase (NNMT) Inventors: Martin, N.I., **Gao, Y.**, van Haren, M.J., Buijs, N., Parsons, R.B., Emanuelli, M., Sartini, D. Priority date: March 30, 2021.
Gao, Y.; van Haren, M.J.; Buijs, N.; Innocenti, P.; Zhang, Y.; Sartini, D. Campagna, R.; Emanuelli, M.; Parsons, R.B.; Jespers, W.; Gutiérrez-de-Terán, H.; van Westen, G.; Martin, N.I.; (2021) Potent Inhibition of Nicotinamide *N*-Methyltransferase by Alkene-Linked Bisubstrate Mimics Bearing Electron Deficient Aromatics. *J. Med. Chem*. In press. DOI:10.1021/acs.jmedchem.1c01094

Abstract

Nicotinamide *N*-methyltransferase (NNMT) methylates nicotinamide (vitamin B3) to generate 1-methylnicotinamide (MNA). NNMT overexpression has been linked to a variety of diseases, most prominently human cancers, indicating its potential as a therapeutic target. The development of small molecule NNMT inhibitors has gained interest in recent years with the most potent inhibitors sharing many similar structural features based on the structures of the nicotinamide substrate and the *S*-adenosyl-L-methionine (SAM) cofactor. We here report the development of a series of inhibitors that depart from some of these conserved structural features through the introduction of alternative electron deficient aromatic groups to mimic the nicotinamide moiety. In addition, the identification of an optimal trans-alkene linker differs from the previously reported alkyl and alkynyl linkers used to connect the substrate and cofactor mimics in these inhibitors. The most potent NNMT inhibitor identified in our study exhibits an IC_{50} value of 3.7 nM placing it among the most active NNMT inhibitors reported to date. Complementary analytical techniques, modeling studies, and cell-based assays provide insight into the binding mode, affinity, and selectivity of these inhibitors.

1. Introduction

The enzyme nicotinamide *N*-methyltransferase (NNMT) catalyzes the methylation of nicotinamide using *S*-adenosyl-L-methionine (SAM) as cofactor and produces *S*-adenosyl-L-homocysteine (SAH) as byproduct (Figure 1). Since its discovery in 1952, its role was considered to be exclusively associated with cell detoxification through the metabolism of xenobiotics.[1] This function is carried out thanks to NNMT's broad substrate recognition that allows for the methylation of pyridines, quinolines and other related heterocyclic metabolites, followed by their excretion.[2] However, the view that NNMT is primarily involved in detoxification has recently changed as a result of numerous studies implicating NNMT in a variety of other critical metabolic pathways.[3,4] For example, NNMT's substrate nicotinamide is the precursor of NAD^+, a compound heavily involved in redox processes and energy management.[5] In addition, while NNMT does not play an epigenetic role *per se*, its influence on the SAM/SAH balance has an indirect impact on gene expression.[6,7] The involvement of NNMT in epigenetic reprogramming as well as in the cell's energetic balance and detoxification pathways provides a broader appreciation of its role in the development and progression of cancer,[3,6,8–12] diabetes,[5,13,14] obesity,[5,14] and neurodegenerative disorders.[15–18]

Improving our understanding of NNMT and its role in disease hinges in significant part on the availability of potent, selective, and cell-active small-molecule inhibitors. Such chemical tools can both lead the way to validate NNMT as a drug target and at the same time be used as templates for the development of new medicines for treating NNMT-driven conditions. At present, the most potent NNMT inhibitors described in the literature are bisubstrate analogues, comprising two covalently linked moieties that mimic the cofactor and substrate, SAM and nicotinamide, respectively. Following our initial reports describing such bisubstrate mimics as NNMT inhibitors,[19,20] significant progress has been made by other groups also working in the

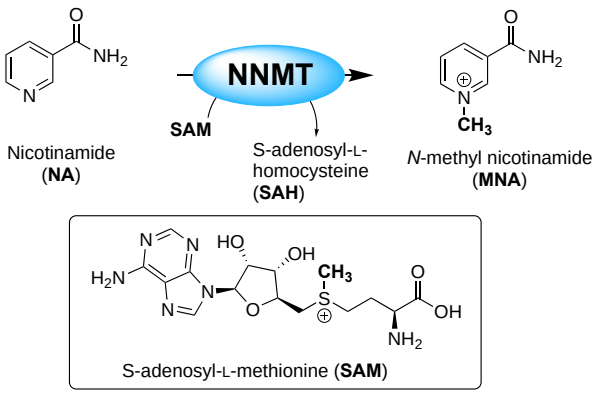

Figure 1. Methylation of nicotinamide (NA) by NNMT using *S*-adenosyl-L-methionine (SAM) as the methyl donor forming *N*-methyl nicotinamide (MNA) and *S*-adenosyl-L-homocysteine (SAH).

field (Figure 2) [21–24] Notably, the potency of bisubstrate NNMT inhibitors has improved from our first reported compounds with IC_{50} values in the micromolar range[19,20,25] to those more recently described by the groups of Shair and Huang with IC_{50} values in the low nanomolar range.[26,27] Collectively, these studies have shown that bisubstrate inhibitor potency is heavily dependent on the relative spacing and spatial orientation of the adenosine, amino acid, and nicotinamide mimicking moieties.[19,20,25–27] Notable in this regard are the different linkers that have been used to connect the SAM and nicotinamide groups, amongst which alkynyl species have been shown to achieve the highest levels of inhibition (Figure 2). Building on our previous endeavors in designing inhibitors for NNMT[19,20] and bisubstrate inhibitors for other methyltransferases containing alkene-based linkers,[28,29] we here describe our most recent efforts at developing novel NNMT inhibitors characterized by innovative design, improved potency, and ease of synthesis. These investigations have culminated in the discovery of a novel styrene scaffold with substitutions in the nicotinamide mimetic that get away from the amide functionality present in the majority of bisubstrate inhibitors reported to date. Our results with this new scaffold also revealed interesting structure-activity relationships of electron-withdrawing substitutions with *para*-cyano compound **17u (Figure 2)** being the most potent inhibitor identified with an IC_{50} value of 3.7 ± 0.2 nM. The extensive SAR results presented here were further corroborated by insights in the compounds' binding mode to NNMT as predicted by molecular modeling. Compound **17u** was further characterized by means of isothermal titration calorimetry (ITC) experiments, biochemical assays to assess selectivity against other methyltransferases, and cell-based studies to assess investigate effects on the viability of several cancer cell lines.

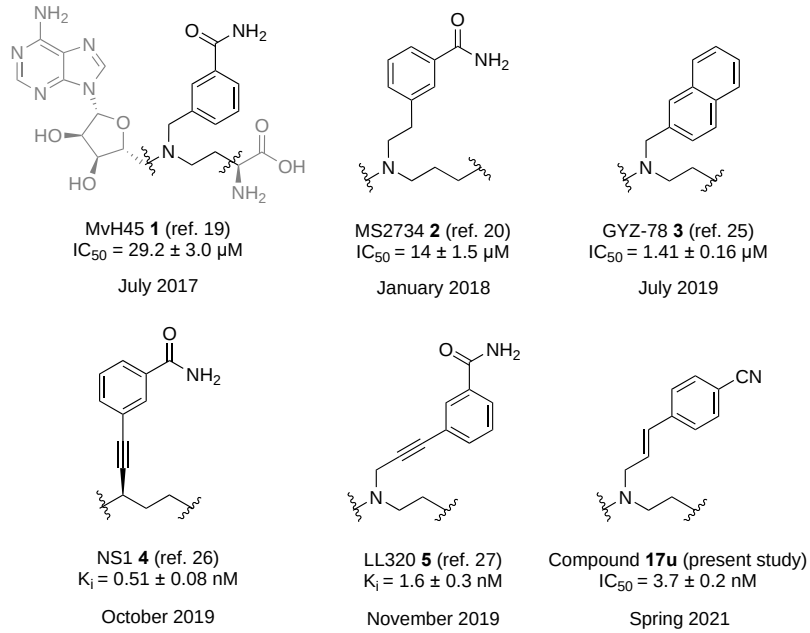

Figure 2. Chemical structures, inhibition data, and publication dates of bisubstrate inhibitors of NNMT.

2. Results and Discussion

Design. The crystal structures reported for NNMT consistently reveal π-π stacking interactions between tyrosine residue Y204 and either the pyridine ring of the natural nicotinamide substrate[30] or the aromatic group that mimics it in the bisubstrate inhibitors.[25–27] In order to capitalize on these interactions and improve the potency of our previously disclosed NNMT ligand **3**,[20] we first undertook a systematic exploration of its naphthalene portion (Figure 3A) where a selection of bicyclic (hetero)aromatics was incorporated. In addition, prompted by the desire for an approach which would allow for the introduction of a wider range of nicotinamide mimics with different shapes and electronic features, a novel styrene-based scaffold was devised. This scaffold-hopping approach, which was based on a naphthalene truncation strategy (Figure 3A), presents two key advantages: i) it allows for the expeditious synthesis of a diverse library of NNMT inhibitors starting from readily available building blocks; and ii) it provides insights into a novel alkenyl linker connecting the SAM-like portion and the nicotinamide mimic moiety. The latter feature is relevant because the resulting ligands complement the published bisubstrate inhibitors (Figure 2), which are generally linked by alkyl or alkynyl spacers.[25–27] In addition, a selection of compounds was designed to assess the importance

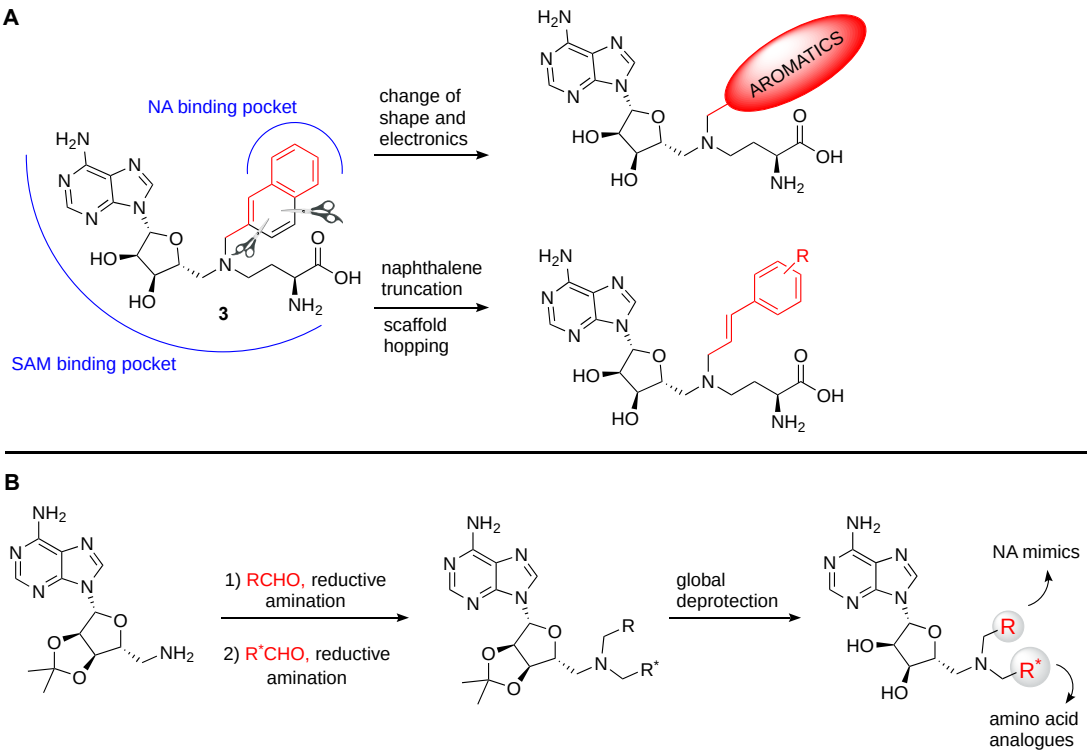

Figure 3. (A) Strategy for the modification and optimization of inhibitor **3** through introduction of a variety of aromatics and the truncation of the naphthalene moiety resulting in the introduction of the alkenyl linker; **(B)** General synthetic route for the preparation of NNMT inhibitors, based on a double reductive amination approach followed by a single deprotection step.

of both the amino acid and adenosine moieties for NNMT active site binding.

Synthesis. The synthesis of the NNMT inhibitors here pursued was based on a convenient, modular strategy that provides access to a wide range of chemically different ligands. Starting from the known adenosine amine building block **9**, all bisubstrate analogues were obtained via a sequential double reductive amination process followed by global deprotection (Figure 3B). The required bicyclic (hetero)aromatic aldehydes **8a-l** used in the reductive amination steps were either commercially available or prepared through formation of the Weinreb amide and subsequent DIBAL-H reduction (Scheme 1). Phenylpropenaldehydes **15a-y** were either commercially available or prepared through a Wittig reaction coupling the corresponding benzaldehydes to (triphenyl-phosphoranylidene)acetaldehyde as shown in Scheme 2. The aldehydes were subsequently coupled to compound **11** (prepared by reductive amination of adenosine amine building block **9** with the appropriate l-Asp derived aldehyde building block **10**). These reductive aminations were found to proceed cleanly using sodium triacetoxyborohydride and acetic acid after which the final compounds were obtained by global deprotection of the acid-labile protecting groups using TFA/CH_2Cl_2, with isopropylidene group cleavage facilitated by the addition of water (Scheme 1 and 2).

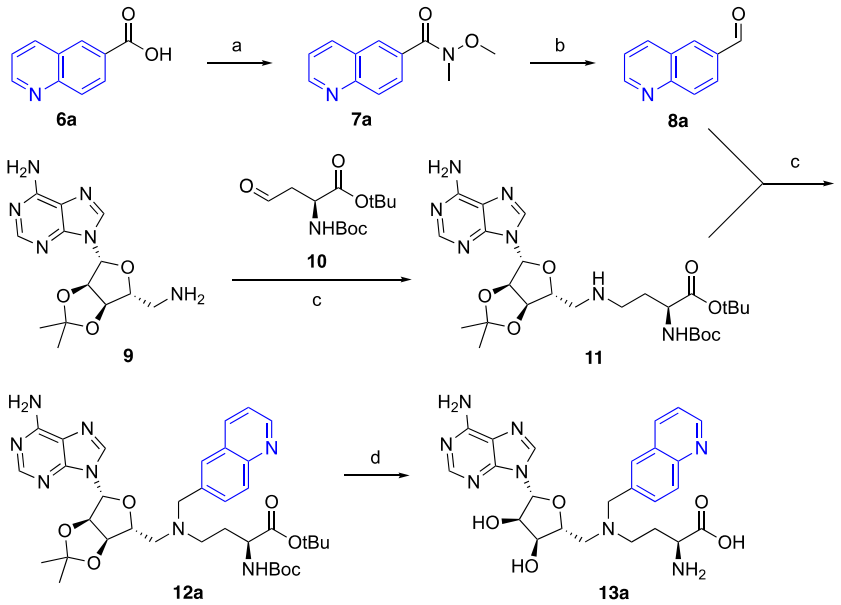

Scheme 1. Representative synthetic scheme for the preparation of bicyclic aromatic compounds **13a-l**, shown for quinoline-containing compound **13a**.[a] The variable group for compounds **6b-l**, **7b-l**, **8b-l**, **12b-l** and **13b-l** is indicated in blue. Reagents and conditions: (a) CH_3NHOCH_3·HCl, BOP, Et_3N, CH_2Cl_2, rt, 2 h (88%); (b) DIBAL-H in hexanes, THF, −78 °C, 2 h (assumed quant.); (c) $NaBH(OAc)_3$, AcOH, DCE, rt, overnight (47%); (d) TFA, CH_2Cl_2, H_2O, rt, 2 h. (86%).

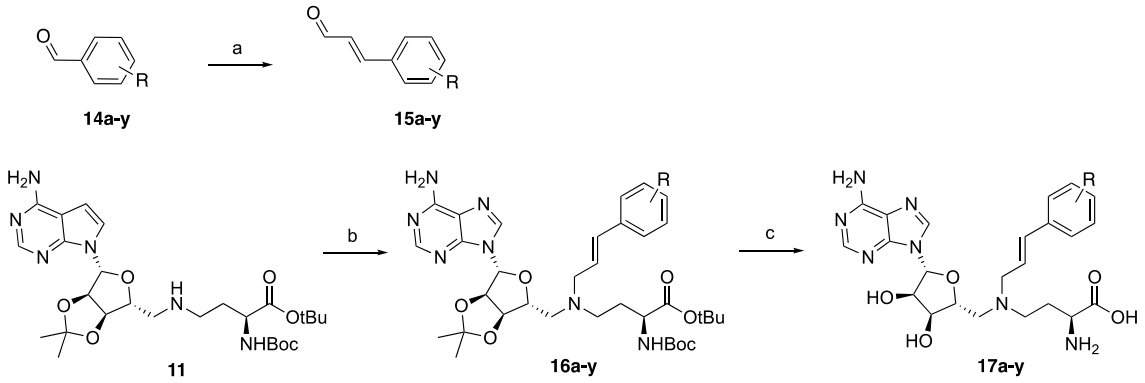

Scheme 2. Representative synthetic scheme for the preparation of substituted cinnamaldehydes **15a-y** and resulting alkenyl linked aromatic compounds **17a-y**. Reagents and conditions: (a) PPh_3=CHCHO, toluene, 80°C, overnight (45-77%); (b) aldehyde **15a-y**, $NaBH(OAc)_3$, AcOH, DCE, rt, overnight (43-81%); (c) TFA, CH_2Cl_2, H_2O, rt, 2 h, (27-86%).

In order to investigate different substitutions of the amino acid moiety, building block **18** containing the *para*-cyano-substituted phenylpropenyl side chain, was prepared through coupling of 4-cyano-phenylpropenaldehyde **15u** to the adenosine amine starting material **9** (Scheme 3). A variety of aldehydes were then coupled to probe the amino acid pocket as exemplified for compound **21a** in which the amino acid linker was extended with an extra carbon. Compounds **24a** and **24b** lacking the adenosine unit were also synthesized in a similar fashion

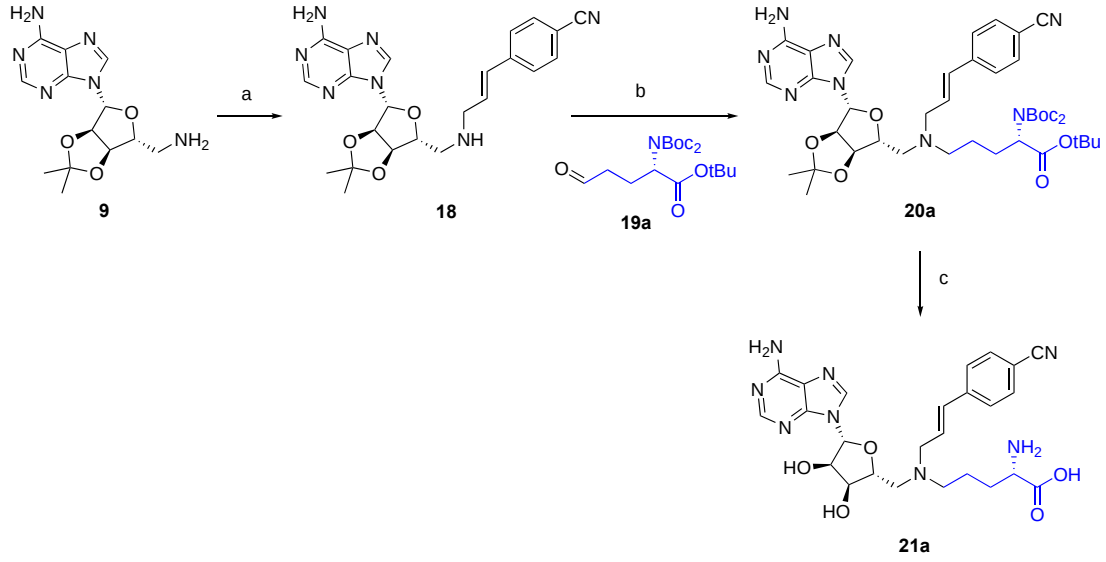

Scheme 3. Representative synthetic scheme for the preparation of 4-cyano-phenylpropenyl compounds with different substitutions of the amino acid side chain, shown for compound **21a** bearing an extended linker to the amino acid moiety. The variable group in compounds **19b-k**, **20b-k** and **21b-k** is indicated in blue. Reagents and conditions: (a) aldehyde **15u**, $NaBH(OAc)_3$, AcOH, DCE, rt, overnight (81%); (b) aldehyde **19a**, $NaBH(OAc)_3$, AcOH, DCE, rt, overnight (81%); (c) TFA, CH_2Cl_2, H_2O, rt, 2 h, (86%).

through coupling of amino acid aldehyde **10** to 4-cyano-phenylpropenylamine **22a** or its methylated analogue **22b (Scheme 4)**. The crude products were purified by preparative high-performance liquid chromatography (HPLC) to yield the desired bisubstrate analogues.

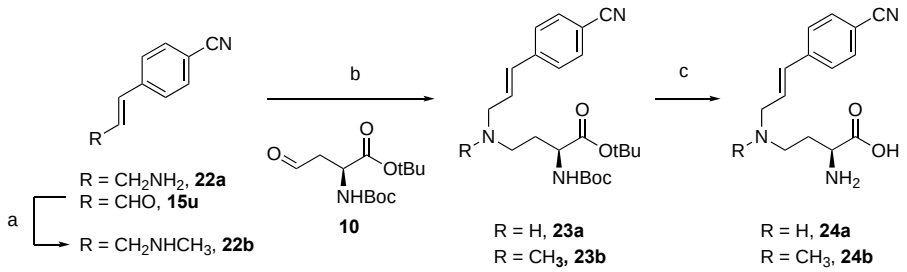

Scheme 4. Synthetic scheme for the preparation of 4-cyano-phenylpropenyl compounds **24a-b** lacking the adenosine unit.[a] Reagents and conditions: (a) methylamine in MeOH (33% w/w), $NaBH(OAc)_3$, AcOH, DCE, rt, overnight (42%); (b) aldehyde **22**, $NaBH(OAc)_3$, AcOH, DCE, rt, overnight (48-77%); (c) TFA, CH_2Cl_2, H_2O, rt, 2 h, (75-87%)

Inhibition Studies. All bisubstrate analogues prepared were tested for NNMT inhibitory activity using a method recently developed in our group.[2] This assay employs hydrophilic liquid interaction chromatography (HILIC) coupled with tandem mass spectrometry (MS/MS) to rapidly and efficiently assess NNMT inhibition through direct analysis of the formation of MNA. For each compound, NNMT inhibition was initially screened at a fixed inhibitor concentration of 25 μM. In cases where at least 50% inhibition was detected at this concentration, full inhibition curves were measured in triplicate to determine the corresponding half-maximal inhibitory concentration (IC_{50}) values. As reference compounds, we included our previously described NNMT inhibitor **3** and the recently described NNMT inhibitor **5**. The structures of these reference compounds are provided above in Figure 2 and the IC_{50} values obtained in our assay were found to be in line with published values.[20,27]

Structure–Activity Relationships (SAR): β-naphthalene modification. As previously mentioned, we aimed at improving the potency of our previously reported inhibitor **3** through further exploitation of the π-π stacking interactions between Y204 and the ligand's nicotinamide mimicking motif. To this end, a small library of compounds was made, in which the naphthalene moiety of compound **3** was replaced with other (hetero)aromatic groups (compounds **13a-l**, Figure 4). The introduction of electron-poor quinolines, which could potentially complement Y204 in a productive π-π stacking interaction, was met with poor results as the IC_{50} values of

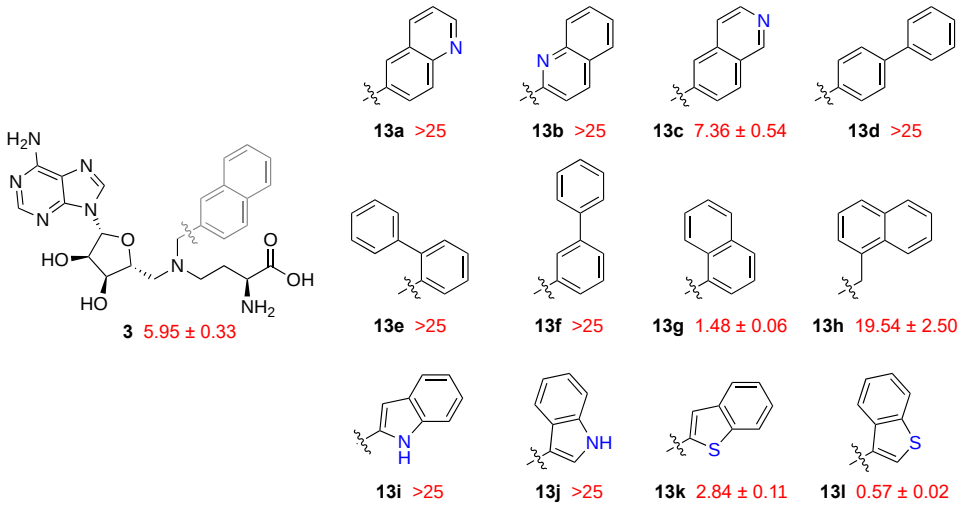

Figure 4. Structure–activity relationship (SAR) studies of bisubstrate NNMT inhibitors **13a-l** carrying bicyclic (hetero)aromatic side-chains to replace the naphthalene group of compound **3**. IC_{50} values (μM) and s.e.m. are shown in red.

compounds **13a** and **13b** were above the 25 μM threshold, with only compound **13c** showing moderate inhibition (IC_{50} = 7.36 μM). Although the incorporation of an α-naphthalene led to good inhibition (**13g**, IC_{50} = 1.48 μM), the addition of an extra carbon to the linker portion abrogated it (**13h**, IC_{50} = 19.54 μM) and switching to biphenyl resulted in a considerable drop in potency (**13d-f**, IC_{50} > 25 μM). A similar trend was observed with the introduction of an indole moiety, with inhibitors **13i** and **13j** failing to display IC_{50} values below 25 μM. Improved potency was achieved when a benzothiophene ring was incorporated (**13k** and **13l**) and especially when the branching point was at its C-3 position. Notable in this regard is compound **13l** which was found to inhibit NNMT with an IC_{50} value of 0.57 μM (Figure 4).

Scaffold hopping to styrene inhibitors. In light of the only moderate level of success obtained by introduction of other bicyclic (hetero)aromatic groups, we next shifted our focus to a different approach. Specifically, we applied a scaffold-hopping/truncation strategy to compound **3**, in which the naphthalene moiety was simplified into styrene derivatives **17a-y** (Figure 3A). Notably, this structural alteration and accompanying synthetic route, along with the wide availability of substituted benzaldehydes, allowed for ready access to a wide range of novel bisubstrate analogues (Figure 5).

The various styrene analogues thus prepared (**17a-y**) bear different electron-donating and electron-withdrawing substituents at *ortho*, *meta* and *para*-positions, and were evaluated for their *in vitro* activity against NNMT. *Ortho* methyl compound **17a** (IC_{50} = 1.16 μM) showed better

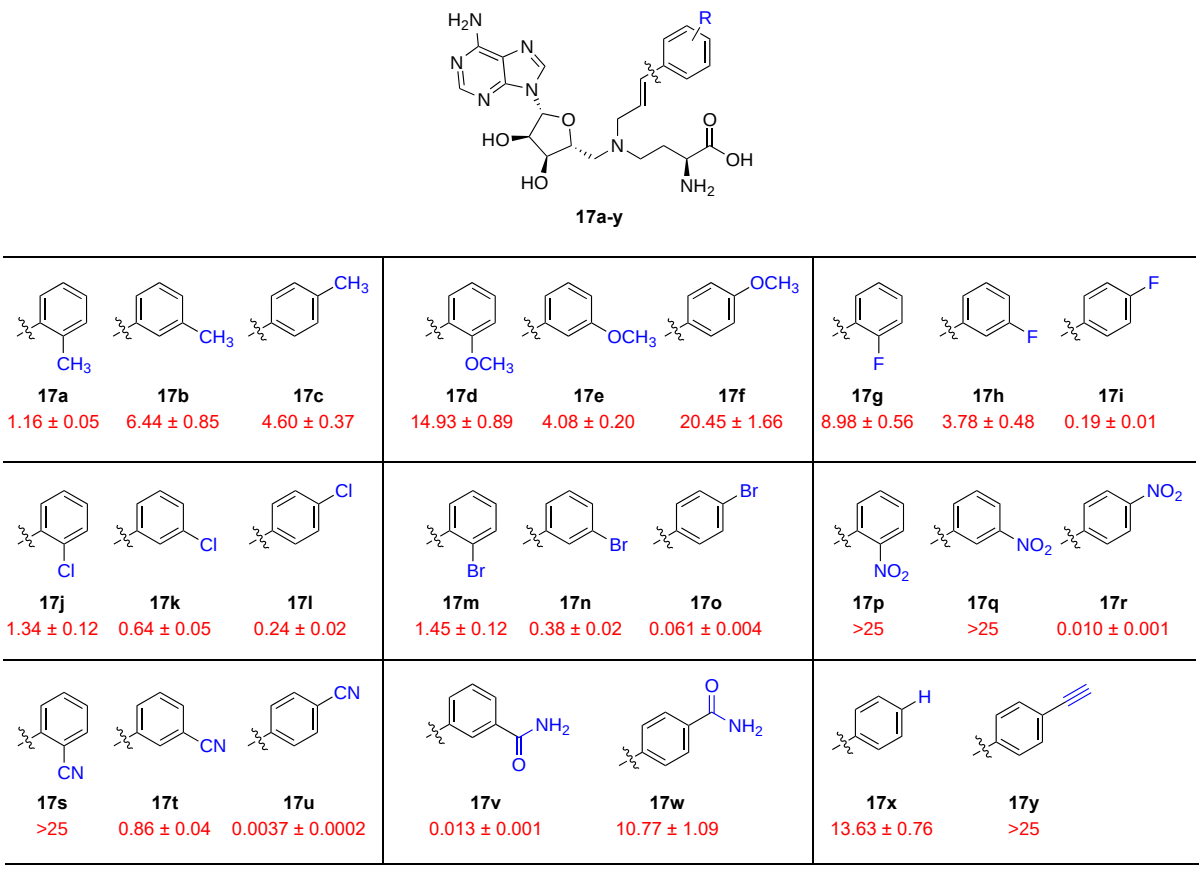

Figure 5. SAR studies of bisubstrate NNMT inhibitors **17a-y** carrying alkenyl linked substituted aromatics. IC_{50} values (μM) and s.e.m. are shown in red and the substitutions are highlighted in blue

activity than the corresponding *meta* (**17b**, IC_{50} = 4.60 μM) and *para* (**17c**, IC_{50} = 6.44 μM) analogues. Methoxy-substituted compounds **17d-f** all showed a somewhat lower potency (IC_{50} ≥ 4 μM). A clear improvement was observed when electron-withdrawing substituents were introduced on the styrene ring. In addition, the orientation of the electron-withdrawing group was directly correlated to its activity with the potency of the compounds increasing from *ortho*- to *meta*- to *para*-substitution. In the case of fluorinated ligands **17g-i**, the activity increased with an IC_{50} value of 8.98 μM for *ortho*-F, to 3.78 μM for *meta*-F and the most potent activity observed for the *para*-F substituted compound displaying an IC_{50} value of 0.19 μM. The introduction of a chlorine atom in the same styrene scaffold resulted in a similar trend in NNMT inhibitory activity. In this instance, the IC_{50} values for the *ortho*-Cl and *meta*-Cl compounds were 1.34 μM and 0.64 μM, respectively (**17j** and **17k**, Figure 5), while *para*-analogue **17l** (IC_{50} = 0.24 μM) was again the most active. Switching chlorine for bromine did not cause any major change in activity for the *ortho*-Br and *meta*-Br analogues (**17m** and **17n**, IC_{50} = 1.45 and 0.38 μM, respectively), but positively impacted NNMT inhibition in the case of the *para*-Br compound **17o**, which displayed

nanomolar activity (IC_{50} = 0.061 μM, Figure 5). Even more striking was the case of nitro-substituted compounds **17p-r**: while the *para*-nitro-substituted analogue was found to be a highly potent inhibitor (**17r**, IC_{50} = 0.010 μM), both *ortho*-nitro and *meta*-nitro compounds failed to show any appreciable activity (**17p** and **17q**, IC_{50} >25 μM). Finally, introduction of nitrile functionality on the styrene core caused yet further improvements in potency, especially when situated at the *para* position. Whereas *ortho*-cyano analogue **17s** did not show inhibition at 25 μM, *meta*-cyano analogue **17t** displayed good inhibition with an IC_{50} of 0.86 μM with another leap in activity for *para*-cyano compound **17u** which exhibits the most potent inhibition of all compounds prepared in the present study with a single digit nanomolar IC_{50} value (IC_{50} = 3.7 nM).

We next assessed the potential for combining structural features of these new NNMT inhibitors with known potent inhibitors **4** and **5** (Figure 2). In doing so, we generated two styrene-based compounds inspired by **17u** in which the nitrile functionality was replaced by a *meta*- or *para*-substituted primary amide (**17v** and **17w**). Notably, the *para*-amide showed a marked decrease in potency (IC_{50} = 10.77 μM) while the *meta*-amide proved to be an active NNMT inhibitor (IC_{50} = 0.013 μM). The behaviour of these two analogues highlighted an interesting trend: whereas for the cyano substituent the *para*-arrangement is superior to the *meta* one, for amides the contrary holds true. Interestingly, unsubstituted compound **17x** exhibited only very modest potency (IC_{50} = 13.63 μM). Finally, it is worth noting that *para*-alkynyl substituted compound **17y**, in which the nitrile group of **17u** was replaced by an acetylene, was completely inactive with an IC_{50} >25 μM. This result clearly indicates as specific role for the nitrile functionality in facilitating productive binding interactions between the inhibitor and the NNMT active site.

From the data presented above, it can be inferred that a strongly electron-rich styrene moiety is not beneficial for NNMT inhibition. Also, it is clear that electron-withdrawing substituents like nitro or cyano are most effective when located at the *para* position on the aromatic ring. The origin of these trends is likely a combination of structural complementarity and electronics. For example, the geometric constraints of the binding pocket could be favouring the *para* substitution pattern, while a particularly effective π-π stacking between NNMT's tyrosine residue Y204 and the electron-poor styrene of compounds **17o**, **17r** and **17u** might lie behind these ligands' potency.

Linker modifications. After having established compound **17u** as our lead inhibitor, we turned our attention to the role of the linker bridging the SAM-derived motif and the nicotinamide mimicking moiety. Our own work in the field had already highlighted the importance of the

correct spacing for achieving potent NNMT inhibition.[20] Moreover, reports by other groups have reinforced the notion that a carefully judged linker, in terms of both length and rigidity, is required for potency (see compounds **2**, **4** and **5**, Figure 2).[25–27] In order to compare our own alkenyl linker with the alternatives devised by others, a series of analogues of inhibitor **17u** were designed featuring a truncated linker (**25**), a fully saturated linker (**26**) and a propargylic linker (**27** and **28**, Figure 6). Additionally, compound **29** was prepared to assess the impact of replacing the core amine functionality with an amide linkage.

Both the truncated analogue **25** and amide-linked compound **29** displayed a clear drop in

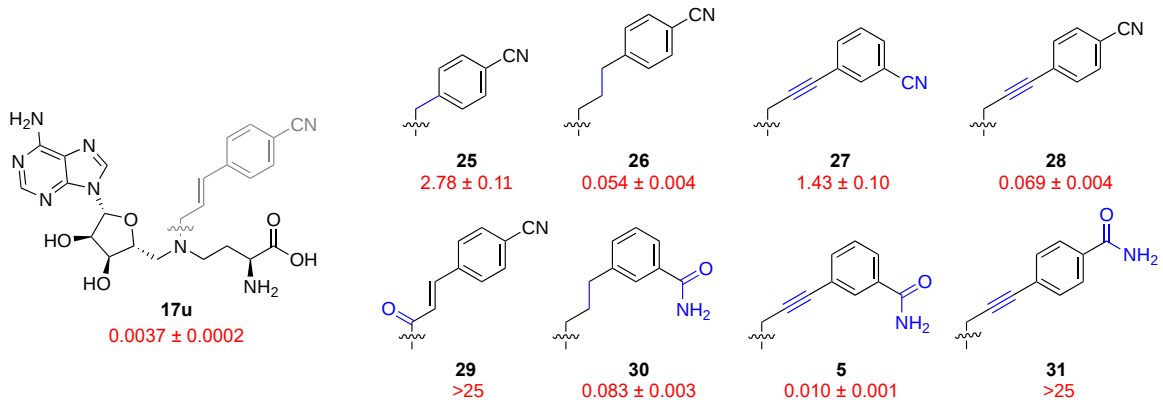

Figure 6. SAR studies of bisubstrate NNMT inhibitors **5** and **25**-**31** carrying different linkers. IC_{50} values (μM) and s.e.m. are shown in red. Changes introduced relative to the lead inhibitor **17u** are indicated in blue.

activity against NNMT (IC_{50} = 2.78 μM and > 25 μM respectively). When the carbon-carbon double bond of inhibitor **17u** was reduced to a saturated three carbon linker, the IC_{50} value increased more than 10-fold (**26**, IC_{50} = 0.054 μM), but the resulting compound still showed high potency. A similar outcome was observed when a propargyl spacer was introduced (**28**, IC_{50} = 0.069 μM).

In recently reported studies involving propargyl linked bisubstrate inhibitors of NNMT, the benzamide fragment featured prominently as the favoured nicotinamide mimic.[25–27] Of note in this regard is the importance of the position of the amide group on the aromatic ring with the *para* substituted amide (**31**) displaying a clear lack of potency (IC_{50} >25 μM) relative to the *meta* compound (**5**[27]) which was measured to have an IC_{50} value of 0.010 μM in our assay. Notably, a similar effect is also observed for the alkenyl linked amides **17v** and **17w** reported in our present study (Figure 5) with the *meta*-substituted analogue displaying a nearly 1000-fold increase in NNMT inhibition. Also of note was the observation that this trend is reversed for the corresponding propargyl-linked *meta*- and *para*-cyano analogues: in this case the *meta* isomer **27**

was a much weaker inhibitor (IC_{50} = 1.43 μM) than the *para* isomer **28** (IC_{50} = 0.069 μM, Figure 6). Finally, as also observed for the fully reduced *para*-cyano analogue **26**, replacement of the unsaturated linker in potent literature inhibitor **5** with a fully saturated alkyl linker led to compound **30** which exhibits reduced activity but retains nanomolar inhibition (IC_{50} = 0.083 μM).

The exploration of different linkers in conjunction with optimized nicotinamide mimicking moieties revealed that nitrile- and amide-substituted aromatics confer high level of NNMT inhibition, with the former narrowly outperforming the latter in our hands. Similarly, our newly developed unsaturated linker compared favourably with the alkyne-based linkers previously described.[26,27] Taking a closer look at this finding, the potency of tight binding alkenyl and alkynyl linked *para*-cyano (**17u** and **28**) and *meta*-amide (**17v** and **5**) inhibitors was reevaluated in the presence of elevated concentrations of cofactor SAM to increase their IC_{50} value, magnifying their differences in potency.[31] The four compounds tested bear the same SAM-mimicking motif and are assumed to be equally SAM-competitive and thus similarly affected by increased levels of the cofactor. Increasing the concentration of SAM to 85 μM (10 times its K_M value) in the biochemical assay, resulted in a 2- to 4-fold increase in IC_{50}, confirming the trend observed under standard assay conditions. In addition, the apparent K_i values were calculated using Morrison's equation for tight binding inhibitors[32] and found to be similar under both SAM concentrations tested (Table 1). These studies confirm compound **17u** as the most potent NNMT inhibitor evaluated in the present study.

Table 1. IC_{50} and Ki_{app} values in nM with standard error of the mean (s.e.m.) for para-cyano compounds **17u** and **28** and meta-amide compounds **17v** and **5** with either propenyl or propargyl linkers. Compounds were tested in the presence of SAM at its K_M value of 8.5 μM or at 10 times its K_M value (85 μM)

	IC_{50} in nM		Ki_{app} in nM	
Compound	**8.5 μM SAM**	**85 μM SAM**	**8.5 μM SAM**	**85 μM SAM**
17u (alkene p-CN)	3.69 ± 0.17	16.00 ± 1.48	1.70 ± 0.12	1.49 ± 0.22
28 (alkyne p-CN)	69.29 ± 4.42	258.25 ± 26.21	34.90 ± 2.58	35.38 ± 0.96
17v (alkene m-$CONH_2$)	12.76 ± 0.78	39.53 ± 4.52	6.93 ± 1.15	5.23 ± 4.52
5 (alkyne m-$CONH_2$)	10.23 ± 0.90	21.66 ± 1.61	5.11 ± 0.44	2.48 ± 0.32

Amino acid and adenosine modifications. After having identified an optimal nicotinamide mimic/linker combination for potent NNMT inhibition, a small selection of ligands with modifications to other parts of the scaffold was next investigated. Structural alterations of the amino acid portion of **17u** (Figure 7) revealed a very steep SAR with all analogues exhibiting IC_{50} values several orders of magnitude higher than the parent compound. Compound **21a**, an

extended three-carbon homolog of **17u**, was significantly less active compared to the parent compound, but still showed submicromolar potency (IC_{50} = 0.36 μM). It is also clear that the amino group of the amino acid moiety is critical for inhibition, as compounds **21f** and **21g** lost all activity. Removal of the carboxylic acid was tolerated slightly better, with amine **21e** showing an IC_{50} value in the low micromolar range (0.96 μM). Amino amide analogue **21b** showed a strong decrease in potency (1.90 μM), which was further diminished upon removal of the primary amine (**21c** and **21d**, IC_{50} >25 μM). Replacement of the amino acid moiety with a pyridinone mimic[33] (**21h**) was also not tolerated. When the entire amino acid chain was swapped for a lipophilic methyl or isopropyl group as in compounds **21j** and **21k**, all activity against NNMT was lost (both IC_{50} >25 μM). Notable, however, is the fully truncated, secondary amine **21i** that was surprisingly found to be active, albeit in the low micromolar range. Taken together, the results presented here demonstrate the crucial role the amino acid motif plays in the interaction of these bisubstrate inhibitors in the NNMT binding pocket. Similarly, two truncated analogues of inhibitor **17u**, lacking the adenosine unit (**24a** and **24b**, see Figure 7) or lacking the nicotinamide mimicking side-chain (AzaAdoMet **32**), displayed a complete loss of potency (IC_{50} >25 μM).

NNMT Inhibitor Binding Studies

The binding of the most potent inhibitor **17u** with NNMT was further characterized using

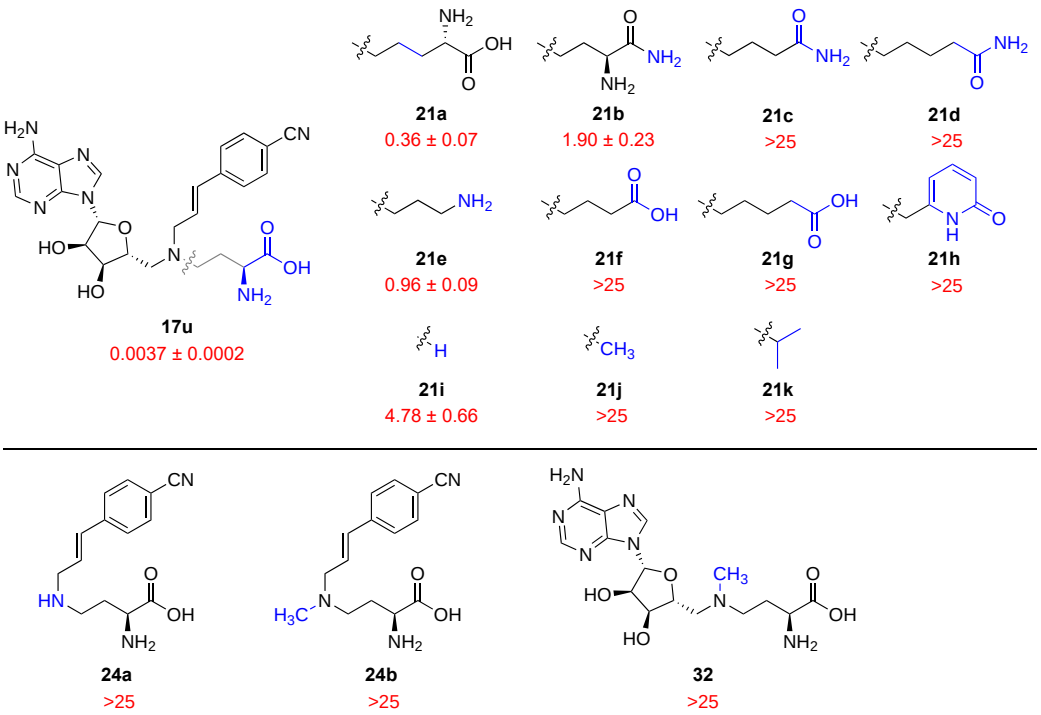

Figure 7. SAR studies of bisubstrate NNMT inhibitors **21a-k** bearing different amino acid substitutions and compounds **24a**, **24b** and **32** lacking either the adenosine unit or the nicotinamide mimicking aromatic sidechain. IC_{50} values (μM) and s.e.m. are shown in red. Changes introduced relative to the lead inhibitor **17u** indicated in blue.

keeping with the bisubstrate inhibitor's capacity to simultaneously compete with both cofactor SAM and substrate NA, the ITC experiment also confirmed a 1:1 stoichiometry between ligand and enzyme. Details and additional thermograms of compound **17u** and NNMT as well as control titrations are provided in the Supplementary Information.

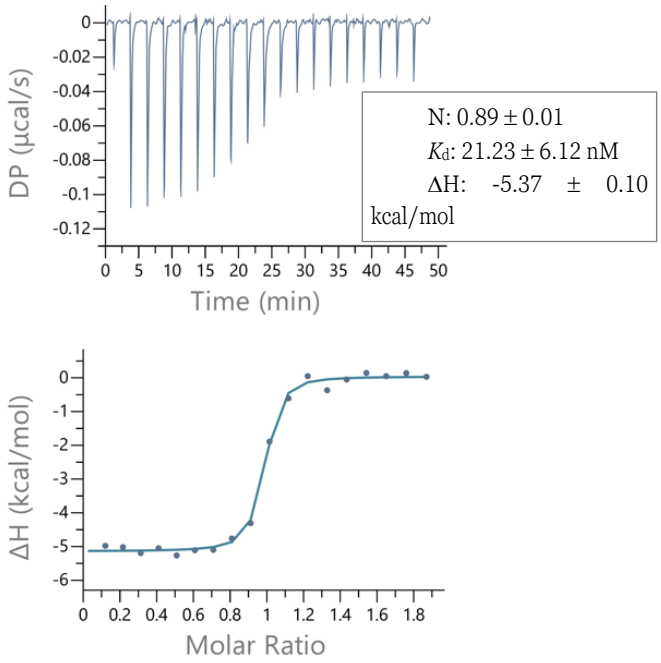

Figure 8. ITC thermogram of compound **17u** including the thermodynamic binding parameters obtained from three independent titration experiments with human wild-type NNMT.

NNMT Inhibitor Modeling

To learn more about the driving force of the *ortho-meta-para* effect observed for the electron-withdrawing (EWG)-substitutions in the styrene compounds, computational studies were performed on nitrile-substituted compounds **17s**, **17t** and **17u**. These studies were specifically aimed at estimating the relative binding affinity shifts, via free energy perturbation (FEP), due to the inclusion of the *ortho*, *meta*, or *para*-nitrile substituent in the unsubstituted reference compound **17x** (Figure 9). From these calculations, it becomes apparent that serine residues S201 and S213 in the nicotinamide binding pocket of NNMT play a crucial role in the potency of compound **17u**. The model predicts hydrogen bonding interactions with the *para*-cyano substituent of compound **17u** involving the sidechains of both S201 and S213. These interactions result in an estimated improvement of the binding affinity due to the *p*-CN substitution of more than 4 kcal/mol, relative to the unsubstituted analogue **17x** in agreement with the experimental data. For the *meta*-cyano compound **17t**, these interactions seem to be much weaker (less frequent),

resulting in only a moderate improvement in the predicted affinity shift arising from the introduction of the *meta*-cyano substitution again in line with the biochemical experiments. Conversely, the *ortho*-cyano compound **17s** cannot reach the serine residues and instead seems to introduce a counterproductive steric hindrance in the binding site, as reflected by the weaker binding affinity predicted relative to the unsubstituted compound **17x**.

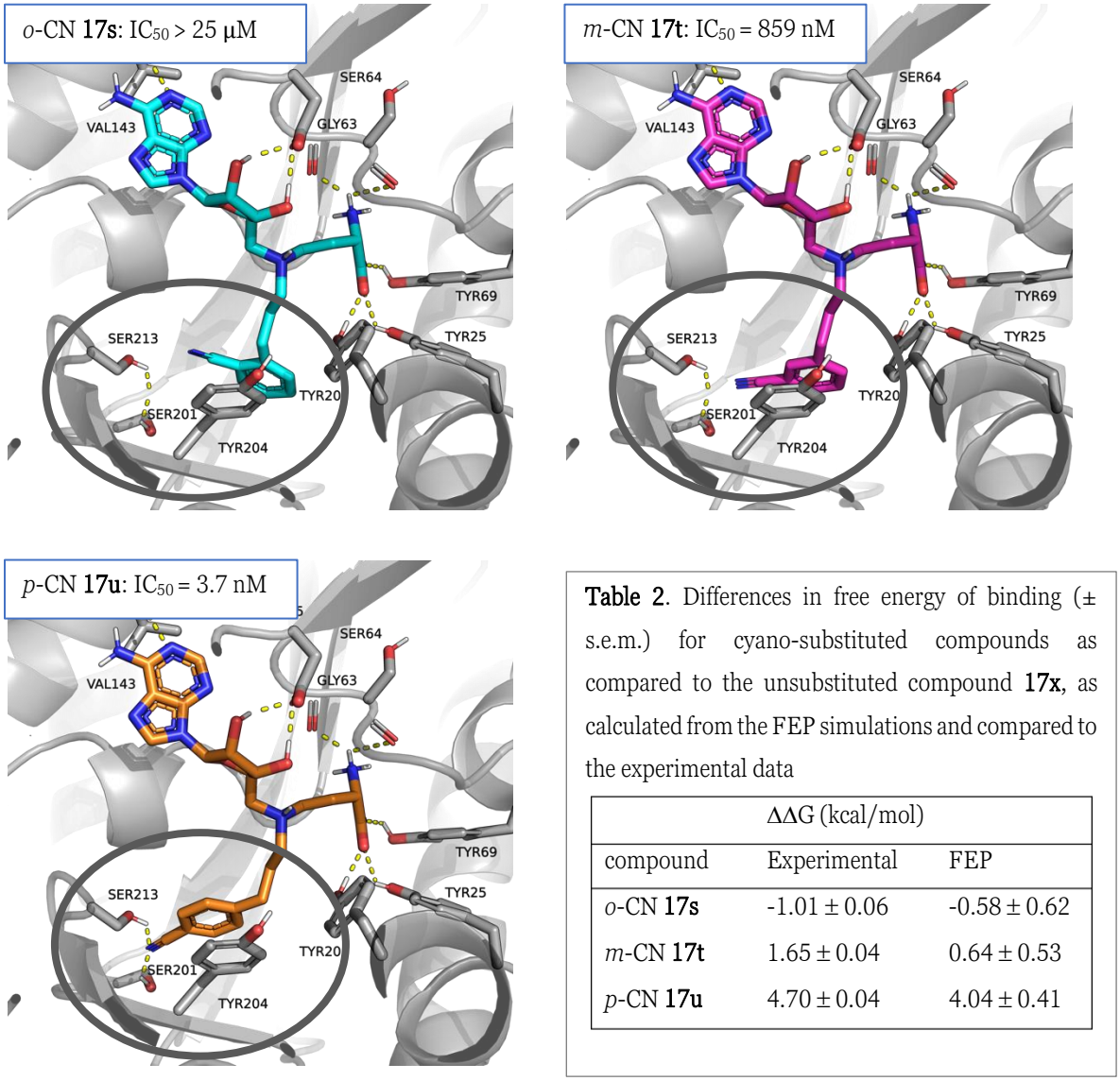

Table 2. Differences in free energy of binding (± s.e.m.) for cyano-substituted compounds as compared to the unsubstituted compound **17x**, as calculated from the FEP simulations and compared to the experimental data

	ΔΔG (kcal/mol)	
compound	Experimental	FEP
o-CN **17s**	-1.01 ± 0.06	-0.58 ± 0.62
m-CN **17t**	1.65 ± 0.04	0.64 ± 0.53
p-CN **17u**	4.70 ± 0.04	4.04 ± 0.41

Figure 9. Results of modeling of compounds **17s-u** bearing the *ortho*-, *meta*- and *para*-cyano substituent. The results indicate strong hydrogen bonding of para-cyano compound **17u** with serine residues S201 and S213, which are not present in the models of compounds **17s** and **17t**. The modelled predictions are supported by the similarity in the difference in Gibbs free energy (ΔΔG) compared to unsubstituted compound **17x** from the biochemical assay and the MD simulations as displayed in Table 2.

Inhibitor Selectivity Studies and Cell-based Assays

To evaluate the NNMT selectivity of the most potent bisubstrate inhibitor, compound **17u** was tested for its activity against 12 representative SAM-dependent methyltransferases. For this

experiment, we selected protein methyltransferases G9a, SETDB1, SETD2, MLL1, SMYD2, PRMT1, CARM1, PRMT5, PRMT7, DNMT1 and DOT1L and small molecule methyltransferase phenylethanolamine *N*-methyltransferase (PNMT). Notably, PNMT has high structural similarity to NNMT sharing 39% sequence identity.[30] Compound **17u** showed good selectivity against all methyltransferases tested. Against PNMT, less than 50% inhibition was observed for compound **17u** at 10 μM. Against PRMT5 and DOT1L, **17u** exhibited more than 50% inhibition at 10 μM, but this activity was abolished at 1 μM. The highest percentage inhibition was observed against lysine methyltransferase SMYD-2, with 19% and 39% activity remaining at the concentrations of 10 μM and 1 μM, respectively. Based on this data, compound **17u** inhibits NNMT with excellent selectivity over other methyltransferases.

To investigate whether the potent activity observed in the biochemical inhibition assays translates to cellular activity, compound **17u** was also tested against human cancer cell lines. In addition to the human oral cancer cell line HSC-2 previously used for assessing the cell-based activity of naphthalene compound **3**,[20] we here also tested compound **17u** against a human lung cancer cell line (A549) and bladder cancer cell line (T24). The results of these studies reveal a clear inhibition of cell viability for the different cancer cell lines upon treatment with compound **17u** at a concentration of 100μM. However, this effect was absent at the lower concentrations tested. As the difference between the biochemical inhibition and the cellular activity spans several orders of magnitude, we investigated the cell permeability of compound **17u** by means of a Parallel Artificial Membrane Permeability Assay (PAMPA). The data revealed very poor cell permeability for **17u**, which is likely to be the explanation for the discrepancy between the nanomolar potency in the biochemical assay and the poor potency in the cellular assay.

3. Conclusion

To date, the majority of bisubstrate NNMT inhibitors have logically employed benzamide groups to mimic the nicotinamide moiety. In addition, recent reports have highlighted the benefit of utilizing alkyne-based linkers to connect the benzamide group to the SAM mimicking moiety. We here report notable departures from both of these strategies to generate novel and potent NNMT inhibitors that: a) include non-benzamide aromatic mimics of the nicotinamide group and b) employ a 3-carbon trans-alkene linker to connect these aromatic groups to the SAM unit. This approach was enabled by a convenient and robust synthetic route utilizing a double reductive amination procedure that allowed for the preparation of a number of novel bisubstrate inhibitors. Biochemical evaluation of the inhibitors thus prepared revealed a striking effect for EWG groups present on the aromatic ring, predominantly when introduced at the position *para* to the linker.

Among these compounds, the *para*-cyano substituted styrene-based inhibitor **17u** was identified as the most potent NNMT inhibitor with an IC_{50} value of 3.7 nM. This compound was subsequently used to further investigate the possibilities of altering and/or replacing the amino acid and adenosine moieties. These studies showed that subtle changes in the amino acid side chain resulted in dramatic decreases in activity. While the removal of the carboxylic acid moiety still yielded a low μM inhibitor, elimination of the primary amine led to inactive compounds. Similarly, the novel *para*-cyano side-chain could not compensate the loss of binding interactions when the adenosine moiety was eliminated. The results from the ITC experiments confirmed compound **17u** to be a tight binder of NNMT with a dissociation constant of 21 nM and a 1:1 stoichiometry. In addition, modelling studies predict the presence of hydrogen bonding interactions of the *para*-cyano group with two active site serine residues in the substrate pocket of NNMT, providing a plausible explanation for the potency of compound **17u**. The low nanomolar potency exhibited in biochemical assays was not maintained in cell-based assays and a significant decrease in cell viability was observed only when compound **17u** was tested at 100 μM against oral, lung, and bladder cancer cell lines. This discrepancy is likely to be explained by the poor cell permeability of compound **17u** found in the PAMPA assay. Taken together, our findings provide valuable new insights towards the design and further optimisation of potent NNMT inhibitors.

EXPERIMENTAL PROCEDURES

General Procedures. All reagents employed were of American Chemical Society grade or finer and were used without further purification unless otherwise stated. For compound characterization, ^{1}H NMR spectra were recorded at 400, 500 or 600 MHz with chemical shifts reported in parts per million downfield relative to H_2O (δ 4.79), CH_3OH (δ 3.31), $CHCl_3$ (δ 7.26), or DMSO (δ 2.50). ^{1}H NMR data are reported in the following order: multiplicity (s, singlet; d, doublet; t, triplet; q, quartet; and m, multiplet), coupling constant (*J*) in hertz (Hz), and the number of protons. Where appropriate, the multiplicity is preceded by br, indicating that the signal was broad. ^{13}C NMR spectra were recorded at 101, 126 or 151 MHz with chemical shifts reported relative to $CDCl_3$ (δ 77.16), methanol (δ 49.00), or DMSO (δ 39.52). The ^{13}C NMR spectra of the compounds recorded in D_2O could not be referenced. Compounds **5**,[27] **9**,[34] **10**,[20] **19a**,[20] **19b**,[35] **19c-d**,[20] **19e**,[36] **19f-g**,[20] **22a**,[37] **30**[27] and **32**[38] were prepared as previously described and had NMR spectra and mass spectra consistent with the assigned structures. Purity was confirmed to be ≥95% by LCMS performed on a Shimadzu LC-20AD system with a Shimadzu Shim-Pack GISS-HP C18 column (3.0 x 150 mm, 3 μm) at 30 °C and equipped with a UV detector monitoring at 214 and 254 nm. The following solvent system, at a flow rate of 0.5 mL/min, was used: solvent A, 0.1 % formic acid in water;

solvent B, acetonitrile. Gradient elution was as follows: 95:5 (A/B) for 2 min, 95:5 to 0:100 (A/B) over 13 min, 0:100 (A/B) for 2 min, then reversion back to 95:5 (A/B) over 1 min, 95:5 (A/B) for 2 min. This system was connected to a Shimadzu 8040 triple quadrupole mass spectrometer (ESI ionisation).

The final compounds were purified via preparative HPLC performed on a BESTA-Technik system with a Dr. Maisch Reprosil Gold 120 C18 column (25 × 250 mm, 10 μm) and equipped with a ECOM Flash UV detector monitoring at 214 nm. The following solvent system, at a flow rate of 12 mL/min, was used: solvent A: 0.1 % TFA in water/acetonitrile 95/5; solvent B: 0.1 % TFA in water/acetonitrile 5/95. Gradient elution was as follows: 95:5 (A/B) for 5 min, 95:5 to 0:100 (A/B) over 40 min, 0:100 (A/B) for 5 min, then reversion back to 95:5 (A/B) over 2 min, 95:5 (A/B) for 8 min.

HRMS analyses were performed on a Shimadzu Nexera X2 UHPLC system with a Waters Acquity HSS C18 column (2.1 × 100 mm, 1.8 μm) at 30 °C and equipped with a diode array detector. The following solvent system, at a flow rate of 0.5 mL/min, was used: solvent A, 0.1 % formic acid in water; solvent B, 0.1 % formic acid in acetonitrile. Gradient elution was as follows: 95:5 (A/B) for 1 min, 95:5 to 15:85 (A/B) over 6 min, 15:85 to 0:100 (A/B) over 1 min, 0:100 (A/B) for 3 min, then reversion back to 95:5 (A/B) for 3 min. This system was connected to a Shimadzu 9030 QTOF mass spectrometer (ESI ionisation) calibrated internally with Agilent's API-TOF reference mass solution kit (5.0 mM purine, 100.0 mM ammonium trifluoroacetate and 2.5 mM hexakis(1*H*,1*H*,3*H*-tetrafluoropropoxy)phosphazine) diluted to achieve a mass count of 10000.

***tert*-butyl (*S*)-4-((((3a*R*,4*R*,6*R*,6a*R*)-6-(6-amino-9*H*-purin-9-yl)-2,2-dimethyltetrahydrofuro[3,4-d][1,3]dioxol-4-yl)methyl)amino)-2-((*tert*-butoxycarbonyl)amino)butanoate (11).** 9-((3a*R*,4*R*,6*R*,6a*R*)-6-(aminomethyl)-2,2-dimethyltetrahydrofuro[3,4-d][1,3]dioxol-4-yl)-9*H*-purin-6-amine **9** (7.3 g, 24 mmol), *tert*-butyl (*S*)-2-((*ter*t-butoxycarbonyl)amino)-4-oxobutanoate **10** (5.5 g, 20 mmol), $NaBH(OAc)_3$ (6.4 g, 30 mmol) and AcOH (1 mL) were added to 1,2-dichloroethane (DCE, 100 mL) in a 250 mL round-bottom flask (RBF) and the mixture was stirred at room temperature under N_2 atmosphere overnight. The reaction was quenched by adding 1 N NaOH (20 mL), and the product was extracted with CH_2Cl_2. The combined organic layers were washed with brine and dried over Na_2SO_4. The solvent was evaporated, and the crude product was purified by column chromatography (10% MeOH in EtOAc) to give compound **11** as a white powder (6.4 g, 57% yield). ^{1}H NMR (400 MHz, $CDCl_3$) δ 8.31 (s, 1H), 7.90 (s, 1H), 6.04 – 5.76 (m, 4H), 5.49 (s, 1H), 5.29 (s, 1H), 5.09 – 5.05

(m, 1H), 4.36 (s, 1H), 4.28 (s, 1H), 2.95 (d, *J* = 9.5 Hz, 1H), 2.85 – 2.70 (m, 2H), 2.63 (s, 1H), 1.93 (br s, 1H), 1.81 (br, 1H), 1.60 (s, 3H), 1.41 (br d, *J* = 26.4 Hz, 21H). ^{13}C NMR (101 MHz, $CDCl_3$) δ 170.8, 156.0, 155.1, 153.0, 149.2, 140.4, 120.2, 113.3, 90.9, 84.9, 83.0, 82.1, 81.5, 79.2, 77.9, 77.3, 77.1, 76.8, 52.9, 50.3, 46.2, 32.1, 28.2, 27.8, 27.2, 25.4. HRMS (ESI): calculated for $C_{26}H_{42}N_7O_7$ $[M+H]^+$ 564.3146, found 564.3150.

tert-butyl (*S*)-4-((((3a*R*,4*R*,6*R*,6a*R*)-6-(6-amino-9*H*-purin-9-yl)-2,2-dimethyltetrahydrofuro[3,4-d][1,3]dioxol-4-yl)methyl)(quinolin-6-ylmethyl)amino)-2-((*tert*-butoxycarbonyl)amino)butanoate (12a). Compound **11** (112 mg, 0.20 mmol), 1-quinoline-6-carbaldehyde **8a** (38 mg, 0.24 mmol), $NaBH(OAc)_3$ (11 mg, 0.30 mmol) and AcOH (one drop) were added to 1,2- dichloroethane (DCE, 10 mL) in a 50 mL round-bottom flask (RBF) and the mixture was stirred at room temperature under N_2 atmosphere overnight. The reaction was quenched by adding 1 N NaOH (10 mL), and the product was extracted with CH_2Cl_2. The combined organic layers were washed with brine and dried over Na_2SO_4. The solvent was evaporated, and the crude product was purified by column chromatography (5% MeOH in EtOAc) to give compound **12a** as a white powder (66 mg, 47% yield). ^{1}H NMR (400 MHz, $CDCl_3$) δ 8.81 (d, *J* = 3.9 Hz, 1H), 8.02 (s, 1H), 7.95 (t, *J* = 9.2 Hz, 2H), 7.78 (s, 1H), 7.62 (d, *J* = 8.5 Hz, 1H), 7.55 (s, 1H), 7.29 (dd, *J* = 8.1, 4.2 Hz, 1H), 6.50 (s, 2H), 5.97 (s, 1H), 5.67 (d, *J* = 7.8 Hz, 1H), 5.28 (d, *J* = 5.4 Hz, 1H), 4.85 – 4.80 (m, 1H), 4.30 (d, *J* = 6.0 Hz, 1H), 4.20 – 4.12 (m, 1H), 3.78 (d, *J* = 8.1, 1H), 3.59 (br d, *J* = 12.0 Hz, 2H), 2.81 – 2.75 (m, 1H), 2.68 – 2.59 (m, 2H), 2.54 – 2.48 (m, 1H), 1.96 (br, 1H), 1.77 (br, 1H), 1.51 (s, 3H), 1.33 – 1.27 (br m, 21H). ^{13}C NMR (101 MHz, $CDCl_3$) δ 171.7, 155.8, 155.4, 152.8, 150.0, 148.9, 139.7, 137.2, 135.7, 130.6, 129.2, 121.1, 120.1, 114.3, 90.6, 85.3, 83.3, 81.6, 58.9, 55.8, 52.8, 50.8, 29.4, 28.3, 27.8, 27.0, 25.3. HRMS (ESI): calculated for $C_{36}H_{49}N_8O_7$ $[M+H]^+$ 705.3724, found 705.3728.

tert-butyl (*S*)-4-((((3aR,4R,6R,6aR)-6-(6-amino-9H-purin-9-yl)-2,2-dimethyltetrahydrofuro[3,4-d][1,3]dioxol-4-yl)methyl)(quinolin-2-ylmethyl)amino)-2-((*tert*-butoxycarbonyl)amino)butanoate (12b). Following the procedure described for compound **12a**, coupling compound **11** (112 mg, 0.20 mmol) with quinoline-2-carbaldehyde **8b** (38 mg, 0.24 mmol) afforded compound **12b**, which was used in the next step without further purification.

tert-butyl (*S*)-4-((((3a*R*,4*R*,6R,6a*R*)-6-(6-amino-9*H*-purin-9-yl)-2,2-dimethyltetrahydrofuro[3,4-d][1,3]dioxol-4-yl)methyl)(isoquinolin-6-ylmethyl)amino)-2-((*tert*-butoxycarbonyl)amino) butanoate (12c). Following the procedure described for compound **12a**, coupling compound **11** (112 mg, 0.20 mmol) with isoquinoline-6-carbaldehyde **8c** (38 mg, 0.24 mmol) afforded compound **12c** as a white powder (77 mg, 55% yield). ^{1}H NMR (400 MHz, $CDCl_3$)

δ 8.07 (s, 1H), 7.98 (dd, *J* = 8.3, 2.0 Hz, 2H), 7.86 (s, 1H), 7.73 (d, *J* = 8.1 Hz, 1H), 7.66 – 7.62 (m, 1H), 7.55 (d, *J* = 8.5 Hz, 1H), 7.49 – 7.45 (m, 1H), 6.04 (br, 3H), 5.57 (d, *J* = 7.7 Hz, 1H), 5.34 (d, *J* = 5.6 Hz, 1H), 4.94 – 4.89 (m, 1H), 4.43 – 4.36 (m, 1H), 4.20 – 4.16 (br, 1H), 3.96 (br, 1H), 3.86 (s, 1H), 2.92 – 2.84 (m, 1H), 2.81 – 2.66 (m, 2H), 2.61 (br, 1H), 2.06 – 1.92 (m, 1H), 1.77 (br, 1H), 1.56 (s, 3H), 1.41 – 1.31 (br m, 21H). ^{13}C NMR (101 MHz, $CDCl_3$) δ 171.8, 159.9, 155.6, 152.9, 149.1, 147.4, 139.9, 136.2, 129.4, 129.0, 127.5, 127.3, 126.2, 124.8, 121.1, 120.2, 114.3, 90.7, 85.5, 83.9, 83.4, 81.6, 79.4, 77.3, 61.6, 56.4, 52.8, 51.2, 30.3, 28.4, 27.9, 27.2, 25.5. HRMS (ESI): calculated for $C_{36}H_{49}N_8O_7$ $[M+H]^+$ 705.3724, found 705.3733.

tert-butyl (2*S*)-4-(([1,1'-biphenyl]-4-ylmethyl)(((3a*R*,4*R*,6*R*,6a*R*)-6-(6-amino-9*H*-purin-9-yl)-2,2-dimethyltetrahydrofuro[3,4-d][1,3]dioxol-4-yl)methyl)amino)-2-((*tert*-butoxycarbonyl)amino) butanoate (12d). Following the procedure described for compound **12a**, coupling compound **11** (112 mg, 0.20 mmol) with [1,1'-biphenyl]-4-carbaldehyde **8d** (44 mg, 0.24 mmol) afforded compound **12d** as a white powder (103 mg, 71% yield). ^{1}H NMR (400 MHz, $CDCl_3$) δ 8.20 (s, 1H), 7.85 (s, 1H), 7.55 (d, *J* = 7.6 Hz, 2H), 7.46 (d, *J* = 7.9 Hz, 2H), 7.40 (t, *J* = 7.6 Hz, 2H), 7.30 (d, *J* = 7.9 Hz, 3H), 6.36 (s, 2H), 6.03 (s, 1H), 5.75 (d, *J* = 7.7 Hz, 1H), 5.37 (d, *J* = 5.4 Hz, 1H), 4.92 – 4.87 (m, 1H), 4.41 – 4.34 (m, 1H), 4.24 – 4.16 (m, 1H), 3.72 (br d, *J* = 12.0 1H), 3.49 (br d, *J* = 12.0 1H), 2.81 (br d, *J* = 19.7 Hz, 1H), 2.71 – 2.60 (m, 2H), 2.52 (d, *J* = 7.0 Hz, 1H), 2.06 – 1.93 (m, 1H), 1.86 – 1.74 (m, 1H), 1.59 (s, 3H), 1.41 – 1.36 (br m, 21H). ^{13}C NMR (101 MHz, $CDCl_3$) δ 171.8, 155.5, 153.1, 149.3, 140.9, 137.6, 129.4, 128.8, 127.2, 127.0, 120.4, 58.7, 55.8, 53.0, 50.7, 30.4, 29.8, 29.4, 28.4, 28.0, 27.2, 25.5. HRMS (ESI): calculated for $C_{39}H_{52}N_7O_7$ $[M+H]^+$ 730.3928, found 730.3956.

tert-butyl (2S)-4-(([1,1'-biphenyl]-2-ylmethyl)(((3a*R*,4*R*,6*R*,6a*R*)-6-(6-amino-9*H*-purin-9-yl)-2,2-dimethyltetrahydrofuro[3,4-d][1,3]dioxol-4-yl)methyl)amino)-2-((*tert*-butoxycarbonyl)amino) butanoate (12e). Following the procedure described for compound **12a**, coupling compound **11** (112 mg, 0.20 mmol) with [1,1'-biphenyl]-2-carbaldehyde **8e** (44 mg, 0.24 mmol) afforded compound **12e** as a white powder (99 mg, 69% yield). ^{1}H NMR (400 MHz, $CDCl_3$) δ 8.22 (s, 1H), 7.79 (s, 1H), 7.57 – 7.51 (m, 1H), 7.39 – 7.11 (m, 8H), 5.97 (br d, *J* = 12.0 Hz, 3H), 5.34 (br, 2H), 4.75 (dd, *J* = 6.4, 3.3 Hz, 1H), 4.22 – 4.17 (m, 1H), 4.07–3.98 (m, 1H), 3.61 (br d, *J* = 12.0, 1H), 3.44 (br d, *J* = 16.0 1H), 2.64 – 2.59 (m, 1H), 2.50 – 2.44 (m, 2H), 2.37 – 2.30 (m, 2H), 1.83 – 1.72 (m, 1H), 1.57 (s, 3H), 1.42 – 1.36 (br m, 21H). ^{13}C NMR (101 MHz, $CDCl_3$) δ 155.4, 153.1, 141.3, 136.1, 130.0, 129.7, 129.4, 128.1, 127.3, 127.0, 126.8, 114.3, 90.8, 85.4, 83.8, 83.3, 56.2, 55.9, 52.8, 50.8, 29.3, 28.4, 28.0, 27.2, 25.5. HRMS (ESI): calculated for $C_{39}H_{51}N_7O_7Na$ $[M+ Na]^+$ 752.3748, found 730.3759.

tert-butyl (2S)-4-(([1,1'-biphenyl]-3-ylmethyl)(((3a*R*,4*R*,6*R*,6a*R*)-6-(6-amino-9*H*-purin-9-yl)-2,2-dimethyltetrahydrofuro[3,4-d][1,3]dioxol-4-yl)methyl)amino)-2-((*tert*-butoxycarbonyl)amino) butanoate (12f). Following the procedure described for compound **12a**, coupling compound **11** (112 mg, 0.20 mmol) with [1,1'-biphenyl]-3-carbaldehyde **8f** (44 mg, 0.24 mmol) afforded compound **12f** as a white powder (108 mg, 74% yield). ^{1}H NMR (400 MHz, $CDCl_3$) δ 8.17 (s, 1H), 7.81 (s, 1H), 7.59–7.51 (m, 3H), 7.44 (d, *J* = 7.6 Hz, 1H), 7.38 (t, *J* = 7.5 Hz, 2H), 7.33 – 7.27 (m, 2H), 7.22 (d, *J* = 7.4 Hz, 1H), 6.51 (s, 2H), 6.02 (s, 1H), 5.68 (d, *J* = 6.6 Hz, 1H), 5.35 (d, *J* = 5.3 Hz, 1H), 4.93 – 4.89 (m, 1H), 4.39 – 4.32 (m, 1H), 4.22 – 4.15 (m, 1H), 3.75 (br, 1H), 3.52 (br, 1H), 2.84 – 2.79 (m, 1H), 2.71–2.60 (m, 2H), 2.59 – 2.49 (m, 1H), 2.06 – 1.94 (m, 1H), 1.83 (br s, 1H), 1.57 (s, 3H), 1.39 – 1.32 (br m, 21H). ^{13}C NMR (101 MHz, $CDCl_3$) δ 171.7, 155.5, 153.1, 141.2, 141.1, 128.8, 127.9, 127.8, 127.3, 127.2, 126.0, 114.4, 90.8, 85.4, 83.9, 83.5, 59.1, 55.7, 52.9, 50.8, 29.5, 28.4, 28.0, 27.2, 25.4. HRMS (ESI): calculated for $C_{39}H_{52}N_7O_7$ $[M+H]^+$ 730.3928, found 730.3938.

tert-butyl (2*S*)-4-((((3a*R*,4*R*,6*R*,6a*R*)-6-(6-amino-9*H*-purin-9-yl)-2,2-dimethyltetrahydrofuro[3,4-d][1,3]dioxol-4-yl)methyl)(naphthalen-1-ylmethyl)amino)-2-((tert-butoxycarbonyl)amino) butanoate (12g). Following the procedure described for compound **12a**, coupling compound **11** (112 mg, 0.20 mmol) with 1-naphthaldehyde **8g** (37 mg, 0.24 mmol), afforded compound **12g** as a white powder (94 mg, 67% yield). ^{1}H NMR (600 MHz, $CDCl_3$) δ 8.14 (d, *J* = 7.7 Hz, 1H), 8.10 (s, 1H), 7.73 (d, *J* = 7.7 Hz, 1H), 7.69 – 7.60 (m, 2H), 7.40 – 7.34 (m, 2H), 7.27–7.19 (m, 2H), 6.24 (br s, 2H), 5.88 (s, 1H), 5.32 (d, *J* = 7.8 Hz, 1H), 5.06 (d, *J* = 5.1 Hz, 1H), 4.54 (s, 1H), 4.30 (s, 1H), 4.10 – 4.05 (m, 2H), 3.78 – 3.73 (m, 1H), 2.72 – 2.64 (m, 2H), 2.60 – 2.56 (m, 1H), 2.53 – 2.47 (m, 1H), 2.02 – 1.93 (m, 1H), 1.86 – 1.73 (m, 1H), 1.46 (s, 3H), 1.33 – 1.29 (br m, 18H), 1.13 (s, 3H). ^{13}C NMR (151 MHz, $CDCl_3$) δ 171.7, 155.7, 155.4, 153.0, 149.1, 139.6, 134.2, 133.76, 132.2, 128.5, 128.1, 127.7, 125.8, 125.6, 125.0, 124.57, 120.18, 91.0, 85.10, 83.5, 83.3, 81.7, 57.6, 55.4, 53.5, 52.8, 51.0, 29.1, 28.4, 27.9, 27.0, 25.1. HRMS (ESI): calculated for $C_{37}H_{50}N_7O_7$ $[M+H]^+$ 704.3772, found 704.3775.

tert-butyl (2*S*)-4-((((3a*R*,4*R*,6*R*,6a*R*)-6-(6-amino-9*H*-purin-9-yl)-2,2-dimethyltetrahydrofuro[3,4-d][1,3]dioxol-4-yl)methyl)(2-(naphthalen-2-yl)ethyl)amino)-2-((*tert*-butoxycarbonyl)amino) butanoate (12h). Following the procedure described for compound **12a**, coupling compound **11** (112 mg, 0.20 mmol) with 2-(naphthalen-2-yl)acetaldehyde **8h** (38 mg, 0.24 mmol) afforded compound **12h** as a white powder (99 mg, 69% yield). ^{1}H NMR (400 MHz, $CDCl_3$) δ 8.36 (s, 1H), 7.90 (s, 1H), 7.79 – 7.69 (m, 3H), 7.52 (s, 1H), 7.45 – 7.36 (m, 2H), 7.21 (dd, *J* = 8.4, 1.5 Hz, 1H), 6.15 (s, 2H), 6.03 (d, *J* = 1.7 Hz, 1H), 5.68 (d, *J* = 8.0 Hz, 1H), 5.48 – 5.46 (d, *J* = 8.0, 1H) 4.96 – 4.93 (m, 1H), 4.39 – 4.31 (m, 1H), 4.20 – 4.15 (m, 1H), 2.90

– 2.50 (m, 8H), 2.05 – 1.97 (m, 1H), 1.70 – 1.75 (m, 1H), 1.59 (s, 3H), 1.43 (d, *J* = 3.4 Hz, 18H), 1.33 (s, 3H). ^{13}C NMR (101 MHz, $CDCl_3$) δ 172.4, 156.6, 153.1, 147.1, 140.2, 138.8, 134.4, 132.5, 128.0, 127.6, 127.4, 126.9, 126.0, 125.3, 120.4, 114.4, 90.2, 85.7, 83.8, 83.3, 81.7, 79.5, 52.9, 50.1, 28.4, 28.1, 27.2, 25.4. HRMS (ESI): calculated for $C_{38}H_{52}N_7O_7$ $[M+H]^+$ 718.3928, found 718.3932.

tert-butyl (2*S*)-4-(((1*H*-indol-2-yl)methyl)(((3a*R*,4*R*,6*R*,6a*R*)-6-(6-amino-9*H*-purin-9-yl)-2,2-dimethyltetrahydrofuro[3,4-d][1,3]dioxol-4-yl)methyl)amino)-2-((*tert*-butoxycarbonyl)amino) butanoate (12i). Following the procedure described for compound **12a**, coupling compound **11** (112 mg, 0.20 mmol) with 1*H*-indole-2-carbaldehyde **8i** (35 mg, 0.18 mmol) afforded compound **12i** as a white powder (77 mg, 56% yield). ^{1}H NMR (600 MHz, $CDCl_3$) δ 9.41 (s, 1H), 8.20 (s, 1H), 7.81 (s, 1H), 7.50 (d, *J* = 7.8 Hz, 1H), 7.28 – 7.23 (m, 1H), 7.10 (t, *J* = 7.5 Hz, 1H), 7.03 (t, *J* = 7.4 Hz, 1H), 6.25 (s, 1H), 6.00 (s, 3H), 5.46 (d, *J* = 8.4 Hz, 1H), 5.30 (d, *J* = 5.3 Hz, 1H), 4.90 (d, *J* = 4.9 Hz, 1H), 4.44 – 4.37 (m, 1H), 4.2 (m 1H), 3.76 (dd, *J* = 8.0, 2H), 2.87 – 2.84 (m, 1H), 2.78 – 2.75 (m, 6.8 Hz, 1H), 2.72 – 2.60 (m, 2H), 2.02 – 1.94 (m, 1H), 1.79 – 1.75 (m, 1H), 1.54 (s, 3H), 1.47– 1.32 (br m, 21H). ^{13}C NMR (151 MHz, $CDCl_3$) δ 172.1, 155.6, 153.0, 149.1, 139.8, 136.4, 128.2, 121.3, 120.2, 120.0, 119.2, 114.6, 110.8, 101.0, 90.2, 84.8, 83.9, 83.4, 82.0, 79.8, 55.9, 52.4, 52.1, 51.2, 30.5, 28.4, 27.9, 27.1, 25.5. HRMS (ESI): calculated for $C_{35}H_{49}N_8O_7$ $[M+H]^+$ 693.3724, found 693.3732.

tert-butyl 3-(((((3a*R*,4*R*,6*R*,6a*R*)-6-(6-amino-9*H*-purin-9-yl)-2,2-dimethyltetrahydrofuro[3,4-d][1,3]dioxol-4-yl)methyl)((*S*)-4-(*tert*-butoxy)-3-((*tert*-butoxycarbonyl)amino)-4-oxobutyl)amino) methyl)-1*H*-indole-1-carboxylate (12j). Following the procedure described for compound **12a**, coupling compound **11** (112 mg, 0.20 mmol) with *tert*-butyl 3-formyl-1*H*-indole-1-carboxylate **8j** (58 mg, 0.24 mmol) afforded compound **12j** as a white powder (79 mg, 50% yield). ^{1}H NMR (600 MHz, $CDCl_3$) δ 8.24 (s, 1H), 8.09 (s, 1H), 7.82 (s, 1H), 7.68 (d, *J* = 7.8 Hz, 1H), 7.44 (s, 1H), 7.28 (d, *J* = 7.4 Hz, 1H), 7.18 (t, *J* = 7.5 Hz, 1H), 5.97 (br d, *J* = 39.0 Hz, 3H), 5.37 – 5.32 (m, 2H), 4.81 (dd, *J* = 6.4, 3.2 Hz, 1H), 4.40 – 4.37 (m, 1H), 4.19 – 4.10 (m, 1H), 3.82 (br d, *J* = 13.7 Hz, 1H), 3.61 – 3.57 (br d, *J* = 13.8 Hz, 1H), 2.85 – 2.82 (br m, 1H), 2.71 – 2.58 (m, 2H), 2.52 – 2.48 (m, 1H), 2.02 – 1.99 (br m, 1H), 1.89 – 1.79 (m, 1H), 1.66 (s, 9H), 1.57 (s, 3H), 1.38 (br d, *J* = 27.7 Hz, 18H), 1.29 (s, 3H).^{13}C NMR (151 MHz, $CDCl_3$) δ 170.7, 154.8, 154.4, 152.0, 148.6, 148.1, 138.7, 134.6, 129.3, 123.7, 123.4, 121.5, 119.2, 119.1, 114.1, 113.3, 89.7, 84.2, 82.6, 82.3, 80.6, 54.6, 52.4, 51.7, 49.7, 49.0, 28.5, 27.3, 27.2, 26.9, 26.1, 24.2. HRMS (ESI): calculated for $C_{40}H_{57}N_8O_9$ $[M+H]^+$ 793.4249, found 793.4256.

tert-butyl (2*S*)-4-((((3a*R*,4*R*,6*R*,6a*R*)-6-(6-amino-9*H*-purin-9-yl)-2,2-dimethyltetrahydrofuro[3,4-d][1,3]dioxol-4-yl)methyl)(benzo[*b*]thiophen-2-ylmethyl)amino)-2-((*tert*-butoxycarbonyl)amino) butanoate (12k). Following the procedure described for compound **12a**, coupling compound **11** (112 mg, 0.20 mmol) with benzo[*b*]thiophene-2-carbaldehyde **8k** (39 mg, 0.24 mmol) afforded compound **12k** as a white powder (89 mg, 63% yield). ^{1}H NMR (400 MHz, $CDCl_3$) δ 8.10 (s, 1H), 7.86 (s, 1H), 7.72 (d, *J* = 7.7 Hz, 1H), 7.61 (d, *J* = 7.4 Hz, 1H), 7.28 (d, *J* = 7.1 Hz, 1H), 7.22 (d, *J* = 7.2 Hz, 1H), 6.99 (s, 1H), 6.27 (s, 2H), 6.04 (s, 1H), 5.61 (d, *J* = 7.8 Hz, 1H), 5.40 (d, *J* = 5.4 Hz, 1H), 5.00 (br s, 1H), 4.42 – 4.36 (m, 1H), 4.23 – 4.15 (m, 1H), 3.95 – 3.91 (br d, *J* = 16.0 Hz, 1H), 3.85 – 3.81 (br d, *J* = 16.0 Hz, 1H), 2.89 – 2.84 (m, 1H), 2.76 – 2.64 (m, 2H), 2.60 – 2.52 (m, 1H), 2.02 – 1.99 (br d, *J* = 12.0 Hz, 1H), 1.83 – 1.81 (d, *J* = 8.0 Hz, 1H), 1.59 (s, 3H), 1.40 – 1.36 (br m, 21H). ^{13}C NMR (101 MHz, $CDCl_3$) δ 171.7, 155.8, 155.4, 153.0, 149.1, 143.1, 139.9, 139.5, 124.1, 123.9, 123.1, 122.2, 120.2, 114.4, 90.6, 85.5, 83.8, 83.2, 81.7, 79.4, 55.3, 54.0, 52.7, 50.3, 29.6, 28.3, 27.9, 27.1, 25.4. HRMS (ESI): calculated for $C_{35}H_{48}N_7O_7S$ $[M+H]^+$ 710.3336, found 710.3348.

tert-butyl (2*S*)-4-((((3a*R*,4*R*,6*R*,6a*R*)-6-(6-amino-9*H*-purin-9-yl)-2,2-dimethyltetrahydrofuro[3,4-d][1,3]dioxol-4-yl)methyl)(benzo[*b*]thiophen-3-ylmethyl)amino)-2-((*tert*-butoxycarbonyl)amino) butanoate (12l). Following the procedure described for compound **12a**, coupling compound **11** (112 mg, 0.20 mmol) with benzo[*b*]thiophene-3-carbaldehyde **8l** (39 mg, 0.24 mmol) afforded compound **12l** as a white powder (79 mg, 50% yield). ^{1}H NMR (400 MHz, $CDCl_3$) δ 8.63 (s, 1H), 8.30 – 8.23 (br d, *J* = 28.0 Hz , 3H), 7.73 – 7.67 (br d, *J* = 24.0 Hz, 3H), 6.94 (s, 2H), 6.44 (s, 1H), 6.06 (s, 1H), 5.72 (s, 1H), 5.20 (s, 1H), 4.81 (s, 1H), 4.63 (s, 1H), 4.35 – 4.32 (br d, *J* = 8.0 Hz, 1H), 4.16 – 4.13 (br d, *J* = 12.0 Hz, 1H), 3.34 – 2.89 (m, 4H), 2.46 (s, 1H), 2.27 (s, 1H), 2.00 (s, 3H), 1.85 – 1.81 (br d, *J* = 16.0 Hz, 18H), 1.71 (s, 3H). ^{13}C NMR (101 MHz, $CDCl_3$) δ 171.7, 155.9, 155.4, 153.0, 149.0, 140.5, 139.6, 138.6, 133.4, 124.6, 124.3, 123.9, 122.6, 122.5, 120.2, 114.2, 90.8, 85.2, 83.6, 83.3, 81.7, 79.4, 77.4, 77.3, 77.1, 76.8, 55.7, 52.9, 52.8, 50.9, 29.3, 28.3, 27.9, 27.0, 25.2. HRMS (ESI): calculated for $C_{35}H_{48}N_7O_7S$ $[M+H]^+$ 710.3336, found 710.3355.

(*S*)-2-amino-4-((((2*R*,3*S*,4*R*,5*R*)-5-(6-amino-9*H*-purin-9-yl)-3,4-dihydroxytetrahydrofuran-2-yl)methyl)(quinolin-6-ylmethyl)amino)butanoic acid (13a). To a solution of compound **12a** (50 mg, 0.071 mmol) in 1 mL of CH_2Cl_2 was added a mixture of 9 mL TFA and 1 mL H_2O, and the solution was stirred for 2 h at room temperature. The mixture was concentrated, and the crude product was purified by preparative HPLC affording compound **13a** as a white powder (33 mg, 74% yield). ^{1}H NMR (400 MHz, D_2O) δ 8.34 (d, *J* = 1.2 Hz, 1H), 8.10 (s, 1H), 7.79 (s, 1H), 7.39 (s, 2H), 7.28 (d, *J* = 8.2 Hz, 1H), 7.06 (t, *J* = 7.6 Hz, 1H), 6.92 (s, 1H), 6.05 (d, *J* = 5.0 Hz, 1H), 4.79

(t, *J* = 5.0 Hz, 1H), 4.56 – 4.49 (m, 2H), 4.38 (d, *J* = 9.9 Hz, 1H), 3.76 – 3.69 (m, 1H), 3.60 – 3.50 (m, 4H), 3.25 (t, *J* = 7.1 Hz, 1H), 2.43 – 2.34 (m, 1H), 2.24 (br s, 1H), 2.14 – 2.08 (m, 1H). ^{13}C NMR (101 MHz, D_2O) δ 169.9, 146.8, 143.6, 126.8, 122.8, 122.7, 120.3, 118.6, 109.0, 108.8, 73.5, 71.7, 52.2, 24.8. HRMS (ESI): calculated for $C_{24}H_{29}N_8O_5$ $[M+H]^+$ 509.2261, found 509.2266.

(*S*)-2-amino-4-((((2*R*,3*S*,4*R*,5*R*)-5-(6-amino-9*H*-purin-9-yl)-3,4-dihydroxytetrahydrofuran-2-yl)methyl)(quinolin-2-ylmethyl)amino)butanoic acid (13b). Following the procedure described for compound **13a**, compound **12b** (50 mg, 0.071 mmol) was deprotected and purified, affording compound **13b** as a white powder (8 mg, 17% yield over two steps). ^{1}H NMR (400 MHz, D_2O) δ 8.45 (d, *J* = 8.6 Hz, 1H), 8.14 (s, 1H), 7.88 – 7.81 (m, 1H), 7.62 – 7.56 (m, 3H), 7.53 (s, 1H), 7.40 (d, *J* = 9.7 Hz, 1H), 5.93 (d, *J* = 4.5 Hz, 1H), 4.58 – 4.48 (m, 3H), 4.46 – 4.41 (m, 1H), 4.29 (t, *J* = 5.1 Hz, 1H), 4.06 (dd, *J* = 7.8, 5.3 Hz, 1H), 3.48 – 3.28 (m, 4H), 2.37 – 2.18 (m, 2H). ^{13}C NMR (101 MHz, D_2O) δ 145.8, 142.4, 133.2, 132.1, 131.6, 129.8, 127.2, 123.0, 120.4, 92.3, 81.3, 80.4, 76.5, 74.4, 71.2, 54.2, 53.1, 27.5. HRMS (ESI): calculated for $C_{24}H_{29}N_8O_5$ $[M+H]^+$ 509.2261, found 509.2265.

(*S*)-2-amino-4-((((2*R*,3*S*,4*R*,5*R*)-5-(6-amino-9*H*-purin-9-yl)-3,4-dihydroxytetrahydrofuran-2-yl)methyl)(isoquinolin-6-ylmethyl)amino)butanoic acid (13c). Following the procedure described for compound **13a**, compound **12c** (50 mg, 0.071 mmol) was deprotected and purified, affording compound **13c** as a white powder (21 mg, 47% yield). ^{1}H NMR (400 MHz, D_2O) δ 8.00 (s, 1H), 7.83 – 7.70 (m, 3H), 7.49 – 7.32 (m, 3H), 6.99 (s, 1H), 5.81 (s, 1H), 4.88 (br d, *J* = 13.7 Hz, 1H), 4.64 (br d, *J* = 14.1 Hz, 1H), 4.44 (dd, *J* = 7.2, 5.7 Hz, 1H), 4.32 (dd, *J* = 5.4, 2.0 Hz, 2H), 3.94 (dd, *J* = 9.1, 4.1 Hz, 1H), 3.71 (t, *J* = 7.0 Hz, 2H), 3.59 (br d, *J* = 12.9 Hz, 1H), 2.50 – 2.45 (m, 1H), 2.38 – 2.28 (m, 1H). ^{13}C NMR (101 MHz, D_2O) δ 171.5, 163.0, 162.6, 153.9, 148.9, 146.8, 144.2, 143.3, 142.9, 139.6, 133.3, 129.1, 128.3, 121.9, 120.8, 118.6, 117.7, 114.8, 90.4, 80.4, 72.9, 71.6, 56.8, 56.5, 51.0, 50.6, 25.9. HRMS (ESI): calculated for $C_{24}H_{29}N_8O_5$ $[M+H]^+$ 509.2261, found 509.2273.

(*S*)-4-(([1,1'-biphenyl]-4-ylmethyl)(((2*R*,3*S*,4*R*,5*R*)-5-(6-amino-9*H*-purin-9-yl)-3,4-dihydroxy-tetrahydrofuran-2-yl)methyl)amino)-2-aminobutanoic acid (13d). Following the procedure described for compound **13a**, compound **12d** (50 mg, 0.068 mmol) was deprotected and purified, affording compound **13d** as a white powder (30 mg, 68% yield). ^{1}H NMR (400 MHz, D_2O) δ 8.13 (br s, 1H), 7.94 (s, 1H), 7.40 – 7.29 (m, 5H), 7.19 (br s, 4H), 5.88 (s, 1H), 4.53 – 4.48 (m, 1H), 4.31 (s, 3H), 4.06 (dd, *J* = 8.3, 4.8 Hz, 1H), 3.69 – 3.49 (m, 4H), 2.49 – 2.37 (br d, *J* = 48.0 Hz, 2H). ^{13}C NMR (101 MHz, D_2O) δ 171.1, 163.0, 162.6, 162.2, 143.6, 140.2, 137.8, 131.1,

129.2, 128.4, 126.0, 118.4, 117.7, 114.8, 111.9, 90.5, 77.7, 73.9, 71.4, 51.0, 24.6. HRMS (ESI): calculated for $C_{27}H_{33}N_7O_5$ $[M+H]^+$ 534.2465, found 534.2474.

(*S*)-4-(([1,1'-biphenyl]-2-ylmethyl)(((2*R*,3*S*,4*R*,5*R*)-5-(6-amino-9*H*-purin-9-yl)-3,4-dihydroxy-tetrahydrofuran-2-yl)methyl)amino)-2-aminobutanoic acid (13e). Following the procedure described for compound **13a**, compound **12e** (50 mg, 0.068 mmol) was deprotected and purified, affording compound **13e** as a white powder (35 mg, 79% yield). ^{1}H NMR (400 MHz, D_2O) δ 8.31 (s, 1H), 8.24 (s, 1H), 7.51 – 7.29 (m, 6H), 7.25 – 7.17 (m, 3H), 5.98 (d, *J* = 3.4 Hz, 1H), 4.63 – 4.53 (m, 2H), 4.48 (d, *J* = 13.8 Hz, 1H), 4.40 (s, 1H), 4.27 – 4.21 (m, 1H), 3.71 (s, 1H), 3.48 – 3.23 (m, 4H), 2.19 – 2.11 (m, 1H), 2.03 – 1.95 (m, 1H). ^{13}C NMR (101 MHz, D_2O) δ 171.2, 149.9, 147.6, 144.2, 143.6, 138.9, 131.2, 130.9, 130.1, 129.32, 128.9, 128.3, 126.2, 119.3, 117.7, 114.8, 90.3, 77.9, 73.3, 71.7, 55.3, 51.1, 24.3. HRMS (ESI): calculated for $C_{27}H_{33}N_7O_5$ $[M+H]^+$ 534.2465, found 534.2472.

(*S*)-4-(([1,1'-biphenyl]-3-ylmethyl)(((2*R*,3*S*,4*R*,5*R*)-5-(6-amino-9*H*-purin-9-yl)-3,4-dihydroxy-tetrahydrofuran-2-yl)methyl)amino)-2-aminobutanoic acid (13f). Following the procedure described for compound **13a**, compound **12f** (50 mg, 0.068 mmol) was deprotected and purified, affording compound **13f** as a white powder (34 mg, 77% yield). ^{1}H NMR (400 MHz, D_2O) δ 7.98 (s, 1H), 7.67 (s, 1H), 7.23 – 7.14 (m, 8H), 7.03 (d, *J* = 6.9 Hz, 2H), 5.86 (s, 1H), 4.38 – 4.32 (br m, 3H), 4.25 – 4.13 (m, 2H), 3.96 (dd, *J* = 8.6, 4.6 Hz, 1H), 3.61 – 3.39 (m, 4H), 2.48 – 2.42 (m, 1H), 2.39 – 2.23 (m, 1H). ^{13}C NMR (101 MHz, D_2O) δ 171.9, 163.3, 162.9, 162.2, 149.0, 146.9, 143.6, 143.0, 139.6, 137.6, 129.5, 129.0, 128.1, 127.2, 125.5, 120.7, 118.5, 117.8, 90.4, 73.6, 71.5, 51.8, 24.7. HRMS (ESI): calculated for $C_{27}H_{33}N_7O_5$ $[M+H]^+$ 534.2465, found 534.2468.

(*S*)-2-amino-4-((((2*R*,3*S*,4*R*,5*R*)-5-(6-amino-9*H*-purin-9-yl)-3,4-dihydroxytetrahydrofuran-2-yl)methyl)(naphthalen-2-ylmethyl)amino)butanoic acid (13g). Following the procedure described for compound **13a**, compound **12g** (50 mg, 0.071 mmol) was deprotected and purified, affording compound **13g** as a white powder (33 mg, 74% yield). ^{1}H NMR (400 MHz, D_2O) δ 7.94 (s, 1H), 7.55 (d, *J* = 8.3 Hz, 4H), 7.39 (d, *J* = 6.9 Hz, 1H), 7.24 (s, 3H), 5.79 (s, 1H), 4.56 (br d, *J* = 12.0, 1H), 4.42 – 4.37 (m, 1H), 4.36 – 4.21 (m, 2H), 3.97 (dd, *J* = 8.6, 4.4 Hz, 1H), 3.76 – 3.42 (m, 4H), 2.53 – 2.25 (m, 2H). ^{13}C NMR (101 MHz, D_2O) δ 171.4, 163.0, 162.7, 149.3, 146.7, 143.4, 143.3, 132.8, 130.1, 128.4, 126.4, 122.2, 118.5, 117.7, 90.7, 73.5, 71.6, 51.4. HRMS (ESI): calculated for $C_{25}H_{30}N_7O_5$ $[M+H]^+$ 508.2308, found 508.2314.

(*S*)-2-amino-4-((((2*R*,3*S*,4*R*,5*R*)-5-(6-amino-9*H*-purin-9-yl)-3,4-dihydroxytetrahydrofuran-2-yl)methyl)(2-(naphthalen-2-yl)ethyl)amino)butanoic acid (13h). Following the procedure described for compound **13a**, compound **12h** (50 mg, 0.069 mmol) was deprotected and purified,

affording compound **13h** as a white powder (33 mg, 76% yield). ^{1}H NMR (400 MHz, CD_3OD) δ 8.45 (s, 1H), 8.23 (s, 1H), 7.78 – 7.63 (m, 3H), 7.58 (s, 1H), 7.46 – 7.39 (m, 2H), 7.26 (d, *J* = 8.4 Hz, 1H), 6.13 (d, *J* = 4.6 Hz, 1H), 4.71 (d, *J* = 9.6 Hz, 1H), 4.62 – 4.55 (m, 1H), 4.44 (t, *J* = 5.1 Hz, 1H), 4.11 (dd, *J* = 8.3, 4.7 Hz, 1H), 3.86 – 3.54 (m, 6H), 3.21 (t, *J* = 8.1 Hz, 2H), 2.56 – 2.46 (m, 1H), 2.36 – 2.28 (m, 1H). ^{13}C NMR (101 MHz, CD_3OD) δ 170.3, 161.6, 161.2, 151.5, 148.1, 133.5, 133.1, 132.5, 119.7, 118.0, 115.1, 90.6, 79.8, 74.2, 68.7, 54.8, 52.0, 51.0, 29.4, 24.5. HRMS (ESI): calculated for $C_{26}H_{32}N_7O_5$ $[M+H]^+$ 522.2465, found 522.2477.

(*S*)-4-(((1*H*-indol-2-yl)methyl)(((2*R*,3*S*,4*R*,5*R*)-5-(6-amino-9*H*-purin-9-yl)-3,4-dihydroxy-tetrahydrofuran-2-yl)methyl)amino)-2-aminobutanoic acid (13i). Following the procedure described for compound **13a**, compound **12i** (50 mg, 0.072 mmol) was deprotected and purified, affording compound **13i** as a white powder (27 mg, 61% yield). ^{1}H NMR (400 MHz, D_2O) δ 8.30 (s, 1H), 7.68 (s, 1H), 7.42 (d, *J* = 7.8 Hz, 1H), 7.13 (t, *J* = 7.5 Hz, 1H), 7.06 (t, *J* = 6.9 Hz, 1H), 6.97 (d, *J* = 8.1 Hz, 1H), 6.08 (s, 1H), 4.69 – 4.64 (m, 1H), 4.61 – 4.45 (m, 4H), 4.03 – 4.00 (m, 2H), 3.70 (t, *J* = 7.3 Hz, 2H), 3.63 – 3.60 (br d, *J* = 12.0, , 1H), 2.57 – 2.45 (m, 1H), 2.38 – 2.33 (m, 1H). ^{13}C NMR (101 MHz, D_2O) δ 170.7, 149.2, 146.7, 143.9, 143.0, 123.0, 120.4, 120.1, 111.0, 91.2, 73.8, 72.0, 25.0. HRMS (ESI): calculated for $C_{23}H_{29}N_8O_5$ $[M+H]^+$ 497.2261, found 497.2263.

(*S*)-4-(((1*H*-indol-3-yl)methyl)(((2*R*,3*S*,4*R*,5*R*)-5-(6-amino-9*H*-purin-9-yl)-3,4-dihydroxy-tetrahydrofuran-2-yl)methyl)amino)-2-aminobutanoic acid (13j). Following the procedure described for compound **13a**, compound **12j** (50 mg, 0.063 mmol) was deprotected and purified, affording compound **13j** as a pink powder (23 mg, 61% yield). ^{1}H NMR (500 MHz, CD_3OD) δ 8.56 – 8.31 (m, 1H), 7.64 (d, *J* = 7.0 Hz, 1H), 7.55 (s, 1H), 7.42 (d, *J* = 8.2 Hz, 1H), 7.18 (t, *J* = 8.2 Hz, 1H), 7.07 (t, *J* = 7.5 Hz, 1H), 6.14 (dd, *J* = 9.4, 4.3 Hz, 1H), 4.75 – 4.56 (m, 3H), 4.51 – 4.38 (m, 1H), 4.02 (dd, *J* = 8.4, 4.7 Hz, 1H), 3.81 – 3.74 (m, 1H), 3.71 – 3.59 (m, 2H), 3.56 – 3.49 (m, 1H), 3.37 (s, 4H), 2.58 – 2.48 (m, 1H), 2.42 – 2.31 (m, 1H). ^{13}C NMR (126 MHz, CD_3OD) δ 170.3, 160.4, 150.5, 148.1, 134.7, 128.0, 127.2, 122.2, 120.1, 116.8, 111.7, 101.8, 91.5, 90.3, 81.0, 78.8, 74.6, 66.4, 49.9, 48.5, 44.6, 26.1, 23.1. HRMS (ESI): calculated for $C_{23}H_{29}N_8O_5$ $[M+H]^+$ 497.2261, found 497.2268.

(*S*)-2-amino-4-((((2*R*,3*S*,4*R*,5*R*)-5-(6-amino-9*H*-purin-9-yl)-3,4-dihydroxytetrahydrofuran-2-yl)methyl)(benzo[*b*]thiophen-2-ylmethyl)amino)butanoic acid (13k). Following the procedure described for compound **13a**, compound **12k** (50 mg, 0.070 mmol) was deprotected and purified, affording compound **13k** as a white powder (34 mg, 78% yield). ^{1}H NMR (400 MHz, D_2O) δ 8.26 (s, 1H), 7.69 (s, 1H), 7.64 – 7.58 (m, 1H), 7.42 – 7.35 (m, 1H), 7.34 – 7.27 (m, 2H), 7.13 (s, 1H), 6.04 (d, *J* = 2.3 Hz, 1H), 4.70 – 4.57 (m, 3H), 4.49 – 4.42 (m, 2H), 4.07 (dd, *J* = 8.7, *J* = 4.5 Hz,

1H), 3.92 – 3.86 (br t, *J* = 12.0 Hz, 1H), 3.73 – 3.67 (m, 2H), 3.63 – 3.59 (br d, *J* = 16.0, 1H), 2.57 – 2.47 (m, 1H), 2.41 – 2.33 (m, 1H). ^{13}C NMR (101 MHz, D_2O) δ 172.7, 162.7, 144.0, 143.0, 128.7, 125.7, 125.0, 123.7, 122.1, 91.2, 78.0, 73.9, 71.9, 53.1, 51.45, 24.1. HRMS (ESI): calculated for $C_{23}H_{28}N_7O_5S$ $[M+H]^+$ 514.1873, found 514.1875.

(*S*)-2-amino-4-((((2*R*,3*S*,4*R*,5*R*)-5-(6-amino-9*H*-purin-9-yl)-3,4-dihydroxytetrahydrofuran-2-yl)methyl)(benzo[*b*]thiophen-3-ylmethyl)amino)butanoic acid (13l). Following the procedure described for compound **13a**, compound **12l** (50 mg, 0.070 mmol) was deprotected and purified, affording compound **13l** as a white powder (29 mg, 67% yield). ^{1}H NMR (400 MHz, CD_3OD) δ 8.37 (s, 1H), 8.06 (s, 1H), 7.93 (s, 1H), 7.85 – 7.80 (m, 2H), 7.35 – 7.26 (m, 2H), 6.12 (d, *J* = 3.0 Hz, 1H), 4.72 (s, 2H), 4.61 – 4.53 (m, 2H), 4.50 – 4.46 (m, 1H), 4.00 (dd, *J* = 8.5, 4.4 Hz, 1H), 3.84 – 3.60 (m, 4H), 2.55 – 2.46 (m, 1H), 2.37 – 2.31 (m, 1H). ^{13}C NMR (101 MHz, CD_3OD) δ 170.8, 162.1, 161.8, 161.4, 161.1, 151.1, 147.8, 140.0, 137.8, 124.8, 120.9, 119.5, 118.0, 115.1, 112.2, 54.7, 51.80, 25.1. HRMS (ESI): calculated for $C_{23}H_{28}N_7O_5S$ $[M+H]^+$ 514.1873, found 514.1877.

(*E*)-3-(4-((trimethylsilyl)ethynyl)phenyl)acrylaldehyde (15y). To a solution of 4-((trimethylsilyl)ethynyl)benzaldehyde **14y** (1.81 g, 8.0 mmol) in THF (40 ml), (triphenyl phosphoramylidene)acetaldehyde (2.20 g, 7.2 mmol) was added. The suspension was stirred at 50°C under N_2 for overnight and concentrated to dryness under vacuum. The crude product was purified by flash chromatography on silica gel (0–90% CH_2Cl_2 in petroleum ether) to give compound **15y** (1.2 g, 73%) as a white solid. ^{1}H NMR (400 MHz, $CDCl_3$) δ 9.72 (d, *J* = 7.7 Hz, 1H), 7.54 – 7.50 (m, 4H), 7.45 (br d, *J* = 12.0 Hz, 1H), 6.75 – 6.69 (m, 1H), 0.28 (s, 9H). ^{13}C NMR (101 MHz, $CDCl_3$) δ 193.5, 151.6, 132.9, 132.6, 128.3, 126.1, 104.3, 97.6. HRMS (ESI): calculated for $C_{14}H_{17}OSi$ $[M+H]^+$ 229.3740, found 229.3744.

***tert*-butyl (2*S*)-4-((((3a*R*,4*R*,6*R*,6a*R*)-6-(6-amino-9*H*-purin-9-yl)-2,2-dimethyltetrahydrofuro[3,4-d][1,3]dioxol-4-yl)methyl)((*E*)-3-(o-tolyl)allyl)amino)-2-((*tert*-butoxycarbonyl)amino)butanoate (16a).** Following the procedure described for compound **12a**, coupling compound **11** (112 mg, 0.20 mmol) with (*E*)-3-(o-tolyl)acrylaldehyde **15a** (35 mg, 0.24 mmol) afforded compound **16a** as a white powder (100 mg, 72% yield) ^{1}H NMR (400 MHz, $CDCl_3$) δ 8.28 (s, 1H), 7.95 (s, 1H), 7.41 – 7.35 (m, 1H), 7.29 (s, 1H), 7.14 (dd, *J* = 5.3, 3.9 Hz, 3H), 6.6 – 6.64 (br d, *J* = 12.0 Hz, 1H), 6.27 (s, 2H), 6.13 – 6.03 (m, 2H), 5.73 (d, *J* = 8.1 Hz, 1H), 5.48 (d, *J* = 5.1 Hz, 1H), 5.05 – 4.96 (m, 1H), 4.43 – 4.39 (m, 1H), 4.25 – 4.21 (m, 1H), 3.42 – 3.33 (m, 1H), 3.31 – 3.23 (m, 1H), 2.89 – 2.84 (m, 1H), 2.72 – 2.55 (m, 3H), 2.30 (s, 3H), 2.07 –1.91 (m, 1H), 1.86 – 1.74 (m, 1H), 1.63 (s, 3H), 1.44 – 1.41 (br m, 21H). ^{13}C NMR (101 MHz, $CDCl_3$) δ 171.9, 155.8, 153.1, 149.3, 140.0, 136.0, 135.2, 130.9, 127.4, 126.1, 125.7, 120.4, 114.5, 90.8,

85.5, 83.9, 83.4, 81.7, 57.2, 55.9, 52.9, 50.6, 29.5, 28.4, 28.0, 27.2, 25.5, 19.9. HRMS (ESI): calculated for $C_{36}H_{52}N_7O_7$ $[M+H]^+$ 694.3928, found 694.3935.

tert-butyl (2*S*)-4-((((3a*R*,4*R*,6*R*,6a*R*)-6-(6-amino-9*H*-purin-9-yl)-2,2-dimethyltetrahydrofuro[3,4-d][1,3]dioxol-4-yl)methyl)((*E*)-3-(m-tolyl)allyl)amino)-2-((*tert*-butoxycarbonyl)amino)butanoate (16b). Following the procedure described for compound **12a**, coupling compound **11** (112 mg, 0.20 mmol) with (*E*)-3-(*m*-tolyl)acrylaldehyde **15b** (35 mg, 0.24 mmol) afforded compound **16b** as a white powder (104 mg, 75% yield). ^{1}H NMR (400 MHz, $CDCl_3$) δ 8.26 (s, 1H), 7.92 (s, 1H), 7.18 – 7.09 (m, 3H), 7.01 (d, *J* = 7.3 Hz, 1H), 6.40 – 6.36 (br d, *J* = 16.0 Hz, 1H), 6.20 – 6.05 (m, 4H), 5.66 (d, *J* = 7.9 Hz, 1H), 5.44 (d, *J* = 6.1 Hz, 1H), 4.96 (d, *J* = 5.8 Hz, 1H), 4.38 (s, 1H), 4.24 – 4.08 (m, 1H), 3.39 – 3.14 (m, 2H), 2.84 – 2.79 (m, 1H), 2.71 – 2.50 (m, 3H), 2.31 (s, 3H), 2.00 – 1.93 (m, 1H), 1.82 – 1.73 (m 1H), 1.60 (s, 3H), 1.41 – 1.38 (br m, 21H). ^{13}C NMR (101 MHz, $CDCl_3$) δ 171.8, 155.8, 153.1, 149.3, 141.0, 140.0, 135.1, 128.5, 126.1, 123.5, 120.4, 114.5, 90.8, 85.4, 83.3, 57.0, 55.9, 52.9, 50.6, 29.5, 28.4, 28.0, 27.2, 25.5. 21.4. HRMS (ESI): calculated for $C_{36}H_{52}N_7O_7$ $[M+H]^+$ 694.3928, found 694.3938.

tert-butyl (2*S*)-4-((((3a*R*,4*R*,6*R*,6a*R*)-6-(6-amino-9*H*-purin-9-yl)-2,2-dimethyltetrahydrofuro[3,4-d][1,3]dioxol-4-yl)methyl)((*E*)-3-(p-tolyl)allyl)amino)-2-((*tert*-butoxycarbonyl)amino)butanoate (16c). Following the procedure described for compound **12a**, coupling compound **11** (112 mg, 0.20 mmol) with (*E*)-3-(*p*-tolyl)acrylaldehyde **15c** (35 mg, 0.24 mmol) afforded compound **16c** as a white powder (109 mg, 79% yield). ^{1}H NMR (400 MHz, $CDCl_3$) δ 8.26 (s, 1H), 7.92 (s, 1H), 7.19 (d, *J* = 8.1 Hz, 2H), 7.07 (d, *J* = 8.0 Hz, 2H), 6.39 – 6.35 (br *J* = 16.1 Hz, 1H), 6.25 – 5.98 (m, 4H), 5.66 (d, *J* = 8.1 Hz, 1H), 5.43 (d, *J* = 6.1 Hz, 1H), 4.96 (d, *J* = 6.1 Hz, 1H), 4.36 (br s, 1H), 4.21 – 4.17 (m, 1H), 3.33 – 3.16 (m, 2H), 2.84 – 2.79 (m, 1H), 2.67 – 2.53 (m, 3H), 2.30 (s, 3H), 1.98 – 1.93 (m, 1H), 1.84 – 1.71 (m, 1H), 1.60 (s, 3H), 1.44 – 1.37 (br m, 21H). ^{13}C NMR (101 MHz, $CDCl_3$) δ 171.8, 155.8, 153.1, 149.3, 140.03, 136.8, 133.0, 128.6, 127.5, 126.3, 120.4, 114.5, 90.8, 85.5, 83.9, 83.4, 81.7, 57.0, 55.9, 52.9, 28.4, 28.0, 27.2, 25.5. HRMS (ESI): calculated for $C_{36}H_{52}N_7O_7$ $[M+H]^+$ 694.3928, found 694.3940.

tert-butyl (2S)-4-((((3a*R*,3a*R*,4*R*,6R,6a*R*,6a*R*)-6-(6-amino-9*H*-purin-9-yl)-2,2-dimethyltetra-hydrofuro[3,4-d][1,3]dioxol-4-yl)methyl)((*E*)-3-(2-methoxyphenyl)allyl)amino)-2-((*tert*-butoxy carbonyl)amino)butanoate (16d). Following the procedure described for compound **12a**, coupling compound **11** (112 mg, 0.20 mmol) with (*E*)-3-(2-methoxyphenyl)acrylaldehyde **15d** (39 mg, 0.24 mmol) afforded compound **16d** as a white powder (75 mg, 53% yield). ^{1}H NMR (400 MHz, $CDCl_3$) δ 8.27 (s, 1H), 7.95 (s, 1H), 7.38 (d, *J* = 7.6 Hz, 1H), 7.24 – 7.17 (m, 1H), 6.93 – 6.75 (m, 3H), 6.33 (br s, 2H), 6.25 – 6.14 (m, 1H), 6.07 (d, *J* = 2.2 Hz, 1H), 5.74 (d, *J* = 8.2 Hz, 1H), 5.44 (d, *J* = 6.5 Hz, 1H), 5.06 – 4.93 (m, 1H), 4.43 – 4.39

(m, 1H), 4.26 – 4.16 (m, 1H), 3.83 (s, 3H), 3.39 – 3.22 (m, 2H), 2.88 – 2.83 (m, 1H), 2.75 – 2.50 (m, 3H), 2.03 – 1.98 (m, 1H), 1.85 – 1.78 (m, 1H), 1.62 (s, 3H), 1.42 – 1.40 (br m, 21H). ^{13}C NMR (101 MHz, $CDCl_3$) δ 171.3, 156.5, 155.8, 155.1, 153.6, 149.9, 141.4, 130.3, 126.8, 125.9, 120.7, 119.7, 114.5, 111.3, 90.8, 85.8, 84.0, 82.7, 81.7, 79.4, 57.4, 55.9, 55.4, 52.9, 49.9, 29.4, 28.4, 27.2, 25.5. HRMS (ESI): calculated for $C_{36}H_{52}N_7O_8$ $[M+H]^+$ 710.3877, found 710.3882.

tert-butyl (2S)-4-((((3a*R*,3a*R*,4*R*,6R,6a*R*,6a*R*)-6-(6-amino-9*H*-purin-9-yl)-2,2-dimethyltetra-hydrofuro[3,4-d][1,3]dioxol-4-yl)methyl)((*E*)-3-(3-methoxyphenyl)allyl)amino)-2-((*tert*-butoxy carbonyl)amino)butanoate (16e). Following the procedure described for compound **12a**, coupling compound **11** (112 mg, 0.20 mmol) with (*E*)-3-(2-methoxyphenyl)acrylaldehyde **15e** (39 mg, 0.24 mmol) afforded compound **16e** as a white powder (82 mg, 58% yield). ^{1}H NMR (400 MHz, $CDCl_3$) δ 8.30 (s, 1H), 7.96 (s, 1H), 7.23 (t, *J* = 7.9 Hz, 1H), 6.97 – 6.88 (m, 2H), 6.80 (dd, *J* = 8.2, 2.4 Hz, 1H), 6.44 – 6.40 (br d, *J* = 16.0 Hz, 1H), 6.28 – 6.17 (m, 1H), 6.09 – 6.03 (br d, *J* = 24.0 Hz, 3H), 5.66 – 5.48 (br m, 2H), 5.05 – 4.97 (m, 1H), 4.48 – 4.36 (m, 1H), 4.23 (d, *J* = 4.7 Hz, 1H), 3.83 (s, 3H), 3.43 – 3.18 (m, 2H), 2.88 – 2.83 (m, 1H), 2.75 – 2.53 (m, 3H), 2.00 – 1.97 (m, 1H), 1.88 – 1.73 (m, 1H), 1.64 (s, 3H), 1.45 – 1.42 (br m, 21H). ^{13}C NMR (101 MHz, $CDCl_3$) δ 171.8, 159.8, 155.7, 151.9, 149.3, 140.1, 138.3, 133.5, 130.0, 127.6, 120.4, 119.9, 114.5, 113.3, 110.8, 93.1, 89.5, 81.7, 83.4, 81.72, 57.0, 55.9, 55.3, 50.6, 28.4, 28.0, 27.2, 25.5. HRMS (ESI): calculated for $C_{36}H_{52}N_7O_8$ $[M+H]^+$ 710.3877, found 710.3885.

tert-butyl (2*S*)-4-((((3a*R*,3a*R*,4*R*,6R,6a*R*,6a*R*)-6-(6-amino-9*H*-purin-9-yl)-2,2-dimethyltetra-hydrofuro[3,4-d][1,3]dioxol-4-yl)methyl)((*E*)-3-(4-methoxyphenyl)/allyl)amino)-2-((*tert*-butoxy carbonyl)amino)butanoate (16f). Following the procedure described for compound **12a**, coupling compound **11** (112 mg, 0.20 mmol) with (*E*)-3-(4-methoxyphenyl)acrylaldehyde **15f** (39 mg, 0.24 mmol) afforded compound **16f** as a white powder (86 mg, 61% yield). ^{1}H NMR (400 MHz, $CDCl_3$) δ 8.29 (s, 1H), 7.96 (s, 1H), 7.26 (d, *J* = 8.7 Hz, 2H), 6.84 (d, *J* = 8.8 Hz, 2H), 6.45 – 6.21 (m, 3H), 6.09 – 6.04 (m, 2H), 5.72 (d, *J* = 8.2 Hz, 1H), 5.47(d, *J* = 8.1 Hz, 1H), 5.01 – 4.99 (m, 1H), 4.41 – 4.40 (br d, *J* = 8.2 Hz, 1H), 4.25 – 4.20 (m, 1H), 3.81 (s, 3H), 3.36 – 3.30 (m, 1H), 3.25 – 3.17 (m, 1H), 2.87 – 2.82 (m, 1H), 2.71 – 2.53 (m, 3H), 2.03 – 1.96 (m, 1H), 1.86 – 1.75 (m, 1H), 1.63 (s, 3H), 1.47 – 1.41 (br m, 21H). ^{13}C NMR (101 MHz, $CDCl_3$) δ 171.8, 159.1, 155.8, 155.6, 153.1, 149.3, 140.1, 132.5, 129.7, 127.5, 124.9, 120.3, 114.5, 114.0, 90.9, 85.5, 83.95, 83.4, 81.7, 57.1, 55.8, 55.3, 52.9, 29.5, 28.4, 28.0, 27.2, 25.5. HRMS (ESI): calculated for $C_{36}H_{52}N_7O_8$ $[M+H]^+$ 710.3877, found 710.3887.

tert-butyl (2*S*)-4-((((3a*R*,3a*R*,4*R*,6R,6a*R*,6a*R*)-6-(6-amino-9*H*-purin-9-yl)-2,2-dimethyltetra-hydrofuro[3,4-d][1,3]dioxol-4-yl)methyl)((*E*)-3-(2-fluorophenyl)allyl)amino)-2-

((*tert*-butoxy carbonyl)amino)butanoate (16g). Following the procedure described for compound **12a**, coupling compound **11** (112 mg, 0.20 mmol) with (*E*)-3-(2-fluorophenyl)acrylaldehyde **15g** (36 mg, 0.24 mmol) afforded compound **16g** as a white powder (96 mg, 69% yield). ^{1}H NMR (600 MHz, $CDCl_3$) δ 8.26 (s, 1H), 7.91 (s, 1H), 7.37 (t, *J* = 7.1 Hz, 1H), 7.19 – 7.15 (m, 1H), 7.04 (t, *J* = 7.9 Hz, 1H), 7.01 – 6.97 (m, 1H), 6.58 (m, 1H), 6.30 – 6.21 (m, 1H), 6.04 (s, 1H), 5.90 (s, 2H), 5.58 (d, *J* = 8.0 Hz, 1H), 5.44 (d, *J* = 5.4 Hz, 1H), 5.01 – 4.92 (m, 1H), 4.38 (s, 1H), 4.22 – 4.15 (m, 1H), 3.35 (d, *J* = 6.2 Hz, 1H), 3.29 – 3.19 (m, 1H), 2.86 – 2.80 (m, 1H), 2.71 – 2.51 (m, 3H), 1.99 – 1.96 (m, 1H), 1.82 – 1.72 (m, 1H), 1.60 (s, 3H), 1.40 – 1.38 (br m, 21H). ^{13}C NMR (151 MHz, $CDCl_3$) δ 171.5, 168.8, 159.4, 156.6, 152.5, 147.4, 145.2, 141.6, 137.1, 127.2, 123.5, 121.5, 119.8, 116.2, 112.4, 91.7, 85.9, 83.3, 81.7, 79.9, 57.1, 54.8, 52.4, 51.8, 49.6, 28.1, 26.1, 24.4. HRMS (ESI): calculated for $C_{35}H_{49}FN_7O_7$ $[M+H]^+$ 698.3678, found 698.3690.

tert-butyl (2*S*)-4-((((3a*R*,3a*R*,4*R*,6R,6a*R*,6a*R*)-6-(6-amino-9*H*-purin-9-yl)-2,2-dimethyltetra-hydrofuro[3,4-d][1,3]dioxol-4-yl)methyl)((*E*)-3-(3-fluorophenyl)allyl)amino)-2-((*tert*-butoxy carbonyl)amino)butanoate (16h). Following the procedure described for compound **12a**, coupling compound **11** (112 mg, 0.20 mmol) with (*E*)-3-(3-fluorophenyl)acrylaldehyde **15h** (36 mg, 0.24 mmol) afforded compound **16h** as a white powder (93 mg, 67% yield). ^{1}H NMR (600 MHz, $CDCl_3$) δ 8.26 (s, 1H), 7.91 (s, 1H), 7.25 – 7.18 (m, 1H), 7.03 (d, *J* = 7.7 Hz, 1H), 7.01 – 6.98 (m, 1H), 6.91 – 6.87 (m 1H), 6.36 (d, *J* = 8.1 Hz , 1H), 6.20 – 6.15 (m, 1H), 6.04 (s, 1H), 5.91 (s, 2H), 5.57 (d, *J* = 8.0 Hz, 1H), 5.45 (d, *J* = 5.5 Hz, 1H), 4.97 (d, *J* = 5.7 Hz, 1H), 4.42 – 4.34 (m, 1H), 4.19 (d, *J* = 4.9 Hz, 1H), 3.32 – 3.28 (m, 1H), 3.23 – 3.19 (m, 1H), 2.82 – 2.79 (m, 1H), 2.70 – 2.50 (m, 3H), 2.03 – 1.91 (m, 1H), 1.79 – 1.75 (m, 1H), 1.60 (s, 3H), 1.42 – 1.38 (br m, 21H). ^{13}C NMR (151 MHz, $CDCl_3$) δ 170.70, 162.85, 161.22, 154.58, 154.49, 152.06, 148.19, 139.03, 138.13, 130.67, 128.94, 128.88, 127.12, 121.17, 119.29, 113.45, 113.28, 113.14, 111.76, 111.61, 89.75, 84.52, 82.87, 82.26, 80.69, 55.83, 54.96, 51.81, 49.61, 28.54, 27.33, 26.95, 26.14, 24.42. HRMS (ESI): calculated for $C_{35}H_{49}FN_7O_7$ $[M+H]^+$ 698.3678, found 698.3682.

tert-butyl (2*S*)-4-((((3a*R*,3a*R*,4*R*,6R,6a*R*,6a*R*)-6-(6-amino-9*H*-purin-9-yl)-2,2-dimethyltetra-hydrofuro[3,4-d][1,3]dioxol-4-yl)methyl)((*E*)-3-(4-fluorophenyl)allyl)amino)-2-((*tert*-butoxy carbonyl)amino)butanoate (16i). Following the procedure described for compound **12a**, coupling compound **11** (112 mg, 0.20 mmol) with (*E*)-3-(4-fluorophenyl)acrylaldehyde **15i** (36 mg, 0.24 mmol) afforded compound **16i** as a white powder (86 mg, 62% yield). ^{1}H NMR (400 MHz, $CDCl_3$) δ 8.21 (s, 1H), 7.89 (s, 1H), 7.21 – 7.16 (m, 2H), 6.90 (t, *J* = 8.6 Hz, 2H), 6.51 (s, 2H), 6.32 – 6.29 (br d, *J* = 16.1 Hz, 1H), 6.08 – 5.99 (m, 2H), 5.74 (d, *J* = 8.1 Hz, 1H), 5.42 (d, *J* = 7.9 Hz, 1H), 4.96 (d, *J* = 3.5 Hz, 1H), 4.36 – 4.32 (m, 1H), 4.22–4.14 (m, 1H), 3.27 – 3.22

(m, 1H), 3.18 – 3.12 (m, 1H), 2.80 – 2.75 (m, 1H), 2.66 – 2.57(m, 2H), 2.54 – 2.46 (m, 1H), 1.99 – 1.88 (m, 1H), 1.78 – 1.69 (m, 1H), 1.56 (s, 3H), 1.36 – 1.34 (br m, 21H). ^{13}C NMR (101 MHz, $CDCl_3$) δ 171.8, 163.3, 160.9, 155.9, 155.5, 153.0, 149.1, 139.9, 132.9, 131.5, 127.7, 126.2, 120.2, 115.4, 115.2, 114.3, 90.7, 85.5, 83.8, 83.2, 81.7, 79.3, 56.9, 55.8, 52.8, 50.5, 29.4, 28.3, 27.9, 27.1, 25.4. HRMS (ESI): calculated for $C_{35}H_{49}FN_7O_7$ $[M+H]^+$ 698.3678, found 698.3694.

tert-butyl (2*S*)-4-((((3a*R*,3a*R*,4*R*,6R,6a*R*,6a*R*)-6-(6-amino-9*H*-purin-9-yl)-2,2-dimethyltetra-hydrofuro[3,4-d][1,3]dioxol-4-yl)methyl)((*E*)-3-(2-chlorophenyl)allyl)amino)-2-((*tert*-butoxy carbonyl)amino)butanoate (16j). Following the procedure described for compound **12a**, coupling compound **11** (112 mg, 0.20 mmol) with (*E*)-3-(2-chlorophenyl)acrylaldehyde **15j** (40 mg, 0.24 mmol) afforded compound **16j** as a white powder (84 mg, 59% yield). ^{1}H NMR (400 MHz, $CDCl_3$) δ 8.25 (s, 1H), 7.91 (s, 1H), 7.44 – 7.41 (m, 1H), 7.29 (dd, *J* = 7.5, 1.7 Hz, 1H), 7.17 – 7.09 (m, 2H), 6.80 (d, *J* = 15.9 Hz, 1H), 6.22 – 6.10 (m, 3H), 6.04 (s, 1H), 5.65 (d, *J* = 8.0 Hz, 1H), 5.44 (d, *J* = 5.6 Hz, 1H), 4.98 (d, *J* = 9.5 Hz, 1H), 4.41 – 4.33 (m, 1H), 4.23 – 4.16 (m, 1H), 3.38 – 3.30 (m, 1H), 3.28 – 3.20 (m, 1H), 2.86 – 2.81 (m, 1H), 2.62 (br s, 2H), 2.56 (d, *J* = 12.9 Hz, 1H), 12.01 – 1.92 (m, 1H), 1.79 – 1.75 (m, 1H), 1.59 (s, 3H), 1.39 – 1.37 (br m, 21H). ^{13}C NMR (101 MHz, $CDCl_3$) δ 174.1, 158.8, 158.6, 156.1, 152.2, 135.8, 132.6, 132.0, 131.5, 129.9, 129.8, 123.4, 117.5, 93.8, 88.5, 86.9, 86.3, 82.4, 59.0, 32.6, 31.4, 31.0, 30.2, 28.5. HRMS (ESI): calculated for $C_{35}H_{49}ClN_7O_7$ $[M+H]^+$ 714.3382, found 714.3389.

tert-butyl (2*S*)-4-((((3a*R*,3a*R*,4*R*,6R,6a*R*,6a*R*)-6-(6-amino-9*H*-purin-9-yl)-2,2-dimethyltetra-hydrofuro[3,4-d][1,3]dioxol-4-yl)methyl)((*E*)-3-(3-chlorophenyl)allyl)amino)-2-((*tert*-butoxy carbonyl)amino)butanoate (16k). Following the procedure described for compound **12a**, coupling compound **11** (112 mg, 0.20 mmol) with (*E*)-3-(3-chlorophenyl)acrylaldehyde **15k** (40 mg, 0.24 mmol) afforded compound **16k** as a white powder (79 mg, 65% yield). ^{1}H NMR (400 MHz, $CDCl_3$) δ 8.22 (s, 1H), 7.88 (s, 1H), 7.17 – 7.09 (m, 3H), 6.32 – 6.28 (br d, *J* = 16.0 Hz, 1H), 6.16 (d, *J* = 5.8 Hz, 3H), 6.01 (s, 1H), 5.62 (d, *J* = 7.9 Hz, 1H), 5.42 (d, *J* = 5.6 Hz, 1H), 4.98 – 4.91 (m, 1H), 4.37 – 4.30 (m, 1H), 4.18 (s, 1H), 3.29 – 3.24 (m, 1H), 3.19 – 3.14 (m, 1H), 2.81 – 2.76 (m, 1H), 2.66 – 2.60 (m, 2H), 2.53 – 2.47 (m, 1H), 1.99 – 1.88 (m, 1H), 1.79 – 1.67 (m, 1H), 1.56 (s, 3H), 1.36 (d, *J* = 6.8, 21H). ^{13}C NMR (101 MHz, $CDCl_3$) δ 174.0, 158.9, 158.7, 157.0, 150.5, 143.2, 141.2, 137.2, 135.1, 132.9, 131.5, 130.5, 129.4, 127.7, 124.1, 118.9, 95.0, 88.7, 87.6, 86.5, 84.8, 84.3, 60.7, 59.1, 53.8, 32.7, 31.6, 31.1, 28.6. HRMS (ESI): calculated for $C_{35}H_{49}ClN_7O_7$ $[M+H]^+$ 714.3382, found 714.3408.

tert-butyl (2*S*)-4-((((3a*R*,3a*R*,4*R*,6R,6a*R*,6a*R*)-6-(6-amino-9*H*-purin-9-yl)-2,2-dimethyltetra-hydrofuro[3,4-d][1,3]dioxol-4-yl)methyl)((*E*)-3-(4-chlorophenyl)allyl)amino)-2-

((*tert*-butoxy carbonyl)amino)butanoate (16l). Following the procedure described for compound **12a**, coupling compound **11** (112 mg, 0.20 mmol) with (*E*)-3-(4-chlorophenyl)acrylaldehyde **15l** (40 mg, 0.24 mmol) afforded compound **16l** as a white powder (79 mg, 56% yield). ^{1}H NMR (400 MHz, $CDCl_3$) δ 8.22 (s, 1H), 7.89 (s, 1H), 7.19 – 7.13 (m, 4H), 6.43 (s, 2H), 6.31 – 6.28 (br , *J* = 16.0 Hz, 1H), 6.12 – 6.05 (m, 1H), 6.02 (d, *J* = 4.1 Hz, 1H), 5.70 (d, *J* = 8.1 Hz, 1H), 5.42 (d, *J* = 5.9 Hz, 1H), 4.97 – 4.94(m, 1H), 4.37 – 4.32 (m, 1H), 4.22 – 4.14 (m, 1H), 3.28 – 3.22 (m, 1H), 3.19 – 3.13 (m, 1H), 2.80 – 2.76 (m, 1H), 2.68 – 2.58 (m, 2H), 2.54 – 2.47 (m, 1H), 2.00 – 1.89 (m, 1H), 1.75 (d, *J* = 9.4 Hz, 1H), 1.57 (s, 3H), 1.37 – 1.35 (br m, 21H). ^{13}C NMR (101 MHz, $CDCl_3$) δ 171.7, 155.8, 155.5, 152.9, 149.1, 139.9, 135.2, 132.9, 131.5, 128.6, 127.4, 120.2, 114.3, 90.7, 85.5, 83.8, 83.3, 81.6, 79.4, 56.9, 55.9, 52.8, 50.5, 29.5, 28.3, 27.1, 25.4. HRMS (ESI): calculated for $C_{35}H_{49}ClN_7O_7$ $[M+H]^+$ 714.3382, found 714.3403.

tert-butyl (*S*)-4-((((3a*R*,4*R*,6*R*,6a*R*)-6-(6-amino-9*H*-purin-9-yl)-2,2-dimethyltetrahydrofuro[3,4-d][1,3]dioxol-4-yl)methyl)((*E*)-3-(2-bromophenyl)allyl)amino)-2-((*tert*-butoxycarbonyl)amino) butanoate (16m). Following the procedure described for compound **12a**, coupling compound **11** (112 mg, 0.20 mmol) with (*E*)-3-(2-bromophenyl)acrylaldehyde **15m** (51 mg, 0.24 mmol) afforded compound **16m** as a white powder (80 mg, 53% yield). ^{1}H NMR (400 MHz, $CDCl_3$) δ 8.33 – 8.22 (m, 1H), 7.93 (s, 1H), 7.50 (dd, *J* = 7.9, 3.9 Hz, 1H), 7.47 – 7.38 (m, 1H), 7.28 (t, *J* = 4.4 Hz, 1H), 7.22 (d, *J* = 7.3 Hz, 1H), 7.06 (d, *J* = 7.4 Hz, 1H), 6.77 (d, *J* = 15.2 Hz, 1H), 6.19 (s, 2H), 6.16 – 6.01 (m, 2H), 5.67 (s, 1H), 5.46 (s, 1H), 5.01 (s, 1H), 4.40 (s, 1H), 4.22 (s, 1H), 3.32 (br d, *J* = 22.6 Hz, 2H), 2.84 (s, 1H), 2.63 (br d, *J* = 42.6 Hz, 3H), 1.98 (s, 1H), 1.79 (s, 1H), 1.61 (d, *J* = 3.8 Hz, 3H), 1.42 (d, *J* = 2.1 Hz, 21H). ^{13}C NMR (101 MHz, $CDCl_3$) δ 171.7, 155.6, 155.5, 152.9, 149.0, 139.9, 136.3, 133.9, 132.3, 128.1, 128.0, 126.3, 124.0, 120.2, 90.9, 85.5, 83.8, 83.5, 81.7, 59.2, 56.0, 53.5, 52., 50.9, 29.5, 28.4, 27.9, 27.1, 25.4. HRMS (ESI): calculated for $C_{35}H_{49}BrN_7O_7$ $[M+H]^+$ 758.2877 found 758.2882.

tert-butyl (2*S*)-4-((((3a*R*,3a*R*,4*R*,6R,6a*R*,6a*R*)-6-(6-amino-9*H*-purin-9-yl)-2,2-dimethyltetra-hydrofuro[3,4-d][1,3]dioxol-4-yl)methyl)((*E*)-3-(3-bromophenyl)allyl)amino)-2-((*tert*-butoxy carbonyl)amino)butanoate (16n). Following the procedure described for compound **12a**, coupling compound **11** (112 mg, 0.20 mmol) with (*E*)-3-(3-bromophenyl)acrylaldehyde **15n** (51 mg, 0.24 mmol) afforded compound **16n** as a white powder (94 mg, 62% yield). ^{1}H NMR (600 MHz $CDCl_3$) δ 8.25 (s, 1H), 7.90 (s, 1H), 7.43 (s, 1H), 7.30 (d, J = 7.8 Hz, 1H), 7.18 – 7.10 (m, 2H), 6.33 – 6.30 (br d, *J* = 12.0 Hz, 1H), 6.19 – 6.14 (m, 1H), 6.05 (d, *J* = 8.1 Hz , 2H), 5.61 (d, *J* = 7.7 Hz, 1H), 5.44 (d, *J* = 5.3 Hz, 1H), 4.98 (s, 1H), 4.36 (s, 1H), 4.19 (s, 1H), 3.31 – 3.18 (m, 2H), 2.82 – 2.78 (m, 1H), 2.70 – 2.50 (m, 3H), 1.96(br d, *J* = 4.0 Hz, 1H), 1.78 (br d, *J* = 4.1 Hz, 1H), 1.59 (s, 3H), 1.39 (d, *J* = 10.7 Hz, 21H). ^{13}C NMR (151 MHz, $CDCl_3$) δ 170.2, 156.2, 153.1,

147.5, 138.5, 131.3, 130.3, 130.0, 129.1, 122.7, 124.5, 122.7, 90.7, 85.2, 84.6, 83.9, 83.3, 81.3, 79.5, 56.0, 52.8, 49.9, 29.58, 29.6, 28.4, 27.2, 24.4. HRMS (ESI): calculated for $C_{35}H_{49}BrN_7O_7$ $[M+H]^+$ 758.2877 found 758.2881.

tert-butyl (2S)-4-((((3a*R*,3a*R*,4*R*,6R,6a*R*,6a*R*)-6-(6-amino-9*H*-purin-9-yl)-2,2-dimethyltetra-hydrofuro[3,4-d][1,3]dioxol-4-yl)methyl)((*E*)-3-(4-bromophenyl)allyl)amino)-2-((*tert*-butoxy carbonyl)amino)butanoate (16o). Following the procedure described for compound **12a**, coupling compound **11** (112 mg, 0.20 mmol) with (*E*)-3-(4-bromophenyl)acrylaldehyde **15o** (51 mg, 0.24 mmol) afforded compound **16o** as a white powder (122 mg, 81% yield). ^{1}H NMR (400 MHz, $CDCl_3$) δ 8.22 (s, 1H), 7.89 (s, 1H), 7.33 (d, *J* = 8.4 Hz, 2H), 7.08 (d, *J* = 8.4 Hz, 2H), 6.41 (s, 2H), 6.26 (s, 1H), 6.14 – 6.07 (m, 1H), 6.03 (d, J = 1.6 Hz, 1H), 5.70 (d, *J* = 8.1 Hz, 1H), 5.43 (d, *J* = 5.8 Hz, 1H), 4.96 (dd, *J* = 6.3 Hz, 3.6 Hz, 1H), 4.37 – 4.31 (m, 1H), 4.22 – 4.14 (m, 1H), 3.27 – 3.22 (m, 1H), 3.18 – 3.13 (m, 1H), 2.80 – 2.75 (m, 1H), 2.69 – 2.57 (m, 2H), 2.54 – 2.47 (m, 1H), 1.99 – 1.88 (m, 1H), 1.79 – 1.69 (m, 1H), 1.57 (s, 3H), 1.37 – 1.35 (br d, *J* = 8.3 Hz, 21H). ^{13}C NMR (101 MHz, $CDCl_3$) δ 171.7, 155.8, 155.5, 153.0, 149.1, 139.9, 135.7, 131.5, 127.7, 127.5, 121.1, 120.2, 114.3, 90.7, 85.5, 83.8, 83.3, 81.6, 79.4, 56.89 55.9, 52.80 50.5, 29.5, 28.3, 27.9, 27.1, 25.4. HRMS (ESI): calculated for $C_{35}H_{49}BrN_7O_7$ $[M+H]^+$ 758.2877, found 758.2895.

tert-butyl (2*S*)-4-((((3a*R*,3a*R*,4*R*,6R,6a*R*,6a*R*)-6-(6-amino-9*H*-purin-9-yl)-2,2-dimethyltetra-hydrofuro[3,4-d][1,3]dioxol-4-yl)methyl)((E)-3-(2-nitrophenyl)allyl)amino)-2-((*tert*-butoxy carbonyl)amino)butanoate (16p). Following the procedure described for compound **12a**, coupling compound **11** (112 mg, 0.20 mmol) with (*E*)-3-(2-nitrophenyl)acrylaldehyde **15p** (42 mg, 0.24 mmol) afforded compound **16p** as a white powder (69 mg, 47% yield). ^{1}H NMR (400 MHz, $CDCl_3$) δ 8.21 (s, 1H), 7.91 (s, 1H), 7.82 (d, *J* = 8.1 Hz, 1H), 7.44 (d, *J* = 4.1 Hz, 2H), 7.29 (dd, *J* = 8.3, 4.2 Hz, 1H), 6.85 – 6.81 (br d, *J* = 16.1 Hz, 1H), 6.46 (s, 2H), 6.15 – 6.06 (m, 1H), 6.03 (d, *J* = 2.0 Hz, 1H), 5.73 (d, *J* = 8.1 Hz, 1H), 5.41 (d, *J* = 5.7 Hz, 1H), 4.96 (dd, *J* = 6.4, 3.6 Hz, 1H), 4.37 – 4.31 (m, 1H), 4.21 – 4.14 (m, 1H), 3.33 – 3.28 (m, 1H), 3.24 – 3.19 (m, 1H), 2.83 – 2.78 (m, 1H), 2.72 – 2.60 (m, 2H), 2.56 – 2.50 (m, 1H), 1.98 – 1.91 (m, 1H), 1.79 – 1.68 (m, 1H), 1.55 (s, 3H), 1.42 – 1.29 (br m, 21H). ^{13}C NMR (101 MHz, $CDCl_3$) δ 171.7, 155.8, 155.5, 153.0, 149.1, 139.9, 135.7, 131.5, 127.7, 121.1, 120.2, 114.3, 90.7, 85.5, 83.8, 83.3, 81.6, 79.4, 56.9, 55.9, 53.4, 52.8, 50.6, 29.5, 28.3, 27.1, 25.4. HRMS (ESI): calculated for $C_{35}H_{49}N_8O_9$ $[M+H]^+$ 725.3633, found 725.3632.

tert-butyl (2*S*)-4-((((3a*R*,3a*R*,4*R*,6R,6a*R*,6a*R*)-6-(6-amino-9*H*-purin-9-yl)-2,2-dimethyltetra-hydrofuro[3,4-d][1,3]dioxol-4-yl)methyl)((*E*)-3-(3-nitrophenyl)allyl)amino)-2-((*tert*-butoxy carbonyl)amino)butanoate (16q). Following the procedure described for compound

12a, coupling compound **11** (112 mg, 0.20 mmol) with (*E*)-3-(3-nitrophenyl)acrylaldehyde **15q** (42 mg, 0.24 mmol) afforded compound **16q** as a white powder (63 mg, 43% yield). 1H NMR (400 MHz, $CDCl_3$) δ 8.21 (s, 1H), 7.91 (s, 1H), 7.82 (d, *J* = 8.1 Hz, 1H), 7.44 (d, *J* = 4.1 Hz, 2H), 7.29 (dd, *J* = 8.3, 4.2 Hz, 1H), 6.85 – 6.81 (br d, *J* = 15.7 Hz, 1H), 6.46 (s, 2H), 6.15 – 6.06 (m, 1H), 6.03 (d, *J* = 2.0 Hz, 1H), 5.73 (d, *J* = 8.1 Hz, 1H), 5.41 (d, *J* = 5.7 Hz, 1H), 4.96 (dd, *J* = 6.4, 3.6 Hz, 1H), 4.37 – 4.31 (m, 1H), 4.21 – 4.14 (m, 1H), 3.33 – 3.19 (m, 2H), 2.83 – 2.78 (m, 1H), 2.72 – 2.60 (m, 2H), 2.56 – 2.50 (m, 1H), 1.98 – 1.93 (m, 1H), 1.79 – 1.68 (m, 1H), 1.55 (s, 3H), 1.42 – 1.29 (m, 21H). ^{13}C NMR (151 MHz, $CDCl_3$) δ 170.7, 154.8, 154.4, 152.0, 148.6, 148.1, 138.7, 134.6, 129.3, 123.7, 123.4, 121.5, 119.2, 119.1, 114.1, 113.3, 89.73, 84.2, 82.6, 82.3, 80.6, 54.6, 52.4, 51.7, 49.7, 49.0, 28.5, 27.3, 27.2, 26.9, 26.1, 24.2. HRMS (ESI): calculated for $C_{35}H_{49}N_8O_9$ $[M+H]^+$ 725.3633, found 725.3634.

***tert*-butyl (2*S*)-4-((((3a*R*,3a*R*,4*R*,6R,6a*R*,6a*R*)-6-(6-amino-9*H*-purin-9-yl)-2,2-dimethyltetra-hydrofuro[3,4-d][1,3]dioxol-4-yl)methyl)((*E*)-3-(4-nitrophenyl)allyl)amino)-2-((*tert*-butoxy carbonyl)amino)butanoate (16r).** Following the procedure described for compound **12a**, coupling compound **11** (112 mg, 0.20 mmol) with (*E*)-3-(4-nitrophenyl)acrylaldehyde **15r** (42 mg, 0.24 mmol) afforded compound **16r** as a white powder (74 mg, 51% yield). ^1H NMR (600 MHz, $CDCl_3$) δ 8.24 (s, 1H), 8.10 (d, *J* = 7.7 Hz, 2H), 7.93 (s, 1H), 7.34 (d, *J* = 7.9 Hz, 2H), 6.45 – 6.43 (br d, *J* = 15.9 Hz, 1H), 6.36 – 6.31 (m, 1H), 6.24 (s, 2H), 6.08 (s, 1H), 5.62 (d, *J* = 7.7 Hz, 1H), 5.46 (d, *J* = 5.0 Hz, 1H), 5.02 (s, 1H), 4.40 (s, 1H), 4.24 (s, 1H), 3.37 – 3.23 (m, 2H), 2.87 – 2.81 (m, 1H), 2.78 (br d, *J* = 19.4 Hz, 1H), 2.66 (s, 1H), 2.61 – 2.57 (m, 1H), 2.03 – 1.99 (br d, *J* = 20.7 Hz, 1H), 1.84 – 1.73 (m, 1H), 1.61 (s, 3H), 1.42 – 1.40 (br d, *J* = 15.3 Hz, 21H). ^{13}C NMR (151 MHz, $CDCl_3$) δ 171.6, 155.7, 153.0, 149.1, 146.7, 143.2, 140.1, 126.6, 123.9, 120.3, 114.43, 90.7, 85.7, 84.0, 83.3, 81.8, 79.5, 56.9, 56.1, 52.8, 50.8, 29.7, 28.4, 28.0, 27.2, 25.4. HRMS (ESI): calculated for $C_{35}H_{49}N_8O_9$ $[M+H]^+$ 725.3633, found 725.3639.

***tert*-butyl (2S)-4-((((3a*R*,3a*R*,4*R*,6R,6a*R*,6a*R*)-6-(6-amino-9*H*-purin-9-yl)-2,2-dimethyltetra-hydrofuro[3,4-d][1,3]dioxol-4-yl)methyl)((*E*)-3-(2-cyanophenyl)allyl)amino)-2-((*tert*-butoxy carbonyl)amino)butanoate (16s).** Following the procedure described for compound **12a**, coupling compound **11** (112 mg, 0.20 mmol) with (*E*)-2-(3-oxoprop-1-en-1-yl)benzonitrile **15s** (58 mg, 0.24 mmol) afforded compound **16s** as a white powder (82 mg, 68% yield). ^1H NMR (600 MHz, $CDCl_3$) δ 8.26 (s, 1H), 7.97 (s, 1H), 7.58 (d, *J* = 7.7 Hz, 1H), 7.54 (d, *J* = 8.0 Hz, 1H), 7.49 (t, *J* = 7.6 Hz, 1H), 7.28 (t, *J* = 7.5 Hz, 1H), 6.78 (br d, *J* = 11.6 Hz, 1H), 6.54 (s, 2H), 6.43 – 6.34 (m, 1H), 6.09 (s, 1H), 5.78 (d, *J* = 8.2 Hz, 1H), 5.47 (d, *J* = 5.6 Hz, 1H), 5.03 (dd, *J* = 6.2, 3.6 Hz, 1H), 4.42 – 4.39 m, 1H), 4.26 – 4.23 (m, 1H), 3.40 – 3.37 (m, 1H), 3.32 – 3.28 (m, 1H), 2.89 – 2.85 (m, 1H), 2.77 – 2.73 (m, 1H), 2.70 – 2.66 (m, 1H), 2.62 – 2.56 (m, 1H), 2.06 – 1.93

(m, 1H), 1.85 – 1.73 (m, 1H), 1.62 (s, 3H), 1.49 – 1.34 (br m, 21H). ^{13}C NMR (151 MHz, $CDCl_3$) δ 171.8, 155.9, 155.5, 153.0, 149.1, 132.7, 128.2, 127.5, 125.6, 120.2, 117.9, 114.4, 110.7, 90.6, 85.4, 83.9, 83.2, 81.6, 57.0, 56.0, 53.5, 52.8, 50.8, 29.6, 28.3, 27.9, 27.2, 25.4. HRMS (ESI): calculated for $C_{36}H_{49}N_8O_7$ $[M+H]^+$ 705.3724, found 705.3734.

tert-butyl (2*S*)-4-((((3a*R*,3a*R*,4*R*,6R,6a*R*,6a*R*)-6-(6-amino-9*H*-purin-9-yl)-2,2-dimethyltetra-hydrofuro[3,4-d][1,3]dioxol-4-yl)methyl)((*E*)-3-(3-cyanophenyl)allyl)amino)-2-((*tert*-butoxy carbonyl)amino)butanoate (16t). Following the procedure described for compound **12a**, coupling compound **11** (112 mg, 0.20 mmol) with (*E*)-3-(3-oxoprop-1-en-1-yl)benzonitrile **15t** (58 mg, 0.24 mmol) afforded compound **16t** as a white powder (69 mg, 49% yield). ^{1}H NMR (400 MHz, $CDCl_3$) δ 8.21 (s, 1H), 7.90 (s, 1H), 7.51 (s, 1H), 7.49 – 7.41 (m, 2H), 7.33 (t, *J* = 7.7 Hz, 1H), 6.33 (d, *J* = 16.0 Hz, 1H), 6.27 – 6.15 (m, 3H), 6.04 (d, *J* = 1.9 Hz, 1H), 5.62 (d, *J* = 8.0 Hz, 1H), 5.43 (d, *J* = 5.9 Hz, 1H), 4.97 (dd, *J* = 6.3, 3.6 Hz, 1H), 4.39 – 4.32 (m, 1H), 4.23 – 4.14 (m, 1H), 3.31 – 3.18 (m, 2H), 2.82 – 2.77 (m, 1H), 2.72 – 2.58 (m, 2H), 2.56 – 2.49 (m, 1H), 2.02 – 1.90 (m, 1H), 1.77 – 1.70 (br, 1H), 1.58 (s, 3H), 1.40 – 1.36 (br m, 21H). ^{13}C NMR (151 MHz, $CDCl_3$) δ 171.7, 155.8, 155.5, 153.0, 149.1, 140.0, 138., 130.7, 130.3, 129.7, 129.3, 120.3, 118.8, 114.4, 112.7, 90.7, 85.6, 83.9, 83.3, 81.7, 79.5, 56.8, 56.0, 52.8, 50.7, 29.6, 28.3, 27.2, 25.4. HRMS (ESI): calculated for $C_{36}H_{49}N_8O_7$ $[M+H]^+$ 705.3724, found 705.3732.

tert-butyl (2*S*)-4-((((3a*R*,3a*R*,4*R*,6R,6a*R*,6a*R*)-6-(6-amino-9*H*-purin-9-yl)-2,2-dimethyltetra-hydrofuro[3,4-d][1,3]dioxol-4-yl)methyl)((*E*)-3-(4-cyanophenyl)allyl)amino)-2-((*tert*-butoxy carbonyl)amino)butanoate (16u). Following the procedure described for compound **12a**, coupling compound **11** (112 mg, 0.20 mmol) with (*E*)-4-(3-oxoprop-1-en-1-yl)benzonitrile **15u** (58 mg, 0.24 mmol) afforded compound **16u** as a white powder (93 mg, 66% yield). ^{1}H NMR (400 MHz, $CDCl_3$) δ 8.23 (s, 1H), 7.90 (s, 1H), 7.53 (d, *J* = 8.4 Hz, 2H), 7.30 (d, *J* = 8.3 Hz, 2H), 6.40 – 6.36 (br d, *J* = 16.0, 1H), 6.33 – 6.22 (m, 1H), 6.08 – 5.91 (m, 3H), 5.53 (d, *J* = 8.0 Hz, 1H), 5.44 (d, *J* = 6.0 Hz, 1H), 5.03 – 4.94 (m, 1H), 4.42 – 4.32 (m, 1H), 4.20 (d, *J* = 4.9 Hz, 1H), 3.36 – 3.20 (m, 2H), 2.84 – 2.79 (m, 1H), 2.72 (d, *J* = 5.2 Hz, 1H), 2.68 – 2.59 (m, 1H), 2.58 – 2.50 (m, 1H), 2.03 – 1.91 (m, 1H), 1.75 (d, *J* = 9.6 Hz, 1H), 1.59 (s, 3H), 1.42 – 1.37 (br m, 21H). ^{13}C NMR (151 MHz, $CDCl_3$) δ 171.6, 155.6, 153.0, 149.1, 140.1, 132.3, 126.7, 120.3, 119.0, 114.5, 110.6, 90.7, 85.7, 83.9, 81.8, 79.5, 56.9, 56.1, 53.4, 52.8, 50.7, 29.1, 28.3, 27.2, 25.5. HRMS (ESI): calculated for $C_{36}H_{49}N_8O_7$ $[M+H]^+$ 705.3724, found 705.3738.

tert-butyl (2S)-4-((((3a*R*,3a*R*,4*R*,6R,6a*R*,6a*R*)-6-(6-amino-9*H*-purin-9-yl)-2,2-dimethyltetra-hydrofuro[3,4-d][1,3]dioxol-4-yl)methyl)((*E*)-3-(3-carbamoylphenyl)allyl)amino)-2-((*tert*-butoxy carbonyl)amino)butanoate (16v). To a solution of compound **16t** (0.21 mmol, 150 mg) in DMSO (10 mL) was added KOH (0.25 mmol, 14 mg). The mixture was cooled to 0 °C and

treated with H_2O_2 (30 % w/w) in H_2O (0.5 mL). The reaction mixture was warmed to room temperature and stirred for 3 hours at room temperature. The reaction was diluted with water and extracted with EtOAc (3x). The combined organic layers were dried over Na_2SO_4. The solvent was evaporated, and the crude product was purified by column chromatography (5% MeOH in EtOAc) to give compound **16v** as a white powder (127 mg, 82% yield). ^{1}H NMR (400 MHz, $CDCl_3$) δ 8.17 (s, 1H), 7.94 (s, 1H), 7.78 (s, 1H), 7.70 (d, *J* = 7.4 Hz, 1H), 7.37 – 7.24 (m, 3H), 7.03 (s, 1H), 6.64 (s, 2H), 6.32 (d, *J* = 15.8 Hz, 1H), 6.23 – 6.12 (m, 1H), 6.06 (d, *J* = 1.5 Hz, 1H), 5.89 (s, 1H), 5.43 (d, *J* = 6.2 Hz, 1H), 4.97 (dd, *J* = 6.2, 3.4 Hz, 1H), 4.39 – 4.35 (m, 1H), 4.22 – 4.17 (m, 1H), 3.26 – 3.13 (m, 2H), 2.78 – 2.55 (m, 4H), 1.97 (dd, *J* = 13.5, 6.0 Hz, 1H), 1.81 – 1.70 (m, 1H), 1.58 (s, 3H), 1.40 – 1.36 (br m, 21H). ^{13}C NMR (101 MHz, $CDCl_3$) δ 172.0, 170.1, 156.0, 155.7, 153.0, 149.0, 137.1, 134.0, 128.7, 128.0, 126.6, 120.1, 114.3, 90.7, 85.8, 84.0, 83.4, 81.8, 79.5, 57.0, 50.6, 45.9, 29.7, 28.4, 28.0, 27.2, 25.5. HRMS (ESI): calculated for $C_{36}H_{51}N_8O_8$ $[M+H]^+$723.3830, found 723.3838.

tert-butyl (*S*)-4-((((3a*R*,4*R*,6*R*,6a*R*)-6-(6-amino-9*H*-purin-9-yl)-2,2-dimethyltetrahydrofuro[3,4-*d*][1,3]dioxol-4-yl)methyl)((*E*)-3-(4-carbamoylphenyl)allyl)amino)-2-((*tert*-butoxycarbonyl) amino)butanoate (16w). Following the procedure described for compound **16v**, compound **16u** was oxidized to afford compound **16w** as a white powder (118 mg, 77% yield). ^{1}H NMR (400 MHz, $CDCl_3$) δ 8.09 (s, 1H), 7.92 (s, 1H), 7.75 (d, *J* = 8.0 Hz, 2H), 7.20 (d, *J* = 8.3 Hz, 2H), 6.72 (s, 2H), 6.34 – 6.30 (br d, *J* = 16 Hz, 1H), 6.20 – 6.10 (m, 1H), 6.04 (d, *J* = 1.6 Hz, 1H), 5.79 (d, *J* = 8.0 Hz, 1H), 5.41 (d, *J* = 6.2 Hz, 1H), 4.98 (dd, *J* = 6.1, 3.7 Hz, 1H), 4.38 – 4.34 (m, 1H), 4.21 – 4.17 (m, 1H), 3.22 (d, *J* = 5.6 Hz, 2H), 3.07 – 3.02 (br m, 1H), 2.80 – 2.67 (m, 2H), 2.61 – 2.55 (m, 2H), 1.58 (s, 3H), 1.44 – 1.36 (br m, 21H). ^{13}C NMR (101 MHz, $CDCl_3$) δ 171.9, 169.9, 156.0, 155.6, 152.9, 149.0, 140.2, 132.3, 131.7, 127.9, 126.2, 90.7, 85.7, 84.0, 83.3, 81.8, 79.5, 56.9, 55.8, 52.9, 45.9, 30.3, 29.7, 28.4, 28.0, 27.2, 25.5. HRMS (ESI): calculated for $C_{36}H_{51}N_8O_8$ $[M+H]^+$ 723.3830, found 723.3832.

tert-butyl (2*S*)-4-((((3a*R*,4*R*,6*R*,6a*R*)-6-(6-amino-9*H*-purin-9-yl)-2,2-dimethyltetrahydrofuro[3,4-d][1,3]dioxol-4-yl)methyl)(cinnamyl)amino)-2-((*tert*-butoxycarbonyl)amino)butanoate (16x). Following the procedure described for compound **12a**, coupling compound **11** (112 mg, 0.20 mmol) with cinnamaldehyde **15x** (32 mg, 0.24 mmol) afforded compound **16x** as a white powder (110 mg, 50% yield). ^{1}H NMR (400 MHz, $CDCl_3$) δ 8.29 (s, 1H), 7.96 (s, 1H), 7.34 – 7.21 (m, 5H), 7.28 (s, 1H), 6.46 – 6.42 (br d, *J* = 16.0 Hz, 1H), 6.31 – 6.16 (m, 3H), 6.08 (d, *J* = 1.7 Hz, 1H), 5.71 (d, *J* = 8.1 Hz, 1H), 5.48 (d, *J* = 5.1 Hz, 1H), 5.02 – 5.00 (m, 1H), 4.50 – 4.35 (m, 1H), 4.22 (d, *J* = 7.4 Hz, 1H), 3.38 – 3.22 (m, 2H), 2.88 – 2.83 (m, 1H), 2.77 – 2.51 (m, 3H), 2.06 – 1.92 (m, 1H), 1.84 – 1.79 (m, 1H), 1.64 (s, 3H), 1.44

– 1.42 (br m, 21H). ^{13}C NMR (101 MHz, $CDCl_3$) δ 171.8, 155.8, 153.1, 149.3, 140.0, 137.3, 134.1, 133.0, 129.3, 126.3, 125.3, 120.3, 114,5, 90.8, 85.5, 83.9, 83.4, 52.9, 50.6, 29.5, 28.41, 28.0, 27.2, 25.5, 21.2. HRMS (ESI): calculated for $C_{35}H_{50}N_7O_7$ $[M+H]^+$ 680.3772, found 680.3780.

tert-butyl (2S)-4-((((3a*R*,3a*R*,4*R*,6R,6a*R*,6a*R*)-6-(6-amino-9*H*-purin-9-yl)-2,2-dimethyltetra-hydrofuro[3,4-d][1,3]dioxol-4-yl)methyl)((*E*)-3-(4-((trimethylsilyl)ethynyl)phenyl)allyl)amino)-2-((*tert*-butoxycarbonyl)amino)butanoate (16y). Following the procedure described for compound **12a**, coupling compound **11** (112 mg, 0.20 mmol) with (*E*)-3-(4-((trimethylsilyl)ethynyl)phenyl)acrylaldehyde **15y** (55 mg, 0.24 mmol) afforded compound **16y** as a white powder (98 mg, 63% yield). ^{1}H NMR (400 MHz, $CDCl_3$) δ 8.27 (s, 1H), 7.93 (s, 1H), 7.38 (d, *J* = 8.4 Hz, 2H), 7.22 (d, *J* = 8.4 Hz, 2H), 6.40 – 6.36 (br d, *J* = 16.0, 1H), 6.25 – 6.15 (m, 1H), 6.19 – 6.06 (m, 2H), 5.68 – 5.66 (br d, *J* = 8.2 Hz, 1H), 5.47 – 5.45 (br d, *J* = 8.6 Hz, 1H), 5.04 – 4.94 (m, 1H), 4.39 (d, *J* = 4.9 Hz, 1H), 4.24 – 4.19 (m, 1H), 3.35 – 3.30 (br m, 1H), 3.25 – 3.19 (br m, 1H), 2.86 – 2.81 (m, 1H), 2.74 – 2.47 (m, 4H), 2.01 – 1.96 (br, 1H), 1.81 – 1.78 (br, 1H), 1.61 (s, 3H), 1.42 – 1.39 (br m, 21H), 0.25 (s, 9H). ^{13}C NMR (101 MHz, $CDCl_3$) δ 171.8, 155.6, 153.1, 149.2, 140.1, 137.0, 132.2, 126.1, 122.2, 120.3, 114.5, 105.2, 90.8, 85.5, 83.9, 83.3, 79.5, 57.0, 56.0, 52.9, 50.7, 29.5, 28.0, 27.2, 25.5. HRMS (ESI): calculated for $C_{40}H_{58}N_7O_7Si$ $[M+H]^+$ 776.4167, found 776.4172.

(*S*)-2-amino-4-((((2*R*,3*S*,4*R*,5*R*)-5-(6-amino-9*H*-purin-9-yl)-3,4-dihydroxytetrahydrofuran-2-yl)methyl)((*E*)-3-(o-tolyl)allyl)amino)butanoic acid (17a). Following the procedure described for compound **13a**, compound **16a** (50 mg, 0.072 mmol) was deprotected and purified, affording compound **17a** as a white powder (31 mg, 71% yield). ^{1}H NMR (400 MHz, CD_3OD) δ 8.50 (s, 1H), 8.21 (s, 1H), 7.38 (d, *J* = 7.5 Hz, 1H), 7.23 – 7.11 (m, 3H), 6.99 – 6.5 (br d, *J* = 16.0 Hz, 1H), 6.29 – 6.23 (m, 2H), 4.69 (t, *J* = 4.2 Hz, 1H), 4.59 (d, *J* = 6.3 Hz, 2H), 4.19 – 4.08 (m, 3H), 3.91 – 3.85 (m, 1H), 3.75 – 3.55 (m, 3H), 2.59 – 2.49 (m, 1H), 2.38 – 2.32 (m, 1H), 2.20 (s, 3H). ^{13}C NMR (101 MHz, CD_3OD) δ 170.53, 151.1, 147.9, 144.7, 143.2, 138.8, 135.8, 134.1, 130.1, 128.7, 126.0, 125.4, 119.63, 116.9, 91.0, 78.9. 735.5, 72.3, 54.39, 51.2, 51.0, 25.02, 18.3. HRMS (ESI): calculated for $C_{24}H_{32}N_7O_5$ $[M+H]^+$ 498.2465, found 498.2572.

(*S*)-2-amino-4-((((2R,3S,4R,5R)-5-(6-amino-9*H*-purin-9-yl)-3,4-dihydroxytetrahydrofuran-2-yl)methyl)((*E*)-3-(m-tolyl)allyl)amino)butanoic acid (17b). Following the procedure described for compound **13a**, compound **16b** (50 mg, 0.072 mmol) was deprotected and purified, affording compound **17b** as a white powder (32 mg, 73% yield). ^{1}H NMR (400 MHz, CD_3OD) δ 8.48 (s, 1H), 8.23 (s, 1H), 7.21 (t, *J* = 7.5 Hz, 1H), 7.11 (dd, *J* = 18.9, 8.4 Hz, 3H), 6.69 (d, *J* = 15.8 Hz, 1H), 6.24 (dt, *J* = 15.3, 7.3 Hz, 1H), 6.17 (d, *J* = 3.6 Hz, 1H), 4.66

(t, *J* = 4.1 Hz, 1H), 4.56 (d, *J* = 6.8 Hz, 2H), 4.10 (dd, *J* = 8.3, 5.0 Hz, 3H), 3.88 (dd, *J* = 13.9, 10.1 Hz, 1H), 3.70 – 3.52 (m, 3H), 2.55 – 2.46 (m, 1H), 2.33 (s, 3H), 2.31 – 2.27 (m, 1H). ^{13}C NMR (101 MHz, CD_3OD) δ 170.3, 151.3, 148.0, 145.0, 143.0, 141.0, 138.3, 135.1, 129.5, 127.0, 123.6, 119.8, 115.3, 91.1, 78.9, 72.3, 54.4, 51.2, 50.9.5.0. 20.0. HRMS (ESI): calculated for $C_{24}H_{32}N_7O_5$ $[M+H]^+$ 498.2465, found 498.2574.

(*S*)-2-amino-4-((((2*R*,3*S*,4*R*,5*R*)-5-(6-amino-9*H*-purin-9-yl)-3,4-dihydroxytetrahydrofuran-2-yl)methyl)((*E*)-3-(p-tolyl)allyl)amino)butanoic acid (17c). Following the procedure described for compound **13a**, compound **16c** (50 mg, 0.072 mmol) was deprotected and purified, affording compound **17c** as a white powder (31 mg, 70% yield). ^{1}H NMR (400 MHz, D_2O) δ 8.47 (s, 1H), 8.22 (s, 1H), 7.16 – 7.09 (m, 4H), 6.69 – 6.65 (br d, *J* = 16.0 Hz, 1H), 6.21 – 6.13 (m, 2H), 4.65 (t, *J* = 4.0 Hz, 1H), 4.54 (d, *J* = 6.2 Hz, 2H), 4.10 – 4.06 (m, 3H), 3.88 – 3.82 (m, 1H), 3.71 – 3.49 (m, 3H), 2.57 – 2.43 (m, 1H), 2.32 – 2.27 (m, 4H). ^{13}C NMR (101 MHz, D_2O) δ 168.7, 163.1, 162.8, 152.7, 149.4, 146.3, 144.5, 142.3, 140.5, 133.73, 127.8, 121.1, 119.4, 116.5, 115.7, 92.4, 80.4, 75.0, 73.7, 55.8, 52.3, 26.40, 21.4. HRMS (ESI): calculated for $C_{24}H_{32}N_7O_5$ $[M+H]^+$ 498.2465, found 498.2570.

(*S*)-2-amino-4-((((2*R*,3*S*,4*R*,5*R*)-5-(6-amino-9*H*-purin-9-yl)-3,4-dihydroxytetrahydrofuran-2-yl)methyl)((*E*)-3-(2-methoxyphenyl)allyl)amino)butanoic acid (17d). Following the procedure described for compound **13a**, compound **16d** (50 mg, 0.070 mmol) was deprotected and purified, affording compound **17d** as a white powder (32 mg, 72% yield). ^{1}H NMR (400 MHz, CD_3OD) δ 8.46 (s, 1H), 8.16 (s, 1H), 7.33 – 7.24 (m, 2H), 6.96 – 6.85 (m, 3H), 6.27 – 6.21 (m, 1H), 6.15 (d, *J* = 3.4 Hz, 1H), 4.62 (dd, *J* = 4.8, 3.5 Hz, 1H), 4.59 – 4.50 (m, 2H), 4.15 – 4.02 (m, 3H), 3.90 (dd, *J* = 13.9, 9.7 Hz, 1H), 3.77 (s, 3H), 3.69 – 3.51 (m, 3H), 2.55 – 2.45 (m, 1H), 2.36 – 2.28 (m, 1H). ^{13}C NMR (101 MHz, CD_3OD) δ 170.3, 157.0, 151.0, 147.9, 144.4, 143.2, 136.0, 130.1, 127.0, 123.56, 119.8, 115.8, 110.8, 91.2, 79.0, 73.6, 72.3, 55.9, 54.6, 54.2, 50.8, 25.0. HRMS (ESI): calculated for $C_{24}H_{32}N_7O_6$ $[M+H]^+$ 514.2414, found 514.2422.

(*S*)-2-amino-4-((((2*R*,3*S*,4*R*,5*R*)-5-(6-amino-9*H*-purin-9-yl)-3,4-dihydroxytetrahydrofuran-2-yl)methyl)((*E*)-3-(3-methoxyphenyl)allyl)amino)butanoic acid (17e). Following the procedure described for compound **13a**, compound **16e** (50 mg, 0.070 mmol) was deprotected and purified, affording compound **17e** as a white powder (34 mg, 77% yield). ^{1}H NMR (400 MHz, CD_3OD) δ 8.46 (s, 1H), 8.21 (s, 1H), 7.21 (t, *J* = 7.9 Hz, 1H), 6.89 – 6.83 (m, 2H), 6.77 (s, 1H), 6.68 – 6.64 (br d, *J* = 16.0 Hz, 1H), 6.27 – 6.19 (m, 1H), 6.15 (d, *J* = 3.5 Hz, 1H), 4.66 – 4.61 (m, 1H), 4.56 – 4.52 (m, 2H), 4.12 – 4.02 (m, 3H), 3.89 – 3.83 (m, 1H), 3.78 (s, 3H), 3.69 – 3.50 (m, 3H), 2.54 – 2.44 (m, 1H), 2.34 – 2.27 (m, 1H). ^{13}C NMR (101 MHz, CD_3OD) δ 170.3, 160.0, 151.2, 148.0,

144.8, 143.1, 140.8, 136.5, 129.5, 119.8, 118.8, 91.1, 78.9, 73.6, 72.3, 54.4, 50.9, 25.0. HRMS (ESI): calculated for $C_{24}H_{32}N_7O_6$ $[M+H]^+$ 514.2414, found 514.2419.

(*S*)-2-amino-4-((((2*R*,3*S*,4*R*,5*R*)-5-(6-amino-9*H*-purin-9-yl)-3,4-dihydroxytetrahydrofuran-2-yl)methyl)((*E*)-3-(4-methoxyphenyl)allyl)amino)butanoic acid (17f). Following the procedure described for compound **13a**, compound **16f** (50 mg, 0.070 mmol) was deprotected and purified, affording compound **17f** as a white powder (35 mg, 80% yield). ^{1}H NMR (400 MHz, D_2O) δ 8.47 (s, 1H), 8.24 (s, 1H), 7.21 (d, *J* = 8.5 Hz, 2H), 6.84 (d, *J* = 8.7 Hz, 2H), 6.65 (d, *J* = 15.7 Hz, 1H), 6.15 (d, *J* = 3.6 Hz, 1H), 6.07 – 6.03 (m, 1H), 4.66 (t, *J* = 4.0 Hz, 1H), 4.54 (d, *J* = 6.4 Hz, 2H), 4.12 – 4.01 (m, 3H), 3.88 – 3.82 (m, 4H), 3.70 – 3.47 (m, 3H), 2.54 – 2.44 (m, 1H), 2.34 – 2.26 (m, 1H). ^{13}C NMR (101 MHz, D_2O) δ 169.0, 161.9, 152.7, 149.44, 146.3, 144.5, 142.0, 129.3, 129.1, 121.1, 115.2, 114.1, 92.4, 80.4, 75.0, 73.7, 55.8, 52.5, 52.1, 26.4. HRMS (ESI): calculated for $C_{24}H_{32}N_7O_6$ $[M+H]^+$ 514.2414, found 514.2425.

(*S*)-2-amino-4-((((2*R*,3*S*,4*R*,5*R*)-5-(6-amino-9*H*-purin-9-yl)-3,4-dihydroxytetrahydrofuran-2-yl)methyl)((*E*)-3-(2-fluorophenyl)allyl)amino)butanoic acid (17g). Following the procedure described for compound **13a**, compound **16g** (50 mg, 0.072 mmol) was deprotected and purified, affording compound **17g** as a white powder (31 mg, 68% yield). ^{1}H NMR (400 MHz, D_2O) δ 8.30 (s, 1H), 8.04 (s, 1H), 7.56 – 7.52 (m, 1H), 7.38 (d, *J* = 5.4 Hz, 2H), 7.21 (s, 1H), 6.85 – 6.56 (m, 1H), 6.10 – 6.05 (m, 1H), 6.02 – 5.93 (m, 1H), 4.70 (dd, *J* = 7.1, 5.6 Hz, 1H), 4.57 (dd, *J* = 5.5, 2.4 Hz, 1H), 4.43 (s, 1H), 4.11 – 4.06 (m, 2H), 3.96 (s, 1H), 3.86 – 3.76 (m, 1H), 3.66 – 3.51 (m, 3H), 2.55 – 2.41 (m, 1H), 2.36 – 2.30 (m, 1H). ^{13}C NMR (101 MHz, D_2O) δ 171.7, 163.2, 162.9, 162.5, 162.2, 149.0, 147.1, 144.0, 133.2, 130.9, 129.9, 128.7, 120.6, 118.7, 117.7, 114.8, 111.9, 91.1, 72.9, 72.3, 50.9, 25.0. HRMS (ESI): calculated for $C_{23}H_{29}FN_7O_5$ $[M+H]^+$ 502.2214, found 502.2215.

(*S*)-2-amino-4-((((2*R*,3*S*,4*R*,5*R*)-5-(6-amino-9*H*-purin-9-yl)-3,4-dihydroxytetrahydrofuran-2-yl)methyl)((*E*)-3-(3-fluorophenyl)allyl)amino)butanoic acid (17h). Following the procedure described for compound **13a**, compound **16h** (50 mg, 0.072 mmol) was deprotected and purified, affording compound **17h** as a white powder (30 mg, 67% yield). ^{1}H NMR (400 MHz, D_2O) δ 8.30 (s, 1H), 8.04 (s, 1H), 7.20 – 7.15 (m, 1H), 6.96 (t, *J* = 8.4 Hz, 1H), 6.75 (d, *J* = 7.6 Hz, 1H), 6.68 (d, *J* = 9.4 Hz, 1H), 6.30 (s, 1H), 6.08 (s, 1H), 6.00 – 5.92 (m, 1H), 4.67 (d, *J* = 6.1 Hz, 1H), 4.54 – 4.48 (m, 1H), 4.39 (s, 1H), 4.07 – 3.76 (m, 4H), 3.46 – 3.45 (m, 3H), 2.42 – 2.36 (m, 1H), 2.30 – 2.15 (m, 1H). ^{13}C NMR (101 MHz, D_2O) δ 172.1, 149.3, 147.2, 144.1, 143.6, 137.0, 130.5, 122.3, 119.2, 115.8, 115.6, 112.42, 112.19, 91.4, 72.0, 51.8. HRMS (ESI): calculated for $C_{23}H_{29}FN_7O_5$ $[M+H]^+$ 502.2214, found 502.2218.

(*S*)-2-amino-4-((((2*R*,3*S*,4*R*,5*R*)-5-(6-amino-9*H*-purin-9-yl)-3,4-dihydroxytetrahydrofuran-2-yl)methyl)((*E*)-3-(4-fluorophenyl)allyl)amino)butanoic acid (17i). Following the procedure described for compound **13a**, compound **16i** (50 mg, 0.072 mmol) was deprotected and purified, affording compound **17i** as a white powder (34 mg, 76% yield). ^{1}H NMR (400 MHz, D_2O) δ 8.32 (s, 1H), 8.02 (s, 1H), 6.98 – 6.81 (m, 4H), 6.28 (br s, 1H), 6.09 (s, 1H), 5.89 – 5.82 (m, 1H), 4.70 (dd, *J* = 6.9, 5.5 Hz, 1H), 4.55 – 4.53 (m, 1H), 4.43 (br s, 1H), 4.11 – 3.79 (m, 4H), 3.65 – 3.47 (m, 3H), 2.52 – 2.38 (m, 1H), 2.31 (s, 1H). ^{13}C NMR (101 MHz, D_2O) δ 171.5, 163.8, 163.0, 161.3, 149.2, 147.1, 144.0, 143.5, 138.8, 131.0, 128.0, 127.9, 115.6, 115.3, 114.0, 112.0, 91.3, 73.6, 51.2, 24.9. HRMS (ESI): calculated for $C_{23}H_{29}FN_7O_5$ $[M+H]^+$ 502.2214, found 502.2216.

(*S*)-2-amino-4-((((2*R*,3*S*,4*R*,5*R*)-5-(6-amino-9*H*-purin-9-yl)-3,4-dihydroxytetrahydrofuran-2-yl)methyl)((*E*)-3-(2-chlorophenyl)allyl)amino)butanoic acid (17j). Following the procedure described for compound **13a**, compound **16j** (50 mg, 0.070 mmol) was deprotected and purified, affording compound **17j** as a white powder (28 mg, 63% yield). ^{1}H NMR (400 MHz, D_2O) δ 8.31 (d, *J* = 10.5 Hz, 1H), 8.00 (br d, *J* = 12.0 Hz, 1H), 7.46 – 6.98 (m, 4H), 6.58 – 6.38 (br d, *J* = 80.0 Hz, 1H), 6.09 (d, *J* = 10.8 Hz, 1H), 6.00 – 5.88 (m, 1H), 4.74 – 4.68 (m, 1H), 4.50 (dd, *J* = 5.4, 2.2 Hz, 1H), 4.43 (s, 1H), 4.15 – 3.81 (m, 4H), 3.67 – 3.48 (m, 3H), 2.47 (s, 1H), 2.36 – 2.30 (m, 1H). ^{13}C NMR (101 MHz, D_2O) δ 171.1, 163.3, 163.0, 162.6, 149.0, 147.0, 144.1, 143.4 138.5, 132.3, 130.3, 129.5, 127.3, 126.33, 125.4, 120.6, 119.1, 117.7, 114.9, 112.0, 91.4, 73.5, 72.0, 55.7, 50.9, 25.0. HRMS (ESI): calculated for $C_{23}H_{29}ClN_7O_5$ $[M+H]^+$ 518.1919, found 518.1922.

(*S*)-2-amino-4-((((2*R*,3*S*,4*R*,5*R*)-5-(6-amino-9*H*-purin-9-yl)-3,4-dihydroxytetrahydrofuran-2-yl)methyl)((*E*)-3-(3-chlorophenyl)allyl)amino)butanoic acid (17k). Following the procedure described for compound **13a**, compound **16k** (50 mg, 0.070 mmol) was deprotected and purified, affording compound **17k** as a white powder (28 mg, 63% yield). ^{1}H NMR (400 MHz, CD_3OD) δ 8.48 (s, 1H), 8.27 (s, 1H), 7.34 – 7.23 (m, 4H), 6.73 (br d, *J* = 16.0 Hz, 1H), 6.37 – 6.29 (m, 1H), 6.16 (d, *J* = 3.8 Hz, 1H), 4.68 – 4.64 (m, 1H), 4.58 – 4.49 (m, 2H), 4.08 (dd, *J* = 8.3, 4.5 Hz, 3H), 3.86 – 3.80 (m, 1H), 3.63 – 3.53 (m, 3H), 2.54 – 2.44 (m, 1H), 2.33 – 2.25 (m, 1H). ^{13}C NMR (101 MHz, CD_3OD) δ 170.5, 162.0, 161.2, 151.3, 148.1, 145.0, 143.0, 139.2, 137.3, 134.4, 130.0, 128.6, 126.2, 125.0, 119.6, 118.0, 117.6, 115.1, 54.66, 78.9, 73.6, 72.2, 54.7, 51.2, 51.0, 25.0, 22.9. HRMS (ESI): calculated for $C_{23}H_{29}ClN_7O_5$ $[M+H]^+$ 518.1919, found 518.1928.

(*S*)-2-amino-4-((((2*R*,3*S*,4*R*,5*R*)-5-(6-amino-9*H*-purin-9-yl)-3,4-dihydroxytetrahydrofuran-2-yl)methyl)((*E*)-3-(4-chlorophenyl)allyl)amino)butanoic acid (17l). Following the procedure described for compound **13a**, compound **16l** (50 mg, 0.070 mmol) was deprotected and purified, affording compound **17l** as a white powder (30 mg, 69% yield). ^{1}H NMR (400 MHz, D_2O) δ 8.33 (s, 1H), 8.05 (d, *J* = 8.2 Hz, 1H), 7.14 (d, *J* =7.8 Hz, 2H), 6.87 (d, *J* = 8.3 Hz, 2H), 6.27 (br s, 1H),

6.10 (s, 1H), 5.97 – 5.89 (m, 1H), 4.72 (dd, *J* = 6.9, 5.6 Hz, 1H), 4.56 – 4.38 (m, 2H), 4.10 – 3.79 (m, 4H), 3.64 – 3.50 (m, 3H), 2.53 – 2.39 (m, 1H), 2.37 – 2.24 (m, 1H). ^{13}C NMR (101 MHz, D_2O) δ 171.8, 163.0, 162.7, 149.1, 147.1, 144.0, 1435, 138.6, 134.0, 133.2, 128.6, 127.4, 119.0, 117.8, 114.9, 91.4, 73.6, 72.0, 25.0. HRMS (ESI): calculated for $C_{23}H_{29}ClN_7O_5$ $[M+H]^+$ 518.1919, found 518.1925.

(*S*)-2-amino-4-((((2*R*,3*S*,4*R*,5*R*)-5-(6-amino-9*H*-purin-9-yl)-3,4-dihydroxytetrahydrofuran-2-yl)methyl)((*E*)-3-(2-bromophenyl)allyl)amino)butanoic acid (17m). Following the procedure described for compound **13a**, compound **16m** (50 mg, 0.066 mmol) was deprotected and purified, affording compound **17m** as a white powder (26 mg, 59% yield). ^{1}H NMR (400 MHz, D_2O) δ 8.21 (s, 1H), 7.86 (s, 1H), 7.29 (d, *J* = 9.3 Hz, 1H), 7.03 (d, *J* = 7.2 Hz, 3H), 6.42 (s, 1H), 5.99 (s, 1H), 5.84 – 5.77 (m, 1H), 4.65 – 4.60 (m, 1H), 4.42 (dd, *J* = 5.4, 2.2 Hz, 1H), 4.34 (s, 1H), 4.02 (dd, *J* = 8.4, 4.9 Hz, 1H), 3.84 – 3.74 (m, 2H), 3.57 – 3.41 (m, 3H), 2.38 (br s, 1H), 2.29 – 2.20 (m, 1H). ^{13}C NMR (101 MHz, D_2O) δ 171.1,163.3, 163.0, 162.2, 149.0, 146.9, 144.1, 143.4, 132.7, 130.5, 127.9, 126.5, 122.7, 120.6, 119.1, 117.7, 114.8, 111.9, 91.5, 73.5,72.0, 55.5, 50.8, 251. HRMS (ESI): calculated for $C_{23}H_{29}BrN_7O_5$ $[M+H]^+$ 562.1414, found 562.1427.

(*S*)-2-amino-4-((((2*R*,3*S*,4*R*,5*R*)-5-(6-amino-9*H*-purin-9-yl)-3,4-dihydroxytetrahydrofuran-2-yl)methyl)((*E*)-3-(3-bromophenyl)allyl)amino)butanoic acid (17n). Following the procedure described for compound **13a**, compound **16n** (50 mg, 0.066 mmol) was deprotected and purified, affording compound **17n** as a white powder (28 mg, 64% yield). ^{1}H NMR (400 MHz, D_2O) δ 8.33 (s, 1H), 8.05 (s, 1H), 7.38 – 7.35 (m, 1H), 7.09 (t, *J* = 7.8 Hz, 1H), 7.00 (s, 1H), 6.95 (d, *J* = 7.8 Hz, 1H), 6.10 (s, 2H), 5.99 – 5.92 (m, 1H), 4.75 – 4.69 (m, 1H), 4.52 –4.43 (m, 2H), 4.09 – 3.91 (m, 4H), 3.66 – 3.51 (m, 3H), 2.53 – 2.45 (m, 1H), 2.36– 2.30 (m, 1H). ^{13}C NMR (101 MHz, D_2O) δ 171.3, 163.4, 162.7, 162.3, 149.0, 147.0, 144.0, 143.4, 138.4, 136.7, 131.6, 130.4, 128.5, 124.9, 122.2, 120.7, 119.1, 117.8, 114.9, 91.5, 73.7, 71.90, 51.1, 25.0. HRMS (ESI): calculated for $C_{23}H_{29}BrN_7O_5$ $[M+H]^+$ 562.1414, found 562.1425.

(*S*)-2-amino-4-((((2*R*,3*S*,4*R*,5*R*)-5-(6-amino-9*H*-purin-9-yl)-3,4-dihydroxytetrahydrofuran-2-yl)methyl)((*E*)-3-(4-bromophenyl)allyl)amino)butanoic acid (17o). Following the procedure described for compound **13a**, compound **16o** (50 mg, 0.066 mmol) was deprotected and purified, affording compound **17o** as a white powder (33 mg, 75% yield).^{1}H NMR (400 MHz, D_2O) δ 8.33 (s, 1H), 7.93 (s, 1H), 7.21 – 7.07 (m, 2H), 6.65 (d, *J* = 8.3 Hz, 2H), 6.00 (s, 2H), 5.86 – 5.78 (m, 1H), 4.62 (d, *J* = 6.3 Hz, 1H), 4.42 – 4.33 (m, 2H), 4.04 – 3.79 (m, 4H), 3.66 – 3.41 (m, 3H), 2.41 – 2.21 (m, 2H). ^{13}C NMR (101 MHz, D_2O) δ 171.3, 163.0, 162.6, 162.3 149.0, 147.0, 143.9, 143.4, 138.7, 135.5, 131.5, 127.6, 122.3, 120.7, 119.0, 117.8, 114.9, 91.4, 73.7, 71.9, 51.1, 25.0. HRMS (ESI): calculated for $C_{23}H_{29}BrN_7O_5$ $[M+H]^+$ 562.1414, found 562.1421.

(*S*)-2-amino-4-((((2*R*,3*S*,4*R*,5*R*)-5-(6-amino-9*H*-purin-9-yl)-3,4-dihydroxytetrahydrofuran-2-yl)methyl)((*E*)-3-(2-nitrophenyl)allyl)amino)butanoic acid (17p). Following the procedure described for compound **13a**, compound **16p** (50 mg, 0.069 mmol) was deprotected and purified, affording compound **17p** as a white powder (18 mg, 43% yield). ^{1}H NMR (400 MHz, D_2O) δ 8.29 (s, 1H), 8.06 (s, 1H), 7.83 – 7.78 (m, 1H), 7.47 (s, 1H), 7.41 (d, *J* = 9.2 Hz, 1H), 7.27 (s, 1H), 6.72 (d, *J* = 13.6 Hz, 1H), 6.07 (s, 1H), 6.00 – 5.93 (m, 1H), 4.67 – 4.59 (m, 2H), 4.49 – 4.40 (m, 1H), 4.13 – 3.91 (m, 3H), 3.80 – 3.73 (m, 1H), 3.68 – 3.49 (m, 3H), 2.50 – 2.43(s, 1H), 2.37 – 2.29 (m, 1H). ^{13}C NMR (101 MHz, D_2O) δ 170.8, 149.2, 147.3, 146.4, 143.9, 143.8, 136.1, 134.1,130.1, 129.8, 124.6, 117.7, 114.8, 111.9, 91.0, 73.2, 71.9, 67.9, 66.5, 50.6, 24.8, 17.9. HRMS (ESI): calculated for $C_{23}H_{29}N_8O_7$ $[M+H]^+$ 529.2159, found 529.2166.

(*S*)-2-amino-4-((((2*R*,3*S*,4*R*,5*R*)-5-(6-amino-9*H*-purin-9-yl)-3,4-dihydroxytetrahydrofuran-2-yl)methyl)((*E*)-3-(3-nitrophenyl)allyl)amino)butanoic acid (17q). Following the procedure described for compound **13a**, compound **16q** (50 mg, 0.069 mmol) was deprotected and purified, affording compound **17q** as a white powder (20 mg, 45% yield). ^{1}H NMR (500 MHz, CD_3OD) δ 8.51 (s, 1H), 8.27 (s, 1H), 7.45 (d, *J* = 8.4 Hz, 2H), 7.24 (d, *J* = 8.1 Hz, 2H), 5.02 (s, 2H), 4.69 (t, *J* = 4.5 Hz, 1H), 4.08 (h, *J* = 7.7 Hz, 3H), 3.85 – 3.80 (m, 1H), 3.68 (6.10 (d, *J* = 8.1 Hz, 1H), 3.64 – 3.55 (m, 2H), 2.54 – 2.46 (m, 1H), 2.32 – 2.24 (m, 1H). ^{13}C NMR (126 MHz, CD_3OD) δ 171.1, 161.9, 161.8, 161.6, 151.4, 148.2, 139.5, 134.3, 131.6, 128.3, 122.6, 119.5, 116.7. 90.5, 79.1, 73.6, 72.2, 54.7, 51.6, 51.2, 29.8, 25.0. HRMS (ESI): calculated for $C_{23}H_{29}N_8O_7$ $[M+H]^+$ 529.2159, found 529.2162.

(*S*)-2-amino-4-((((2*R*,3*S*,4*R*,5*R*)-5-(6-amino-9*H*-purin-9-yl)-3,4-dihydroxytetrahydrofuran-2-yl)methyl)((*E/Z*)-3-(4-nitrophenyl)allyl)amino)butanoic acid (17r, mixture of isomers). Following the procedure described for compound **13a**, compound **16r** (50 mg, 0.069 mmol) was deprotected and purified, affording compound **17r** as a pink powder (mixture of E- and Z-isomers, 23 mg, 51% yield). ^{1}H NMR (500 MHz, CD_3OD) δ 8.48 (s, 1H), 8.38 (d, *J* = 6.2 Hz, 1H), 8.30 (s, 1H), 8.20 – 8.12 (m, 3H), 7.54 (s, 2H), 7.42 (d, *J* = 7.1 Hz, 1H), 7.01 – 6.85 (br m, 2H), 6.56 – 6.51 (m, 1H), 6.17 (d, *J* = 3.6 Hz, 1H), 6.12 – 5.99 (m, 1H), 4.70 – 4.66 (m, 1H), 4.61 – 4.53 (m, 3H), 4.42 – 4.35 (m, 1H), 4.30 (d, *J* = 6.3 Hz, 1H), 4.21 – 4.04 (m, 4H), 3.90 – 3.82 (m, 1H), 3.79 – 3.50 (m, 5H), 2.56 – 2.19 (m, 3H). (E/Z mixture). ^{13}C NMR (126 MHz, CD_3OD) δ 171.1, 153.9, 148.4, 147.71, 141.6, 137.7, 134.5, 129.5, 123.6, 123.3, 121.6, 90.8, 79.3, 73.4, 73.3, 72.4, 72.1, 54.8,52.0, 25.0. HRMS (ESI): calculated for $C_{23}H_{29}N_8O_7$ $[M+H]^+$ 529.2159, found 529.2178.

(*S*)-2-amino-4-((((2*R*,3*S*,4*R*,5*R*)-5-(6-amino-9*H*-purin-9-yl)-3,4-dihydroxytetrahydrofuran-2-yl)methyl)((*E*)-3-(2-cyanophenyl)allyl)amino)butanoic acid (17s). Following the procedure

described for compound **13a**, compound **16s** (50 mg, 0.071 mmol) was deprotected and purified, affording compound **17s** as a white powder (34 mg, 78% yield). ^{1}H NMR (400 MHz, D_2O) δ 8.33 (s, 1H), 8.03 (s, 1H), 7.52 – 7.42 (m, 2H), 7.33 (t, *J* = 7.2 Hz, 2H), 6.44 (s, 1H), 6.22 – 6.15 (m, 1H), 6.11 (d, *J* = 2.3 Hz, 1H), 4.70 – 4.65 (m, 1H), 4.45 (t *J* = 7.8, 1H), 4.14 – 4.04 (m, 3H), 3.86 (d, *J* = 10.2 Hz, 1H), 3.67 – 3.51 (m, 3H), 2.53 – 2.43 (m, 1H), 2.37 – 2.29 (m, 1H). ^{13}C NMR (101 MHz, D_2O) δ 171.0, 163.2, 162.9, 162.5, 162.2, 149.1, 147.1, 144.2, 143.7, 137.3, 135.2, 133.6, 133.0, 129.4, 125.6, 120.6, 119.0, 117.7, 117.3, 114.8, 109.1, 91.4, 73.4, 72.0, 55.4, 50.8, 24.9. HRMS (ESI): calculated for $C_{24}H_{29}N_8O_5$ $[M+H]^+$ 509.2261, found 509.2271.

(*S*)-2-amino-4-((((2*R*,3*S*,4*R*,5*R*)-5-(6-amino-9*H*-purin-9-yl)-3,4-dihydroxytetrahydrofuran-2-yl)methyl)((*E*)-3-(3-cyanophenyl)allyl)amino)butanoic acid (17t). Following the procedure described for compound **13a**, compound **16t** (50 mg, 0.071 mmol) was deprotected and purified, affording compound **17t** as a white powder (34 mg, 77% yield). ^{1}H NMR (400 MHz, D_2O) δ 8.36 (s, 1H), 8.10 (s, 1H), 7.60 – 7.58 (m, 1H), 7.39 – 7.29 (m, 3H), 6.40 (br s, 1H), 6.13 – 6.05 (m, 2H), 4.71 (dd, *J* = 7.1, 5.5 Hz, 1H), 4.56 – 4.51 (m, 1H), 4.45 (s, 1H), 4.11 – 3.86 (m, 4H), 3.68 – 3.52 (m, 3H), 2.53 – 2.44 (m, 1H), 2.37 – 2.31 (m, 1H). ^{13}C NMR (101 MHz, D_2O) δ 171.1, 149.2, 147.2, 144.1, 143.6, 137.8, 135.7, 132.3, 130.8, 129.7, 119.1, 118.9, 118.5, 117.7, 114.8, 111.5, 91.4, 71.8, 50.9, 24.9. HRMS (ESI): calculated for $C_{24}H_{29}N_8O_5$ $[M+H]^+$ 509.2261, found 509.2264.

(*S*)-2-amino-4-((((2*R*,3*S*,4*R*,5*R*)-5-(6-amino-9*H*-purin-9-yl)-3,4-dihydroxytetrahydrofuran-2-yl)methyl)((*E*)-3-(4-cyanophenyl)allyl)amino)butanoic acid (17u). Following the procedure described for compound **13a**, compound **16u** (50 mg, 0.071 mmol) was deprotected and purified, affording compound **17u** as a white powder (35 mg, 80% yield). ^{1}H NMR (400 MHz, D_2O) δ 8.38 (s, 1H), 8.14 (s, 1H), 7.59 (d, *J* = 8.0 Hz, 2H), 7.16 (d, *J* = 8.1 Hz, 2H), 6.47 (d, *J* = 8.1, 1H), 6.23 – 6.13 (m, 2H), 4.75 – 4.72 (m, 1H), 4.58 – 4.56 (m, 1H), 4.47 (br s, 1H), 4.09 – 4.01 (m, 4H), 3.67 – 3.54 (m, 3H), 2.52 – 2.42 (m, 1H), 2.35 – 2.29 (m, 1H). ^{13}C NMR (101 MHz, D_2O) δ 171.8, 149.3, 147.2, 144.1, 143.6, 138.1, 132.63, 126.6, 119.2, 114.9, 110.8, 91.4, 73.6, 71.9, 51.6, 20.5. HRMS (ESI): calculated for $C_{24}H_{29}N_8O_5$ $[M+H]^+$ 509.2261, found 509.2266.

(*S*)-2-amino-4-((((2*R*,3*S*,4*R*,5*R*)-5-(6-amino-9*H*-purin-9-yl)-3,4-dihydroxytetrahydrofuran-2-yl)methyl)((*E*)-3-(3-carbamoylphenyl)allyl)amino)butanoic acid (17v). Following the procedure described for compound **13a**, compound **16v** (50 mg, 0.069 mmol) was deprotected and purified, affording compound **17v** as a white powder (34 mg, 77% yield). ^{1}H NMR (400 MHz, CD_3OD) δ 8.46 (s, 1H), 8.26 (s, 1H), 7.91 (s, 1H), 7.82 (d, *J* = 7.6 Hz, 1H), 7.53 – 7.41 (m, 2H), 6.16 (d, *J* = 3.8 Hz, 1H), 4.72 – 4.68 (m, 1H), 4.60 – 4.49 (m, 2H), 4.17 – 4.02 (m, 3H), 3.86 – 3.80 (m, 1H), 3.71 – 3.52 (m, 3H), 2.51 – 2.45 (m, 1H), 2.30 – 2.20 (m, 1H). ^{13}C NMR (101

MHz, CD_3OD) δ 170.7, 148.7, 144.6, 139.7, 137.0, 134.8, 129.8, 128.7, 127.5, 126.2, 118.0, 90.7, 79.5, 73.4, 71.9, 53.5, 52.4, 50.8, 25.0. HRMS (ESI): calculated for $C_{24}H_{31}N_8O_6$ $[M+H]^+$ 527.2367, found 527.2378.

(*S*)-2-amino-4-((((2*R*,3*S*,4*R*,5*R*)-5-(6-amino-9*H*-purin-9-yl)-3,4-dihydroxytetrahydrofuran-2-yl)methyl)((*E*)-3-(4-carbamoylphenyl)allyl)amino)butanoic acid (17w). Following the procedure described for compound **13a**, compound **16w** (50 mg, 0.069 mmol) was deprotected and purified, affording compound **17w** as a white powder (34 mg, 77% yield). ^1H NMR (400 MHz, CD_3OD) δ 8.45 (s, 1H), 8.26 (s, 1H), 7.85 (d, *J* = 8.4 Hz, 2H), 7.41 (s, 2H), 6.81 (br d, *J* = 15.8 Hz, 1H), 6.45 – 6.37 (m, 1H), 6.16 (s, 1H), 4.73 – 4.68 (m, 1H), 4.55 (dd, *J* = 5.6, 2.8 Hz, 2H), 4.16 – 4.01 (m, 3H), 3.88 – 3.79 (m, 1H), 3.69 – 3.57 (m, 4H), 2.51 – 2.45 (m, 1H), 2.29 – 2.20 (m, 1H). ^{13}C NMR (101 MHz, CD_3OD) δ 171.9, 148.2, 138.5, 129.0, 126.5, 120.9, 118.4, 51.40, 90.9, 79.0, 72.9, 72.3, 51.7, 51.4, 25.0. HRMS (ESI): calculated for $C_{24}H_{31}N_8O_6$ $[M+H]^+$ 527.2367, found 527.2373.

(*S*)-2-amino-4-((((2*R*,3*S*,4*R*,5*R*)-5-(6-amino-9*H*-purin-9-yl)-3,4-dihydroxytetrahydrofuran-2-yl)methyl)(cinnamyl)amino)butanoic acid (17x). Following the procedure described for compound **13a**, compound **16x** (50 mg, 0.074 mmol) was deprotected and purified, affording compound **17x** as a white powder (35 mg, 79% yield). ^1H NMR (500 MHz, CD_3OD) δ 8.49 (s, 1H), 8.24 (s, 1H), 7.31 – 7.26 (s, 5H), 6.74 – 6.71 (br d, *J* = 12.0, 1H), 6.29 – 6.23 (m, 1H), 6.18 (d, *J* = 3.8 Hz, 1H), 4.70 – 4.68 (m, 1H), 4.60 – 4.56 (m, 2H), 4.14 – 4.10 (m, 3H), 3.90 – 3.85 (br m, 1H), 3.76 – 3.52 (m, 3H), 2.57 – 2.51 (m, 1H), 2.41 – 2.34 (m, 1H). ^{13}C NMR (126 MHz, CD_3OD) δ 169.5, 162.0, 161.7, 161.4, 149.7, 151.0,148.0, 140.9, 135.1, 128.8, 128.5, 125.7, 120.0, 119.8, 117.7, 115.5, 115.4, 91.1, 79.4, 73.6, 72.3, 55.5, 54.5, 50.9, 50.6, 25.0. HRMS (ESI): calculated for $C_{23}H_{30}N_7O_5$ $[M+H]^+$ 484.2308, found 484.2311.

(*S*)-2-amino-4-((((2*R*,3*S*,4*R*,5*R*)-5-(6-amino-9*H*-purin-9-yl)-3,4-dihydroxytetrahydrofuran-2-yl)methyl)((*E*)-3-(4-ethynylphenyl)allyl)amino)butanoic acid (17y). Following the procedure described for compound **13a**, compound **16y** (50 mg, 0.064 mmol) was deprotected and purified, affording compound **17y** as a white powder (8 mg, 21% yield). ^1H NMR (500 MHz, CD_3OD) δ 8.41 (s, 1H), 8.28 (s, 1H), 7.43 (d, *J* = 8.3 Hz, 2H), 7.30 (d, *J* = 8.3 Hz, 2H), 6.77 – 6.73 (br d, *J* = 12.0, 1H), 6.37 – 6.25 (m, 1H), 6.14 (d, *J* = 3.5 Hz, 1H), 4.70 – 4.66 (m, 1H), 4.53 (dd, *J* = 5.5, 2.5 Hz, 2H), 4.14 – 3.94 (m, 3H), 3.82 – 3.77 (m, 1H), 3.66 – 3.63 (br d, *J* = 16.0, 1H), 3.61 (s, 1H), 3.60 – 3.47 (m, 2H), 2.48 – 2.40 (m, 1H), 2.24 – 2.16 (m, 1H). ^{13}C NMR (126 MHz, CD_3OD) δ 148.6, 139.6, 135.6, 132.0, 126.5, 91.1, 79.1, 78.9, 73.4, 71.7, 54.6, 51.5, 25.2. HRMS (ESI): calculated for $C_{25}H_{30}N_7O_5$ $[M+H]^+$ 508.2308, found 508.2315.

4-((*E*)-3-((((3a*R*,3a*R*,4*R*,6R,6a*R*,6a*R*)-6-(6-amino-9*H*-purin-9-yl)-2,2-dimethyltetrahydrofuro[3,4-d][1,3]dioxol-4-yl)methyl)amino)prop-1-en-1-yl)benzonitrile (18). Following the procedure described for compound **12a**, coupling 9-((3a*R*,4*R*,6*R*,6a*R*)-6-(aminomethyl)-2,2-dimethyltetrahydrofuro[3,4-d][1,3]dioxol-4-yl)-9*H*-purin-6-amine **9** (67 mg, 0.22 mmol) with (*E*)-4-(3-oxoprop-1-en-1-yl)benzonitrile **15u** (31 mg, 0.20 mmol) afforded compound **18** as a yellow powder (49 mg, 55% yield). ^{1}H NMR (400 MHz, $CDCl_3$) δ 8.26 (s, 1H), 7.92 (s, 1H), 7.59 (d, *J* = 8.4 Hz, 2H), 7.41 (d, *J* = 8.3 Hz, 2H), 6.51 (s, 1H), 6.41 – 6.36 (m, 1H), 6.15 (s, 2H), 6.01 (d, *J* = 3.3 Hz, 1H), 5.52 – 5.47 (m, 1H), 5.10 (dd, *J* = 6.4, 3.3 Hz, 1H), 4.45 – 4.41 (m, 1H), 3.46 (t, *J* = 5.5 Hz, 2H), 3.06 – 2.93 (m, 2H), 2.61 (s, 3H), 1.64 (s, 3H), 1.41 (s, 3H). ^{13}C NMR (101 MHz, $CDCl_3$) δ 155.7, 153.1, 149.3, 141.5, 140.1, 132.5, 129.8, 126.8, 114.8, 110.6, 91.1, 85.5, 83.3, 82.3, 51.6, 50.9, 27.4, 25.5. HRMS (ESI): calculated for $C_{23}H_{26}N_7O_3$ $[M+H]^+$448.2097, found 448.2106.

***tert*-butyl (*S*)-5-((((3 3a*R*,3a*R*,4*R*,6R,6a*R*,6a*R*)-6-(6-amino-9*H*-purin-9-yl)-2,2-dimethyltetrahydrofuro[3,4-d][1,3]dioxol-4-yl)methyl)((*E*)-3-(4-cyanophenyl)allyl)amino)-2-(bis(*tert*-butoxycarbonyl)amino)pentanoate (20a).** Following the procedure described for compound **12a**, coupling compound **18** (112 mg, 0.20 mmol) with *tert*-butyl (*S*)-2-(bis(*tert*-butoxycarbonyl)amino)-5-oxopentanoate **19a** (82 mg, 0.24 mmol) afforded protected intermediate **20a** as a white powder (113 mg, 69% yield). ^{1}H NMR (400 MHz, $CDCl_3$) δ 8.23 (s, 1H), 7.92 (s, 1H), 7.51 (d, *J* = 8.3 Hz, 2H), 7.28 (d, *J* = 8.2 Hz, 2H), 6.44 – 6.21 (m, 4H), 6.04 (d, *J* = 1.9 Hz, 1H), 5.44 (dd, *J* = 6.4, 1.9 Hz, 1H), 4.97 (dd, *J* = 6.4, 3.6 Hz, 1H), 4.71 (dd, *J* = 9.6, 5.2 Hz, 1H), 4.38 – 4.34 (m, 1H), 3.26 (d, *J* = 6.0 Hz, 2H), 2.79 – 2.69 (m, 2H), 2.56 – 2.51 (m, 2H), 2.07 – 2.00 (m, 1H), 1.91 – 1.75 (m, 1H), 1.59 (s, 3H), 1.44 (br d, *J* = 21.0, 27H), 1.37 (s, 3H). ^{13}C NMR (101 MHz, $CDCl_3$) δ 169.8, 155.8, 153.0, 152.6, 149.2, 141.4, 140.0, 132.4, 131.7, 130.6, 126.6, 119.1, 114.4, 110.4, 107.0, 90.8, 85.7, 83.9, 83.3,82.8, 81.2, 77.5, 77.2, 76.9, 58.6, 54.3, 28.1, 27.2, 26.9, 25.5, 23.9. HRMS (ESI): calculated for $C_{42}H_{59}N_8O_9$ $[M+H]^+$ 819.4405, found 819.4410.

methyl (*S*)-4-((((3a*R*,3a*R*,4*R*,6R,6a*R*,6a*R*)-6-(6-amino-9*H*-purin-9-yl)-2,2-dimethyltetrahydro-furo[3,4-d][1,3]dioxol-4-yl)methyl)((*E*)-3-(4-cyanophenyl)allyl)amino)-2-((*tert*-butoxycarbonyl) amino)butanoate (20b). Following the procedure described for compound **12a**, coupling compound **18** (112 mg, 0.20 mmol) with methyl (*S*)-2-((*tert*-butoxycarbonyl)amino)-4-oxobutanoate **19b** (82 mg, 0.24 mmol) afforded protected intermediate **20b** as a white powder (97 mg, 73% yield). ^{1}H NMR (400 MHz, $CDCl_3$) δ 8.21 (s, 1H), 7.94 (s, 1H), 7.49 (d, *J* = 8.3 Hz, 2H), 7.27 (d, *J* = 8.3 Hz, 2H), 6.60 (s, 2H), 6.41 – 6.25 (m, 1H), 6.26 – 6.19 (m, 1H), 6.06 (s, 1H), 5.94 (d, *J* = 8.1 Hz, 1H), 5.45 (d, *J* = 6.2 Hz, 1H), 5.03 – 4.95 (m, 1H),

4.41 – 4.30 (m, 2H), 3.64 (s, 3H), 3.23 (d, *J* = 6.0 Hz, 2H), 2.79 – 2.69 (m, 2H), 2.58 – 2.50 (m, 2H), 2.07 – 2.00 (m, 1H), 1.86 – 1.79 (m, 1H), 1.58 (s, 3H), 1.41 – 1.33 (br m, 12H). ^{13}C NMR (101 MHz, $CDCl_3$) δ 173.3, 155.9, 155.6, 155.3, 153.0, 149.0, 141.3, 140.1, 132.3, 131.0, 126.7, 120.2, 119.0, 114.4, 110.5, 90.7, 85.7, 83.9, 83.3, 56.6, 56.1, 53.6, 52.2, 50.6, 44.8, 29.2, 28.4, 27.2, 25.4. HRMS (ESI): calculated for $C_{33}H_{43}N_8O_7$ $[M+H]^+$ 663.3255, found 663.3258.

4-((((3a*R*,3a*R*,4*R*,6R,6a*R*,6a*R*)-6-(6-amino-9*H*-purin-9-yl)-2,2-dimethyltetrahydrofuro[3,4-d][1,3]dioxol-4-yl)methyl)((*E*)-3-(4-cyanophenyl)allyl)amino)-*N*-tritylbutanamide (20c). Following the procedure described for compound **12a**, coupling compound **18** (112 mg, 0.20 mmol) with 4-oxo-*N*-tritylbutanamide **19c** (82 mg, 0.24 mmol) afforded protected intermediate **20c** as a white powder (79 mg, 51% yield). ^{1}H NMR (400 MHz, $CDCl_3$) δ 8.27 (s, 1H), 7.90 (s, 1H), 7.54 (d, *J* = 6.6 Hz, 2H), 7.33 – 7.19 (m, 20H), 6.72 (br s, 1H), 6.43 – 6.39 (br d, *J* = 16.0 Hz, 1H), 6.32 – 6.23 (m, 1H), 6.04 (d, *J* = 2.1 Hz, 1H), 5.82 (s, 2H), 5.47 (dd, *J* = 6.4, 2.1 Hz, 1H), 4.99 (dd, *J* = 6.4, 3.5 Hz, 1H), 4.42 – 4.38 (m, 1H), 3.28 (t, *J* = 6.4 Hz, 2H), 2.77 (d, *J* = 6.7 Hz, 2H), 2.57 – 2.51 (m, 2H), 2.35 – 2.25 (m, 2H), 1.87 – 1.73 (m, 2H), 1.59 (s, 3H), 1.38 (s, 3H). ^{13}C NMR (101 MHz, $CDCl_3$) δ 171.7, 154.9, 153.6, 149.2, 144.0, 140.8, 132.4, 128.7, 128.0, 127.0, 126.7, 120.8, 119.1, 114.4, 110.5, 90.9, 86.7, 83.9, 82.7, 69.1, 56.6, 56.0, 54.5, 35.6, 26.5, 25.4, 22.6. HRMS (ESI): calculated for $C_{46}H_{47}N_8O_4$ $[M+H]^+$ 775.3720, found 775.3733.

5-((((3a*R*,4*R*,6*R*,6a*R*)-6-(6-amino-9*H*-purin-9-yl)-2,2-dimethyltetrahydrofuro[3,4-d][1,3]dioxol-4-yl)methyl)((*E*)-3-(4-cyanophenyl)allyl)amino)-*N*-tritylpentanamide (20d). Following the procedure described for compound **12a**, coupling compound **18** (112 mg, 0.20 mmol) with 5-oxo-*N*-tritylpentanamide **19d** (86 mg, 0.24 mmol) afforded protected intermediate **20d** as a white powder (88 mg, 56% yield). ^{1}H NMR (500 MHz, $CDCl_3$) δ 8.15 (s, 1H), 7.97 (s, 1H), 7.52 (d, *J* = 8.4 Hz, 2H), 7.29 – 7.27 (m, 7H), 7.25 – 7.18 (m, 11H), 7.07 (s, 2H), 6.75 (s, 1H), 6.05 (d, *J* = 2.0 Hz, 1H), 5.40 (dd, *J* = 6.4, 2.0 Hz, 1H), 4.97 (dd, *J* = 6.4, 3.5 Hz, 1H), 4.45 – 4.41 (m, 1H), 3.30 (d, *J* = 6.5 Hz, 2H), 2.78 (d, *J* = 6.6 Hz, 2H), 2.54 (dd, *J* = 10.8, 4.0 Hz, 2H), 2.28 – 2.25 (m, 2H), 1.60 (s, 3H), 1.46 – 1.41 (m, 2H), 1.37 (s, 3H). ^{13}C NMR (126 MHz, $CDCl_3$) δ 175.9, 171.9, 155.8, 152.3, 148.9, 144.8, 141.2, 132.5, 131.5, 130.6, 128.8, 127.1, 126.8, 119.5, 119.1, 114.6, 110.7, 91.1, 86.1, 84.4, 83.3, 70.5, 60.5, 56.4, 55.8, 54.0, 37.2, 26.1, 23.2, 21.5. HRMS (ESI): calculated for $C_{47}H_{49}N_8O_4$ $[M+H]^+$ 789.3877, found 789.3886.

***tert*-butyl (3-((((3a*R*,4*R*,6*R*,6a*R*)-6-(6-amino-9*H*-purin-9-yl)-2,2-dimethyltetrahydrofuro[3,4-d][1,3]dioxol-4-yl)methyl)((*E*)-3-(4-cyanophenyl)allyl)amino)propyl)carbamate (20e).** Following the procedure described for compound **12a**, coupling compound **18** (112 mg, 0.20 mmol) with *tert*-butyl (3-oxopropyl)carbamate **19e** (41 mg, 0.24 mmol) afforded protected intermediate **20e** as a white

powder (88 mg, 73% yield). ^{1}H NMR (500 MHz, $CDCl_3$) δ 8.09 (s, 1H), 7.97 (s, 1H), 7.54 (d, *J* = 8.4 Hz, 1H), 7.30 (d, *J* = 8.4 Hz, 2H), 6.98 (s, 2H), 6.40 (d, *J* = 15.9 Hz, 1H), 6.32 – 6.22 (m, 1H), 6.06 (s, 1H), 5.41 (d, *J* = 7.8 Hz, 1H), 4.40 – 4.37 (m, 1H), 3.26 (d, *J* = 6.5 Hz, 2H), 3.17 – 3.13 (m, 1H), 2.75 (d, *J* = 4.7 Hz, 1H), 2.56 (s, 1H), 1.42 (d, *J* = 8.6 Hz, 12H), 1.38 (s, 3H). ^{13}C NMR (126 MHz, $CDCl_3$) δ 175.8, 154.8, 152.4, 149.7, 141.2, 132.6, 126.8, 119.6, 119.0, 114.6, 112.1, 90.9, 86.4, 84.1, 57.0, 51.2, 39.2, 28.5, 27.2, 26.5, 25.4, 22.0. HRMS (ESI): calculated for $C_{31}H_{41}N_8O_5$ $[M+H]^+$ 605.3200, found 605.3211.

tert-butyl 4-((((3a*R*,3a*R*,4*R*,6R,6a*R*,6a*R*)-6-(6-amino-9*H*-purin-9-yl)-2,2-dimethyltetrahydro-furo[3,4-d][1,3]dioxol-4-yl)methyl)((*E*)-3-(4-cyanophenyl)allyl)amino)butanoate (20f). Following the procedure described for compound **12a**, coupling compound **18** (89 mg, 0.20 mmol) with *tert*-butyl 4-oxobutanoate **19f** (35 mg, 0.22 mmol) to afford protected intermediate **20f** as a white powder (84 mg, 71% yield). ^{1}H NMR (400 MHz, $CDCl_3$) δ 8.27 (s, 1H), 7.93 (s, 1H), 7.55 (d, *J* = 8.4 Hz, 2H), 7.32 (d, *J* = 8.4 Hz, 2H), 6.43 (d, *J* = 15.9 Hz, 1H), 6.33 – 6.26 (m, 1H), 6.10 (s, 2H), 6.07 (d, *J* = 2.1 Hz, 1H), 5.47 (dd, *J* = 6.5, 2.1 Hz, 1H), 5.01 (dd, *J* = 6.5, 3.6 Hz, 1H), 4.40 – 4.36 (m, 1H), 3.30 (d, *J* = 6.5 Hz, 2H), 2.83 – 2.73 (m, 2H), 2.54 (t, *J* = 7.3 Hz, 2H), 2.26 – 2.23 (m, 2H), 1.79 – 1.69 (m, 2H), 1.61 (s, 3H), 1.43 – 1.38 (br m, 12H). ^{13}C NMR (101 MHz, $CDCl_3$) δ 173.7, 157.1, 153.0, 150.2, 142.2, 141.7, 140.1, 138.9, 136.8, 134.2, 130.7, 127.0, 120.9, 119.0, 114.4, 111.2, 90.8, 85.8, 84.6, 83.2, 79.5, 56.8, 56.0, 52.4, 33.1, 28.7, 27.2, 25.4, 22.4. HRMS (ESI): calculated for $C_{31}H_{40}N_7O_5$ $[M+H]^+$ 590.3091, found 590.3097.

tert-butyl 5-((((3a*R*,3a*R*,4*R*,6R,6a*R*,6a*R*)-6-(6-amino-9*H*-purin-9-yl)-2,2-dimethyltetrahydro-furo[3,4-d][1,3]dioxol-4-yl)methyl)((*E*)-3-(4-cyanophenyl)allyl)amino)pentanoate (20g). Following the procedure described for compound **12a**, coupling compound **18** (112 mg, 0.20 mmol) with *tert*-butyl 5-oxopentanoate **19g** (41 mg, 0.24 mmol) afforded protected intermediate **20g** as a white powder (82 mg, 68% yield). ^{1}H NMR (500 MHz, $CDCl_3$) δ 8.23 (s, 1H), 7.92 (s, 1H), 7.53 (d, *J* = 6.7 Hz, 2H), 7.29 (d, *J* = 8.4 Hz, 2H), 6.40 (d, *J* = 16.0 Hz, 1H), 6.31– 6.25 (m, 1H), 6.20 (s, 2H), 6.05 (d, *J* = 2.1 Hz, 1H), 5.45 (dd, *J* = 6.4, 2.1 Hz, 1H), 4.99 (dd, *J* = 6.4, 3.6 Hz, 1H), 4.39 – 4.34 (m, 1H), 3.69 – 3.59 (m, 3H), 3.28 (d, *J* = 6.8 Hz, 2H), 2.75 (d, *J* = 6.7 Hz, 2H), 2.53 – 2.45 (m, 3H), 2.18 (t, *J* = 7.3 Hz, 2H), 1.76 – 1.68 (m, 1H), 1.65 – 1.48 (m, 8H), 1.47 – 1.43 (m, 2H), 1.41 (s, 9H), 1.37 (s, 3H). ^{13}C NMR (126 MHz, $CDCl_3$) δ 173.0, 155.7, 153.1, 149.2, 141.4, 132.4, 126.7, 120.3, 119.1, 114.4, 111.3, 90.9, 85.8, 84.0, 83.3, 80.2, 62.5, 62.0, 56.9, 56.0, 54.4, 35.3, 32.4, 28.2, 27.2, 25.5, 23.5. HRMS (ESI): calculated for $C_{32}H_{42}N_7O_5$ $[M+H]^+$ 604.3247, found 604.3255.

4-((*E*)-3-((((3a*R*,3a*R*,4*R*,6R,6a*R*,6a*R*)-6-(6-amino-9*H*-purin-9-yl)-2,2-dimethyltetrahydrofuro[3,4-d][1,3]dioxol-4-yl)methyl)((6-(*tert*-butoxy)pyridin-2-yl)methyl)amino)prop-1-en-1-yl)benzonitrile (20h). Following the procedure described for compound **12a**, coupling compound **18** (112 mg, 0.20 mmol) with 6-(*tert*-butoxy)picolinaldehyde **19h** (43 mg, 0.24 mmol) afforded protected intermediate **20h** as a white powder (73 mg, 60% yield). ^{1}H NMR (400 MHz, $CDCl_3$) δ 8.15 (s, 1H), 7.95 (s, 1H), 7.54 (d, *J* = 6.6 Hz, 2H), 7.45 – 7.41 (m, 1H), 7.30 (d, *J* = 6.5 Hz, 2H), 6.88 (d, *J* = 7.4 Hz, 1H), 6.59 (d, *J* = 6.8 Hz, 2H), 6.52 (dd, *J* = 8.2, 0.8 Hz, 1H), 6.44 (d, *J* = 16.0 Hz, 1H), 6.37 – 6.29 (m, 1H), 6.08 (d, *J* = 2.1 Hz, 1H), 5.42 (dd, *J* = 6.4, 2.1 Hz, 1H), 4.97 (dd, *J* = 6.4, 3.5 Hz, 1H), 4.50 – 4.56 (m, 1H), 3.75 (s, 2H), 3.46 – 3.32 (m, 2H), 2.90 (d, *J* = 6.6 Hz, 2H), 1.60 (s, 3H), 1.56 (s, 9H), 1.39 (s, 3H). ^{13}C NMR (101 MHz, $CDCl_3$) δ 163.3, 156.0, 153.0, 149.2, 141.5, 139.9, 132.4, 131.8, 130.7, 126.6, 120.3, 119.1, 115.4, 114.3, 111.5, 110.5, 90.8, 85.8, 84.0, 83.2, 79.4, 60.2, 56.9, 56.0, 28.8, 27.2, 25.5. HRMS (ESI): calculated for $C_{33}H_{39}N_8O_4$ $[M+H]^+$ 611.3094, found 611.3102.

4-((*E*)-3-((((3a*R*,3a*R*,4*R*,6*R*,6a*R*,6a*R*)-6-(6-amino-9*H*-purin-9-yl)-2,2-dimethyltetrahydrofuro[3,4-d][1,3]dioxol-4-yl)methyl)amino)prop-1-en-1-yl)benzonitrile (20j). Following the procedure described for compound **12a,** coupling 9-((3a*R*,4*R*,6*R*,6a*R*)-2,2-dimethyl-6-((methylamino)methyl)tetrahydrofuro[3,4-d][1,3]dioxol-4-yl)-9*H*-purin-6-amine[39] (64 mg, 0.20 mmol) with **15u** (34 mg, 0.22 mmol) afforded protected intermediate **20j** as a yellow powder (66 mg, 72% yield). ^{1}H NMR (400 MHz, CDCl3) δ 8.20 (s, 1H), 7.97 (s, 1H), 7.52 (d, *J* = 8.1 Hz, 2H), 7.28 (d, *J* = 8.5 Hz, 2H), 6.57 (s, 2H), 6.42 (d, *J* = 16.0 Hz, 1H), 6.34 – 6.23 (m, 1H), 6.08 (s, 1H), 5.45 (d, *J* = 7.9 Hz, 1H), 4.98 (dd, *J* = 6.3, 3.7 Hz, 1H), 4.48 – 4.35 (m, 1H), 3.28 – 3.11 (m, 2H), 2.80 – 2.74 (m, 1H), 2.65 – 2.60 (br m, 1H), 2.33 (s, 3H), 1.61 (s, 3H), 1.38 (s, 3H). ^{13}C NMR (101 MHz, CDCl3) δ 155.8, 152.9, 149.1, 140.0, 132.4, 131.0, 126.6, 120.2, 119.1, 114.5, 110.6, 90.8, 85.2, 84.1, 83.2, 60.4, 59.0, 42.8, 29.7, 27.2, 25.4. HRMS (ESI): calculated for $C_{24}H_{28}N_7O_3$ $[M+H]^+$ 462.2254, found 462.2259.

4-((*E*)-3-((((3a*R*,3a*R*,4*R*,6R,6a*R*,6a*R*)-6-(6-amino-9*H*-purin-9-yl)-2,2-dimethyltetrahydrofuro[3,4-d][1,3]dioxol-4-yl)methyl)(isopropyl)amino)prop-1-en-1-yl)benzonitrile (20k). Following the procedure described for compound **12a**, coupling compound **18** (112 mg, 0.20 mmol) with 2 mL dry acetone afforded protected intermediate **20k** as a white powder (47 mg, 48% yield). ^{1}H NMR (400 MHz, $CDCl_3$) δ 8.29 (s, 1H), 7.92 (s, 1H), 7.54 (d, *J* = 8.4 Hz, 2H), 7.33 (d, *J* = 8.3 Hz, 2H), 6.49 – 6.38 (m, 3H), 6.37 – 6.29 (m, 1H), 6.06 (d, *J* = 2.0 Hz, 1H), 5.49 (dd, *J* = 6.4, 2.0 Hz, 1H), 5.04 (dd, *J* = 6.4, 3.5 Hz, 1H), 4.35 – 4.31 (m, 1H), 3.35 – 3.22 (m, 2H), 3.04 – 2.97 (m, 1H), 2.83 – 2.78 (m, 1H), 2.69 – 2.60 (m, 1H), 1.58 (s, 3H), 1.40 (s, 3H), 1.05 (d, *J* = 6.6 Hz, 3H), 0.93 (d, *J* = 6.6 Hz, 3H). ^{13}C NMR (101 MHz, $CDCl_3$) δ 155.8, 153.0, 149.2, 141.6, 140.2,

133.7, 132.4, 129.6, 126.6, 120.3, 119.1, 114.3, 110.3, 90.9, 86.6, 83.9, 83.1, 53.8, 51.7, 27.2, 25.5, 18.6, 17.9. HRMS (ESI): calculated for $C_{26}H_{32}N_7O_3$ $[M+H]^+$ 490.2567, found 490.2573.

(*S*)-2-amino-5-((((*2R,3S,4R,5R*)-5-(6-amino-9*H*-purin-9-yl)-3,4-dihydroxytetrahydrofuran-2-yl)methyl)((*E*)-3-(4-cyanophenyl)allyl)amino)pentanoic acid (21a). Following the procedure described for compound **13a**, compound **20a** (50 mg, 0.061 mmol) was deprotected and purified, affording compound **21a** as a white powder (24 mg, 63% yield). ^{1}H NMR (400 MHz, CD_3OD) δ 8.47 (s, 1H), 8.33 (s, 1H), 7.68 (d, *J* = 8.3 Hz, 2H), 7.48 (d, *J* = 8.2 Hz, 2H), 6.82 – 6.78 (br d, *J* = 15.8 Hz, 1H), 6.51 – 6.43 (m, 1H), 6.18 (d, *J* = 3.2 Hz, 1H), 4.71 – 4.65 (m, 1H), 4.62 – 4.51 (m, 2H), 4.19 – 4.00 (m, 3H), 3.89 – 3.84 (m, 1H), 3.69 (d, *J* = 8.9 Hz, 1H), 3.47 – 3.37 (m, 2H), 2.13 – 1.91 (m, 4H). ^{13}C NMR (101 MHz, CD_3OD) δ 170.0, 151.3, 148.1, 145.0, 143.1, 139.7, 138.5, 132.3, 127.2, 120.0, 119.7, 118.1, 118.0, 115.1, 111.9, 91.3, 73.5, 72.2, 55.3, 52.8, 27.1, 20.0. HRMS (ESI): calculated for $C_{25}H_{32}N_8O_5$ $[M+H]^+$ 523.2417, found 523.2423.

(*S*)-2-amino-4-((((2*R*,3*S*,4*R*,5*R*)-5-(6-amino-9*H*-purin-9-yl)-3,4-dihydroxytetrahydrofuran-2-yl)methyl)((*E*)-3-(4-cyanophenyl)allyl)amino)butanamide (21b). Compound **20b** (50 mg, 0.076 mmol) was added to ammonia in MeOH (33% w/w, 5 mL) in a sealed tube and the mixture was stirred overnight at room temperature. The solvent was evaporated and the crude intermediate was deprotected and purified following the procedure described for compound **13a** affording compound **21b** as a white powder (33 mg, 71% yield, two steps). ^{1}H NMR (400 MHz, CD_3OD) δ 8.44 (s, 1H), 8.32 (s, 1H), 7.70 (d, *J* = 8.4 Hz, 2H), 7.50 (d, *J* = 8.4 Hz, 2H), 6.85 – 6.81 (br d, *J* = 15.8 Hz, 1H), 6.50 – 6.41 (m, 1H), 6.15 (d, *J* = 3.3 Hz, 1H), 4.68 (dd, *J* = 5.0, 3.4 Hz, 1H), 4.58 – 4.48 (m, 2H), 4.15 – 4.03 (m, 3H), 3.86 – 3.80 (m, 1H), 3.67 – 3.64 (br d, *J* = 9.0 Hz, 1H), 3.51 – 3.40 (m, 2H), 2.47 – 2.34 (m, 2H). ^{13}C NMR (101 MHz, CD_3OD) δ 169.4, 163.1, 161.0, 152.6, 148.1, 140.1, 138.3, 132.7, 119.8, 118.0, 111.8, 91.1, 78.6, 73.4, 72.2, 55.4, 54.8, 49.3, 26.8. HRMS (ESI): calculated for $C_{24}H_{40}N_9O_4$ $[M+H]^+$ 508.2421, found 508.2427.

4-((((2*R*,3*S*,4*R*,5*R*)-5-(6-amino-9*H*-purin-9-yl)-3,4-dihydroxytetrahydrofuran-2-yl)methyl)((*E*)-3-(4-cyanophenyl)allyl)amino)butanamide (21c). Following the procedure described for compound **13a**, compound **20c** (50 mg, 0.065 mmol) was deprotected and purified, affording compound **21c** as a white powder (19 mg, 59% yield). ^{1}H NMR (400 MHz, CD_3OD) δ 8.46 (s, 1H), 7.70 (d, *J* = 8.1 Hz, 2H), 7.53 (s, 2H), 6.88 – 6.84 (br d, *J* =9.0 Hz, 1H), 6.54 – 6.40 (m, 1H), 4.75 (br s, 1H), 4.57 (d, *J* = 6.1 Hz, 2H), 4.12 (dd, *J* = 7.4, 3.7 Hz, 2H), 3.88 – 3.82 (m, 1H), 3.68 – 3.64 (br d, *J* = 16.0 Hz, 1H), 3.37(s, 1H), 2.46 (t, *J* = 6.5 Hz, 2H), 2.10 – 2.04 (m, 2H). ^{13}C NMR (101 MHz, CD_3OD) δ 174.8, 151.7, 149.1, 141.3, 137.9, 132.8, 127.2, 120.1, 117.0, 110.2, 91.0, 73.8, 71.1, 55.1, 30.1, 19.3. HRMS (ESI): calculated for $C_{24}H_{29}N_8O_4$ $[M+H]^+$ 493.2312, found 493.2320.

5-((((2*R*,3*S*,4*R*,5*R*)-5-(6-amino-9*H*-purin-9-yl)-3,4-dihydroxytetrahydrofuran-2-yl)methyl)((*E*)-3-(4-cyanophenyl)allyl)amino)pentanamide (21d). Following the procedure described for compound **13a**, compound **20d** (50 mg, 0.063 mmol) was deprotected and purified, affording compound **21d** as a white powder (22 mg, 57% yield). ^{1}H NMR (400 MHz, CD_3OD) δ 8.44 (s, 1H), 8.32 (s, 1H), 7.71 (d, *J* = 7.9 Hz, 2H), 7.51 (s, 2H), 6.87 (s, 1H), 6.52 (s, 1H), 6.16 (d, *J* = 3.5 Hz, 1H), 4.70 (s, 1H), 4.60 – 4.48 (m, 2H), 4.11 (d, *J* = 7.2 Hz, 2H), 3.87 – 3.81 (m, 1H), 3.66 (br d, *J* = 15.8 Hz, 1H), 2.31 (t, *J* = 7.0 Hz, 2H), 1.89 – 1.77 (m, 2H), 1.72 – 1.64 (m, 2H). ^{13}C NMR (101 MHz, CD_3OD) δ 175.5, 140.8, 138.6, 132.3, 127.2, 118.0, 112.7, 91.1, 73.4, 72.3, 54.4, 31.4, 23.1, 21.8. HRMS (ESI): calculated for $C_{25}H_{31}N_8O_4$ $[M+H]^+$ 507.2468, found 507.2479.

3-((*E*)-3-((((2*R*,3*S*,4*R*,5*R*)-5-(6-amino-9*H*-purin-9-yl)-3,4-dihydroxytetrahydrofuran-2-yl)methyl) (3-aminopropyl)amino)prop-1-en-1-yl)benzonitrile (21e). Following the procedure described for compound **13a**, compound **20e** (50 mg, 0.083 mmol) was deprotected and purified, affording compound **21e** as a white powder (41 mg, 72% yield). ^{1}H NMR (500 MHz, CD_3OD) δ 8.48 (s, 1H), 8.33 (s, 1H), 7.64 (d, *J* = 8.4 Hz, 2H), 7.47 (s, 2H), 6.18 (d, *J* = 3.3 Hz, 1H), 4.68 (d, *J* = 3.3 Hz, 1H), 4.60 – 4.55 (m, 2H), 4.14 (d, *J* = 7.3 Hz, 2H), 3.90 – 3.83 (m, 1H), 3.73 – 3.70 (br d, *J* = 9.0 Hz, 1H), 3.08 (t, *J* = 7.5 Hz, 2H), 2.26 – 2.20 (m, 2H). ^{13}C NMR (126 MHz, CD_3OD) δ 151.1, 148.1, 139.7, 138.6, 132.3, 127.2, 120.0, 119.8, 118.2, 111.8, 91.3, 73.6, 72.3, 55.4, 54.6, 50.6, 36.51, 48.6, 36.5, 22.2. HRMS (ESI): calculated for $C_{23}H_{29}N_8O_3$ $[M+H]^+$ 465.2363, found 465.2372.

4-((((2*R*,3*S*,4*R*,5*R*)-5-(6-amino-9*H*-purin-9-yl)-3,4-dihydroxytetrahydrofuran-2-yl)methyl)((*E*)-3-(4-cyanophenyl)allyl)amino)butanoic acid (21f). Following the procedure described for compound **13a**, compound **20f** (50 mg, 0.085 mmol) was deprotected and purified, affording compound **21f** as a white powder (37 mg, 71% yield). ^{1}H NMR (CD_3OD) δ 8.44 (s, 1H), 8.34 (s, 1H), 6.87 (d, *J* = 15.8 Hz, 1H), 6.51 – 6.43 (m, 1H), 6.16 (d, *J* = 3.7 Hz, 1H), 4.74 (t, *J* = 4.1 Hz, 1H), 4.55 (d, *J* = 6.9 Hz, 2H), 4.13 (d, *J* = 7.4 Hz, 2H), 3.37 (dd, *J* = 9.5, 6.9 Hz, 2H), 2.47 (t, *J* = 6.8 Hz, 2H), 2.11 – 2.02 (m, 2H). ^{13}C NMR (101 MHz, CD_3OD) δ 178.8, 151.1, 147.5, 139.7, 139.2, 132.3, 127.3, 120.5, 118.1, 112.3, 95.4, 78.3, 73.4, 72.3, 57.9, 52.9, 32.6, 22.2. HRMS (ESI): calculated for $C_{24}H_{28}N_7O_5$ $[M+H]^+$ 494.2152, found 494.2160.

5-((((2*R*,3*S*,4*R*,5*R*)-5-(6-amino-9*H*-purin-9-yl)-3,4-dihydroxytetrahydrofuran-2-yl)methyl)((*E*)-3-(4-cyanophenyl)allyl)amino)pentanoic acid (21g). Following the procedure described for compound **13a**, compound **20g** (50 mg, 0.083 mmol) was deprotected and purified, affording compound **21g** as a white powder (39 mg, 75% yield). ^{1}H NMR (400 MHz, CD_3OD) δ 8.45 (s, 1H), 8.33 (s, 1H), 7.71 (d, *J* = 8.0 Hz, 2H), 7.52 (br s, 2H), 6.85 (br d, *J* = 15.7 Hz, 1H),

6.48 – 6.41 (m, 1H), 6.17 (d, *J* = 4.3 Hz, 1H), 4.59 – 4.48 (m, 2H), 4.12 (d, *J* = 7.3 Hz, 2H), 3.86 – 3.81 (br m, 1H), 3.68 – 3.65 (br d, *J* = 12.2 Hz, 1H), 2.38 (t, *J* = 7.0 Hz, 2H), 1.86 (t, *J* = 7.8 Hz, 1H), 1.70 – 1.63 (m, 2H). ^{13}C NMR (101 MHz, CD_3OD) δ 171.7, 139.1, 138.6, 131.7, 119.9, 118.0, 111.9, 91.1, 73.4, 72.2, 55.1, 53.0, 31.7, 23.0, 20.7. HRMS (ESI): calculated for $C_{25}H_{30}N_7O_5$ $[M+H]^+$ 508.2308, found 508.2317.

4-((*E*)-3-((((2*R*,3*S*,4*R*,5*R*)-5-(6-amino-9*H*-purin-9-yl)-3,4-dihydroxytetrahydrofuran-2-yl)methyl) ((6-oxo-1,6-dihydropyridin-2-yl)methyl)amino)prop-1-en-1-yl)benzonitrile (21h). Following the procedure described for compound **13a**, compound **20h** (50 mg, 0.082 mmol) was deprotected and purified, affording compound **21h** as a white powder (25 mg, 59% yield). ^{1}H NMR (400 MHz, CD_3OD) δ 8.43 (s, 1H), 8.26 (s, 1H), 7.64 (d, *J* = 8.4 Hz, 2H), 7.57 (dd, *J* = 8.8, 7.0 Hz, 1H), 7.46 (d, *J* = 8.4 Hz, 2H), 6.79 – 6.69 (m, 2H), 6.57 – 6.43 (m, 2H), 6.14 (d, *J* = 3.1 Hz, 1H), 4.63 (dd, *J* = 4.9, 3.1 Hz, 1H), 4.58 – 4.49 (m, 2H), 4.35 (s, 2H), 4.13 – 4.00 (m, 2H), 3.76 – 3.57 (m, 2H). ^{13}C NMR (101 MHz, CD_3OD) δ 164.1, 150.9, 148.0, 144.3, 143.3, 141.4, 137.3, 132.3, 127.1, 122.2, 119.8, 118.2, 117.8, 115.8, 114.9, 112.3, 111.5, 91.2, 79.4, 73.7, 72.3, 56.1, 55.4, 55.1. HRMS (ESI):) calculated for $C_{26}H_{27}N_8O_4$ $[M+H]^+$ 515.2155, found 515.2164.

4-((*E*)-3-((((2*R*,3*S*,4*R*,5*R*)-5-(6-amino-9*H*-purin-9-yl)-3,4-dihydroxytetrahydrofuran-2-yl)methyl) amino)prop-1-en-1-yl)benzonitrile (21i). Following the procedure described for compound **13a**, compound **18** (50 mg, 0.11 mmol) was deprotected and purified, affording compound **21i** as a white powder (30 mg, 52% yield). ^{1}H NMR (500 MHz, CD_3OD) δ 8.49 (s, 1H), 8.38 (s, 1H), 7.69 (d, *J* = 8.4 Hz, 2H), 7.58 (d, *J* = 8.4 Hz, 2H), 6.86 (d, *J* = 15.9 Hz, 1H), 6.49 – 6.40 (m, 1H), 6.15 (d, *J* = 4.6 Hz, 1H), 4.83 (d, *J* = 4.9 Hz, 2H), 4.50 (t, *J* = 5.1 Hz, 1H), 4.47 – 4.43 (m, 1H), 3.95 (d, *J* = 7.2 Hz, 2H), 3.66 – 3.61 (br m, 1H), 3.56 – 3.53 (br m, 1H). ^{13}C NMR (126 MHz, CD_3OD) δ 161.3, 150.8, 148.3, 140.3, 136.7, 132.5, 128.3, 122.2, 119.7, 118.6, 108.9, 90.6, 80.3, 73.7, 71.9, 50.7. HRMS (ESI): calculated for $C_{20}H_{22}N_7O_3$ $[M+H]^+$408.1784, found 408.1792.

4-((*E*)-3-((((2*R*,3*S*,4*R*,5*R*)-5-(6-amino-9*H*-purin-9-yl)-3,4-dihydroxytetrahydrofuran-2-yl)methyl) (methyl)amino)prop-1-en-1-yl)benzonitrile (21j). Following the procedure described for compound **13a**, compound **20j** (50 mg, 0.11 mmol) was deprotected and purified, affording compound **21j** as a white powder (37 mg, 64% yield). ^{1}H NMR (400 MHz, CD_3OD) δ 8.46 (s, 1H), 8.37 (s, 1H), 7.73 (d, *J* = 8.3 Hz, 2H), 7.59 (d, *J* = 8.0 Hz, 2H), 6.94 – 6.90 (br d, *J* =16.0, 1H), 6.53 – 6.45 (m, 1H), 6.16 (d, *J* = 4.2 Hz, 1H), 4.81 – 4.76 (m, 1H), 4.59 – 4.46 (m, 2H), 4.09 (d, *J* = 5.0 Hz, 2H), 3.84 (br t, *J* = 9.0 Hz, 1H), 3.63 – 3.61 (br d, *J* = 8.0 Hz, 1H), 3.00 (s, 3H). ^{13}C NMR (101 MHz, CD_3OD) δ 151.82, 148.9, 139.7, 138.7, 132.3, 127.8, 118.05, 111.1, 89.5, 78.7, 73.3, 72.2, 56.9. HRMS (ESI): calculated for $C_{21}H_{24}N_7O_3$ $[M+H]^+$ 422.1941, found 422.1945.

4-((*E*)-3-((((2*R*,3*S*,4*R*,5*R*)-5-(6-amino-9*H*-purin-9-yl)-3,4-dihydroxytetrahydrofuran-2-yl)methyl) (isopropyl)amino)prop-1-en-1-yl)benzonitrile (21k). Following the procedure described for compound **13a**, compound **20k** (50 mg, 0.10 mmol) was deprotected and purified, affording compound **21k** as a white powder (32 mg, 69% yield). ^{1}H NMR (500 MHz, CD_3OD) δ 8.34 (s, 1H), 8.28 (s, 1H), 7.62 (d, *J* = 8.2 Hz, 2H), 7.44 (d, *J* = 6.9 Hz, 2H), 6.82 (d, *J* = 8.9 Hz, 1H), 6.44 – 6.38 (m, 1H), 6.12 – 6.10 (m, 1H), 4.64 (dd, *J* = 5.3, 3.2 Hz, 1H), 4.58 – 4.53 (m, 2H), 4.47 – 4.43 (m, 1H), 4.07 (d, *J* = 8.1 Hz, 2H), 3.89 – 3.81 (m, 1H), 3.69 (d, *J* = 4.2 Hz, 2H), 1.44 (d, *J* = 6.6 Hz, 3H), 1.41 (d, *J* = 6.6 Hz, 3H). ^{13}C NMR (101 MHz, CD_3OD) δ 161.9, 161.6, 161.2, 160.8, 142.9, 139.8, 132.3, 119.7, 118.1, 115.1, 111.7, 91.3, 73.7, 72.1, 51.7. HRMS (ESI): calculated for $C_{23}H_{28}N_7O_3$ $[M+H]^+$ 450.2254, found 450.2262.

(*E*)-4-(3-(methylamino)prop-1-en-1-yl)benzonitrile (22b). Aldehyde **15u** (157 mg, 1.0 mmol), 5 mL methylamine in MeOH (33% w/w), $NaBH(OAc)_3$ (57 mg, 1.5 mmol) and AcOH (one drop) were added to DCE (10 mL) in a sealed tube and the mixture was stirred at room temperature overnight. The reaction was quenched by adding 1 N NaOH (10 mL), and the product was extracted with CH_2Cl_2. The combined organic layers were washed with brine and dried over Na_2SO_4. The solvent was evaporated, and the crude product was purified by column chromatography (20% MeOH in EtOAc) to give compound **22b** as a white powder (72 mg, 42% yield). ^{1}H NMR (400 MHz, CD_3OD) δ 7.76 (d, *J* = 8.6 Hz, 2H), 7.68 (d, *J* = 8.7 Hz, 2H), 6.97 – 6.93 (br d, *J* = 12.0 Hz, 1H), 6.52 – 6.45 (m, 1H), 3.85 (dd, *J* = 7.1, 1.3 Hz, 2H), 2.77 (s, 3H). ^{13}C NMR (101 MHz, CD_3OD) δ 140.1, 136.5, 132.4, 127.3, 122.2, 118.1, 111.7, 50.0, 31.5. HRMS (ESI): calculated for $C_{11}H_{13}N_2$ $[M+H]^+$ 173.1079, found 173.1084.

***tert*-butyl (*S*,*E*)-2-((*tert*-butoxycarbonyl)amino)-4-((3-(4-cyanophenyl)allyl)amino)butanoate (23a).** Following the procedure described for compound **12a**, coupling (*E*)-4-(3-aminoprop-1-en-1-yl)benzonitrile **22a** (35 mg, 0.22 mmol) with *tert*-butyl (*S*)-2-((*tert*-butoxycarbonyl)amino)-4-oxobutanoate **10** (55 mg, 0.20 mmol) afforded compound **23a** as a white powder (40 mg, 48% yield).^{1}H NMR (400 MHz, $CDCl_3$) δ 7.57 (d, *J* = 8.3 Hz, 2H), 7.43 (d, *J* = 8.3 Hz, 2H), 6.56 – 6.52 (br d, *J* = 16.0 Hz , 1H), 6.45 – 6.35 (m, 1H), 5.57 (d, *J* = 8.1 Hz, 1H), 4.30 – 4.18 (m, 1H), 3.48 – 3.40 (m, 2H), 2.76 – 2.67 (m, 2H), 2.04 – 1.92 (m, 2H), 1.81 – 1.75 (m, 1H), 1.45 – 1.42 (m, 18H). ^{13}C NMR (101 MHz, $CDCl_3$) δ 171.9, 155.7, 141.7, 132.4, 129.5, 126.8, 119.0, 110.5, 81.9, 79.6, 52.6, 51.5, 45.4, 32.9, 28.4. HRMS (ESI): calculated for $C_{23}H_{34}N_3O_4$ $[M+H]^+$ 416.2549, found 416.2563.

***tert*-butyl (*S*,*E*)-2-((*tert*-butoxycarbonyl)amino)-4-((3-(4-cyanophenyl)allyl)(methyl)amino) butanoate (23b).** Following the procedure described for compound **12a**, coupling (*E*)-4-(3-(methylamino)prop-1-en-1-yl)benzonitrile **22b** (34 mg, 0.20 mmol) with *tert*-butyl (*S*)-2-((*tert*-

butoxycarbonyl)amino)-4-oxobutanoate **10** (66 mg, 0.24 mmol) afforded compound **23b** as a white powder (66 mg, 77% yield).^{1}H NMR (400 MHz, $CDCl_3$) δ 7.59 (d, *J* = 8.3 Hz, 2H), 7.46 (d, *J* = 8.2 Hz, 2H), 6.53 (d, *J* = 16.0 Hz, 1H), 6.46 – 6.34 (m, 1H), 5.83 (d, *J* = 7.9 Hz, 1H), 4.23 (d, *J* = 6.4 Hz, 1H), 3.26 – 3.21 (m, 1H), 3.14 – 3.09 (m, 1H), 2.58 – 2.49 (m, 1H), 2.44 – 2.38 (m, 1H), 2.26 (s, 3H), 2.07 – 1.97 (m, 1H), 1.87 – 1.79 (m, 1H), 1.46 – 1.42 (br m, 18H).^{13}C NMR (101 MHz, $CDCl_3$) δ 171.7, 156.9, 141.5, 132.4, 131.8, 130.8, 126.9, 119.0, 110.6, 81.7, 79.5, 60.2, 53.6, 53.3, 42.3, 28.4, 28.0. HRMS (ESI): calculated for $C_{24}H_{35}N_3O_4$ $[M+H]^+$ 430.2706, found 430.2715.

(*S*,*E*)-2-amino-4-((3-(4-cyanophenyl)allyl)amino)butanoic acid (24a). Following the procedure described for compound **13a**, compound **23a** (20 mg, 0.048 mmol) was deprotected and purified, affording compound **24a** as a white powder (14 mg, 76% yield). ^{1}H NMR (400 MHz, CD_3OD) δ 7.75 (d, *J* = 8.4 Hz, 2H), 7.68 (d, *J* = 8.4 Hz, 2H), 6.96 (d, *J* = 15.9 Hz, 1H), 6.54 – 6.47 (m, 1H), 4.10 (dd, *J* = 8.1, 5.3 Hz, 1H), 3.91 (d, *J* = 8.3 Hz, 2H), 3.43 – 3.35 (m, 1H), 2.45 – 2.21 (m, 2H). ^{13}C NMR (101 MHz, CD_3OD) δ 169.4, 144.8, 136.5, 131.3, 127.8, 126.2, 122.5, 118.0, 114.1, 111.7, 50.7, 48.7, 42.8, 28.7. HRMS (ESI): calculated for $C_{14}H_{18}N_3O_2$ $[M+H]^+$ 260.1399, found 260.1408.

(*S*,*E*)-2-amino-4-((3-(4-cyanophenyl)allyl)(methyl)amino)butanoic acid (24b). Following the procedure described for compound **13a**, compound **23b** (13 mg, 0.046 mmol) was deprotected and purified, affording compound **24b** as a white powder (9 mg, 72% yield). ^{1}H NMR (400 MHz, CD_3OD δ 7.76 (d, *J* = 8.6 Hz, 2H), 7.71 (d, *J* = 8.5 Hz, 2H), 7.04 – 7.00 (br d, *J* = 15.8 Hz, 1H), 6.62 – 6.51 (m, 1H), 4.13 (dd, *J* = 8.0, 5.3 Hz, 1H), 4.06 (d, *J* = 7.3 Hz, 2H), 3.53 – 3.30 (br m, 2H), 2.96 (s, 3H), 2.53 – 2.42 (m, 1H), 2.41 – 2.30 (m, 1H). ^{13}C NMR (101 MHz, CD_3OD) δ 171.7, 143.8, 140.9, 138.7, 132.3, 127.5, 120.3, 117.0, 115.1, 110.6, 54.9, 53.0, 50.8, 39.3, 23.8. HRMS (ESI): calculated for $C_{15}H_{20}N_3O_2$ $[M+H]^+$ 274.1556, found 274.1561.

***tert*-butyl (2*S*)-4-((((3 3a*R*,3a*R*,4*R*,6R,6a*R*,6a*R*)-6-(6-amino-9*H*-purin-9-yl)-2,2-dimethyltetra-hydrofuro[3,4-d][1,3]dioxol-4-yl)methyl)(4-cyanobenzyl)amino)-2-((*tert*-butoxycarbonyl) amino)butanoate (25a).** Following the procedure described for compound **12a**, coupling compound **11** (112 mg, 0.20 mmol) with 4-formylbenzonitrile (31 mg, 0.24 mmol) afforded protected intermediate **25a** as a white powder (79 mg, 50% yield). ^{1}H NMR (500 MHz, $CDCl_3$) δ 8.14 (s, 1H), 7.86 (s, 1H), 7.46 (d, *J* = 8.3 Hz, 2H), 7.32 (d, *J* = 8.2 Hz, 2H), 6.42 (s, 2H), 6.03 (s, 1H), 5.43 – 5.37 (m, 2H), 4.93 (dd, *J* = 6.5, 3.6 Hz, 1H), 4.38 – 4.33 (m, 1H), 4.21 – 4,17 (m, 1H), 3.69 – 3.53 (m, 2H), 2.82 – 2.67 (m, 2H), 2.65 – 2.48 (m, 2H), 2.00 – 1.96 (br m, 1H), 1.77 – 1.71 (br m, 1H), 1.59 (s, 3H), 1.43 – 1.37 (br m, 21H). ^{13}C NMR (126 MHz, $CDCl_3$) δ 175.4, 171.7, 155.7, 148.9, 132.1, 129.3, 120.1, 119.0, 115.8, 109.5, 90.8, 85.7, 84.0, 83.5,

59.4, 52.7, 50.73, 29.8, 28.4, 27.2, 25.5. HRMS (ESI): calculated for $C_{34}H_{47}N_8O_7$ $[M+H]^+$ 679.3568, found 679.3571.

(*S*)-2-amino-4-((((2*R*,3*S*,4*R*,5*R*)-5-(6-amino-9*H*-purin-9-yl)-3,4-dihydroxytetrahydrofuran-2-yl)methyl)(4-cyanobenzyl)amino)butanoic acid (25). Following the procedure described for compound **13a**, compound **25a** (50 mg, 0.074 mmol) was deprotected and purified, affording compound **25** as a white powder (33 mg, 75% yield). ^{1}H NMR (500 MHz, CD_3OD) δ 8.40 (s, 1H), 8.34 (s, 1H), 7.69 (d, *J* = 8.5 Hz, 2H), 7.64 (d, *J* = 8.6 Hz, 2H), 6.11 (d, *J* = 3.2 Hz, 1H), 4.60 (dd, *J* = 5.3, 3.3 Hz, 1H), 4.48 – 4.40 (m, 3H), 4.33 (br d, *J* = 13.7 Hz, 1H), 3.98 (dd, *J* = 7.9, 5.1 Hz, 1H), 3.53 – 3.37 (m, 4H), 2.39 – 2.33 (m, 1H), 2.22 – 2.18 (m, 1H). ^{13}C NMR (126 MHz, CD_3OD) δ 172.2, 161.2, 151.5, 147.8, 132.4, 128.0, 119.6, 118.3, 112.8, 90.8, 79.4, 73.1, 70.9, 57.3, 55.1, 51.7, 51.0, 39.1, 25.5. HRMS (ESI): calculated for $C_{24}H_{27}N_8O_5$ $[M+H]^+$ 483.2104, found 483.2115.

***tert*-butyl (2*S*)-4-((((3a*R*,3a*R*,4*R*,6R,6a*R*,6a*R*)-6-(6-amino-9*H*-purin-9-yl)-2,2-dimethyltetra-hydrofuro[3,4-d][1,3]dioxol-4-yl)methyl)(3-(4-cyanophenyl)propyl)amino)-2-((*tert*-butoxy carbonyl)amino)butanoate (26a).** Following the procedure described for compound **12a**, coupling compound **11** (112 mg, 0.20 mmol) with 4-(3-oxopropyl)benzonitrile (38 mg, 0.24 mmol) afforded protected intermediate compound **26a** as a white powder (80 mg, 57% yield). ^{1}H NMR (400 MHz, $CDCl_3$) δ 8.30 (s, 1H), 7.92 (s, 1H), 7.54 (d, *J* = 8.1 Hz, 2H), 7.22 (d, *J* = 8.2 Hz, 2H), 6.24 (br s, 2H), 6.07 (d, *J* = 1.7 Hz, 1H), 5.76 (d, *J* = 8.0 Hz, 1H), 5.52 (d, *J* = 6.0 Hz, 1H), 5.02 (s, 1H), 4.32 – 4.28 (m, 1H), 4.20 – 4.14 (m, 2H), 3.01 – 2.73 (m, 2H), 2.67 – 2.57 (m, 4H), 2.50 – 2.34 (m, 3H), 2.16 – 1.88 (m, 2H), 1.75 – 1.64 (m, 3H), 1.62 (s, 3H), 1.48 – 1.38 (br m, 21H). ^{13}C NMR (101 MHz, $CDCl_3$) δ 171.9, 153.1, 149.2, 148.0, 140.3, 132.2, 129.2, 120.4, 119.2, 114.4, 109.6, 90.9, 85.7, 83.9, 83.4, 81.7, 79.5, 60.4, 54.0, 53.7, 53.0, 52.6, 50.9, 42.1, 33.6, 30.8, 29.3, 28.4, 28.2, 27.2, 25.5, 20.0, 14.3. HRMS (ESI): calculated for $C_{36}H_{51}N_8O_7$ $[M+H]^+$ 707.3881, found 707.3882.

(*S*)-2-amino-4-((((2*R*,3*S*,4*R*,5*R*)-5-(6-amino-9*H*-purin-9-yl)-3,4-dihydroxytetrahydrofuran-2-yl)methyl)(3-(4-cyanophenyl)propyl)amino)butanoic acid (26). Following the procedure described for compound **13a**, compound **26a** (50 mg, 0.071 mmol) was deprotected and purified, affording compound **26** as a white powder (35 mg, 79% yield). ^{1}H NMR (400 MHz, CD_3OD) δ 8.47 (s, 1H), 8.38 (s, 1H), 7.61 (d, *J* = 8.3 Hz, 2H), 7.33 (d, *J* = 8.2 Hz, 2H), 6.12 (d, *J* = 3.9 Hz, 1H), 4.70 (t, *J* = 4.3 Hz, 1H), 4.50 – 4.43 (m, 2H), 4.08 (dd, *J* = 8.2, 4.7 Hz, 1H), 3.84 – 3.78 (m, 1H), 3.71 – 3.67 (br d, *J* = 16.0 Hz, 1H), 3.64 – 3.47 (m, 2H), 2.81 – 2.68 (m, 2H), 2.47 – 2.38 (m, 1H), 2.30 – 2.22(m, 1H), 2.07 (h, *J* = 7.4 Hz, 2H). ^{13}C NMR (101 MHz, CD_3OD) δ 170.2, 161.9, 161.5, 161.2, 160.8, 151.6, 148.3, 146.1, 145.4, 142.8, 132.1, 129.1, 119.6, 118.4, 115.1,

109.9, 90.6, 78.7, 73.3, 72.2, 54.9, 51.1, 31.9, 24.7, 24.3. HRMS (ESI): calculated for $C_{24}H_{31}N_8O_5$ $[M+H]^+$ 511.2417, found 511.2425.

tert-butyl (2*S*)-4-((((3a*R*,3a*R*,4*R*,6R,6a*R*,6a*R*)-6-(6-amino-9*H*-purin-9-yl)-2,2-dimethyltetra-hydrofuro[3,4-d][1,3]dioxol-4-yl)methyl)(3-(3-cyanophenyl)prop-2-yn-1-yl)amino)-2-((*tert*-butoxycarbonyl)amino)butanoate (27a). Following the procedure described for compound **12a**, coupling compound **11** (112 mg, 0.20 mmol) with 3-(3-oxoprop-1-yn-1-yl)benzonitrile (37 mg, 0.24 mmol) afforded protected intermediate compound **27a** as a white powder (90 mg, 64% yield). ^{1}H NMR (400 MHz, $CDCl_3$) δ 8.31 (s, 1H), 7.99 (s, 1H), 7.63 (s, 1H), 7.55 (dd, *J* = 7.7, 2.1 Hz, 2H), 7.39 (t, *J* = 7.8 Hz, 1H), 6.34 (d, *J* = 11.2 Hz, 2H), 6.09 (d, *J* = 2.3 Hz, 1H), 5.64 – 5.49 (br m, 2H), 5.08 – 5.00 (m 1H), 4.42 – 4.23 (m, 2H), 3.66 (s, 2H), 2.91 – 2.86 (m, 1H), 2.81 – 2.73 (br m, 1H), 2.65 (t, *J* = 6.9 Hz, 2H), 2.02 – 1.96 (m, 1H), 1.87 – 1.80 (m, 1H), 1.62 (s, 3H), 1.50 – 1.35 (br m, 21H). ^{13}C NMR (101 MHz, $CDCl_3$) δ 175.9, 171.7, 155.8, 155.5, 153.0, 149.2, 140.1, 135.83, 135.8, 135.1, 131.4, 129.2, 124.5, 120.2, 118.1, 114.5, 112.8, 86.8, 85.7, 83.9, 83.4, 55.6, 52.67,50.6, 43.5, 29.7, 28.4, 28.0, 27.2, 25.5. HRMS (ESI): calculated for $C_{36}H_{47}N_8O_7$ $[M+H]^+$ 703.3568, found 703.3582.

(*S*)-2-amino-4-((((2*R*,3*S*,4*R*,5*R*)-5-(6-amino-9*H*-purin-9-yl)-3,4-dihydroxytetrahydrofuran-2-yl)methyl)(3-(3-cyanophenyl)prop-2-yn-1-yl)amino)butanoic acid (27). Following the procedure described for compound **13a**, compound **27a** (50 mg, 0.074 mmol) was deprotected and purified, affording compound **27** as a white powder (33 mg, 73% yield). ^{1}H NMR (500 MHz, CD_3OD) δ 8.48 (s, 1H), 8.38 (s, 1H), 7.83 (t, *J* = 1.3 Hz, 1H), 7.78 – 7.75 (m, 1H), 7.74 – 7.72 (m, 1H), 7.59 – 7.55 (m, 1H), 6.14 (d, *J* = 4.1 Hz, 1H), 4.74 – 4.71 (m, 1H), 4.50 – 4.46 (m, 1H), 4.44 (t, *J* = 5.4 Hz, 1H), 4.23 (s, 2H), 4.13 (t, *J* = 6.4 Hz, 1H), 3.60 – 3.49 (m, 2H), 3.40 (t, *J* = 6.9 Hz, 2H), 2.42 – 2.35 (m, 1H), 2.24 – 2.17 (m, 1H). ^{13}C NMR (126 MHz, CD_3OD) δ 170.3, 161.0, 160.8, 151.2, 148.4, 135.8, 134.9, 132.4, 129.6, 123.1, 119.6, 117.4, 115.2, 112.8, 90.3, 86.1, 81.44, 80.2, 73.7, 72.2, 55.9, 51.7, 51.1, 42.7, 25.6. HRMS (ESI): calculated for $C_{24}H_{27}N_8O_5$ $[M+H]^+$ 507.2104, found 507.2108.

tert-butyl (2S)-4-((((3a*R*,3a*R*,4*R*,6R,6a*R*,6a*R*)-6-(6-amino-9*H*-purin-9-yl)-2,2-dimethyltetra-hydrofuro[3,4-d][1,3]dioxol-4-yl)methyl)(3-(4-cyanophenyl)prop-2-yn-1-yl)amino)-2-((*tert*-butoxycarbonyl)amino)butanoate (28a). Following the procedure described for compound **12a**, coupling compound **11** (112 mg, 0.20 mmol) with 4-(3-oxoprop-1-yn-1-yl)benzonitrile (37 mg, 0.24 mmol) afforded protected intermediate compound **28a** as a white powder (104 mg, 74% yield). ^{1}H NMR (500 MHz, $CDCl_3$) δ 8.32 (s, 1H), 7.96 (s, 1H), 7.56 (s, 2H), 7.40 (d, *J* = 8.4 Hz, 2H), 6.09 (d, *J* = 9.8 Hz, 3H), 5.57 (d, *J* = 8.2 Hz, 1H), 5.50 (d, *J* = 8.7 Hz, 1H), 5.09 – 4.99 (m, 1H), 4.43 – 4.36 (m, 1H), 4.25 – 4.23 (m, 1H), 3.66 (d, *J* = 2.9 Hz, 2H),

2.90 – 2.75 (m, 2H), 2.64 (t, *J* = 6.9 Hz, 2H), 2.01 – 1.97 (m, 1H), 1.85 – 1.80 (m, 1H), 1.61 (s, 3H), 1.45 – 1.38 (br m, 21H). ^{13}C NMR (126 MHz, $CDCl_3$) δ 171.7, 154.5, 153.1, 150.6, 132.3, 132.0, 129.0, 120.9, 118.5, 113.9, 110.2, 90.9, 89.0, 85.8, 83.2, 81.9, 80.2, 55.2, 50.6, 42.1, 30.1, 28.4, 28.1, 27.2, 25.5. HRMS (ESI): calculated for $C_{36}H_{47}N_8O_7$ $[M+H]^+$ 703.3568, found 703.3577.

(*S*)-2-amino-4-((((2*R*,3*S*,4*R*,5*R*)-5-(6-amino-9*H*-purin-9-yl)-3,4-dihydroxytetrahydrofuran-2-yl)methyl)(3-(4-cyanophenyl)prop-2-yn-1-yl)amino)butanoic acid (28). Following the procedure described for compound **13a**, compound **28a** (50 mg, 0.074 mmol) was deprotected and purified, affording compound **28** as a white powder (36 mg, 81% yield). ^{1}H NMR (500 MHz, CD_3OD) δ 8.48 (s, 1H), 8.37 (s, 1H), 7.73 (d, *J* = 8.6 Hz, 2H), 7.59 (d, *J* = 8.6 Hz, 2H), 6.13 (d, *J* = 4.1 Hz, 1H), 4.74 – 4.71 (m, 1H), 4.48 – 4.41 (m, 2H), 4.19 (s, 2H), 4.12 (t, *J* = 6.4 Hz, 1H), 3.53 – 3.42 (m, 2H), 3.35 (d, *J* = 6.5 Hz, 2H), 2.39 – 2.32 (m, 1H), 2.20 – 2.13 (m, 1H). ^{13}C NMR (126 MHz, CD_3OD) δ 170.5, 161.0, 151.50, 148.4, 132.1, 126.6, 117.8, 115.3, 112.2, 90.2, 86.2, 84.2, 73.7, 72.2, 55.9, 52.2, 51.1, 42.7, 25.8. HRMS (ESI): calculated for $C_{24}H_{27}N_8O_5$ $[M+H]^+$ 507.2104, found 507.2113.

***tert*-butyl (2*S*)-4-((*E*)-*N*-(((3a*R*,3a*R*,4*R*,6R,6a*R*,6a*R*)-6-(6-amino-9*H*-purin-9-yl)-2,2-dimethyl-tetrahydrofuro[3,4-d][1,3]dioxol-4-yl)methyl)-3-(4-cyanophenyl)acrylamido)-2-((tert-butoxy carbonyl)amino)butanoate (29a)** To a stirred solution of (*E*)-3-(4-cyanophenyl)acrylic acid (35 mg, 0.20 mmol) in CH_2Cl_2 (10 mL) under N_2 atmosphere were added BOP (97 mg, 0.22 mmol), compound **11** (112mg, 0.20 mmol) and Et_3N (0.1 mL) sequentially. The resulting reaction mixture was then stirred for 16 hours at room temperature. After washing with 5% $KHSO_4$ (2 × 80 mL), 5% $NaHCO_3$ (2 × 80 mL), and H_2O (80 mL), the organic phase was dried over Na_2SO_4. The solvent was evaporated, and the crude product was purified by column chromatography (5% MeOH in EtOAc) to give protected intermediate compound **29a** as a white powder (83 mg, 58% yield). ^{1}H NMR (400 MHz, $CDCl_3$) δ 8.32 (d, *J* = 8.1 Hz, 1H), 7.93 (d, *J* = 43.7 Hz, 1H), 7.73 – 7.59 (m, 2H), 7.52 – 7.36 (m, 2H), 7.08 – 6.87 (m, 2H), 6.76 (s, 1H), 6.70 – 6.47 (m, 1H), 6.07 (d, *J* = 9.4 Hz, 1H), 5.63 – 5.47 (br m, 1H), 5.27 (d, *J* = 6.4 Hz, 1H), 5.17 – 5.12 (m, 1H), 4.27 – 3.80 (m, 3H), 3.70 – 3.66 (br d, *J* = 16.0 Hz, 1H), 3.60 – 3.13 (m, 2H), 2.11 (s, 1H), 1.61 (d, *J* = 10.2 Hz, 3H), 1.46 – 1.36 (br m, 21H) ^{13}C NMR (101 MHz, $CDCl_3$) δ 175.7, 141.4, 166.2, 155.0, 153.1, 140.2, 139.5, 132.5, 128.5, 127.6, 124.8, 121.5, 118.7, 90.6, 89.9, 84.7, 81.8, 52.2, 50.5, 43.4, 28.4, 28.0, 25.5. HRMS (ESI): calculated for $C_{36}H_{47}N_8O_8$ $[M+H]^+$ 719.3517, found 719.3524.

(*S*)-2-amino-4-((*E*)-*N*-(((2*R*,3*S*,4*R*,5*R*)-5-(6-amino-9*H*-purin-9-yl)-3,4-dihydroxytetrahydro-furan-2-yl)methyl)-3-(4-cyanophenyl)acrylamido)butanoic acid (29). Following the procedure described for compound **13a**, compound **29a** (50 mg, 0.070 mmol) was

deprotected and purified, affording compound **29** as a white powder (18 mg, 49% yield). ^{1}H NMR (400 MHz, CD_3OD) δ 8.40 (s, 1H), 8.32 (s, 1H), 7.68 (d, *J* = 8.4 Hz, 2H), 7.46 (d, *J* = 6.7 Hz, 2H), 7.43 – 7.39 (br d, *J* = 16.0, 1H), 7.18 (br s, 1H), 6.09 – 6.04 (m, 1H), 4.69 – 4.63 (m, 2H), 4.39 – 4.25 (m, 1H), 4.07 – 4.01 (m, 2H), 3.97 (dd, *J* = 7.7, 5.4 Hz, 1H), 3.89 – 3.82 (m, 1H), 3.74 – 3.63 (m, 1H), 2.40 – 2.35 (m, 1H), 2.27 – 2.20(m, 1H). ^{13}C NMR (101 MHz, CD_3OD) δ 170.0, 168.4, 162.5, 151.6, 148.3, 140.1, 139.3, 133.2, 127.9, 121.2, 117.96, 112.52, 90.6, 82.5, 72.5, 70.9, 50.2, 42.6, 27.9. HRMS (ESI): calculated for $C_{24}H_{27}N_8O_6$ $[M+H]^+$ 523.2054, found 523.2061.

tert-butyl (2*S*)-4-((((3a*R*,3a*R*,4*R*,6R,6a*R*,6a*R*)-6-(6-amino-9*H*-purin-9-yl)-2,2-dimethyltetra-hydrofuro[3,4-d][1,3]dioxol-4-yl)methyl)(3-(4-carbamoylphenyl)prop-2-yn-1-yl)amino)-2-((*tert*-butoxycarbonyl)amino)butanoate (31a). Following the procedure described for compound **16v**, compound **28a** was oxidized to afford protected intermediate compound **31a** as a white powder (109 mg, 82% yield). ^{1}H NMR (400 MHz, $CDCl_3$) δ 8.31 (s, 1H), 7.99 (s, 1H), 7.76 (d, *J* = 8.3 Hz, 2H), 7.38 (d, *J* = 8.2 Hz, 2H), 6.47 (s, 2H), 6.18 (s, 2H), 6.10 (s, 1H), 5.62 (d, *J* = 8.0 Hz, 1H), 5.51 (d, *J* = 5.7 Hz, 1H), 5.12 – 5.03 (m, 1H), 4.43 (s, 1H), 4.32 – 4.21 (m, 1H), 3.67 (s, 2H), 2.92 – 2.80 (m, 2H), 2.69 – 2.63 (m, 2H), 1.99 (d, *J* = 5.5 Hz, 1H), 1.87 – 1.82 (br m, 1H), 1.64 (s, 3H), 1.44 – 1.42 (br d, *J* = 8.0 Hz, 21H). ^{13}C NMR (101 MHz, $CDCl_3$) δ 171.8, 169.0, 155.6, 153.0, 149.2, 140.2, 132.7, 131.8, 127.4, 120.3, 114.5, 90.9, 86.8, 86.0, 83.0, 83.3, 55.7, 52.8, 50.7, 28.4, 28.0, 27.2, 25.50. HRMS (ESI): calculated for $C_{36}H_{51}N_8O_8$ $[M+H]^+$ 723.3830, found 723.3841

(*S*)-2-amino-4-((((2*R*,3*S*,4*R*,5*R*)-5-(6-amino-9*H*-purin-9-yl)-3,4-dihydroxytetrahydrofuran-2-yl)methyl)(3-(4-carbamoylphenyl)prop-2-yn-1-yl)amino)butanoic acid (31). Following the procedure described for compound **13a**, compound **31a** (50 mg, 0.074 mmol) was deprotected and purified, affording compound **31** as a white powder (34 mg, 80% yield). ^{1}H NMR (400 MHz, CD_3OD) δ 8.59 (s, 1H), 8.32 (s, 1H), 7.87 (d, *J* = 8.5 Hz, 2H), 7.53 (d, *J* = 8.4 Hz, 2H), 6.20 (d, *J* = 4.8 Hz, 1H), 4.79 (t, *J* = 4.8 Hz, 1H), 4.61 (dd, *J* = 7.9, 4.6 Hz, 1H), 4.50 (t, *J* = 4.9 Hz, 1H), 4.44 (s, 2H), 4.20 (dd, *J* = 8.1, 4.7 Hz, 1H), 3.85 – 3.68 (m, 2H), 3.67 – 3.53 (m, 2H), 2.57 – 2.48 (m, 1H), 2.35 – 2.22 (m, 1H). ^{13}C NMR (101 MHz, CD_3OD) δ 171.4, 169.9, 162.2, 161.8, 161.5, 161.1, 151.2, 148.3, 144.9, 148.3, 144.9, 143.0, 134.2, 127.5, 124.6, 121.0, 119.2, 118.1, 115.2, 112.3, 89.9, 88.4, 73.7, 72.2, 55.7,52.1, 51.8, 42.3, 25.3. HRMS (ESI): calculated for $C_{24}H_{28}N_8O_6$ $[M+H]^+$ 525.2210, found 525.2223.

Enzymatic activity assay: Expression and purification of full-length wild-type NNMT protein (NNMTwt) were performed as previously described.[30] The purity of the enzyme was confirmed

using sodium dodecyl sulfate-polyacrylamide gel electrophoresis (SDS-PAGE) with Coomassie blue staining, and NNMT identity was confirmed using SDS-PAGE and Western blotting. Catalytic activity of the recombinant protein was evaluated with 1 unit of enzyme activity representing the formation of 1 nmol of MNA/h of incubation. The specific activity of the batch used in the inhibitory activity assays was 18060 units/mg of protein at a protein concentration of 0.98 mg/mL. NNMT was used at a final concentration of 100 nM diluted in assay buffer (50 mM Tris buffer (pH 8.4) and 1 mM dithiothreitol final concentrations). The compounds were dissolved in DMSO and diluted with water to concentrations ranging from 1 nM to 500 μM (DMSO was kept constant at 1.25% final concentration). The compounds were screened for activity at fixed concentrations of 25 and 5 μM. When at least 50% inhibition was observed at 25 μM, full IC_{50} curves were generated. The compounds were incubated with the enzyme for 10 minutes at room temperature before initiating the reaction with a mixture of NA and SAM at their K_M concentrations of 400 μM and 8.5 μM, respectively. The formation of MNA was measured after 30 minutes at room temperature. The reaction was quenched by addition of 30 μL of the sample to 70 μL of acetonitrile containing 50 nM deuteromethylated nicotinamide (d_3-MNA) as internal standard. Sample analysis was performed using Multiple Reaction Monitoring (MRM) on an LC-MS system as previously described with minor modifications.[20] The LC-MS system consisted of a Shimadzu 8040 triple quadrupole mass spectrometer (ESI ionization). Isocratic elution was performed after 5 μL injections on a Waters Acquity BEH Amide HILIC column (3.0 × 100 mm, 1.7 μm particle size, Waters, Milford), using water containing 300 mM formic acid and 550 mM NH_4OH (pH 9.2) at 40% v/v and acetonitrile at 60% v/v, with a runtime of 1.7 min. Calibration samples were prepared using 70 μL of internal standard d_3-MNA at 50 nM in acetonitrile and 30 μL of an aqueous solution of reference standard MNA with concentrations ranging from 1 to 1024 nM. All compounds exhibiting an IC_{50} value below 500 nM were considered tight binding inhibitors and were retested using an enzyme concentration of 10 nM and a reaction time of 45 minutes.

Isothermal Titration Calorimetry: All binding experiments are performed using a MicroCal PEAQ-ITC Automated microcalorimeter (Malvern). The samples are equilibrated to 20°C prior to the measurement. The hNNMT enzyme (8.4 mg/mL in 50mM NaH_2PO_4, pH 8, 300mM NaCl, 200mM imidazole, 0.5mM DTT, 1mM PMSF, 20% glycerol) was diluted with 20 mM Tris HCl, pH 7.0 to reach a final concentration of 11.4 μM. Compound **17u** was diluted to a final concentration of 114 μM in 20 mM Tris HCl, pH 7.0 with the addition of enzyme buffer to avoid any buffer mismatch during titration. Compound **17u** (114μM) was titrated into hNNMT (11.4 μM). The titrations are conducted at 25 °C under constant stirring at 750 rpm. Each binding

experiment consisted of an initial injection of 0.4 μL followed by 18 separate injections of 2.0 μL into the sample cell of 200 μL. The time between each injection is 150 seconds, the measurements are performed with the reference power set at 10 μcal s^{-1} and the feedback mode set at 'high'. The calorimetric data obtained is analyzed using MicroCal PEAQ-ITC Analysis Software Version 1.20. ITC data fitting is made based on the "One set of sites" fitting model of the software. The best fit is defined by chi-square minimization. All thermodynamic parameters and thermograms are reported based on the measurements of three independent experiments.

Enzyme assays for selectivity: The PRMT4/CARM1 methyltransferase inhibition assay was performed as previously described[29] by using a commercially available chemiluminescent assay kit for PRMT4/CARM1 (purchased from BPS Bioscience). Compound **17u** was tested at concentrations of 3.7, 11.1, 33.3 and 100 μM and no inhibition was observed at the concentrations tested. The phenylethanolamine *N*-methyltransferase (PNMT) assay was developed using the Promega MTase-Glo™ Methyltransferase Assay (purchased from Promega Corporation, US). Compound **17u** was tested at concentrations of 1 and 10 μM and less than 50% inhibition was observed at the concentrations tested. Full details of the PNMT assay are provided below. All other methyltransferase assays are performed as previously described.[25]

PNMT selectivity assay: The phenylethanolamine N-methyltransferase (PNMT) assay was developed using the Promega MTase-Glo™ Methyltransferase Assay (Promega Corporation, US, #V7601). In the coupled luminescence-based assay, the enzymatic product SAH is converted into ADP and subsequently into light.[1] Human recombinant PNMT was purchased from ProSpec-Tany TechnoGene Ltd, Israel (#ENZ-457). After establishing the concentration of enzyme to use in the assay, the K_M values for cofactor SAM and substrate (+)-norepinephrine were determined. The measured K_M values were 2.6 μM for SAM and 5.9 μM for (+)-norepinephrine. The final conditions of the assay were set at 125 nM PNMT, 5 μM SAM, 10 μM (+)-norepinephrine and a reaction time of 45 minutes. The reactions were performed in half area, flat bottom, white 96 well plates (Greiner Bio-One #675074) with a final volume of the reaction mixture of 10 μL. Inhibitors (2 μL) were pre-incubated with the enzyme in the presence of substrate (4 μL) for 10 minutes before the methyltransferase reaction was initiated through addition of cofactor SAM (4 μL). After 45 minutes, the MTase Glo detection solution (10 μL) was added and incubated for 60 minutes followed by analysis of the luminescent signal in a plate reader. Compound **17u** was tested at 3.7, 11.1, 33.3 and 100 μM in duplicate.

The luminescence data were analysed using GraphPad Prism (version 8.4.3). The luminescence of the positive control (Lp) in each dataset was defined as 100% activity. This value was included in the IC_{50} graphs at a concentration of 1.5 log values below the lowest concentration tested. The luminescence data of the negative controls (Ln) in each dataset were subtracted from the obtained luminescence data. The percent activity in the presence of each inhibitor was calculated according to the following equation: % activity = (L – Ln)/(Lp – Ln), where L = the luminescence in the presence of the compound, Ln = the luminescence in the absence of the enzyme, and Lp = the luminescence in the absence of the inhibitor. The percent activity values were plotted as a function of inhibitor concentrations and fitted using non-linear regression analysis of the Sigmoidal dose–response curve generated using the equation Y=100/(1+10^((LogIC50-X)*HillSlope))). The IC_{50} value was determined by the concentration resulting in a half- maximal percent activity at 21.34 ± 1.28 μM.

Modelling: The structure of NNMT was taken from PDB entry 6PVE[27] and subsequently prepared using the Protein Preparation Wizard in Maestro (Schrodinger, version 2020-3). Compounds were aligned to the co-crystallized ligand using flexible ligand alignment in Maestro, based on their chemical similarity. The generated protein-ligand complexes were used as starting point for molecular dynamics (MD) simulations performed in the software package Q.[40] This software is tailored for different types of free energy calculations under spherical boundary conditions, and in particular we used the QligFEP utility as a free energy perturbation (FEP) protocol[41] for the generation of all input files and subsequent analysis. A 25 Å radius sphere was solvated, based on the center of geometry of the ligand. Protein atoms in the boundary of the sphere (22-25 Å outer shell) had a positional restraint of 20 kcal/mol/Å^2, while solvent atoms were subject to polarization and radial restrains using the surface constrained all-atom solvent (SCAAS)[42,43] model to mimic the properties of bulk water at the sphere surface. Atoms lying outside the simulation sphere are tightly constrained (200 kcal/mol/Å^2 force constant) and excluded from the calculation of non-bonded interactions. Long range electrostatics interactions beyond a 10 Å cut off were treated with the local reaction field method,[43] except for the atoms undergoing the FEP transformation where no cut-off was applied. Solvent bonds and angles were constrained using the SHAKE algorithm.[44] All titratable residues outside the sphere were neutralized and histidine protonation states were assigned by the Protein Preparation Wizard. The OPLS-AA/M force field [45] was adopted for protein and solvent (TIP3P model) parameters, while compatible OPLS2005 ligand parameters were generated using the ffld_server[46] and translated to Q format using QligFEP. The simulation sphere was warmed up from 0.1 to 298 K, during a first equilibration period of 0.61

nanoseconds, where an initial restraint of 25 kcal/mol/Å^2 imposed on all heavy atoms was slowly released for all complexes. Thereafter the system was subject to ten parallel replicates of unrestrained MD, starting in all cases with a 0.25 nanosecond unbiased equilibration period using randomized initial velocities. Thereafter the FEP protocol follows for every investigated ligand pair, which consists of 101 FEP λ-windows, where the coupling parameter λ is unevenly distributed using a sigmoidal function, each window sampled for 10 ps. In order to close a thermodynamic cycle and calculate relative binding free energies, for each ligand pair an analogous FEP transformation is run in parallel in a sphere of water. In these water simulations, the same parameters apply (i.e., sphere size, simulation time, etc.), and the relative binding free energy difference was estimated by solving the thermodynamic cycle utilizing the Bennett acceptance ratio (BAR).[47] The corresponding experimental values were extracted from the herein reported IC_{50} values for each ligand using equation 1:

$$\Delta\Delta G_{exp} = -RT \ln\left(\frac{IC50_{17s-v}}{IC50_{17x}}\right) \qquad \text{Equation (1)}$$

where R = 1.987x10^{-3} kcal/mol/K, and T = 298K.

Cell culture and treatment with compounds: HSC-2 human oral cancer cell line, T24 human bladder cancer cell line and A549 human lung cancer line were purchased from the American Type Culture Collection (ATCC, Rockville, MD, USA), and cultured in DMEM/F12 medium, supplemented with 10% fetal bovine serum and 50 μg/ml gentamicin, at 37 °C in a humidified 5% CO_2 incubator. Compound **17u** was dissolved in DMSO at 100mM concentration. This stock solution was then diluted in culture medium to final concentration values ranging between 1μM and 100μM. For each sample, DMSO was kept constant at 0.1% final concentration. The day before starting treatment, cells were seeded in 96-well plates, at a density of 2x10^3 cells/well. Cells were allowed to attach overnight and then incubated with compound **17u** at different final concentrations, or with DMSO only, for 24, 48 and 72 hours. All experiments were performed in triplicate. Cell proliferation was determined using a colorimetric assay with 3-(4,5-dimethylthiazol-2-yl)-2,5-diphenyl tetrazolium bromide (MTT). The MTT assay measures the conversion of MTT to insoluble formazan by dehydrogenase enzymes of the intact mitochondria of living cells. Cell proliferation was evaluated by measuring the conversion of the tetrazolium salt MTT to formazan crystals upon treatment with compound **17u** or DMSO only for 24, 48 and 72 hours. Briefly, cells were incubated for 2 hours at 37 °C with 100 μl fresh culture medium containing 5μl of MTT

reagent (5 mg/ml in PBS). The medium was removed and 200µl isopropanol were added. The amount of formazan crystals formed correlated directly with the number of viable cells. The reaction product was quantified by measuring the absorbance at 540nm using an ELISA plate reader. Experiments were repeated three times. Results were expressed as percentage of the control (control equals 100% and corresponds to the absorbance value of each sample at time zero) and presented as mean values ± standard deviation of three independent experiments performed in triplicate. Data were analysed using GraphPad Prism (GraphPad Software, San Diego, CA). Significant differences between groups were determined using the one-way analysis of variance (ANOVA). A p-value <0.05 was considered statistically significant.

Parallel Artificial Membrane Permeability Assay

The PAMPA assay was carried out with a Corning® BioCoat™ Pre-coated PAMPA Plate System (cat. 353015). The stock solutions were prepared at 10 mM concentration in DMSO and diluted with PBS to achieve a final sample concentration of 200 µM (2% DMSO (v/v)). The bottom plate (donor) was filled with 300 µL of diluted sample solution, while the top plate (acceptor, containing the synthetic phospholipid membrane) was filled with 200 µL of PBS. The acceptor plate was then placed on the donor plate and the system incubated for 5 h at 25 ˚C. The plate sandwich was separated, and the concentrations of samples in both the donor and acceptor compartments were evaluated by means of UV spectrometry using a Tecan plate reader set at 280 nM.

References

1. Aksoy S, Szumlanski CL, Weinshilboum RM. Human liver nicotinamide N-methyltransferase. cDNA cloning, expression, and biochemical characterization. J Biol Chem. 1994;269(20):14835-40. http://www.ncbi.nlm.nih.gov/pubmed/8182091
2. van Haren MJ, Sastre Toraño J, Sartini D, Emanuelli M, Parsons RB, Martin NI. A Rapid and Efficient Assay for the Characterization of Substrates and Inhibitors of Nicotinamide N -Methyltransferase. Biochemistry. 2016;55(37):5307-15.
3. Pissios P. Nicotinamide N-Methyltransferase: More Than a Vitamin B3 Clearance Enzyme. Trends Endocrinol Metab. 2017;28(5):340-53.
4. Alston TA, Abeles RH. Substrate specificity of nicotinamide methyltransferase isolated from porcine liver. Arch Biochem Biophys. 1988;260(2):601-8.
5. Kraus D, Yang Q, Kong D, Banks AS, Zhang L, Rodgers JT, et al. Nicotinamide N-methyltransferase knockdown protects against diet-induced obesity. Nature. 2014;508(7495):258-62.
6. Ulanovskaya OA, Zuhl AM, Cravatt BF. NNMT promotes epigenetic remodeling in cancer by creating a metabolic methylation sink. Nat Chem Biol. 2013;9(5):300-6.
7. Sperber H, Mathieu J, Wang Y, Ferreccio A, Hesson J, Xu Z, et al. The metabolome regulates the epigenetic landscape during naive-to-primed human embryonic stem cell transition. Nat Cell Biol. 2015;17(12):1523-35.
8. You Z, Liu Y, Liu X. Nicotinamide N-methyltransferase enhances the progression of prostate cancer by stabilizing sirtuin 1. Oncol Lett. 2018;15(6):9195-201.
9. Xie X, Yu H, Wang Y, Zhou Y, Li G, Ruan Z, et al. Nicotinamide N-methyltransferase enhances the capacity of tumorigenesis associated with the promotion of cell cycle progression in human colorectal cancer cells. Arch Biochem Biophys. 2014;564:52-66.
10. Eckert MA, Coscia F, Chryplewicz A, Chang JW, Hernandez KM, Pan S, et al. Proteomics reveals NNMT as a master metabolic regulator of cancer-associated fibroblasts. Nature. 2019;569(7758):723-8.
11. Sartini D, Morganti S, Guidi E, Rubini C, Zizzi A, Giuliante R, et al. Nicotinamide N-methyltransferase in Non-small Cell Lung Cancer: Promising Results for Targeted Anti-cancer Therapy. Cell Biochem Biophys. 2013;67(3):865-73.
12. Tomida M, Ohtake H, Yokota T, Kobayashi Y, Kurosumi M. Stat3 up-regulates expression of nicotinamide N-methyltransferase in human cancer cells. J Cancer Res Clin Oncol. 2008;134(5):551-9.
13. Brachs S, Polack J, Brachs M, Jahn-Hofmann K, Elvert R, Pfenninger A, et al. Genetic

Nicotinamide N-Methyltransferase (Nnmt) Deficiency in Male Mice Improves Insulin Sensitivity in Diet-Induced Obesity but Does Not Affect Glucose Tolerance. Diabetes. 2019;68(3):527-42.

14. Liu M, Li L, Chu J, Zhu B, Zhang Q, Yin X, et al. Serum N1-methylnicotinamide is associated with obesity and diabetes in Chinese. J Clin Endocrinol Metab. 2015;100(8):3112-7.
15. Parsons RB, Smith M-L, Williams AC, Waring RH, Ramsden DB. Expression of Nicotinamide N-Methyltransferase (E.C. 2.1.1.1) in the Parkinsonian Brain. J Neuropathol Exp Neurol. 2002;61(2):111-24.
16. Thomas MG, Saldanha M, Mistry RJ, Dexter DT, Ramsden DB, Parsons RB. Nicotinamide N-methyltransferase expression in SH-SY5Y neuroblastoma and N27 mesencephalic neurones induces changes in cell morphology via ephrin-B2 and Akt signalling. Cell Death Dis. 2013;4(6):e669-e669.
17. van Haren MJ, Thomas MG, Sartini D, Barlow DJ, Ramsden DB, Emanuelli M, et al. The kinetic analysis of the N-methylation of 4-phenylpyridine by nicotinamide N-methyltransferase: Evidence for a novel mechanism of substrate inhibition. Int J Biochem Cell Biol. 2018;98(March):127-36.
18. Kocinaj A, Chaudhury T, Uddin MS, Junaid RR, Ramsden DB, Hondhamuni G, et al. High Expression of Nicotinamide N-Methyltransferase in Patients with Sporadic Alzheimer's Disease. Mol Neurobiol. 2021;58(4):1769-81.
19. van Haren MJ, Taig R, Kuppens J, Sastre Toraño J, Moret EE, Parsons RB, et al. Inhibitors of nicotinamide N-methyltransferase designed to mimic the methylation reaction transition state. Org Biomol Chem. 2017;15(31):6656-67.
20. Gao Y, van Haren MJ, Moret EE, Rood JJM, Sartini D, Salvucci A, et al. Bisubstrate Inhibitors of Nicotinamide N -Methyltransferase (NNMT) with Enhanced Activity. J Med Chem. 2019;62(14):6597-614.
21. Neelakantan H, Wang HY, Vance V, Hommel JD, McHardy SF, Watowich SJ. Structure-Activity Relationship for Small Molecule Inhibitors of Nicotinamide N-Methyltransferase. J Med Chem. 2017;60(12):5015-28.
22. Kannt A, Rajagopal S, Kadnur SV, Suresh J, Bhamidipati RK, Swaminathan S, et al. A small molecule inhibitor of Nicotinamide N-methyltransferase for the treatment of metabolic disorders. Sci Rep. 2018;8(1):3660.
23. Lee H-Y, Suciu RM, Horning BD, Vinogradova E V., Ulanovskaya OA, Cravatt BF. Covalent inhibitors of nicotinamide N-methyltransferase (NNMT) provide evidence for target engagement challenges in situ. Bioorg Med Chem Lett. 2018;28(16):2682-7.

24. Bach D-H, Kim D, Bae SY, Kim WK, Hong J-Y, Lee H-J, et al. Targeting Nicotinamide N-Methyltransferase and miR-449a in EGFR-TKI-Resistant Non-Small-Cell Lung Cancer Cells. Mol Ther - Nucleic Acids. 2018;11(June):455-67.
25. Babault N, Allali-Hassani A, Li F, Fan J, Yue A, Ju K, et al. Discovery of Bisubstrate Inhibitors of Nicotinamide N-Methyltransferase (NNMT). J Med Chem. 2018;61(4):1541-51.
26. Policarpo RL, Decultot L, May E, Kuzmič P, Carlson S, Huang D, et al. High-Affinity Alkynyl Bisubstrate Inhibitors of Nicotinamide N-Methyltransferase (NNMT). J Med Chem. 2019;62(21):9837-73.
27. Chen D, Li L, Diaz K, Iyamu ID, Yadav R, Noinaj N, et al. Novel Propargyl-Linked Bisubstrate Analogues as Tight-Binding Inhibitors for Nicotinamide N -Methyltransferase. J Med Chem. 2019;62(23):10783-97.
28. Van Haren M, Van Ufford LQ, Moret EE, Martin NI. Synthesis and evaluation of protein arginine N-methyltransferase inhibitors designed to simultaneously occupy both substrate binding sites. Org Biomol Chem. 2015;13(2).
29. van Haren MJ, Marechal N, Troffer-Charlier N, Cianciulli A, Sbardella G, Cavarelli J, et al. Transition state mimics are valuable mechanistic probes for structural studies with the arginine methyltransferase CARM1. Proc Natl Acad Sci. 2017;114(14):3625-30.
30. Peng Y, Sartini D, Pozzi V, Wilk D, Emanuelli M, Yee VC. Structural Basis of Substrate Recognition in Human Nicotinamide N -Methyltransferase. Biochemistry. 2011;50(36):7800-8.
31. Yang J, Copeland RA, Lai Z. Defining balanced conditions for inhibitor screening assays that target bisubstrate enzymes. J Biomol Screen. 2009;14(2):111-20.
32. Copeland RA. Enzymes. A Practical Introduction to Structure, Mechanism, and Data Analysis, Second ed. Anal Biochem. 2001;291(1):172.
33. Brooun A, Gajiwala KS, Deng Y-L, Liu W, Bolaños B, Bingham P, et al. Polycomb repressive complex 2 structure with inhibitor reveals a mechanism of activation and drug resistance. Nat Commun. 2016;7(1):11384.
34. Kai K, Fujii H, Ikenaka R, Akagawa M, Hayashi H. An acyl-SAM analog as an affinity ligand for identifying quorum sensing signal synthases. Chem Commun. 2014;50(62):8586-9.
35. Hernández JN, Ramírez MA, Martín VS. A new selective cleavage of N,N-dicarbamoyl-protected amines using lithium bromide. J Org Chem. 2003;68(3):743-6.
36. Evans CG, Smith MC, Carolan JP, Gestwicki JE. Improved synthesis of 15-deoxyspergualin analogs using the Ugi multi-component reaction. In: Bioorganic and Medicinal Chemistry

Letters. Vol 21. ; 2011:2587-90.

37. Mennie KM, Banik SM, Reichert EC, Jacobsen EN. Catalytic Diastereo- and Enantioselective Fluoroamination of Alkenes. J Am Chem Soc. 2018;140(14):4797-802.
38. Thompson MJ, Mekhalfia A, Jakeman DL, Phillips SEV, Phillips K, Porter J, et al. Homochiral synthesis of an aza analogue of S-adenosyl-L-methionine (AdoMet) and its binding to the E. coli methionine repressor protein (MetJ). Chem Commun. 1996;(6):791-2.
39. Joce C, Caryl J, Stockley PG, Warriner S, Nelson A. Identification of stable S-adenosylmethionine (SAM) analogues derivatised with bioorthogonal tags: Effect of ligands on the affinity of the E. coli methionine repressor, MetJ, for its operator DNA. Org Biomol Chem. 2009;7(4):635-8.
40. Marelius J, Kolmodin K, Feierberg I, Åqvist J. Q: A molecular dynamics program for free energy calculations and empirical valence bond simulations in biomolecular systems. J Mol Graph Model. 1998;16(4-6):213-25.
41. Jespers W, Esguerra M, Åqvist J, Gutiérrez-de-Terán H. QligFEP: an automated workflow for small molecule free energy calculations in Q. J Cheminform. 2019;11(1):26.
42. King G, Warshel A. A surface constrained all-atom solvent model for effective simulations of polar solutions. J Chem Phys. 1989;91(6):3647-61.
43. Lee FS, Warshel A. A local reaction field method for fast evaluation of long-range electrostatic interactions in molecular simulations. J Chem Phys. 1992;97(5):3100-7.
44. Ryckaert J-P, Ciccotti G, Berendsen HJC. Numerical integration of the cartesian equations of motion of a system with constraints: molecular dynamics of n-alkanes. J Comput Phys. 1977;23(3):327-41.
45. Robertson MJ, Tirado-Rives J, Jorgensen WL. Improved Peptide and Protein Torsional Energetics with the OPLS-AA Force Field. J Chem Theory Comput. 2015;11(7):3499-509.
46. Banks JL, Beard HS, Cao Y, Cho AE, Damm W, Farid R, et al. Integrated Modeling Program, Applied Chemical Theory (IMPACT). J Comput Chem. 2005;26(16):1752-80.
47. Bennett CH. Efficient estimation of free energy differences from Monte Carlo data. J Comput Phys. 1976;22(2):245-68.

Chapter 4

Esterase-sensitive prodrug forms of a potent NNMT inhibitor translate its biochemical potency into cellular activity

Manuscript under review

Abstract

A recently discovered NNMT inhibitor with single digit nanomolar IC_{50} values (compound **17u** from **Chapter 3**) was found to be highly potent in biochemical assays but lacking in cellular activity. In order to translate the observed potent inhibitory activity into strong cellular activity, a prodrug strategy was investigated. This prodrug strategy focused on the temporary protection of the amine and carboxylic acid moieties of the highly polar amino acid side chain present in bisubstrate inhibitor **17u**. The modification of the carboxylic acid into a range of esters in the absence or presence of a trimethyllock (TML) protecting group at the amine group yielded a range of candidate prodrugs. Based on stability in buffers combined with conformed esterase-dependent conversion to the parent compound, the isopropyl ester was selected as the preferred acid prodrug. The isopropyl ester and isopropyl ester-TML prodrugs demonstrated improved cell permeability, which importantly also translated into significantly enhanced cellular activity in assays designed to measure the enzymatic activity of NNMT in live cells.

1. Introduction

Nicotinamide *N*-methyltransferase (NNMT) is a small molecule methyltransferase enzyme responsible for the conversion of nicotinamide (NA, vitamin b3) to 1-methylnicotinamide (MNA). NNMT utilizes the cofactor *S*-adenosyl-L-methionine (SAM) as a methyl donor, which is converted to *S*-adenosyl-L-homocysteine (SAH) upon methylation of nicotinamide.[1] Under normal physiological conditions, NNMT is mainly expressed in the liver and in adipose tissue.[2] One of the primary roles of NNMT is the detoxification of xenobiotics. This function is achieved through NNMT's broad substrate recognition that allows for the methylation of different metabolites, including pyridines, quinolines, and other related heterocyclic aromatics.[3]

The overexpression of NNMT has been described in a wide variety of tissues and diseases, generally with detrimental effects. Elevated NNMT activity in cancer has been correlated with tumour aggressiveness and is proposed to promote migration, invasion, proliferation, leading to its potential a biomarker predictive of worsened clinical outcomes.[4–11] The overexpression of NNMT has been shown to cause depletion of the cellular pool of SAM, distorting the SAM/SAH balance, subsequently leading to a hypomethylated state with downstream effects on gene expression beneficial for tumour growth and metastasis.[12] This process is supported by recent proteomics-based research revealing NNMT to be the master regulator of the differentiation of cancer-associated fibroblasts (CAFs).[13] In another recent investigation upregulated MNA levels in the tumour microenvironment were found to lead to the inhibition of T-cell functions resulting in their deregulated killing capacity and increased tumour growth.[14]

Potent, selective, and cell-active NNMT inhibitors are valuable tools to probe the complex regulatory functions mediated by NNMT and to also investigate a number of different pharmacological hypotheses that suggest NNMT as a therapeutic target. Although the increase in reports describing the roles of NNMT in disease have led to an increase in the development of inhibitors of NNMT, to date very few cell-active inhibitors have been described. In this regard, the bisubstrate inhibitors of NNMT pioneered by our group and others exhibit very potent enzyme inhibition in biochemical assays but due to the polar nature of their structures, show only limited cellular activity.[15–19] Recent work in our group yielded compound **17u** (see **Chapter 3**), which showed an IC_{50} value of 3.7 nM and was found to be more potent than similar bisubstrate inhibitors reported by other groups. However, when tested against a range of human cancer cell lines, compound **17u** only showed significant antiproliferative effects at the high concentration tested of 100 μM, more than four orders of magnitude higher than the concentration needed for enzyme inhibition in the biochemical assay. The absence of cellular activity of compound **17u** is presumably due to the compound's poor cell permeability which is most likely caused by the presence of two

highly polar functional groups that are present in all of the potent bisubstrate inhibitors of NNMT; the carboxylic acid and amine moieties of the amino acid sidechain. Notably, previous structure activity relationship studies of the bisubstrate inhibitors revealed that both the carboxylic acid and amine moieties of the amino acid sidechain are required for potent inhibitory activity and attempts at replacing them with less polar bio-isosteres in all cases resulted in a significant loss of potency.

Therefore, a prodrug strategy was applied to the structure of compound **17u** with the aim of improving its cellular activity (Figure 1A). The carboxylic acid moiety was converted into a variety of esters, which can be cleaved by cellular esterases. In the case of the amino group a different prodrug strategy was applied. The derivatization of amines to give amides has not been widely used as a prodrug strategy due to the high chemical stability of amide linkages[20,21] and the lack of amidase enzymes necessary for hydrolysis[22]. To circumvent these problems, the trimethyl-lock (TML) moiety[23] was selected for the prodrug form of the amine (Figure 1B). After esterase-mediated hydrolysis of the acetyl group, the liberated hydroxyl group of the TML moiety spontaneously cyclizes to form the corresponding lactone ring, with concomitant release of the free amine. Using these strategies, a series of prodrugs were prepared in which either one, or both, of the ester and TML-groups were incorporated.

To investigate the most suitable prodrug form of compound **17u**, the different ester and TML modified analogues were evaluated for their hydrolytic stability in buffer after which the most stable prodrugs were evaluated for the esterase-mediated release of the parent compound. After confirming the esterase mediated conversion to the active compound, the prodrugs were evaluated for cellular activity in a range of cellular assays and compared to the activity of the parent compound.

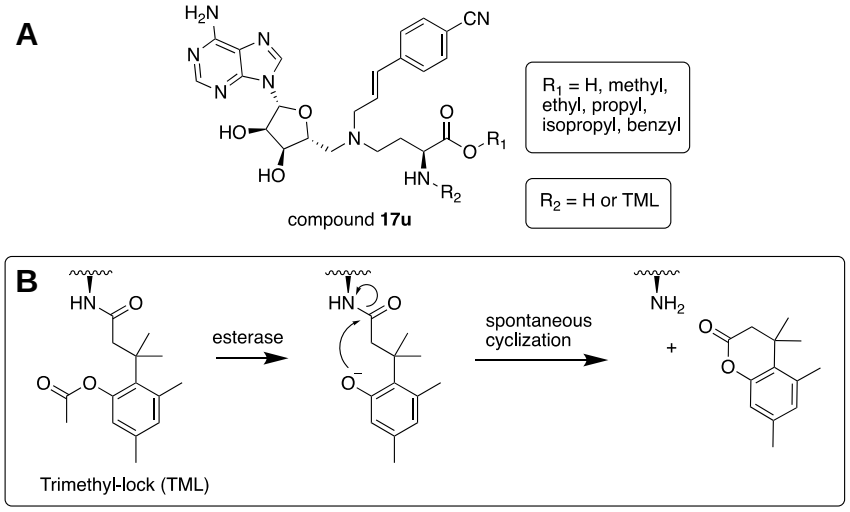

Figure 1. A) Prodrug strategy of compound **17u**. The carboxylic acid can be masked as an ester and the amine can be masked as an amide using the esterase-sensitive trimethyl-lock (TML). **B)** The mechanism of the trimethyl-lock cleavage. Deacetylation by esterases results in subsequent spontaneous lactonization releasing the free amine.

2. Results and Discussion

The prodrugs of parent compound **17u** were prepared following the syntheses depicted in Scheme 1 and 2. This synthetic route was developed during the investigation of structure activity relationships of **17u** and allows for the convenient modification of different parts of the molecule. The ester building blocks were synthesised (Scheme 1) starting from the Boc-Asp(Bn)-OH **1** which is esterified with the appropriate iodides in the presence of potassium carbonate as base to produce compounds **2b-e**, followed by the deprotection of the benzyl protecting group to obtain compounds **3b-e**. Compounds **3a** and **3f** were commercially available. Free carboxylic acids **3a-f** were then first converted into Weinreb amides **4a-f** using BOP-coupling conditions and subsequently reduced to the corresponding aldehyde (**5b-f**) with DIBAL-H. Compound **4a** followed a different route to produce TML-prodrug **8a** which contains the free carboxylic acid. In order to do so, the Boc group was selectively deprotected using HCl in dioxanes to produce free amine **6a**. The free amine can then be coupled to the trimethyllock acid[24] **7** with BOP and triethylamine to yield Weinreb amide intermediate **8a** followed by DIBAL reduction to form aldehyde **9a**.

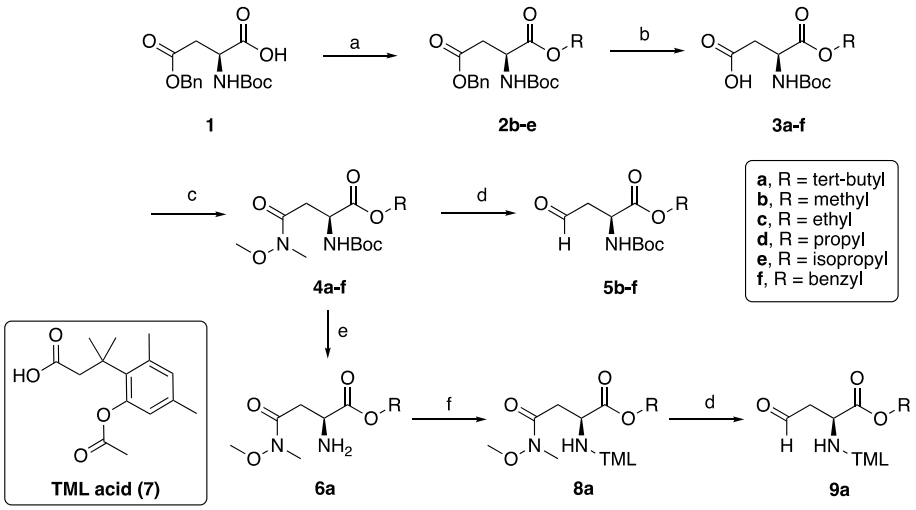

Scheme 1. Synthesis of the prodrug forms of the amino acid building blocks. Reagents and conditions: (a) RI, DMF, K_2CO_3, rt, overnight (65–79%); (b) 10% Pd/C, MeOH, overnight (82–90%); (c) CH_3NHOCH_3·HCl, BOP, Et_3N, CH_2Cl_2, rt, 2 h (77–83%); (d) DIBAL-H (1 M in hexanes), THF, −78 °C, assumed quant; (e) HCl (4N in dioxanes), 0°C to rt, 2.25 h; (f) TML acid **7**, BOP, Et_3N, CH_2Cl_2, rt, overnight, 88% over 2 steps.

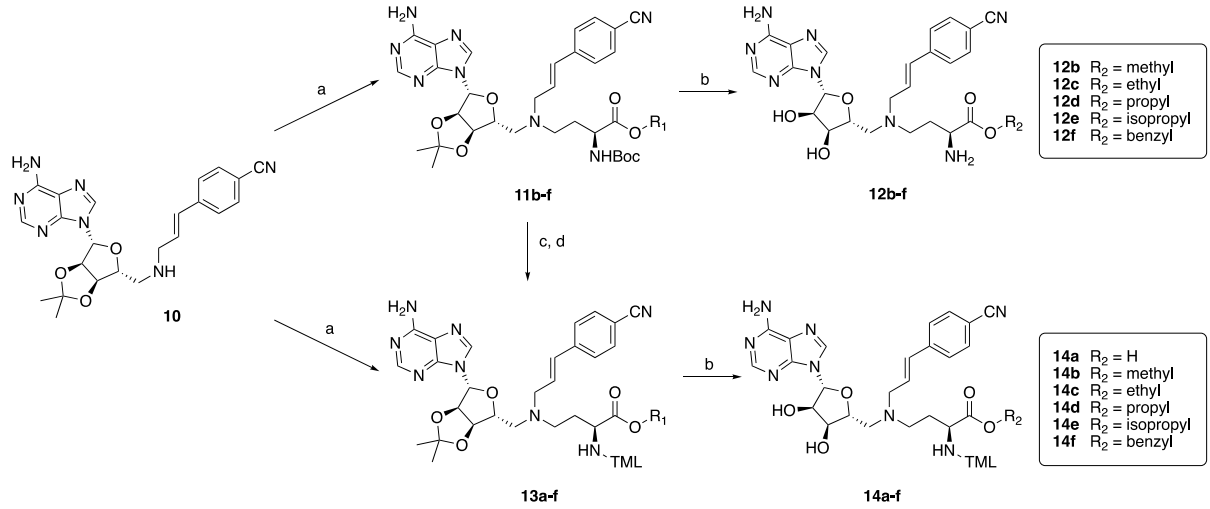

Scheme 2. Synthesis of prodrugs **12b-f** and **14a-f**. Reagents and conditions: (a) aldehydes **5b-f** or **9a**, $NaBH(OAc)_3$, AcOH, DCE, rt, overnight (34–73%); (b) TFA, CH_2Cl_2, H_2O, rt, 2h (70–93%); (c) TFA, CH_2Cl_2, rt, 2h; (d) TML acid **7**, BOP, Et_3N, CH_2Cl_2, rt, 2h (77–83%);

The aldehydes were subsequently coupled to intermediate **10** using reductive amination conditions forming intermediates **11b-f**, which can be deprotected to form ester prodrugs **12b-f (Scheme 2)**. Compounds **11b-f** can alternatively be selectively Boc-deprotected using TFA/DCM to form intermediates **13b-f** and subsequently coupled to trimethyllock acid **7** with BOP and triethylamine. Compound **13a** was synthesized through coupling of aldehyde **9a** with compound **10**. The intermediates were then deprotected under acidic conditions to yield ester-TML dual prodrugs **14a-f**. Initially, the prodrugs were tested for their residual activity in the enzymatic activity assay. However, several prodrugs unexpectedly showed significant inhibition at fixed concentrations of 5 and 25 μM. In order to evaluate the validity of these results, the prodrugs were subsequently evaluated for their hydrolytic stability in both PBS buffer at pH 7.4 and Tris buffer at pH 8.4. Both these buffers and pHs have been used in the different biochemical and cellular assays described in this report. Compounds were dissolved in DMSO at a concentration of 40 mM and diluted with the respective buffer to a final concentration of 1 mM. Compounds were tested directly (t_0) and subsequently every 2 hours over a time period of 16 hours by HPLC. The formation of the parent compound was evaluated and normalized by measuring the peak area at 214 nm and comparing it to the initial timepoint. The results presented in Table 1 below show significant hydrolysis over time for most of the ester prodrugs. Only the isopropyl ester seems to be stable under these conditions. Interestingly, the stability of the prodrugs increased significantly in the presence of the trimethyllock (TML) moiety at the amine position. Even for the rather labile methyl ester **12b**, the TML group in **14b** results in a decrease in hydrolysis of the methyl ester. Benzyl ester

8f was found to be the least stable and due to its poor aqueous solubility, the benzyl ester-TML dual prodrug **14f** was not evaluated further.

Table 1. Stability data of the prodrugs in Tris buffer at pH 8.4 and in PBS buffer at pH 7.4. The values indicate the percentage of compound peak area present after 16 hours of incubation at room temperature.

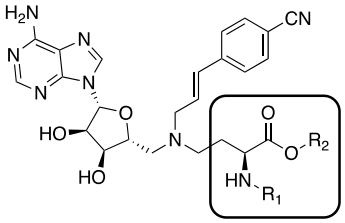

compound	Ester R_2 (R_1=H)	Tris	PBS
17u	H	n.a.	n.a.
12b	Methyl	22.59	36.97
12c	Ethyl	54.84	68.36
12d	Propyl	61.32	71.96
12e	Isopropyl	93.70	98.59
12f	Benzyl	21.60	33.43

compound	Ester R_2 (R_1=TML)	Tris	PBS
14a	H	93.97	99.10
14b	Methyl	73.88	88.08
14c	Ethyl	87.00	90.44
14d	Propyl	87.52	90.30
14e	Isopropyl	87.69	91.13
14f	Benzyl	n.d.	n.d.

n.a. not applicable; n.d. not determined

The most stable esters were found to be the isopropyl ester (compound **12e**), the trimethyllock (compound **14a**) and the isopropyl-trimethyllock dual prodrug (compound **14e**). However, as compound **14a** was not found to improve the cellular activity of the parent compound (discussed below), this compound was not evaluated further. The next step was to establish whether compounds **12e** and **14e** can be converted to the parent compound in the presence of an esterase. Using commercially available pig liver esterase (PLE), both compounds were shown to be readily converted to the parent compound as measured by HPLC (Figure 2). Within 4 hours the prodrugs were fully converted to the parent compound, while no hydrolysis was observed in the absence of PLE. Of note is the sequential conversion of dual prodrug **14e** in which the TML is hydrolysed first followed by the isopropyl ester. No trace of compound **14a** could be observed in which the ester is cleaved and the TML is still in place. This finding suggests that the TML group hinders the esterase-mediated hydrolysis of the isopropyl ester moiety and only after deacetylation of the TML moiety followed by its spontaneous loss, can the ester moiety be cleaved by the esterase.

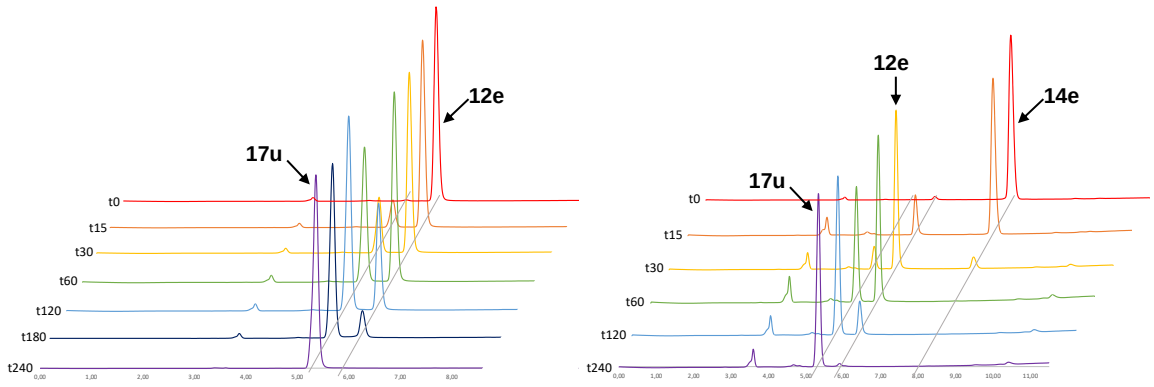

Figure 2. Esterase-mediated hydrolysis of isopropyl ester prodrug **12e** (left) and isopropyl-TML dual prodrug **14e** (right). The data shows clean conversion of the prodrugs to the parent compound **17u**. For the dual prodrug **14e**, conversion of the TML happens first followed by the hydrolysis of the isopropyl ester moiety.

The prodrugs shown in Table 1 were also subjected to a variety of cellular assays to screen for the most suitable prodrug form of compound **17u**. Initially, the prodrugs were tested in an MTT assay to evaluate their effect on cell viability against three different cancer cell lines: HSC-2 (oral cancer), T24 (bladder cancer), and A549 (lung cancer) (Figure 3). The results of these assays did not show an appreciable effect for ester prodrugs **12b-f** or TML prodrug **14a** compared to parent compound **17u**. Selected dual prodrugs **14b** and **14c** did show some activity, but only against HSC-2 cells, which overall seemed to be the more sensitive cell-line towards NNMT inhibition compared to the T24 and A549 cell lines. By comparison, when tested at the highest concentration evaluated (100 μM) compound **14e** did cause reduction of cell viability in a time dependent manner.

Compound **14e** was then tested in a neon electroporation assay in which the cell membrane is made highly permeable by energy pulses without killing the cells. With this technique, the effect of poorly cell permeable compounds can be evaluated. As control measurements, cells were either treated with DMSO alone, were not electroporated, or were treated with the parent compound **17u**. The results depicted in the bar graph in Figure 4 indicate an effect of the treatment of compounds **17u** and **14e** on the cell viability of the electroporated A549 cells. Again, however, the effects on cell viability were only found at a concentration of 100μM, more than 10,000 times higher than the activity of the parent compound in biochemical assays (IC_{50} = 3.7 nM).

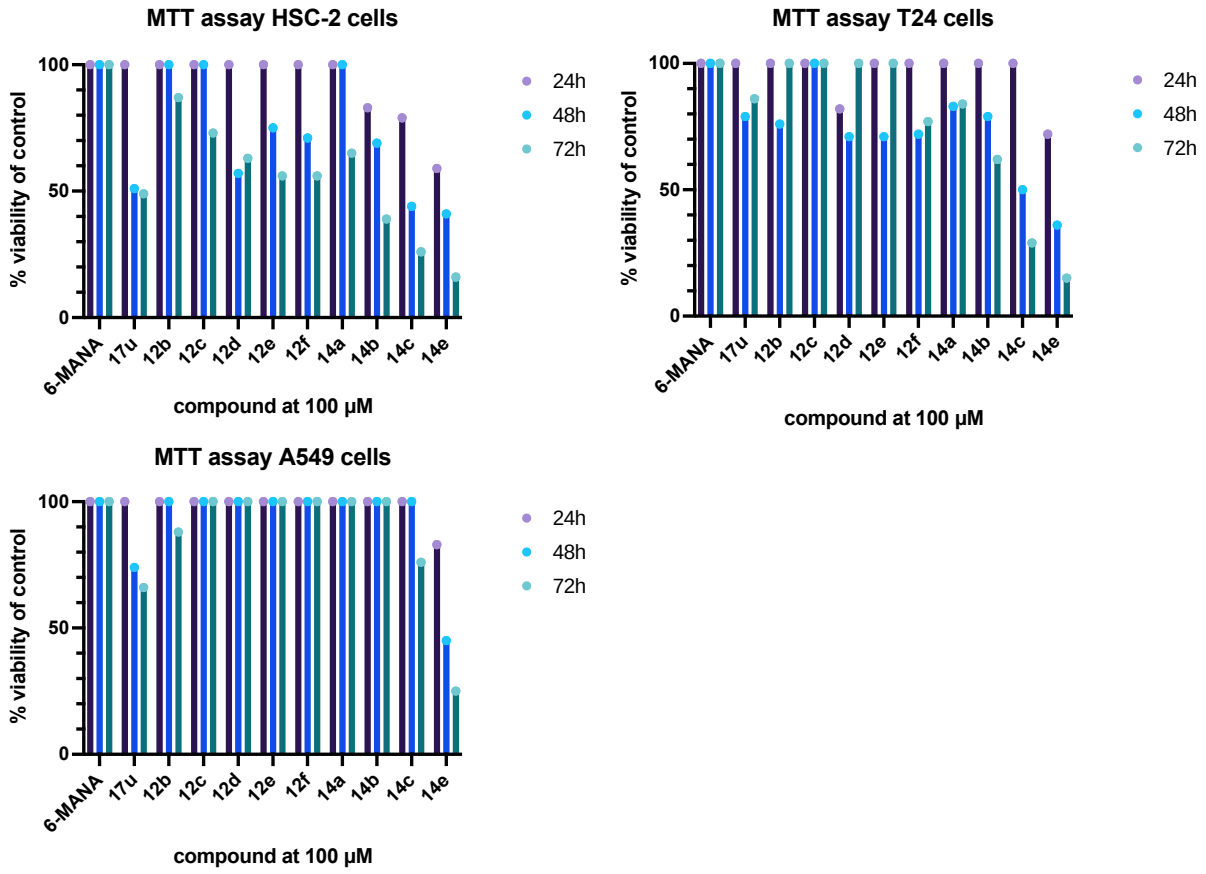

Figure 3. MTT cell viability data presented as percentage of DMSO control in three different cancer cell lines tested with 100µM compound after 24, 48 and 72 hours of incubation. Experiments were performed in triplicate.

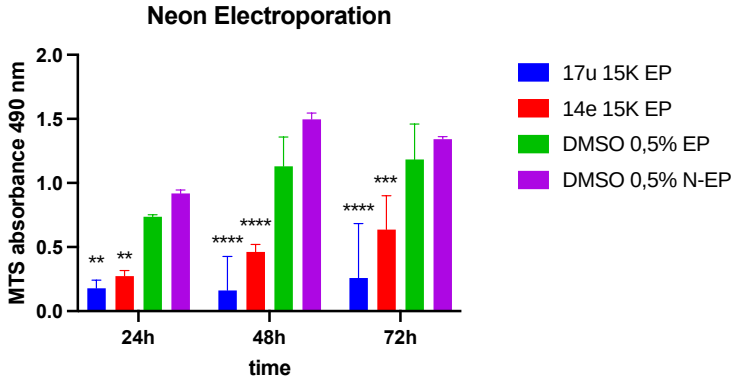

Figure 4. Effect of compounds **17u** and **14e** on the cell viability of A549 cells after neon electroporation. Absorbance of the water-soluble formazan product was measured at 490 nm using the MTS cell viability assay. The cell viability after treatment with compounds **17u** (blue) and **14e** (red) are significantly lower than the DMSO control (green) and non-electroporated DMSO control (purple).

The findings from both the conventional MTT and neon electroporation assays reveal that the prodrug inhibitors have little effect on cell viability unless tested at very high concentrations. One explanation for these finding may be that prodrugs are not effectively entering the cells. An alternative explanation could be that the compounds do enter the cells but that NNMT inhibition is simply not inherently toxic to these cells. If this is the case, the impact on cell viability observed when applying the compounds at the highest concentration tested (100 μM) could instead by ascribed to a non-specific toxic effect.

To investigate the cellular activity of the prodrugs in a more direct manner, compounds **12b-f** and **14a-e** were screened in a cellular MNA assay and compared to parent compound **17u** at a fixed concentration of 10 μM (Figure 5). In this assay the levels of MNA produced by an immortalized human microvascular endothelial cell line (HMEC-1) are quantified using a sensitive LC-MS assay. The results of the treatment of HMEC-1 cells with the different prodrugs show significant improvement of cellular activity over the parent compound for all prodrugs tested except for TML prodrug **14a**. These results indicate that masking the carboxylic acid is more important to promote cell permeability than masking the amine functionality. Of note is the comparable efficacy compared to reference compound 6-methylamino-nicotinamide (6-MANA), for which *in vivo* effects have been previously demonstrated[25], and the absence of any effect for 5-amino-1-methylquinolium (5-MQ), another reference compound used in cellular assays[26].

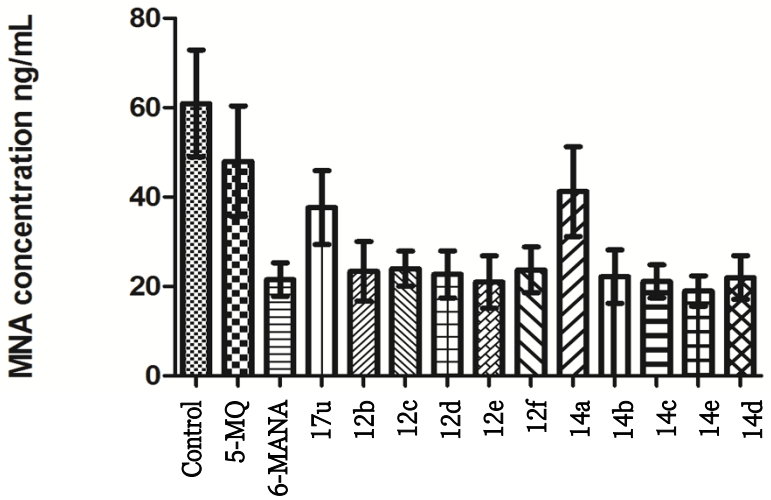

Figure 5. MNA concentrations in endothelial HMEC-1 cells after 24-hour incubation with 10 μM of compounds 5-amino-methylquinolinum (5-MQ), 6-methylamino-nicotinamide (6-MANA), compound **17u** or prodrug compounds **12b-f** and **14a-e**.

From this data, the best prodrugs in terms of stability and potency are compounds **12e** and **14e**, corresponding to the isopropyl ester prodrugs with and without the TML group on the amine. The study was therefore continued focusing on compounds **12e** and **14e**, which were further evaluated for their effect on cellular levels of MNA in a dose-dependent manner. The results presented in Figure 6 demonstrate that parent compound **17u** and reference compound 6-MANA require higher concentrations to substantially decrease the levels of MNA in A549 lung cancer cells. In contract, when the isopropyl ester **12e** was tested, a clear and significant decrease in MNA levels were observed. This effect is even further enhanced by the introduction of the TML moiety as present in compound **14e**. These findings indicate that the prodrug strategy here applied was able to convert a potent, but non-permeable inhibitor, into a compound with cellular activity. Notably, our findings also seem to suggest that the capacity for a small molecule to inhibit NNMT in cells does not *per se* lead to an impact on cell viability. This is in keeping with recent reports showing that the addition of NNMT inhibitors to cancer associated fibroblasts do not kill the cells but rather cause a reversion of cell morphology to one that more-closely resembles normal fibroblasts.[13]

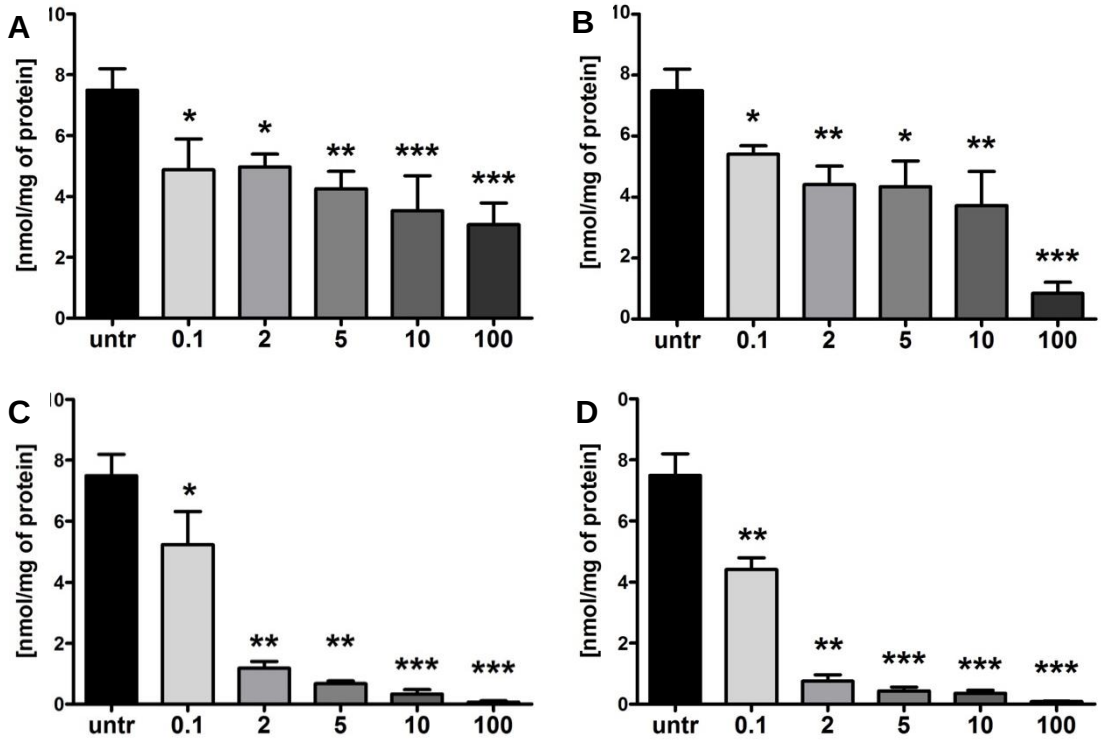

Figure 6. Concentration of MNA in A549 cells after 24-hour treatment with compounds 6-MANA (**A**), **17u** (**B**), **12e** (**C**) and **14e** (**D**).

3. Conclusion

In this report we describe a prodrug strategy to translate the potent activity of lead compound **17u** found in biochemical assays into cellular activity. The prodrug strategy focussed specifically on the amino acid functionality of the bisubstrate inhibitor. The carboxylic acid was masked as an ester using a variety of alkyl and benzyl groups and the amine was masked using the trimethyl-lock technology, in which the amine is masked as an amide, but can be released by an esterase. The different combination of prodrugs led to the selection of the isopropyl ester and the isopropyl ester/TML dual prodrug as the compounds with the most promising profile in terms of stability and cellular activity. The prodrugs were found to have little impact on cell viability. However, when evaluated in an assay allowing for the direct quantification of cellular MNA production, a clear dose-dependent effect was observed. The data presented here demonstrate the suitability of a prodrug strategy for the delivery of polar NNMT inhibitors into cells. Ongoing research is focussing on the effect of NNMT inhibition in a range of cell systems covering oncology as well as metabolic disorders.

4. Experimental procedures

All reagents employed were of American Chemical Society grade or finer and were used without further purification unless otherwise stated. For compound characterization, 1H NMR spectra were recorded at 400, 500 MHz with chemical shifts reported in parts per million downfield relative to $CHCl_3$ (7.26) or CH_3OH (δ 3.31).^{1}H NMR data are reported in the following order: multiplicity (s, singlet; d, doublet; t, triplet; q, quartet; and m, multiplet), coupling constant (*J*) in hertz (Hz), and the number of protons. Where appropriate, the multiplicity is preceded by br, indicating that the signal was broad. ^{13}C NMR spectra were recorded at 101 or 126 MHz with chemical shifts reported relative to $CHCl_3$ (77.16) or CH_3OH (δ 49.00). High-resolution mass spectrometry (HRMS) analysis was performed using a Q-TOF instrument. Purity was confirmed to be ≥95% by LCMS performed on a Shimadzu LC-20AD system with a Shimadzu Shim-Pack GISS-HP C18 column (3.0 x 150 mm, 3 μm) at 30 °C and equipped with a UV detector monitoring at 214 and 254 nm. The following solvent system, at a flow rate of 0.5 mL/min, was used: solvent A, 0.1 % formic acid in water; solvent B, acetonitrile. Gradient elution was as follows: 95:5 (A/B) for 2 min, 95:5 to 0:100 (A/B) over 13 min, 0:100 (A/B) for 2 min, then reversion back to 95:5 (A/B) over 1 min, 95:5 (A/B) for 2 min. This system was connected to a Shimadzu 8040 triple quadrupole mass spectrometer (ESI ionization). The compounds were purified via preparative HPLC performed on a BESTA-Technik system with a Dr. Maisch Reprosil Gold 120 C18 column (25 × 250 mm, 10 μm) and equipped with an ECOM Flash UV detector monitoring at 214 nm.

The following solvent system, at a flow rate of 12 mL/min, was used: solvent A: 0.1 % TFA in water/acetonitrile 95/5; solvent B: 0.1 % TFA in water/acetonitrile 5/95. Gradient elution was as follows: 95:5 (A/B) for 5 min, 95:5 to 0:100 (A/B) over 40 min, 0:100 (A/B) for 5 min, then reversion back to 95:5 (A/B) over 2 min, 95:5 (A/B) for 8 min. HRMS analyses were performed on a Shimadzu Nexera X2 UHPLC system with a Waters Acquity HSS C18 column (2.1 × 100 mm, 1.8 μm) at 30°C and equipped with a diode array detector. The following solvent system, at a flow rate of 0.5 mL/min, was used: solvent A, 0.1 % formic acid in water; solvent B, 0.1 % formic acid in acetonitrile. Gradient elution was as follows: 95:5 (A/B) for 1 min, 95:5 to 15:85 (A/B) over 6 min, 15:85 to 0:100 (A/B) over 1 min, 0:100 (A/B) for 3 min, then reversion back to 95:5 (A/B) for 3 min. This system was connected to a Shimadzu 9030 QTOF mass spectrometer (ESI ionization) calibrated internally with Agilent's API-TOF reference mass solution kit (5.0 mM purine, 100.0 mM ammonium trifluoroacetate and 2.5 mM hexakis(1H,1H,3H-tetrafluoropropoxy)phosphazine) diluted to achieve a mass count of 10000.

Compounds **2c**[27], **2d**[28], **2e**[29], **3c**[30], **3d**[28], **4a**[15], **4b**[31], **4f**[32], **5a**[17] were prepared as previously described and had NMR spectra and mass spectra consistent with the assigned structures.

4.1 Synthetic procedures

(*S*)-3-((*tert*-butoxycarbonyl)amino)-4-isopropoxy-4-oxobutanoic acid (3e). To a stirred suspension of 4-benzyl 1-*iso*propyl (*tert*-butoxycarbonyl)-L-aspartate (**2e**) (1200 mg, 3.3 mmol), 10% Pd-C (120 mg) under H_2 atmosphere. After completion of reaction (TLC), the mixture was filtered through celite, and the filtrate was concentrated under vacuum to get **3e** (900 mg, 99% yield) as a colorless oil. ^{1}H NMR (400 MHz, $CDCl_3$) δ 5.55 (d, *J* = 8.4 Hz, 1H), 5.11 – 5.03 (m, 1H), 4.54 – 4.50 (m, 1H), 3.05 (dd, *J* = 17.4, 4.5 Hz, 1H), 2.99 (s, 2H), 2.91 (s, 2H), 2.85 (dd, *J* = 17.3, 4.3 Hz, 1H), 1.46 (s, 9H), 1.25 (dd, *J* = 10.2, 6.3 Hz, 6H). ^{13}C NMR (101 MHz, $CDCl_3$) δ 176.1, 170.5, 155.6, 80.3, 69.7, 50.0, 36.7, 28.3, 21.6. HRMS (ESI): calculated for C12H22NO6 $[M+H]^+$ 276.1447, found 276.1450.

ethyl *N*^{2}-(tert-butoxycarbonyl)-*N*^{4}-methoxy-*N*^{4}-methyl-L-asparaginate (4c). To a stirred suspension of **3c** (100 mg, 0.4 mmol) in 10 mL CH_2Cl_2, benzotriazol-1-yloxytris(dimethylamino)phosphonium hexafluorophosphate (BOP) (194 mg, 0.44 mmol) and 0.1 mL Et_3N were added and after 10 mins *N,O*-dimethylhydroxylamine hydrogen chloride (43 mg, 0.44) was added followed by another 0.1 mL Et_3N. The resulting mixture was stirred at room temperature for 2 hours, 10 mL water was added to quench the reaction, the product extracted with CH_2Cl_2 (10 mL × 3), the organic layer washed with water, brine, dried over $NaSO_4$. Solvent was removed and the crude compound purified by column chromatography to get compound **4c** as a

colorless oil (960 mg, 80% yield). ^{1}H NMR (400 MHz, $CDCl_3$) δ 5.73 (d, *J* = 8.8 Hz, 1H), 4.59 – 4.55 (m, 1H), 4.24 – 4.19 (m, 2H), 3.70 (s, 3H), 3.18 (s, 3H), 2.97 – 2.91 (m, 1H), 1.46 (s, 9H), 1.28 (t, *J* = 7.1 Hz, 3H). LRMS (ESI): calculated for $C_{13}H_{25}N_2O_6$ $[M+H]^+$ 305.17, found 305.19.

propyl *N*^{2}-(*tert*-butoxycarbonyl)-*N*^{4}-methoxy-*N*^{4}-methyl-L-asparaginate (4d). Following the procedure described for compound **4c**, coupling compound **3d** (730 mg, 2.6 mmol) with *N*,O-dimethylhydroxylamine hydrogen chloride (284 mg, 2.9 mmol) yielded compound **4d** as a colourless oil (708 mg, 84% yield).^{1}H NMR (400 MHz, $CDCl_3$) δ 5.70 (d, *J* = 8.9 Hz, 1H), 4.53 (dt, *J* = 9.3, 4.4 Hz, 1H), 4.08 – 4.01 (m, 2H), 3.66 (s, 3H), 3.21 – 3.15 (m, 1H), 3.12 (s, 3H), 2.91 – 2.86 (br m, 1H), 1.67 – 1.56 (m, 2H), 1.41 (s, 9H), 0.90 (t, *J* = 7.4 Hz, 3H).^{13}C NMR (101 MHz, $CDCl_3$) δ 171.8, 155.8, 80.6, 67.1, 62.1, 49.1, 34.7, 32.4, 21.9, 4.8. HRMS (ESI): calculated for $C_{14}H_{27}N_2O_6$ $[M+H]^+$ 319.1869, found 318.1873.

***iso*propyl *N*^{2}-(*tert*-butoxycarbonyl)-*N*^{4}-methoxy-*N*^{4}-methyl-L-asparaginate (4e).** Following the procedure described for compound **4c**, coupling compound **3e** (800 mg, 2.9 mmol) with *N*,O-dimethylhydroxylamine hydrogen chloride (312 mg, 3.2 mmol) yielded compound **4e** as a colourless oil (760 mg, 82% yield). ^{1}H NMR (400 MHz, $CDCl_3$) δ 5.71 (d, *J* = 8.8 Hz, 1H), 5.11 – 5.01 (m, 1H), 4.55 – 4.50 (m, 1H), 3.70 (s, 3H), 3.25 – 3.18 (m, 1H), 3.17 (s, 3H), 2.95 –2.89 (br m, 1H), 1.46 (s, 10H), 1.25 (dd, *J* = 13.5, 6.3 Hz, 6H). ^{13}C NMR (101 MHz, $CDCl_3$) δ 171.1, 155.8, 69.1, 61.3, 50.0, 34.7, 32.0, 28.4, 21.7. HRMS (ESI): calculated for $C_{14}H_{27}N_2O_6$ $[M+H]^+$ 319.1869, found 318.1872.

methyl (*S*)-2-((*tert*-butoxycarbonyl)amino)-4-oxobutanoate (5b). To a solution of methyl *N*^{2}-(*tert*-butoxycarbonyl)-*N*^{4}-methoxy-*N*^{4}-methyl-L-asparaginate **4b** (1000 mg, 4.1 mmol) in CH_2Cl_2 (20 mL) at -78 ^{o}C was added DIBAL-H (1M in hexane, 6.0 mL) and the resulting mixture was stirred at -78 ^{o}C for 2 hours. 10 mL water was added to quench the reaction, 10 mL 1M HCl (aq) was added to the solution, the product was extracted with Et_2O. Combined organic layer wash with H_2O, brine, dried over Na_2SO_4. The solvent was removed to yield compound **5b** as a colorless oil used in the next step without further purification.

ethyl (*S*)-2-((*tert*-butoxycarbonyl)amino)-4-oxobutanoate (5c). Following the procedure described for compound **5a**, compound ethyl *N*^{2}-(*tert*-butoxycarbonyl)-*N*^{4}-methoxy-*N*^{4}-methyl-L-asparaginate **4c** (560 mg, 1.84 mmol) was reduced using DIBAL-H (1M in hexane, 3 mL) to yield compound **5c,** which was used in the next step without further purification.

propyl (*S*)-2-((*tert*-butoxycarbonyl)amino)-4-oxobutanoate (5d). Following the procedure described for compound **5a**, compound propyl *N*^{2}-(*tert*-butoxycarbonyl)-*N*^{4}-methoxy-*N*^{4}-methyl-L-asparaginate **4d** (400 mg, 1.3 mmol) was reduced by DIBAL-H (1M in hexane, 2 mL) to yield compound **5d** which was used in the next step without further purification.

***iso*propyl (*S*)-2-((*tert*-butoxycarbonyl)amino)-4-oxobutanoate (5e).** Following the procedure described for compound **5a**, compound *iso*propyl N^2-(*tert*-butoxycarbonyl)-N^4-methoxy-N^4-methyl-L-asparaginate **4e** (450 mg, 1.4 mmol) was reduced by DIBAL-H (1M in hexane, 2 mL) to yield compound **5e** which was used in the next step without further purification.

benzyl (*S*)-2-((*tert*-butoxycarbonyl)amino)-4-oxobutanoate (5f). Following the procedure described for compound **5a**, compound benzyl N^2-(*tert*-butoxycarbonyl)-N^4-methoxy-N^4-methyl-L-asparaginate **4f** (370 mg, 1.0mmol) was reduced by DIBAL-H (1M in hexane, 1.2 mL) to yield compound **5f** which was used in the next step without further purification.

***tert*-butyl N^2-(3-(2-acetoxy-4,6-dimethylphenyl)-3-methylbutanoyl)-N^4-methoxy-N^4-methyl-*L*-asparaginate (8a).** *tert*-butyl N^2-(*tert*-butoxycarbonyl)-N^4-methoxy-N^4-methyl-*L*-asparaginate **4a** (300 mg, 0.9 mmol) in dioxane (5 mL) is selectively deprotected using 4N HCl in dioxanes (10 mL) while stirring for 1 hour at 0 °C and 75 minutes at room temperature. The mixture is concentrated and added to a mixture of TML acid **7** (220 mg, 0.83 mmol, 0.9 eq), Et_3N (330 µL, 2.4 mmol, 2.8 eq) and BOP (450 mg, 1 mmol, 1.1 eq) in CH_2Cl_2 (10 mL). The mixture was stirred overnight, diluted with CH_2Cl_2 to 100 mL, washed with saturated $NaHCO_3$, water and Brine, dried over sodium sulfate and concentrated. The crude product was purified by column chromatography (30% EtOAc in petroleum ether, followed by flushing with 20% MeOH in EtOAc) yielding compound **8a** (350 mg, 88%) of an off-white powder. ^{1}H NMR (300 MHz, $CDCl_3$) δ 6.77 (d, *J* = 2.0 Hz, 1H), 6.56 (d, *J* = 2.1 Hz, 1H), 6.51 (d, *J* = 8.4 Hz, 1H), 4.66 (dt, *J* = 8.4, 4.2 Hz, 1H), 3.62 (s, 3H), 3.11 (s, 3H), 2.98 (dd, *J* = 17.3, 4.2 Hz, 1H), 2.78 (d, *J* = 13.8 Hz, 1H), 2.64 – 2.41 (m, 5H), 2.30 (s, 3H), 2.19 (s, 3H), 1.61 (s, 3H), 1.54 (s, 3H), 1.40 (s, 9H). ^{13}C NMR (75 MHz, $CDCl_3$) δ 170.66, 170.19, 170.08, 149.60, 138.14, 136.15, 133.61, 132.47, 123.21, 81.76, 61.15, 49.28, 48.51, 39.54, 34.32, 31.97, 31.64, 27.88, 25.45, 21.92, 20.24. LRMS (ESI): calculated for $C_{25}H_{39}N_2O_7$ $[M+H]^+$ 479.28, found 479.35.

***tert*-butyl (*S*)-2-(3-(2-acetoxy-4,6-dimethylphenyl)-3-methylbutanamido)-4-oxobutanoate (9a).** Following the procedure described for compound **5a**, compound **8a** (110 mg, 0.23 mmol) was reduced by DIBAL-H (1M in hexane, 0.4 mL) to yield compound **9a** which was used in the next step without further purification.

methyl (*S*)-4-((((3a*R*,4*R*,6*R*,6a*R*)-6-(6-amino-9*H*-purin-9-yl)-2,2-dimethyltetrahydrofuro[3,4-d][1,3]dioxol-4-yl)methyl)((*E*)-3-(4-cyanophenyl)allyl)amino)-2-((*tert*-butoxycarbonyl)amino)butanoate (11b). 4-((*E*)-3-((((3a*R*,4*R*,6*R*,6a*R*)-6-(6-amino-9*H*-purin-9-yl)-2,2-dimethyltetrahydrofuro[3,4-*d*][1,3]dioxol-4-yl)methyl)amino)prop-1-en-1-yl)benzonitrile **10** (50 mg, 0.11 mmol), **5b** (30, 0.13 mmol), $NaBH(OAc)_3$ (36 mg, 0.17 mmol) and AcOH (one drop) were dissolved in 1,2- dichloroethane (DCE, 10 mL) and stirred at room temperature under

a N_2 atmosphere overnight. The reaction was quenched by adding 1 N NaOH (10 mL), and the product was extracted with CH_2Cl_2. The combined organic layers were washed with brine and dried over Na_2SO_4. The solvent was evaporated, and the crude product was purified by column chromatography (5% MeOH in CH_2Cl_2) to give compound **11b** as a white powder (47 mg, 65% yield). ^{1}H NMR (400 MHz, $CDCl_3$) δ 8.21 (s, 1H), 7.94 (s, 1H), 7.49 (d, *J* = 8.3 Hz, 2H), 7.27 (d, *J* = 8.3 Hz, 2H), 6.60 (s, 2H), 6.35 (d, *J* = 16.0 Hz, 1H), 6.27 – 6.22 (m, 1H), 6.06 (s, 1H), 5.94 (d, *J* = 8.1 Hz, 1H), 5.45 (d, *J* = 6.2 Hz, 1H), 5.03 – 4.95 (m, 1H), 4.41 – 4.30 (m, 2H), 3.64 (s, 3H), 3.23 (d, *J* = 6.0 Hz, 2H), 2.79 – 2.69 (m, 2H), 2.58 – 2.54 (m, 2H), 2.00 – 1.89 (m, 1H), 1.82-1.77 (br m, 1H), 1.58 (s, 3H), 1.38 (br s, 12H). ^{13}C NMR (101 MHz, $CDCl_3$) δ 173.3, 155.9, 155.6, 153.0, 149.0, 141.3, 140.1, 132.3, 131.0, 126.7, 120.2, 119.0, 114.4, 110.5, 90.7, 85.7, 83.9, 83.3, 56.6, 56.1, 53.6, 52.2, 50.6, 44.8, 29.2, 28.4, 27.2, 25.4. HRMS (ESI): calculated for $C_{33}H_{43}N_8O_7$ $[M+H]^+$ 663.3255, found 663.3262.

ethyl (*S*)-4-((((3a*R*,4*R*,6*R*,6a*R*)-6-(6-amino-9*H*-purin-9-yl)-2,2-dimethyltetrahydrofuro [3,4-d][1,3]dioxol-4-yl)methyl)((*E*)-3-(4-cyanophenyl)allyl)amino)-2-((*tert*-butoxycarbonyl)amino)butanoate (11c). Following the procedure described for compound **11b**, coupling compound **10** (50 mg, 0.11 mmol) with **5c** (32 mg, 0.13 mmol) afforded compound **11c** as a white powder (53 mg, 72% yield). ^{1}H NMR (400 MHz, $CDCl_3$) δ 8.15 (s, 1H), 7.91 (s, 1H), 7.46 (d, *J* = 8.3 Hz, 2H), 7.24 (d, *J* = 8.3 Hz, 2H), 6.58 (s, 2H), 6.32 (d, *J* = 16.0 Hz, 1H), 6.26 – 6.16 (br, 1H), 6.01 (s, 1H), 5.85 (d, *J* = 8.0 Hz, 1H), 5.39 (t, *J* = 8.2 Hz, 2H), 4.95-4.89 (m, 2H), 4.36 – 4.17 (m, 2H), 3.74 – 3.51 (m, 6H), 3.43 (s, 4H), 3.29 – 3.03 (m, 4H), 2.80 – 2.52 (m, 6H), 2.49 (s, 5H), 1.83-1.64 (m, 3H), 1.53 (s, 3H), 1.34 (br d, *J* = 7.8 Hz, 15H). ^{13}C NMR (101 MHz, $CDCl_3$) δ 172.2, 156.1, 155.8, 153.0, 148.9, 141.3, 132.3, 126.7, 120.2, 114.4, 110.4, 90.6, 85.6, 83.9, 83.2, 68.8, 65.0, 59.7, 56.8, 56.0, 52.4, 51.0, 44.8, 29.3, 28.3, 25.4, 21.7. HRMS (ESI): calculated for $C_{33}H_{43}N_8O_7$ $[M+H]^+$677.3411, found 677.3420.

propyl (*S*)-4-((((3a*R*,4*R*,6*R*,6a*R*)-6-(6-amino-9*H*-purin-9-yl)-2,2-dimethyltetrahydrofuro [3,4-d][1,3]dioxol-4-yl)methyl)((*E*)-3-(4-cyanophenyl)allyl)amino)-2-((*tert*-butoxycarbonyl)amino)butanoate (11d). Following the procedure described for compound **11b**, coupling compound **10** (50 mg, 0.11 mmol) with **5d** (34 mg, 0.13 mmol) afforded compound **11d** as a white powder (46 mg, 60% yield). ^{1}H NMR (400 MHz, $CDCl_3$) δ 8.18 (s, 1H), 7.93 (s, 1H), 7.48 (d, *J* = 8.3 Hz, 2H), 7.26 (d, *J* = 8.3 Hz, 2H), 6.55 (s, 2H), 6.34 (d, *J* = 15.9 Hz, 1H), 6.27 – 6.17 (m, 1H), 6.03 (s, 1H), 5.88 (d, *J* = 8.1 Hz, 1H), 5.41 (d, *J* = 5.6 Hz, 2H), 4.96 (dd, *J* = 6.3, 3.7 Hz, 1H), 4.33 (t, *J* = 8.1 Hz, 2H), 3.98 (t, *J* = 6.7 Hz, 2H), 3.64 (d, *J* = 2.7 Hz, 1H), 3.59 (d, *J* = 3.1 Hz, 1H), 3.26 – 3.19 (m, 2H), 3.11 (d, *J* = 6.8 Hz, 1H), 2.79 – 2.50 (m, 8H), 2.02 – 1.65 (m, 4H), 1.62-1.52 (m, 6H), 1.39 – 1.34 (m, 19H). ^{13}C NMR (101 MHz, $CDCl_3$) δ 172.8, 155.9,

153.0, 149.0, 141.3, 132.3, 130.9, 126.7, 120.1, 119.0, 114.4, 110.5, 90.6, 85.6, 83.9, 79.6, 66.6, 65.1, 59.6, 52.31, 44.8, 28.4, 25.4, 21.8. HRMS (ESI): calculated for $C_{33}H_{43}N_8O_7$ $[M+H]^+$ 691.3568, found 691.3573.

***iso*propyl (*S*)-4-((((3a*R*,4*R*,6*R*,6a*R*)-6-(6-amino-9*H*-purin-9-yl)-2,2-dimethyltetrahydrofuro[3,4-d][1,3]dioxol-4-yl)methyl)((*E*)-3-(4-cyanophenyl)allyl)amino)-2-((*tert*-butoxycarbonyl)amino)butanoate (11e).** Following the procedure described for compound **11b**, coupling compound **10** (50 mg, 0.11 mmol) with **5e** (34 mg, 0.13 mmol) afforded compound **11e** as a white powder (47 mg, 62% yield). ^{1}H NMR (400 MHz, $CDCl_3$) δ 8.16 (s, 1H), 7.92 (s, 1H), 7.45 (d, *J* = 8.3 Hz, 2H), 7.24 (d, *J* = 8.4 Hz, 2H), 6.62 (br s, 2H), 6.32 (br s, 1H), 6.24-6.16 (m, 1H), 6.04 – 5.99 (m, 1H), 5.91 (d, *J* = 8.1 Hz, 1H), 5.40 (t, *J* = 8.1 Hz, 2H), 4.33-4.25(m, 2H), 3.61 (d, *J* = 2.3 Hz, 1H), 3.56 (d, *J* = 3.6 Hz, 2H), 3.44 (s, 3H), 3.20 (t, *J* = 5.6 Hz, 2H), 3.09 (d, *J* = 4.8 Hz, 1H), 2.78 – 2.52 (m, 6H), 2.49 (s, 3H), 1.85 – 1.62 (m, 3H), 1.53 (s, 3H), 1.34 (br s, 20H). ^{13}C NMR (101 MHz, $CDCl_3$) δ 172.7, 156.1, 153.0, , 132.29, 141.3, 132.3, 130.9, 126.6, 119.0, 114.3, 110.4, 90.6, 85.6, 83.9, 83.2, 59.7, 52.3, 51.0, 44.8, 29.2, 28.3, 27.1, 25.4. HRMS (ESI): calculated for $C_{33}H_{43}N_8O_7$ $[M+H]^+$ 691.3568, found 691.3577.

benzyl (*S*)-4-((((3a*R*,4*R*,6*R*,6a*R*)-6-(6-amino-9*H*-purin-9-yl)-2,2-dimethyltetrahydrofuro[3,4-d][1,3]dioxol-4-yl)methyl)((*E*)-3-(4-cyanophenyl)allyl)amino)-2-((*tert*-butoxycarbonyl)amino)butanoate (11f). Following the procedure described for compound 11b, coupling compound **5f** (50 mg, 0.11 mmol) with compound **10** (40 mg, 0.13 mmol) afforded compound **11f** as a white powder (54 mg, 66% yield). ^{1}H NMR (400 MHz, $CDCl_3$) δ 8.18 (s, 1H), 7.91 (s, 1H), 7.48 (d, *J* = 8.4 Hz, 2H), 7.25 (s, 7H), 6.48 (s, 2H), 6.02 (s, 1H), 5.92 (d, *J* = 8.1 Hz, 1H), 5.38 (d, *J* = 6.4 Hz, 2H), 5.19 – 4.99 (m, 2H), 4.98 – 4.90 (m, 1H), 4.38 – 4.31 (br m, 2H), 3.78 – 3.68 (m, 2H), 3.66 (s, 1H), 3.60 (d, *J* = 3.9 Hz, 3H), 3.48 (s, 5H), 3.23-3.17 (m, 2H), 2.79 – 2.59 (m, 6H), 1.88 – 1.82 (m, 2H), 1.74-1.69 (m, 2H), 1.56 (s, 3H), 1.38 (br, 12H). ^{13}C NMR (101 MHz, $CDCl_3$) δ 172.6, 156.1, 155.8, 153.0, 149.0, 141.2, 135.5, 132.3, 128.2, 126.7, 120.0, 90.6, 85.6, 83.9, 83.3, 66.9, 65.1, 59.8, 56.6, 56.1, 52.4, 44.8, 28.4, 27.2, 25.4. HRMS (ESI): calculated for $C_{33}H_{43}N_8O_7$ $[M+H]^+$ 739.3568, found 739.3571.

methyl (*S*)-2-amino-4-((((2*R*,3*S*,4*R*,5*R*)-5-(6-amino-9*H*-purin-9-yl)-3,4-dihydroxytetrahydrofuran-2-yl)methyl)((*E*)-3-(4-cyanophenyl)allyl)amino)butanoate (12b). To a solution of compound **11b** (30 mg, 0.045 mmol) in 1 mL of CH_2Cl_2 was added a mixture of 9 mL TFA and 1 mL H_2O, and the solution was stirred for 2 h at room temperature. The mixture was concentrated, and the crude product was purified by preparative HPLC affording compound **12b** as a white powder (24mg, 93% yield). ^{1}H NMR (400 MHz, CD_3OD) δ 8.47 (s, 1H), 8.33 (s, 1H), 7.69 (d, *J* = 8.4 Hz, 2H), 7.51 (d, *J* = 8.5 Hz, 2H), 6.84 (d, *J* = 15.8 Hz, 1H), 6.49 (dt, *J* = 15.8, 7.2 Hz,

1H), 6.17 (d, *J* = 3.4 Hz, 1H), 4.70 (dd, *J* = 4.8, 3.4 Hz, 1H), 4.60 – 4.53 (m, 2H), 4.25 (dd, *J* = 7.4, 5.7 Hz, 1H), 4.14 (d, *J* = 7.3 Hz, 2H), 3.92 – 3.85 (m, 1H), 3.84 (s, 3H), 3.74 – 3.66 (m, 1H), 3.64 – 3.47 (m, 2H), 2.58 – 2.47 (m, 1H), 2.46 – 2.34 (m, 1H). ^{13}C NMR (101 MHz, CD_3OD) δ 168.3, 161.84, 161.5, 151.6, 148.2, 139.75, 145.5, 143.0, 139.8, 138.4, 132.3, 127.2, 119.8, 118.191.2, 78.7, 73.5, 72.2, 55.5, 54.9, 52.8, 50.2, 49.8, 24.9. HRMS (ESI): calculated for $C_{25}H_{31}N_8O_5$ $[M+H]^+$ 523.2417, found 523.2422.

ethyl (*S*)-2-amino-4-((((2*R*,3*S*,4*R*,5*R*)-5-(6-amino-9*H*-purin-9-yl)-3,4-dihydroxytetrahydrofuran-2-yl)methyl)((*E*)-3-(4-cyanophenyl)allyl)amino)butanoate (12c). Following the procedure described for compound **12b**, compound **11c** (30 mg, 0.044 mmol) was deprotected and purified, affording compound **12c** as a white powder (19 mg, 67% yield). ^{1}H NMR (400 MHz, CD_3OD) δ 8.42 (s, 1H), 8.30 (s, 1H), 7.70 (d, *J* = 8.4 Hz, 2H), 7.50 (d, *J* = 8.4 Hz, 2H), 6.84 (br d, *J* = 15.9 Hz, 1H), 6.53 – 6.42 (m, 1H), 6.15 (d, *J* = 3.4 Hz, 1H), 4.69 (dd, *J* = 5.1, 3.5 Hz, 1H), 4.59 – 4.48 (m, 2H), 4.33 – 4.25 (m, 2H), 4.21 (t, *J* = 6.6 Hz, 1H), 4.09 (t, *J* = 7.2 Hz, 2H), 3.80 (dd, *J* = 13.9, 9.8 Hz, 1H), 3.65 – 3.61 (dd, *J* = 13.2, 5.8 Hz, 1H), 3.56 – 3.44 (m, 2H), 2.52 – 2.44 (m, 1H), 2.41 – 2.30 (m, 1H), 1.30 (t, *J* = 7.1 Hz, 3H). ^{13}C NMR (101 MHz, CD_3OD) δ 167.9, 161.6, 152.5, 148.3, 139.8, 138.0, 132.3, 127.2, 121.0, 119.7, 118.1, 111.7, 91.0, 78.8, 73.4, 72.2, 62.9, 55.5, 55.0, 50.4, 49.9, 25.0. HRMS (ESI): calculated for $C_{26}H_{33}N_8O_5$ $[M+H]^+$ 537.2574, found 537.2579.

propyl (*S*)-2-amino-4-((((2*R*,3*S*,4*R*,5*R*)-5-(6-amino-9*H*-purin-9-yl)-3,4-dihydroxytetrahydrofuran-2-yl)methyl)((*E*)-3-(4-cyanophenyl)allyl)amino)butanoate (12d). Following the procedure described for compound **12b**, compound **11d** (30 mg, 0.043 mmol) was deprotected and purified, affording compound **12d** as a white powder (20 mg, 69% yield). ^{1}H NMR (400 MHz, CD_3OD) δ 8.46 (s, 1H), 8.33 (s, 1H), 7.69 (d, *J* = 8.3 Hz, 2H), 7.51 (d, *J* = 8.3 Hz, 2H), 6.84 (d, *J* = 15.8 Hz, 1H), 655-6.45 (m, 1H), 6.16 (d, *J* = 3.4 Hz, 1H), 4.75 – 4.67 (m, 1H), 4.59 – 4.53 (m, 2H), 4.28 – 4.09 (m, 5H), 3.90 – 3.77 (m, 1H), 3.69 (d, *J* = 13.4 Hz, 1H), 3.63 – 3.47 (m, 2H), 2.57 – 2.33 (m, 2H), 1.73-1.64 (m, 2H), 1.24 (s, 6H), 0.94 (t, *J* = 7.4 Hz, 3H). ^{13}C NMR (101 MHz, CD_3OD) δ 168.0, 152.0, 148.3, 146.1, 142.8, 139.81, 120.6, 118.1, 111.8, 91.1, 78.8, 73.5, 72.2, 68.3, 55.6, 55.0, 29.8, 25.0, 21.4. HRMS (ESI): calculated for $C_{27}H_{35}N_8O_5$ $[M+H]^+$551.2730, found 551.2732.

***iso*propyl (*S*)-2-amino-4-((((2*R*,3*S*,4*R*,5*R*)-5-(6-amino-9*H*-purin-9-yl)-3,4-dihydroxytetrahydrofuran-2-yl)methyl)((*E*)-3-(4-cyanophenyl)allyl)amino)butanoate (12e).** Following the procedure described for compound **12b**, compound **11e** (30 mg, 0.043 mmol) was deprotected and purified, affording compound **12e** as a white powder (21 mg, 73% yield). ^{1}H NMR (400 MHz, CD_3OD) δ 8.41 (s, 1H), 8.30 (s, 1H), 7.70 (d, *J* = 8.4 Hz, 2H), 7.50 (d, *J* = 8.3 Hz, 2H),

6.84 (br d, *J* = 15.8 Hz, 1H), 6.53 – 6.42 (m, 1H), 6.14 (d, *J* = 3.4 Hz, 1H), 5.14 – 5.07 (m, 1H), 4.70 (dd, *J* = 5.1, 3.5 Hz, 1H), 4.59 – 4.54 (m, 1H), 4.54 – 4.48 (m, 1H), 4.18 (t, *J* = 6.6 Hz, 1H), 4.07 (d, *J* = 7.1 Hz, 2H), 2.51 – 2.29 (m, 2H), 1.29 (t, *J* = 6.1 Hz, 6H). ^{13}C NMR (101 MHz, CD_3OD) δ 167.5, 152.7, 139.8, 137.8, 132.3, 127.2, 119.7, 118.1, 111.7, 91.0, 78.9, 73.4, 72.2, 71.4, 55.1, 50.6, 50.0, 25.1, 20.3. HRMS (ESI): calculated for $C_{27}H_{35}N_8O_5$ $[M+H]^+$ 551.2730, found 551.2734.

benzyl (*S*)-2-amino-4-((((2*R*,3*S*,4*R*,5*R*)-5-(6-amino-9*H*-purin-9-yl)-3,4-dihydroxytetrahydrofuran-2-yl)methyl)((*E*)-3-(4-cyanophenyl)allyl)amino)butanoate (12f). Following the procedure described for compound **12b**, compound **11f** (30 mg, 0.041 mmol) was deprotected and purified, affording compound **12f** as a white powder (22 mg, 77% yield). ^{1}H NMR (400 MHz, CD_3OD) δ 8.41 (s, 1H), 8.29 (s, 1H), 7.48 (s, 1H), 7.46 (s, 1H), 7.43 – 7.36 (m, 5H), 6.79 (br d, *J* = 15.9 Hz, 1H), 6.47 – 6.37 (m, 1H), 6.13 (d, *J* = 3.4 Hz, 1H), 5.29 (d, *J* = 2.8 Hz, 2H), 4.67 (dd, *J* = 5.1, 3.4 Hz, 1H), 4.57 – 4.45 (m, 2H), 4.28 (t, *J* = 6.6 Hz, 1H), 4.03 (d, *J* = 7.2 Hz, 2H), 3.76 (dd, *J* = 13.9, 9.9 Hz, 1H), 3.60 (br d, *J* = 12.8 Hz, 1H), 3.53 – 3.40 (m, 2H), 2.54 – 2.33 (m, 2H). ^{13}C NMR (101 MHz, CD_3OD) δ 167.9, 152.1, 148.2, 134.7, 132.3, 119.7, 118.1, 111.78, 91.0, 78.8, 73.4, 72.2, 68.2, 55.5, 54.9, 50.4, 49.9, 25.0. HRMS (ESI): calculated for $C_{31}H_{34}N_8O_5$ $[M+H]^+$598.2652, found 598.2656.

***tert*-butyl (*S*)-2-(3-(2-acetoxy-4,6-dimethylphenyl)-3-methylbutanamido)-4-((((3a*R*,4*R*,6*R*,6a*R*)-6-(6-amino-9*H*-purin-9-yl)-2,2-dimethyltetrahydrofuro[3,4-d][1,3]dioxol-4-yl)methyl)((*E*)-3-(4-cyanophenyl)allyl)amino)butanoate (13a).** Following the procedure described for compound **11b**, coupling compound **10** (95 mg, 0.21 mmol, 1.1 eq) with compound **9a** (80 mg, 0.19 mmol, 1.0 eq) afforded compound **13a** as a yellowish oil (55 mg, 34% yield). ^{1}H NMR (400 MHz, $CDCl_3$) δ 8.24 (s, 1H), 7.90 (s, 1H), 7.55 (d, *J* = 8.4 Hz, 1H), 7.31 (d, *J* = 8.4 Hz, 2H), 6.79 (d, *J* = 2.1 Hz, 1H), 6.58 (d, *J* = 2.1 Hz, 1H), 6.43 – 6.19 (m, 3H), 6.14 (s, 2H), 6.04 (d, *J* = 2.0 Hz, 1H), 5.44 (dd, *J* = 6.4, 2.0 Hz, 1H), 4.98 (dd, *J* = 6.4, 3.6 Hz, 1H), 4.38 – 4.27 (m, 2H), 3.21 (d, *J* = 6.3 Hz, 2H), 2.77 – 2.66 (m, 2H), 2.57 (q, *J* = 13.5 Hz, 2H), 2.49 (s, 3H), 2.31 (s, 3H), 2.20 (s, 3H), 1.85 – 1.73 (m, 1H), 1.67 – 1.56 (m, 11H), 1.52 – 1.38 (m, 16H), 1.26 (s, 9H). ^{13}C NMR (101 MHz, $CDCl_3$) δ 171.15, 170.94, 170.76, 155.65, 153.02, 149.87, 149.12, 141.25, 140.14, 138.46, 136.51, 133.68, 132.73, 132.39, 130.90, 126.69, 124.82, 123.39, 119.05, 114.43, 114.13, 110.59, 90.80, 85.71, 83.96, 83.25, 81.71, 56.83, 56.01, 51.56, 50.84, 49.26, 43.53, 39.80, 31.97, 31.81, 31.69, 30.35, 29.74, 29.55, 29.46, 27.96, 27.94, 27.20, 25.53, 25.43, 21.97, 20.27. HRMS (ESI): calculated for $C_{46}H_{59}N_8O_8$ $[M+H]^+$ 851.4450, found 851.4456.

methyl (*S*)-2-(3-(2-acetoxy-4,6-dimethylphenyl)-3-methylbutanamido)-4-((((3a*R*,4*R*,6*R*,6a*R*)-6-(6-amino-9*H*-purin-9-yl)-2,2-dimethyltetrahydrofuro[3,4-d][1,3]dioxol-

4-yl)methyl)((*E*)-3-(4-cyanophenyl)allyl)amino)butanoate (13b). To a solution of compound **11b** (30 mg, 0.045 mmol) in 9 mL dry of CH_2Cl_2 was added a 1 mL TFA and the solution was stirred for 1 h at room temperature. The mixture was concentrated. 5mL CH_2Cl_2 was added to the mixture, followed by adding benzotriazol-1-yloxytris(dimethylamino)phosphonium hexafluorophosphate (BOP, 20 mg), 3-(2-acetoxy-4,6-dimethylphenyl)-3-methylbutanoic acid **7** (TML acid, 0.045 mmol, 12 mg) and 0.5 ml Et_3N. The reaction mixture stirred 2 hours at r.t. 10 mL water wad added, then extracted with CH_2Cl_2 (10 ml ×3), the combined organic phase dried over Na_2SO_4. The solvent was evaporated, and the crude product was purified by column chromatography (100% EtOAc) to give compound **13b** as a white powder (15 mg, 42% yield over 2 steps). ^{1}H NMR (400 MHz, $CDCl_3$) δ 8.20 (s, 1H), 7.91 (s, 1H), 7.54 (d, *J* = 8.3 Hz, 2H), 7.30 (d, *J* = 8.5 Hz, 2H), 6.79 (d, *J* = 1.5 Hz, 1H), 6.58 (d, *J* = 7.3 Hz, 3H), 6.43 – 6.32 (m, 2H), 6.27 – 6.17 (m, 1H), 6.04 (d, *J* = 2.0 Hz, 1H), 5.43 (dd, *J* = 6.4, 2.0 Hz, 1H), 4.97 (dd, *J* = 6.4, 3.4 Hz, 1H), 4.48-4.43 (m, 1H), 4.37-4.32 (m, 1H), 3.62 (s, 3H), 3.19 (d, *J* = 6.2 Hz, 2H), 2.69 (d, *J* = 6.8 Hz, 2H), 2.55 (d, *J* = 4.8 Hz, 2H), 2.48 (s, 3H), 2.41 – 2.32 (m, 1H), 2.30 (s, 3H), 2.19 (s, 3H), 2.12 (s, 1H), 1.81-1.74 (m, 1H), 1.69 – 1.55 (m, 9H), 1.38 (s, 3H). ^{13}C NMR (101 MHz, $CDCl_3$) δ 172.5, 171.1, 155.8, 152.7, 149.9, 141.2, 140.1, 138.5, 136.6, 132.7, 133.6, 132.4, 131.0, 130.9, 126.7, 123.4, 114.4, 110.6, 90.9, 85.6, 83.9, 83.2, 56.4, 55.9, 52.2, 50.9, 49.2, 39.8, 31.7, 29.1, 27.2, 25.5, 25.3, 22.0, 20.2. HRMS (ESI): calculated for $C_{43}H_{53}N_8O_8$ $[M+H]^+$809.3986, found 809.3991.

ethyl (*S*)-2-(3-(2-acetoxy-4,6-dimethylphenyl)-3-methylbutanamido)-4-((((3a*R*,4*R*,6*R*,6a*R*)-6-(6-amino-9*H*-purin-9-yl)-2,2-dimethyltetrahydrofuro[3,4-d][1,3]dioxol-4-yl)methyl)((*E*)-3-(4-cyanophenyl)allyl)amino)butanoate (13c). Following the procedure described for compound **13b**, compound **11c** (85 mg, 0.126 mmol) was selectively deprotected and coupled with TML acid **7** (40 mg, 0.15 mmol), affording crude 13c which was used in the next step without further purification.

propyl (*S*)-2-(3-(2-acetoxy-4,6-dimethylphenyl)-3-methylbutanamido)-4-((((3a*R*,4*R*,6*R*,6a*R*)-6-(6-amino-9*H*-purin-9-yl)-2,2-dimethyltetrahydrofuro[3,4-d][1,3]dioxol-4-yl)methyl)((*E*)-3-(4-cyanophenyl)allyl)amino)butanoate (13d). Following the procedure described for compound **13b**, compound **11d** (31 mg, 0.045 mmol) was selectively deprotected and coupled with TML acid **7** (12 mg, 0.045 mmol), affording crude **13d** which was used in the next step without further purification.

***iso*propyl (*S*)-2-(3-(2-acetoxy-4,6-dimethylphenyl)-3-methylbutanamido)-4-((((3a*R*,4*R*,6*R*,6a*R*)-6-(6-amino-9*H*-purin-9-yl)-2,2-dimethyltetrahydrofuro[3,4-d][1,3]dioxol-4-yl)methyl)((*E*)-3-(4-cyanophenyl)allyl)amino)butanoate (13e).** Following the procedure described for compound **13b**, compound **11e** (31 mg, 0.045 mmol) was selectively deprotected and

coupled with TML acid **7** (15 mg, 0.045 mmol), affording compound **13e** as a white powder (18 mg, 39% yield over 2 steps). ^{1}H NMR (400 MHz, $CDCl_3$) δ 8.22 (s, 1H), 7.90 (s, 1H), 7.54 (d, *J* = 8.3 Hz, 2H), 7.30 (d, *J* = 6.4 Hz, 2H), 6.79 (d, *J* = 1.6 Hz, 1H), 6.59 (d, *J* = 1.6 Hz, 1H), 6.43 – 6.32 (m, 4H), 6.23 (dt, *J* = 15.9, 6.4 Hz, 1H), 6.04 (d, *J* = 2.0 Hz, 1H), 5.44 (dd, *J* = 6.4, 2.0 Hz, 1H), 5.01 – 4.92 (m, 2H), 4.46 – 4.30 (m, 2H), 3.20 (d, *J* = 6.2 Hz, 2H), 2.70 (d, *J* = 7.9 Hz, 2H), 2.64 – 2.51 (m, 3H), 2.49 (s, 3H), 2.41 – 2.36 (m, 2H), 2.30 (s, 3H), 2.20 (s, 3H), 1.83 – 1.78 (m, 1H), 1.67 – 1.57 (m, 11H), 1.38 (s, 3H), 1.26 (s, 4H), 1.20 (d, *J* = 6.3 Hz, 3H), 1.15 (d, *J* = 6.2 Hz, 3H). ^{13}C NMR (101 MHz, $CDCl_3$) δ 171.6, 171.0, 170.8, 155.7, 152.9, 149.9, 141.2, 140.1, 138.6, 132.7, 132.4, 123.42, 120.2, 119.0, 114.4, 109.8, 90.9, 85.7, 84.0, 83.2, 68.9, 56.7, 56.0, 51.1, 50.8, 49.2, 39.8, 31.7, 29.7, 27.2, 25.5, 25.4, 22.0, 21.7, 20.3. HRMS (ESI): calculated for $C_{45}H_{57}N_8O_8$ $[M+H]^+$ 837.4299, found 837.4303.

benzyl (*S*)-2-(3-(2-acetoxy-4,6-dimethylphenyl)-3-methylbutanamido)-4-((((3a*R*,4*R*,6*R*,6a*R*)-6-(6-amino-9*H*-purin-9-yl)-2,2-dimethyltetrahydrofuro[3,4-d][1,3]dioxol-4-yl)methyl)((*E*)-3-(4-cyanophenyl)allyl)amino)butanoate (13f). Following the procedure described for compound **13b**, compound **11f** (82 mg, 0.13 mmol) was selectively deprotected and coupled with TML acid **7** (34 mg, 0.13 mmol), affording crude **13f** which was used in the next step without further purification.

(*S*)-2-(3-(2-acetoxy-4,6-dimethylphenyl)-3-methylbutanamido)-4-((((2*R*,3*S*,4*R*,5*R*)-5-(6-amino-9*H*-purin-9-yl)-3,4-dihydroxytetrahydrofuran-2-yl)methyl)((*E*)-3-(4-cyanophenyl)allyl)amino)butanoic acid (14a). Following the procedure described for compound **12a**, compound **13a** (55 mg, 0.065 mmol) was deprotected and purified, affording compound **14a** as a white powder (28 mg, 54% yield). ^{1}H NMR (400 MHz, CD_3OD) δ 8.47 (s, 1H), 8.35 (s, 1H), 7.72 (d, *J* = 8.1 Hz, 2H), 7.54 (d, *J* = 8.1 Hz, 2H), 6.85 – 6.75 (m, 2H), 6.61 (d, *J* = 2.1 Hz, 1H), 6.44 – 6.34 (m, 1H), 6.15 (d, *J* = 3.5 Hz, 1H), 4.54 – 4.47 (m, 2H), 4.32 (dd, *J* = 8.6, 4.8 Hz, 1H), 3.93 (d, *J* = 7.5 Hz, 2H), 3.84 – 3.76 (m, 1H), 3.62 (d, *J* = 13.8 Hz, 1H), 3.27 – 3.16 (m, 2H), 2.76 (d, *J* = 14.9 Hz, 1H), 2.69 – 2.60 (m, 1H), 2.55 (s, 3H), 2.33 (s, 3H), 2.16 (s, 3H), 2.08 – 1.96 (m, 1H), 1.60 (s, 3H), 1.56 (s, 3H). ^{13}C NMR (101 MHz, CD_3OD) δ 175.2, 171.7, 162.9, 157.1, 150.4, 147.3, 139.6, 138.7, 138.3, 136.0, 134.4, 133.0, 132.3, 131.9, 127.3, 123.0, 119.8, 118.1, 117.7, 114.8, 112.4, 91.1, 77.0, 73.4, 71.7, 54.9, 50.9, 50.5, 36.9, 31.0, 29.7, 26.3, 20.5, 18.5. HRMS (ESI): calculated for $C_{39}H_{47}N_8O_8$ $[M+H]^+$ 755.3511, found 755.3508.

methyl (*S*)-2-(3-(2-acetoxy-4,6-dimethylphenyl)-3-methylbutanamido)-4-((((2*R*,3*S*,4*R*,5*R*)-5-(6-amino-9*H*-purin-9-yl)-3,4-dihydroxytetrahydrofuran-2-yl)methyl)((*E*)-3-(4-cyanophenyl)allyl)amino)butanoate (14b). Following the procedure described for compound **12a**, compound **13b** (10 mg, 0.012 mmol) was deprotected and purified, affording compound **14b**

as a white powder (5 mg, 48% yield). ^{1}H NMR (400 MHz, CD_3OD) δ 8.48 (s, 1H), 8.36 (s, 1H), 7.70 (d, *J* = 8.3 Hz, 2H), 7.53 (d, *J* = 8.1 Hz, 2H), 6.87 – 6.77 (m, 2H), 6.61 (d, *J* = 1.5 Hz, 1H), 6.42 – 6.35 (m, 1H), 6.17 (d, *J* = 3.5 Hz, 1H), 4.69 (t, *J* = 3.8 Hz, 1H), 4.51 (d, *J* = 6.6 Hz, 2H), 4.40 (dd, *J* = 8.7, 5.0 Hz, 1H), 3.95 (br s, 2H), 3.82 – 3.74 (m, 1H), 3.69 (s, 3H), 3.62 (br d, *J* = 13.6 Hz, 1H), 3.25 – 3.18 (m, 2H), 2.76 (d, *J* = 14.9 Hz, 1H), 2.64 (br d, *J* = 14.8 Hz, 1H), 2.54 (s, 3H), 2.16 (s, 3H), 2.00 (s, 1H), 1.61 (s, 3H), 1.55 (s, 3H). ^{13}C NMR (101 MHz, CD_3OD) δ 172.9, 170.9, 160.96, 161.3, 161.0, 160.6, 160.2, 151.1, 149.7, 148.1, 139.66, 138.7, 136.0, 133.6, 132.3, 131.9, 127.3, 123.0, 119.9, 118.1, 117.7, 114.8, 111.9, 91.1, 78.5, 73.4, 72.2, 54.3, 51.8, 49.5, 39.1, 31.1, 30.8, 26.1, 24.4, 20.6, 18.9. HRMS (ESI): calculated for $C_{40}H_{49}N_8O_8$ $[M+H]^+$ 769.3673, found 769.3681.

ethyl (*S*)-2-(3-(2-acetoxy-4,6-dimethylphenyl)-3-methylbutanamido)-4-((((2*R*,3*S*,4*R*,5*R*)-5-(6-amino-9*H*-purin-9-yl)-3,4-dihydroxytetrahydrofuran-2-yl)methyl)((*E*)-3-(4-cyanophenyl)allyl)amino)butanoate (14c). Following the procedure described for compound **12a**, compound **13c** (10 mg, 0.012 mmol) was deprotected and purified, affording compound **14c** as a white powder (6 mg, 56% yield). ^{1}H NMR (400 MHz, Methanol-*d*$_4$) δ 8.46 (s, 1H), 8.34 (s, 1H), 7.72 (d, *J* = 8.4 Hz, 2H), 7.53 (d, *J* = 8.2 Hz, 2H), 6.86 – 6.78 (m, 2H), 6.61 (d, *J* = 2.1 Hz, 1H), 6.42 – 6.31 (m, 1H), 6.16 (d, *J* = 3.6 Hz, 1H), 4.70 (s, 1H), 4.55 – 4.46 (m, 2H), 4.38 (dd, *J* = 8.8, 5.0 Hz, 1H), 4.18 – 4.13 (m, 2H), 3.93 (s, 2H), 3.81 – 3.75 (m, 1H), 3.61 (br d, *J* = 14.9 Hz, 1H), 3.26 – 3.15 (m, 2H), 2.55 (s, 3H), 2.34 (s, 3H), 2.16 (s, 3H), 1.62 (s, 3H), 1.56 (s, 3H), 1.24 (t, *J* = 7.1 Hz, 3H). ^{13}C NMR (101 MHz, Methanol-*d*$_4$) δ 172.9, 171.0, 151.6, 149.7, 147.1, 139.6, 138.7, 138.3, 136.0, 133.6, 132.7, 131.9, 128.1, 123.6, 119.8, 118.9, 112.0, 91.0, 78.5, 78.5, 73.4, 72.2, 61.6, 55.5, 50.9, 49.6, 39.1, 29.9, 26.1, 24.4, 20.6, 18.8. HRMS (ESI): calculated for $C_{41}H_{51}N_8O_8$ $[M+H]^+$ 783.3830, found 783.3835.

propyl (*S*)-2-(3-(2-acetoxy-4,6-dimethylphenyl)-3-methylbutanamido)-4-((((2*R*,3*S*,4*R*,5*R*)-5-(6-amino-9*H*-purin-9-yl)-3,4-dihydroxytetrahydrofuran-2-yl)methyl)((*E*)-3-(4-cyanophenyl)allyl)amino)butanoate (14d). Following the procedure described for compound **12a**, compound **13d** (10 mg, 0.012 mmol) was deprotected and purified, affording compound **14d** as a white powder (4 mg, 42% yield). ^{1}H NMR (500 MHz, CD_3OD) δ 8.45 (s, 1H), 8.34 (s, 1H), 7.70 (d, *J* = 8.3 Hz, 2H), 7.51 (d, *J* = 8.1 Hz, 2H), 6.85 – 6.78 (m, 2H), 6.60 (d, *J* = 1.8 Hz, 1H), 6.40 – 6.34 (m, 1H), 6.15 (d, *J* = 3.5 Hz, 1H), 4.68 (t, *J* = 4.0 Hz, 1H), 4.52 –4.47 (m, 2H), 4.37 (dd, *J* = 8.6, 5.1 Hz, 1H), 4.04 (t, *J* = 6.7 Hz, 2H), 3.97 –3.89 (m, 2H), 3.79 – 3.74 (m, 1H), 3.64 – 3.57 (m, 1H), 3.24 – 3.17 (m, 2H), 2.79 – 2.70 (m, 2H), 2.67 (d, *J* = 4.2 Hz, 1H), 2.64 (s, 1H), 2.53 (s, 3H), 2.32 (s, 3H), 2.15 (s, 3H), 2.04 – 1.94 (m, 1H), 1.67 – 1.58 (m, 6H), 1.54 (s, 3H), 0.91 (t, *J* = 7.4 Hz, 3H). ^{13}C NMR (126 MHz, CD_3OD) δ 172.9, 171.1, 170.6, 149.8, 139.7, 138.4,

136.1, 133.7, 134.4, 132.0, 127.4, 123.1, 119.9, 118.1, 112.0, 91.1, 78.6, 73.5, 72.3, 67.1, 54.5, 50.9, 49.7, 39.2, 31.1, 30.9, 24.5, 21.6, 20.7, 18.9. HRMS (ESI): calculated for $C_{42}H_{53}N_8O_8$ $[M+H]^+$ 783.3986, found 797.3991.

*iso*propyl (*S*)-2-(3-(2-acetoxy-4,6-dimethylphenyl)-3-methylbutanamido)-4-((((2*R*,3*S*,4*R*,5*R*)-5-(6-amino-9*H*-purin-9-yl)-3,4-dihydroxytetrahydrofuran-2-yl)methyl)((*E*)-3-(4-cyanophenyl)allyl)amino)butanoate (14e). Following the procedure described for compound **12a**, compound **13e** (10 mg, 0.012 mmol) was deprotected and purified, affording compound **14e** as a white powder (5.3 mg, 49% yield). ^{1}H NMR (400 MHz, CD_3OD) δ 8.47 (s, 1H), 8.35 (s, 1H), 7.71 (d, *J* = 8.1 Hz, 2H), 7.53 (d, *J* = 8.1 Hz, 2H), 6.86 – 6.77 (m, 2H), 6.61 (d, *J* = 2.1 Hz, 1H), 6.42 – 6.35 (m, 1H), 6.17 (d, *J* = 3.5 Hz, 1H), 4.72 – 4.66 (m, 1H), 4.54 – 4.49 (m, 2H), 4.33 (dd, *J* = 8.8, 5.0 Hz, 1H), 3.93 (d, *J* = 7.5 Hz, 2H), 3.78 (dd, *J* = 14.0, 9.6 Hz, 1H), 3.62 (d, *J* = 13.8 Hz, 1H), 3.27 – 3.17 (m, 2H), 2.77 (d, *J* = 14.9 Hz, 1H), 2.64 (br d, *J* = 14.9 Hz, 1H), 2.55 (s, 3H), 2.33 (s, 3H), 2.16 (s, 3H), 2.07 – 1.93 (m, 1H), 1.61 (s, 3H), 1.56 (s, 3H), 1.22 (dd, *J* = 6.3, 1.8 Hz, 6H). ^{13}C NMR (101 MHz, CD_3OD) δ 175.2, 171.7, 162.9, 157.1, 150.4, 147.3, 139.6, 138.7, 138.3, 136.0, 134.4, 133.0, 132.3, 131.9, 127.3, 123.0, 119.8, 118.1, 117.7, 114.8, 112.4, 91.1, 77.0, 73.4, 71.7, 69.2, 54.9, 50.9, 50.5, 36.9, 31.0, 29.7, 26.3, 24.4, 20.5, 18.5. HRMS (ESI): calculated for $C_{42}H_{53}N_8O_8$ $[M+H]^+$ 783.3986, found 797.3994.

benzyl *(S)*-2-(3-(2-acetoxy-4,6-dimethylphenyl)-3-methylbutanamido)-4-((((2*R*,3*S*,4*R*,5*R*)-5-(6-amino-9H-purin-9-yl)-3,4-dihydroxytetrahydrofuran-2-yl)methyl)((*E*)-3-(4-cyanophenyl)allyl)amino)butanoate (14f). compound **13f** (13mg, 0.015 mmol) was deprotected and purified, affording compound **14f** as a white powder (5 mg, 39%). ^{1}H NMR (500 MHz, CD_3OD) δ 8.41 (s, 1H), 8.31 (s, 1H), 7.69 (d, *J* = 6.3 Hz, 2H), 7.49 (d, *J* = 8.1 Hz, 2H), 7.33 (d, *J* = 9.1 Hz, 5H), 6.82 – 6.75 (m, 2H), 6.57 (d, *J* = 2.1 Hz, 1H), 6.36 – 6.27 (m, 1H), 6.12 (d, *J* = 3.5 Hz, 1H), 5.12 (d, *J* = 2.9 Hz, 2H), 4.65 (t, *J* = 4.2 Hz, 1H), 4.50 – 4.38 (m, 3H), 3.89 (d, *J* = 11.8 Hz, 2H), 3.76 – 3.70(m, 1H), 3.56 (br d, *J* = 14.6 Hz, 1H), 3.35 (s, 1H), 3.23 – 3.11 (m, 2H), 2.28 (s, 3H), 2.12 (s, 3H), 2.01 – 1.93 (m, 1H), 1.56 (s, 3H), 1.49 (s, 3H). 13C NMR (126 MHz, CD3OD) δ 171.1, 149.8, 139.6, 138.4, 136.1, 133.7, 1132.4, 128.3, 128.1, 123.1, 91.1, 72.3, 67.1, 42.4, 31.7, 24.4, 20.6, 18.9. HRMS (ESI): calculated for $C_{46}H_{52}N_8O_8$ $[M+H]^+$ 844.3908, found 844.3911.

4.2 Ester stability assay

The prodrugs were evaluated for their stability in both PBS buffer at pH 7.4 and Tris buffer at pH 8.4. The compounds were dissolved in DMSO at a concentration of 40 mM and diluted with the respective buffer to a final concentration of 1 mM. Compounds were tested directly (t_0) and

subsequently every 2 hours over a time period of 16 hours by HPLC. Compounds were eluted from a Dr. Maisch reprosil-pur C18 column (4.6 x 250 mm, 10µm) with the following solvent system at a flow rate of 0.5 mL/min: solvent A, 0.1 % trifluoroacetic acid in water/acetonitrile (95:5) ; solvent B, 0.1 % trifluoroacetic acid in water/acetonitrile (5:95). Gradient elution was as follows: 100:0 (A/B) to 0:100 (A/B) over 8 min, 0:100 (A/B) for 1 min, then reversion back to 100:0 (A/B) over 1 min, 100:0 (A/B) for 2 min. The formation of the parent compound was evaluated and normalized by measuring the peak area at 214 nm and comparing it to the initial timepoint.

4.3 Esterase-mediated hydrolysis

The conversion of the prodrugs to the parent compound by esterases was evaluated using pig liver esterase (PLE, 18 U/mg, Sigma-Aldrich) in PBS at pH 7.4. Compounds were dissolved in DMSO at 40 mM, diluted to a final concentration of 2 mM with PBS and added to an equal volume of a 10 mg/mL solution of PLE in PBS (pH 7.4), resulting in final concentrations of 2.5% DMSO, 1 mM compound and 5 mg/mL PLE. At different time-points 50 µL aliquots were taken, added to 100µL acetonitrile to precipitate the proteins and centrifuged for 5 minutes at 10,000 rpm. The supernatant was subsequently analyzed by HPLC as described in section 4.2 above.

4.4 Neon electroporation assay

4.4.1. Cell culture

A549 lung cancer cells were grown in Dulbecco's Modified Eagle's Medium (DMEM) with 10% fetal bovine serum and seeded at 50,000 cells per well in a 48 well plate. After addition of compound (1, 10 or 100µM) or DMSO (0.5%), the cells were electroporated in 10µL Neon transfection tips with 2 pulses with a pulse voltage of 1700 mV and a pulse width of 20ms. Cells were resuspended in 250 mM sucrose buffer with Mg2+ and transferred to 96 well plates (100 µL, 15,000 cells/well) and incubated for 24, 48 or 72 hours at 37 °C with 5% CO2. The cells were subsequently checked for their viability using the MTS cell viability assay and compared to both non-treated cells (DMSO) and non-electroporated cells. All experiments were performed in triplicate.

4.4.2. MTS cell viability assay

Cell proliferation was determined using a colorimetric assay with 3-(4,5-dimethylthiazol-2-yl)-5-(3-carboxymethoxyphenyl)-2-(4-sulfophenyl)-2H-tetrazolium (MTS). The MTS assay measures the conversion of MTS to a water-soluble formazan product by dehydrogenase enzymes of the intact mitochondria of living cells. Cell proliferation was evaluated by measuring the absorbance at 490 nm upon treatment with compounds or DMSO only for 24, 48 and 72 hours. Briefly, medium was aspirated from the cells and MTS in DMEM/FBS medium was added. The

cells were incubated for 1 hour at 37°C. The reaction product was quantified by measuring the absorbance at 490 nm using a plate reader. Experiments were repeated three times. Results were expressed as percentage of the control (control equals 100% and corresponds to the absorbance value of each sample at time zero) and presented as mean values ± standard deviation of three independent experiments performed in triplicate.

4.5 Cell proliferation assay

4.5.1. Cell culture

HSC-2 human oral cancer cell line, T24 human bladder cancer cell line and A549 human lung cancer line were cultured in DMEM/F12 medium, supplemented with 10% fetal bovine serum and 50 μg/ml gentamicin, at 37 °C in a humidified 5% CO2 incubator. For each compound tested, powder was dissolved in DMSO at 100mM concentration. This stock solution was then diluted in culture medium to final concentration values ranging between 1μM and 100μM. For each sample, DMSO was kept constant at 0.1% final concentration. The day before starting treatment, cells were seeded in 96-well plates, at a density of 2,000 cells/well. Cells were allowed to attach overnight and then incubated with compounds at different concentrations, or with DMSO only, for 24, 48 and 72 hours. All experiments were performed in triplicate.

4.5.2. MTT cell viability assay

Cell proliferation was determined using a colorimetric assay with 3-(4,5-dimethylthiazol-2-yl)-2,5-diphenyl tetrazolium bromide (MTT). The MTT assay measures the conversion of MTT to insoluble formazan by dehydrogenase enzymes of the intact mitochondria of living cells. Cell proliferation was evaluated by measuring the conversion of the tetrazolium salt MTT to formazan crystals upon treatment with compounds or DMSO only for 24, 48 and 72 hours. Briefly, cells were incubated for 2 hours at 37 °C with 100 μl fresh culture medium containing 5μl of MTT reagent (5mg/ml in PBS). The medium was removed and 200μl isopropanol were added. The amount of formazan crystals formed correlated directly with the number of viable cells. The reaction product was quantified by measuring the absorbance at 540nm using a plate reader. Experiments were repeated three times. Results were expressed as percentage of the control (control equals 100% and corresponds to the absorbance value of each sample at time zero) and presented as mean values ± standard deviation of three independent experiments performed in triplicate.

4.6. 1-methylnicotinamide (MNA) quantification in A549 cells

4.6.1. Cell culture

Human lung adenocarcinoma line (A549, ATCC, VA, USA) was cultured according to the provider's indications and seeded in 6-well format. After 24h stabilization, when cells reached ≈100% confluence, A549 line was preincubated with normal Hank's buffer (HBSS), then treated with NNMT peptide inhibitors (1 or 10 μM), applied for 1h-incubation in a presence of nicotinamide 100 μM ans S-adenosyl-mehionine 10 μM (Sigma Aldrich. MO, USA). After incubation, effluent samples were taken and frozen (-80 °C) for further MNA measurement. Cells also were collected, centrifuged (2 x 500 G/5 min.) and frozen both for the measurement of intracellular MNA and for BCA protein assay.

4.6.2. Quantification of 1-methylnicotinamide (MNA)

The quantification of 1-methylnicotinamide (MNA), nicotinamide (NAM), nicotinic acid (NicA), 1-methyl-2-pyridone-5-carboxamide (Met-2Pyr) and 1-methyl-4-pyridone-5-carboxamide (Met-4Pyr) was performed applying ultra-high pressure liquid chromatography coupled to tandem mass spectrometry (UPLC-MS) according to the methodology previously described with minor modifications. An UPLC-MS system comprised of an UPLC Ultimate 3000 (Dionex, Thermo Scientific, USA) connected to a TSQ Quantum Ultra mass spectrometer (Thermo Scientific, USA) equipped with a heated electrospray ionization interface (HESI-II Probe) was used. Chromatographic separation of analytes was carried out on an Aquasil C18 analytical column (4.6 mm x 150 mm, 5 mm; Thermo Scientific) under isocratic elution using acetonitrile with 0.1% of formic acid (A) and 5 mM ammonium formate in water (B) as mobile phases delivered at the flow rate of 0.8 ml/min (A:B, 80:20, v/v). The cell pellet was resuspended in 60 μL of deionized water and 50 μL of suspension was transferred to a fresh test tube. 50 μl of effluent sample was used for the measurement of extracellular MNA. The internal standard (IS) containing MNA-d_3 was added to each sample (5 μL) obtaining the final concentration of 500 ng/mL. After the sample mixing, the proteins were precipitated using 100 μL of acidified acetonitrile (0.1% of formic acid), and samples were mixed (10 min), cooled at 4 °C (15 min) and finally centrifuged (15 000 x g, 15 min, 4 °C). A clear supernatant was transferred to a chromatographic vial and directly injected (5 μL) into UPLC-MS system. The mass spectrometer was operating in the positive ionisation mode using selected reactions monitoring (SRM) mode monitoring the following ion transitions for analysed metabolite: m/z 137→ 94 for MNA and 140 → 97 for MNA-d3. The concentration of MNA was calculated based on the calibration curve plotted for the analyte as the relationship between the peak area ratios of analyte/IS to the nominal concentration of the analyte. The concentration of analytes was normalized to milligram of proteins, which was assessed using Pierce™ BCA Protein Assay Kit (Thermo Fisher, Waltham, MA, USA) and a Synergy4 multiplate reader (BioTek, Winooski, VT, USA). MNA was obtained from Sigma-Aldrich, and the deuterated internal standard MNA-d_3 was

synthesized by Dr. Adamus (Technical University, Lodz, Poland). LC-MS–grade acetonitrile, ammonium formate and formic acid were purchased from Sigma-Aldrich. Ultrapure water was obtained from a Millipore system (Direct-Q 3UV).

4.7 Statistical Analysis

Data were analysed using GraphPad Prism software for Windows (GraphPad Software, San Diego, CA). Significant differences between groups were determined using the one-way analysis of variance (ANOVA). A p value <0.05 was considered as statistically significant.

5. References

1. Martin JL, McMillan FM. SAM (dependent) I AM: the S-adenosylmethionine-dependent methyltransferase fold. Curr Opin Struct Biol. 2002;12(6):783-93.
2. Aksoy S, Szumlanski CL, Weinshilboum RM. Human liver nicotinamide N-methyltransferase. cDNA cloning, expression, and biochemical characterization. J Biol Chem. 1994;269(20):14835-40. http://www.ncbi.nlm.nih.gov/pubmed/8182091
3. van Haren MJ, Sastre Toraño J, Sartini D, Emanuelli M, Parsons RB, Martin NI. A Rapid and Efficient Assay for the Characterization of Substrates and Inhibitors of Nicotinamide N -Methyltransferase. Biochemistry. 2016;55(37):5307-15.
4. Tomida M, Ohtake H, Yokota T, Kobayashi Y, Kurosumi M. Stat3 up-regulates expression of nicotinamide N-methyltransferase in human cancer cells. J Cancer Res Clin Oncol. 2008;134(5):551-9.
5. Kim J, Hong SJ, Lim EK, Yu Y, Kim SW, Roh JH, et al. Expression of nicotinamide N-methyltransferase in hepatocellular carcinoma is associated with poor prognosis. J Exp Clin Cancer Res. 2009;28(1):20.
6. Zhang J, Wang Y, Li G, Yu H, Xie X. Down-Regulation of Nicotinamide N-methyltransferase Induces Apoptosis in Human Breast Cancer Cells via the Mitochondria-Mediated Pathway. Filleur S, ed. PLoS One. 2014;9(2):e89202.
7. Markert JM, Fuller CM, Gillespie GY, Bubien JK, McLean LA, Hong RL, et al. Differential gene expression profiling in human brain tumors. Physiol Genomics. 2001;2001(5):21-33.
8. Xu J, Moatamed F, Caldwell JS, Walker JR, Kraiem Z, Taki K, et al. Enhanced Expression of Nicotinamide N-Methyltransferase in Human Papillary Thyroid Carcinoma Cells. J Clin Endocrinol Metab. 2003;88(10):4990-6.
9. Yu T, Wang YT, Chen P, Li YH, Chen YX, Zeng H, et al. Effects of nicotinamide n-methyltransferase on PANC-1 cells proliferation, metastatic potential and survival under metabolic stress. Cell Physiol Biochem. 2015;35(2):710-21.
10. Jung J, Kim LJY, Wang X, Wu Q, Sanvoranart T, Hubert CG, et al. Nicotinamide metabolism regulates glioblastoma stem cell maintenance. JCI Insight. 2017;2(10):1-23.
11. Lim BH, Cho BI, Yu NK, Jae WK, Park ST, Lee CW. Overexpression of nicotinamide N-methyltransferase in gastric cancer tissues and its potential post-translational modification. Exp Mol Med. 2006;38(5):455-65.
12. Ulanovskaya OA, Zuhl AM, Cravatt BF. NNMT promotes epigenetic remodeling in cancer by creating a metabolic methylation sink. Nat Chem Biol. 2013;9(5):300-6.
13. Eckert MA, Coscia F, Chryplewicz A, Chang JW, Hernandez KM, Pan S, et al. Proteomics

reveals NNMT as a master metabolic regulator of cancer-associated fibroblasts. Nature. 2019;569(7758):723-8.

14. Kilgour MK, MacPherson S, Zacharias LG, Ellis AE, Sheldon RD, Liu EY, et al. 1-Methylnicotinamide is an immune regulatory metabolite in human ovarian cancer. Sci Adv. 2021;7(4):eabe1174.
15. van Haren MJ, Taig R, Kuppens J, Sastre Toraño J, Moret EE, Parsons RB, et al. Inhibitors of nicotinamide N-methyltransferase designed to mimic the methylation reaction transition state. Org Biomol Chem. 2017;15(31):6656-67.
16. Babault N, Allali-Hassani A, Li F, Fan J, Yue A, Ju K, et al. Discovery of Bisubstrate Inhibitors of Nicotinamide N -Methyltransferase (NNMT). J Med Chem. 2018;61(4):1541-51.
17. Gao Y, van Haren MJ, Moret EE, Rood JJM, Sartini D, Salvucci A, et al. Bisubstrate Inhibitors of Nicotinamide N -Methyltransferase (NNMT) with Enhanced Activity. J Med Chem. 2019;62(14):6597-614.
18. Policarpo RL, Decultot L, May E, Kuzmič P, Carlson S, Huang D, et al. High-Affinity Alkynyl Bisubstrate Inhibitors of Nicotinamide N -Methyltransferase (NNMT). J Med Chem. 2019;62(21):9837-73.
19. Chen D, Li L, Diaz K, Iyamu ID, Yadav R, Noinaj N, et al. Novel Propargyl-Linked Bisubstrate Analogues as Tight-Binding Inhibitors for Nicotinamide N-Methyltransferase. J Med Chem. 2019;62(23):10783-97.
20. Kemnitz CR, Loewen MJ. "Amide Resonance" Correlates with a Breadth of C–N Rotation Barriers. J Am Chem Soc. 2007;129(9):2521-8.
21. Mujika JI, Mercero JM, Lopez X. Water-Promoted Hydrolysis of a Highly Twisted Amide: Rate Acceleration Caused by the Twist of the Amide Bond. J Am Chem Soc. 2005;127(12):4445-53.
22. Mahesh S, Tang K-C, Raj M. Amide Bond Activation of Biological Molecules. Molecules. 2018;23(10):2615.
23. Amsberry KL, Borchardt RT. The lactonization of 2'-hydroxyhydrocinnamic acid amides: a potential prodrug for amines. J Org Chem. 1990;55(23):5867-77.
24. Amsberry KL, Gerstenberger AE, Borchardt RT. Amine Prodrugs Which Utilize Hydroxy Amide Lactonization. Pharm Res. 1991;8(4):455-61.
25. Kannt A, Rajagopal S, Kadnur SV, Suresh J, Bhamidipati RK, Swaminathan S, et al. A small molecule inhibitor of Nicotinamide N-methyltransferase for the treatment of metabolic disorders. Sci Rep. 2018;8(1):3660.

26. Neelakantan H, Brightwell CR, Graber TG, Maroto R, Wang H-YL, McHardy SF, et al. Small molecule nicotinamide N-methyltransferase inhibitor activates senescent muscle stem cells and improves regenerative capacity of aged skeletal muscle. Biochem Pharmacol. 2019;163(January):481-92.
27. Watanabe T, Kawabata T. Asymmetric dieckmann condensation via memory of chirality: synthesis of the key intermediate for as-3201, an aldose reductase inhibitor. Heterocycles. 2008;76(2):1593-606.
28. Mandal PK, McMurray JS. Pd-C-induced catalytic transfer hydrogenation with triethylsilane. J Org Chem. 2007;72(17):6599-601.
29. Bitta J, Kubik S. Cyclic Hexapeptides with Free Carboxylate Groups as New Receptors for Monosaccharides. Org Lett. 2001;3(17):2637-40.
30. Winiecka I, Dudkiewicz-Wilczyńska J, Roman I, Paruszewski R. New potential renin inhibitors with dipeptide replacements in the molecule. Acta Pol Pharm. 67(4):367-74. http://www.ncbi.nlm.nih.gov/pubmed/20635532
31. Sharnabai KM, Nagendra G, Vishwanatha TM, Sureshbabu V V. Efficient synthesis of N-protected amino/peptide Weinreb amides from T3P and DBU. Tetrahedron Lett. 2013;54(6):478-82.
32. Shekharappa M, Roopesh Kumar L, Sureshbabu V V. One-pot synthesis of Weinreb amides employing 3,3-dichloro-1,2-diphenylcyclopropene (CPI-Cl) as a chlorinating agent. Synth Commun. 2019;49(6):790-8.

Chapter 5

Bisubstrate inhibitors of nicotinamide *N*-methyltransferase bearing warheads for covalent interaction with cysteine and serine residues

Manuscript in preparation

Abstract

Nicotinamide *N*-methyltransferase (NNMT) catalyses the methylation of nicotinamide using the cofactor *S*-adenosyl-L-methionine (SAM) as a methyl donor. NNMT has been implicated in various diseases, including cancer and metabolic disorders. Therefore, potent, and selective NNMT inhibitors are valuable tools to study the biological functions and therapeutic potential of NNMT. Covalent inhibition is a rapidly growing discipline within drug discovery. Here, we describe our efforts to design covalent inhibitors targeting non-catalytic cysteine residues (C159 and C165) and serine residues (S201 and S213) involved in substrate binding in the NNMT active site. Acrylamides and chloroacetamides were used as warheads to target the cysteine residues and sulfonyl fluoride and boronic acid groups were used to target serine. After linker optimization, a chloroacetamide-containing inhibitor gave good inhibition of NNMT (compound **17b**, IC_{50} = 400 nM) and was found to be the first example of a potent NNMT bisubstrate type inhibitor lacking the amino acid motif present in SAM. The replacement of the aromatic nitrile in lead compound **17u** (chapter 3) with a sulfonyl fluoride at either the *meta*- or *para*-position gave potent inhibition of NNMT with IC_{50} values of 68-89 nM for compounds **39a** and **39b**. Modelling data predicts that the distance and orientation of the sulfonyl fluoride moieties may allow for covalent interaction with active site serine residues Experiments to further characterize the mechanistic details of these inhibitors are currently ongoing.

1. Introduction

Nicotinamide *N*-methyltransferase (NNMT) is a key cytoplasmic enzyme in the human body, which is responsible for the methylation of the nicotinamide (NA), using *S*-adenosyl-L-methionine (SAM) as the methyl donor.[1–3] The physiological function of NNMT is related to various human diseases in the past years. The main functions of NNMT were assumed to be linked to NA metabolism and xenobiotic detoxification of endogenous metabolites. However, the role that NNMT plays in human health and disease is becoming more apparent and seems to be much more complex.[4] Overexpressed NNMT has been observed in various disorders, including cardiovascular disease,[5,6] metabolic disorders,[7–9] neurodegenerative disease,[10,11] and cancer.[12–16] It seems that NNMT has a role in regulating epigenetic modifications and signal transduction, making it a promising and valuable therapeutic target.[17,18] Given the increased interest in NNMT as a potential therapeutic target, a variety of NNMT inhibitors have recently been disclosed, including SAM-competitive inhibitors, nicotinamide-competitive inhibitors, bisubstrate inhibitors, natural product inhibitors, peptides inhibitors, and covalent inhibitors.[19] Generally speaking, covalent inhibitors have several potential advantages, including sustained duration of action, increased ligand efficiency, the ability to overcome endogenous ligands, optimized capability to avoid resistant mutations, and increased selectivity of some clinically isolated variants.[20]

In this chapter, we aimed to expand upon the available set of bisubstrate NNMT inhibitors developed in our group (**chapters 2 and 3**) by the introduction of covalent warheads. The active site of NNMT contains several non-catalytic cysteine residues, specifically C159 and C165, which can be targeted for covalent modification. In addition, the NA substrate pocket of NNMT contains two important, but non-essential active site serine residues (S201 and S213) which are involved in the interaction of the amide moiety of NA. Mutation of these cysteine and serine residues to alanine does not impair the activity of the enzyme.[21–23] Previous work by Cravatt and co-workers has also demonstrated the feasibility of covalent inhibition of NNMT.[22] In their work, an activity-based protein profiling study was performed using probes based on *S*-adenosyl-L-homocysteine (SAH), the biproduct of the NNMT enzymatic methylation reaction, to profile methyltransferases in various human cancer cell lines (renal carcinoma 769P, ovarian cancer OVCAR3, and melanoma MUM2C). Subsequently, the SAH-probe was used as a fluorescence polarization (FP) probe to screen a set of electrophilic fragments identifying the first covalent NNMT inhibitor (RS004 (**1**), Figure 1) which displayed an IC_{50} value of 10 μM. Through mutation of active site cysteine residue C165 to alanine, the compound was confirmed to covalently engage with this residue.[22] The structure of RS004 was optimized through a structure-activity relationship (SAR) study, resulting in the more potent compounds HS58a (**2**) and HS312 (**3**) which showed

submicromolar IC_{50} values (Figure 1).[24] In an alternative approach, Sen et al. reported 4-chloropyridine analogs (**4-6**) as NNMT suicide substrates. Upon NNMT mediated *N*-methylation of the chlorinated substrates, the now positively charged pyridine ring enhances the electrophilicity of the C4 position, thereby facilitating an aromatic nucleophilic substitution by the non-catalytic C159 residue.[23] In a third approach, Resnick et al. described the high-throughput screening of ca. 1000 electrophilic fragments against cysteine-containing enzymes, identifying several fragments that covalently modified NNMT (compounds **7-9**).[25] However, when we evaluated these compounds using our in-house NNMT inhibition assay, none of them showed significant NNMT inhibition when tested at a concentration of 100 µM (unpublished data).

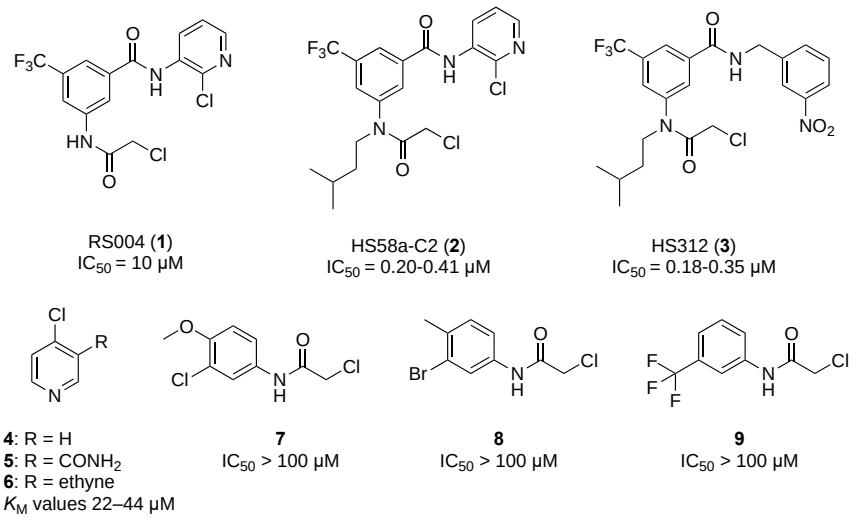

Figure 1. The structures of published covalent NNMT inhibitors featuring the chloroacetamide moiety as a warhead (compounds **1-3** and **7-9**). Compounds **4-6** are substrates which become covalent modifiers of an active site cysteine upon NNMT-mediated methylation.

Compound Design

The crystal structure of NNMT bound to its natural substrate NA and the product of the enzymatic reaction SAH (PDB ID: 3ROD) reveals multiple interactions with active site residues, including cysteine C165 that interacts with the ribose oxygen, and serine residues S201 and S213 that interact with the carbonyl of the NA substrate (Figure 2A).[21] Notably, results of a modelling study performed with the very potent NNMY inhibitor **17u** (**chapter 3**) suggest that the nitrile group is interacting with two active site serine residues (S201 and S213, Figure 2B).

In an NMR-based activity assay Gilbert et al. measured the reactivity of various covalent warheads against serine and cysteine residues: the two most common residues targeted for covalent inhibition.[26] Building from this information, as well as from the structures of recdently reported covalent NNMT inhibitors (Figure 1), we selected the acrylamide and chloroacetamide

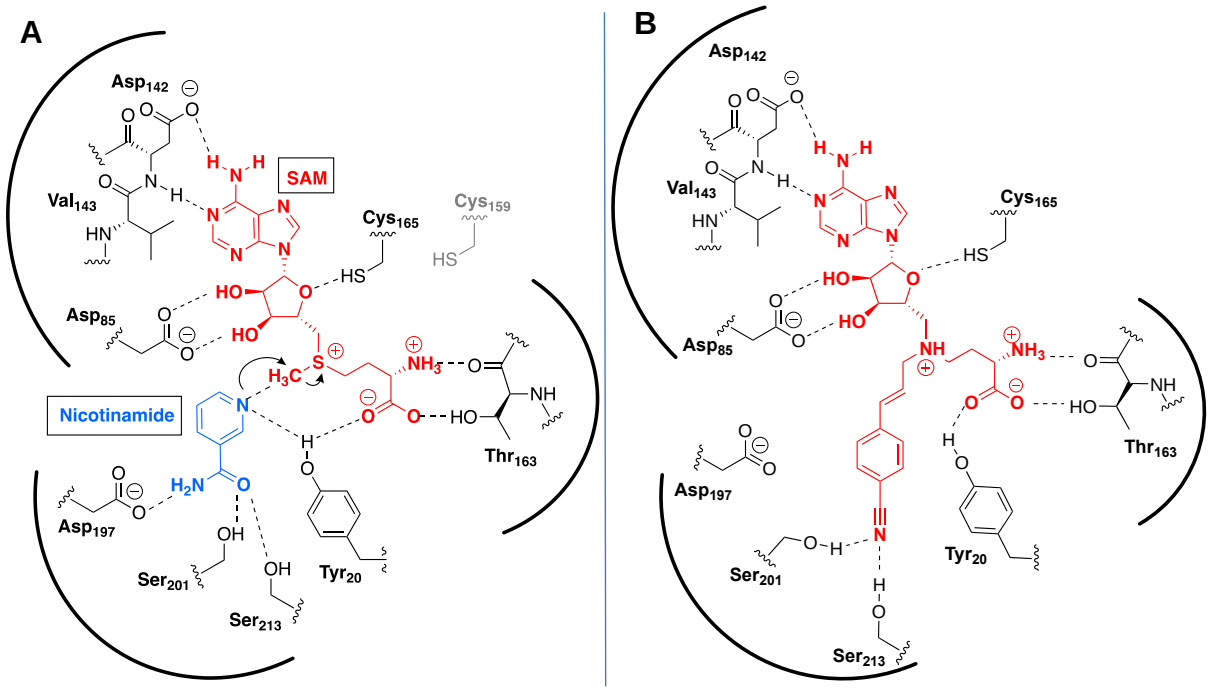

Figure 2. Schematic overview of the active site of NNMT. A) Interactions of active site residues with substrate NA and product SAH indicating the presence of cysteine residues C159 and C165 and serine residues S201 and S213. B) Compound **17u** (**chapter 3**) modelled in the active site of NNMT

moieties as Michael acceptor "warheads" in an attempt to target cysteine residues C159 and C165. In search of other warheads to covalently modifying serine residues S201 and S213, we selected the boronic acid and sulfonyl fluoride moieties. The boronic acid motif is found in a variety of clinically approved drugs, like Bortezomib, Tavaborole, and Vaborbactam, which have been approved for treatment of cancer and fungal infections, and bacterial infections.[27] The boric acids form a reversible covalent interaction with serine or threonine residues in their protein targets. The use of the sulfonyl fluoride moiety as a covalent warhead was first reported by Fahrney,[28] and was subsequently broadly investigated as a covalent warhead for protein modification. As a covalent warhead, sulfonyl fluorides show good reactivity towards active site serine residues and as such are often used in protease inhibitors. Furthermore, sulfonyl fluorides are known to interact with threonine, lysine, tyrosine, cysteine and histidine residues.[29] This feature may help in identifying other residues in NNMT that can be targeted for covalent inhibition.

Based on the structural and modelling data available, our design of covalent bisubstrate NNMT inhibitors focussed on the introduction of the acrylamide and chloroacetamide moieties in place of the amino acid functionality as well as the introduction of boronic acid and sulfonyl fluoride warheads on the aromatic ring in the substrate pocket (Figure 3). The Michael acceptors

were incorporated with a variety of linkers to probe the optimal length and rigidity for the position of the warheads. The warheads on the aromatic ring were investigated at both the meta and para-position. as both para-cyano and meta-amide lead compounds **17u** and **17v** (Figure 3) showed potent inhibition of NNMT and are predicted to interact with serine residues S201 and S213.

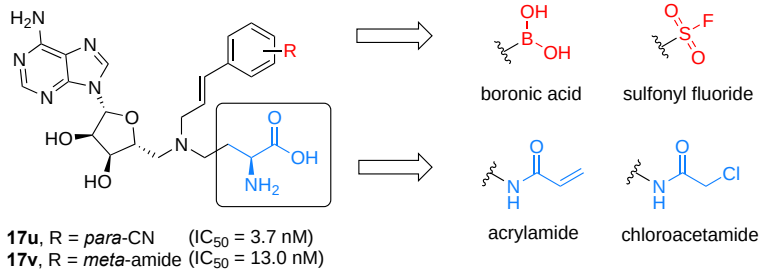

Figure 3. The design of the covalent NNMT inhibitors was based on the structure of lead compounds **17u** and **17v**, which were modified to target active site serine residues with boronic acids and sulfonyl fluoride motifs (red) or modified with acrylamide and chloroacetamide motifs to target active site cysteine residues.

Synthesis of cysteine targeting compounds

Using our modular double reductive amination procedure, we first prepared compounds **12a-d** to investigate the role of the aromatic sidechain and the choice of warhead. In this route, 5'-amino-5'-deoxy-2',3'-O-isopropylideneadenosine **10a** or the propenyl-4-cyanophenyl linked compound **10b** was treated with acryloyl chloride or chloroacetyl chloride to obtain intermediates **11a-d** which were subsequently deprotected using TFA and purified by preparative HPLC to give final compounds **12a-d** (Scheme 1). Unfortunately, compounds **12a-c** did not show any measurable activity against NNMT and compound **12d** showed only poor inhibition with an IC_{50} of 45.76 ± 2.07 μM. These findings hinted at the importance of the aromatic sidechain and the

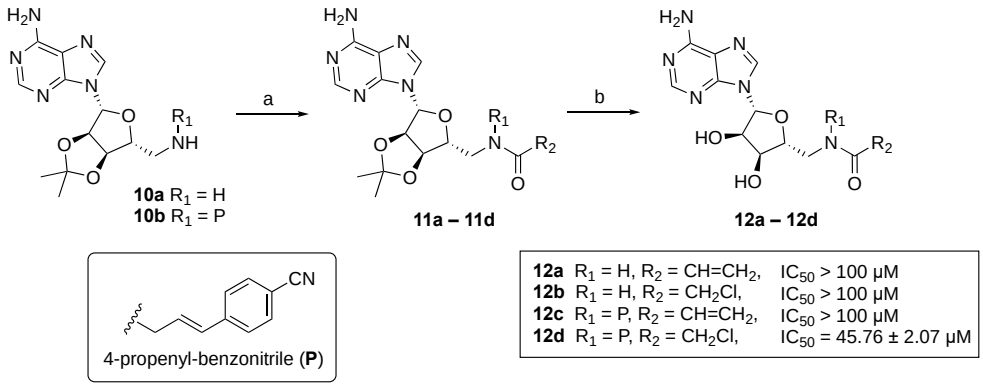

Scheme 1. Synthetic Route for compounds **12a – 12d**. Reagents and conditions: (a) acryloyl chloride or chloroacetyl chloride, DIPEA, DCM, 2h; (b) TFA, DCM, H_2O, rt. 2h (two steps, 18 – 38%).

need to optimize the spacing of the warhead.

We then prepared compounds **17a-17f** (Scheme 2), in which the propenyl-4-cyanophenyl was maintained and the linker between the central nitrogen and the warhead was varied from 2 to 4 carbons. Starting from compound **1b**, aldehydes **13a-c** were coupled to offer intermediates **14a-c**. Next, the Boc-group was removed selectively using water-free acidic conditions and the corresponding amines **15a-c** coupled with acryloyl chloride or chloroacetyl chloride. Finally, the isopropylidene group was cleaved using aqueous acidic conditions and the crude products were purified to yield compounds **17a-f**. For acrylamide **17a** only moderate activity was observed (IC_{50} = 20.98 ± 1.06 μM) while compounds **17c** and **17e** bearing longer spacers, showed no inhibition of NNMT. The chloroacetamides, however, showed more promising results with increasing activity with decreasing spacer length. While no activity was observed for compound **17f**, compound **17d** exhibited moderate activity (IC_{50} = 11.86 ± 0.53 μM), which was further improved in the case of compound **17b**, which exhibits sub-micromolar inhibition of NNMT (IC_{50} = 0.40 ± 0.01 μM). Notably, this is the first example of a bisubstrate inhibitor of NNMT in which the amino acid functionality is replaced by a less polar functionality while retaining significant activity.

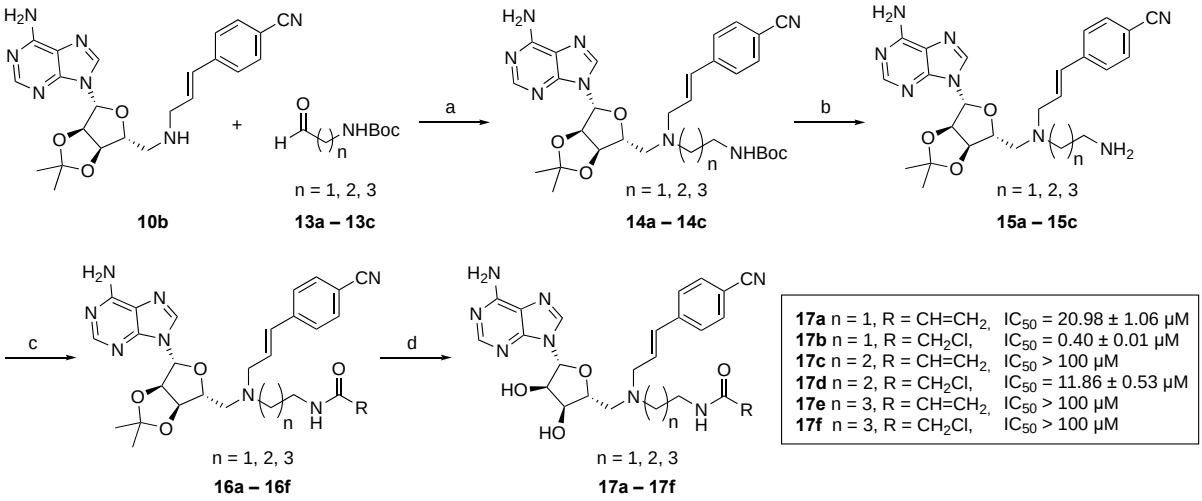

Scheme 2. Synthetic route for compounds **17a – 17f**. Reagents and conditions: (a) $NaBH(OAc)_3$, DCE, AcOH (65-72% yield); (b) TFA, dry DCM; (c) acryloyl chloride or chloroacetyl chloride, DIPEA, DCM (d) TFA, DCM, H_2O, rt. 2h (18-47% yield, 3 steps).

Building on the promising results obtained with compound **17b,** we next focussed on the further optimization of the linker. Instead of the linear linkers, we investigated a series of 4-, 5- or 6-membered cyclic linkers (Scheme 3 and 4). To synthesize these compounds, amine **1b** was subjected to reductive amination with ketones **18a-c** (Scheme 3) or aldehyde **23** (Scheme 4). As

before, the Boc group was then selectively deprotected and the resulting amine coupled to acryloyl chloride or chloroacetyl chloride to form intermediates **21a-f** and **26a-b** which were then deprotected and purified to give final compounds **22a-f** and **27a-b**. For the chloroacetamide-containing compounds, no improvement in activity was found with the best results found for compound **27b** (IC_{50} = 19.77 ± 0.96 μM). For the acrylamides however, compounds **22e** (IC_{50} = 8.46 ± 0.40 μM), and **27a** (IC_{50} = 4.16 ± 0.32 μM), now showed low micromolar inhibition.

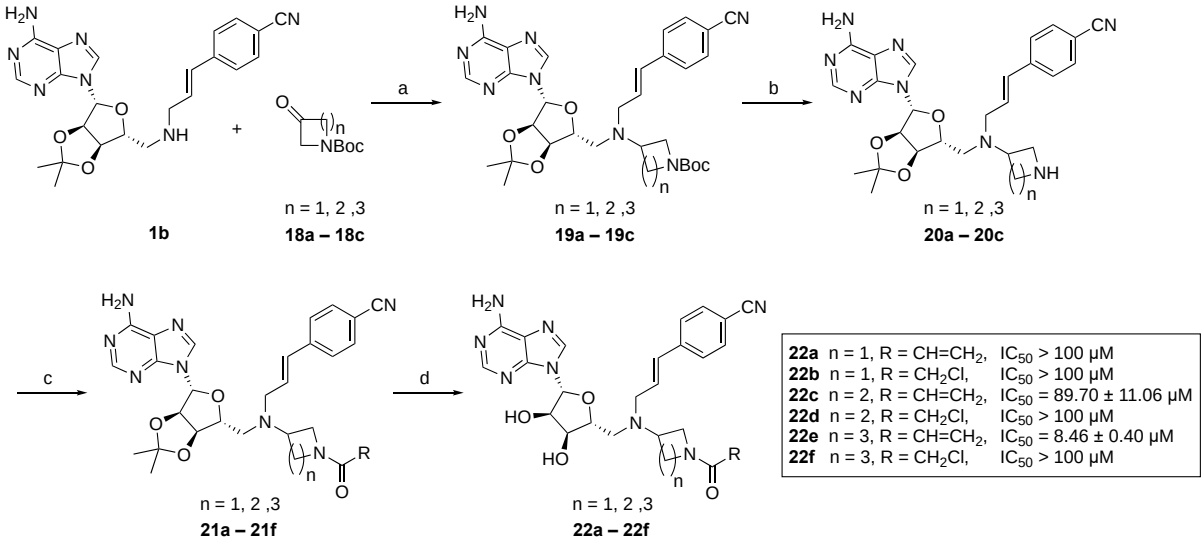

Scheme 3. Synthetic route for compounds **22a – 22f.** Reagents and conditions: (a) $NaBH(OAc)_3$, DCE, AcOH (17-63% yield); (b) TFA, dry DCM; (c) acryloyl chloride or chloroacetyl chloride, DIPEA, DCM (d) TFA, DCM, H_2O, rt. 2h (23-39% yield, 3 steps) .

To investigate aromatic linkers, a benzyl-based moiety was introduced bearing the

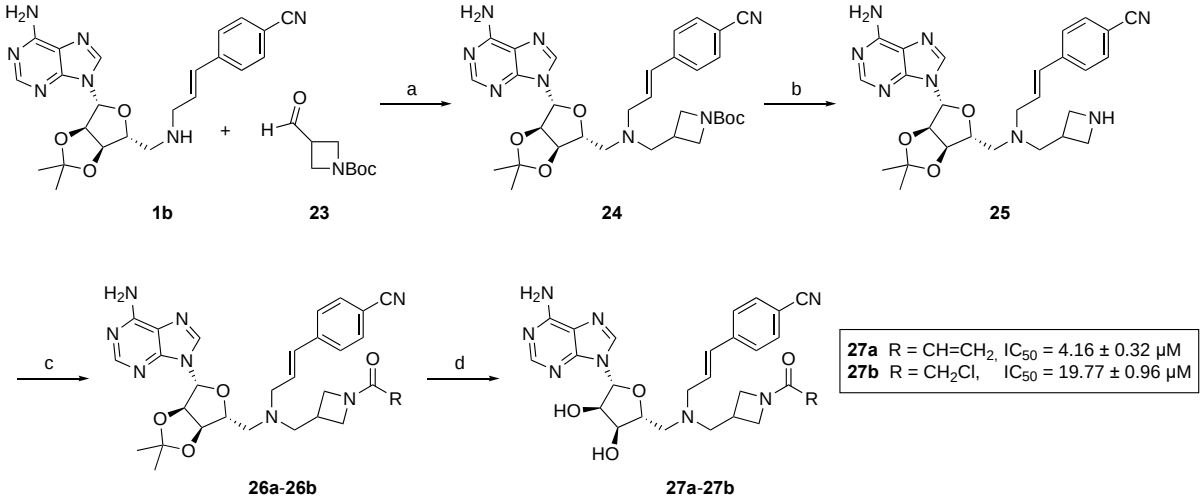

Scheme 4. Synthetic route for compounds **27a – 27b**. Reagents and conditions: (a) $NaBH(OAc)_3$, DCE, AcOH, (35%); (b) TFA, dry DCM; (c) acryloyl chloride or chloroacetyl chloride, DIPEA, DCM (d) TFA, DCM, H_2O, rt. 2h (20–28%, over 3 steps).

acrylamide or chloroacetamide warhead at the *ortho*, *meta* or *para* position (Scheme 5). To this end, compound **1b** was coupled with *tert*-butyl 4-formylphenylcarbamates **28a-c**. As before, the Boc group was selectively deprotected and the resulting anilines **29a-c** coupled to acryloyl chloride or chloroacetyl chloride to form intermediates **30a-f**. Final deprotection and purification gave compounds **31a-f**. Unfortunately, the introduction of the aromatic ring did not improve the activity of the compounds.

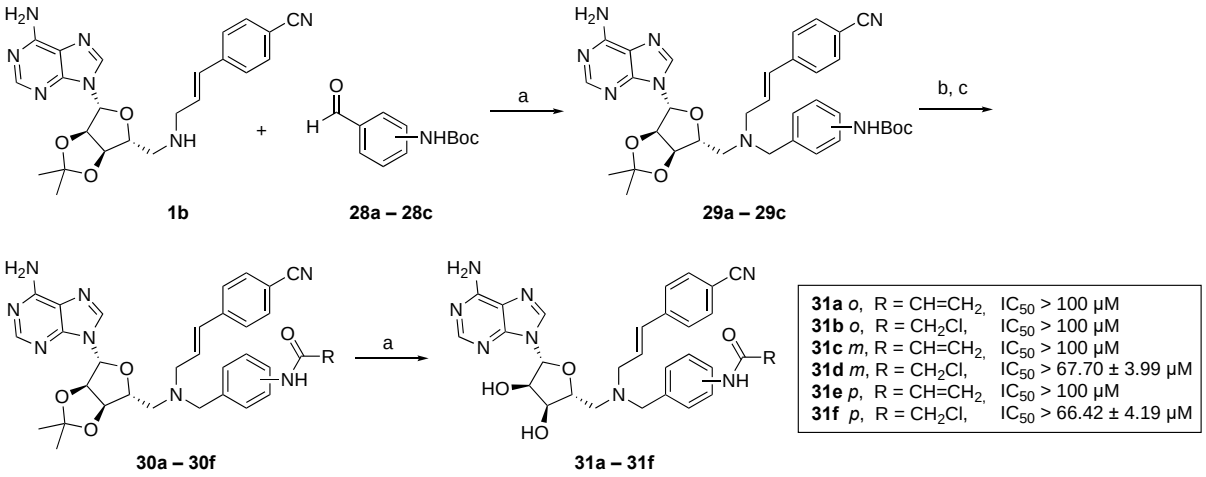

Scheme 5. Synthetic route for compounds **31a – 31f**. Reagents and conditions: (a) $NaBH(OAc)_3$, DCE, AcOH (21 – 56% yield); (b) TFA, dry DCM; (c) acryloyl chloride or chloroacetyl chloride, DIPEA, DCM (d) TFA, DCM, H_2O, rt. 2h (22-41% yield, 3 steps).

As noted above, in our attempts to develop covalent bisubstrate NNMT inhibitors, compound **17b** was identified as the most potent compound and bears the chloroacetamide moiety in place of the amino acid functionality. Ongoing work is focussing on establishing the proposed covalent mechanism of this inhibitor both by whole protein mass spectrometry to analyse the formation of the enzyme-inhibitor adduct as well as biochemical assays using enzyme mutants in which one or more of the target cysteine residues is mutated to an alanine. For these experiments we recently obtained the C159A, C165A and C159A/C165A mutants, all of which are catalytically still active. Should a covalent interaction with either of these cysteine residues play a covalent role in the activity of 17b, the activity of the inhibitor would be expected to be reduced against the mutant enzyme.

Synthesis of serine targeting compounds

For the serine-targeting compounds containing the sulfonyl fluoride warheads, commercially available methylbenzenesulfonyl chlorides **32a-b** were brominated with benzoyl peroxide (BPO) and *N*-bromo-succinimide to form bromomethylbenzenesulfonyl chlorides **33a-b** and subsequently converted to the corresponding sulfonyl fluorides **34a-b** using hydrogen fluoride (Scheme 6). Compounds **34a-b** were then oxidized directly using *N*-methylmorpholine *N*-oxide (NMO) in the presence of 4Å molsieves to offer the corresponding aldehydes **35a-b** which were extended via a Wittig reaction to obtain cinnamic aldehydes **36a-b**. The aldehydes were coupled with amine **37** via a reductive amination reaction to obtain intermediates **38a-b** and after deprotection using TFA and purification by preparative HPLC, final compounds **39a-b** were obtained.

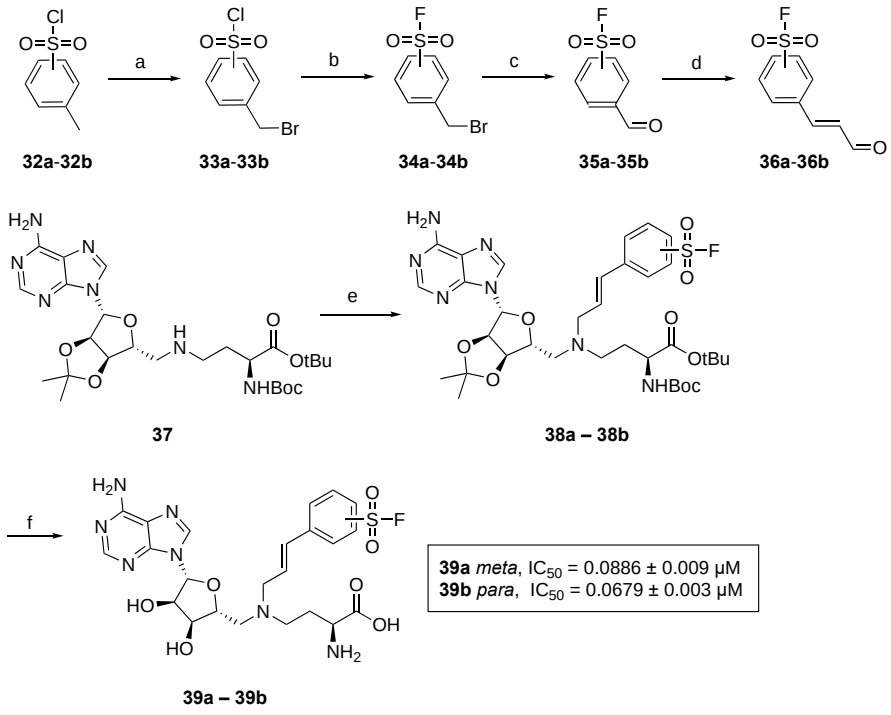

Scheme 6. Synthetic route for compounds **39a** – **39b**. Reagent and conditions: (a) Benzoyl peroxide, N-bromosuccinimide, ACN, reflux (8-25%); (b) HF.KF, H_2O/ACN, rt, (31-80%); (c) *N*-methylmorpholine *N*-oxide, 4Å molsives, ACN, rt (50-75%); (d) PPh_3=CHCHO, THF, 50°C, overnight (44 – 67%); (e) **36a** or **36b**, $NaBH(OAc)_3$, DCE, AcOH (67% – 71%); (f) TFA, DCM, H_2O, rt, 2h (71– 82%).

When evaluating the sulfonyl fluoride compounds, we found that incorporation of the sulfonyl fluoride at either the *meta*- and *para*-position relative to the alkene linker, both resulted in potent inhibition of NNMT with IC_{50} values of 89 and 68 nM respectively. Until now, the position on the aromatic ring at which a substitution was incorporated had a significant impact

into its activity. However, for compounds **39a** and **39b**, no significant difference is observed. Experiments are ongoing to establish the mode of action of these inhibitors. Specifically, looking into the covalent nature of the mechanism through whole protein MS and biochemical assays. For these experiments we have obtained the single and double serine-to-alanine mutants (S201A, S213A, S201A/S213A), all of which are catalytically still active. Should a covalent interaction with either of these serine residues play a role in the mechanism of action for 39a or 39b, the activity of the compound(s) will likely be significantly impacted against NNMT mutants wherein these serine residues are exchanged for alanine.

For the synthesis of the boronic acid containing compounds, we started from pinacolatoboron aldehydes **40a-b** which were extended via Wittig reaction to obtain cinnamic aldehydes **41 (**Scheme 7). The aldehydes were subsequently coupled with amine **37** to offer compounds **42a-b**. The pinacol protecting groups were cleaved under oxidative conditions using $NaIO_4$ yielding compounds **43a-b**. Final compounds **44a-b** were obtained by global deprotection of the acid-labile protecting groups using TFA.

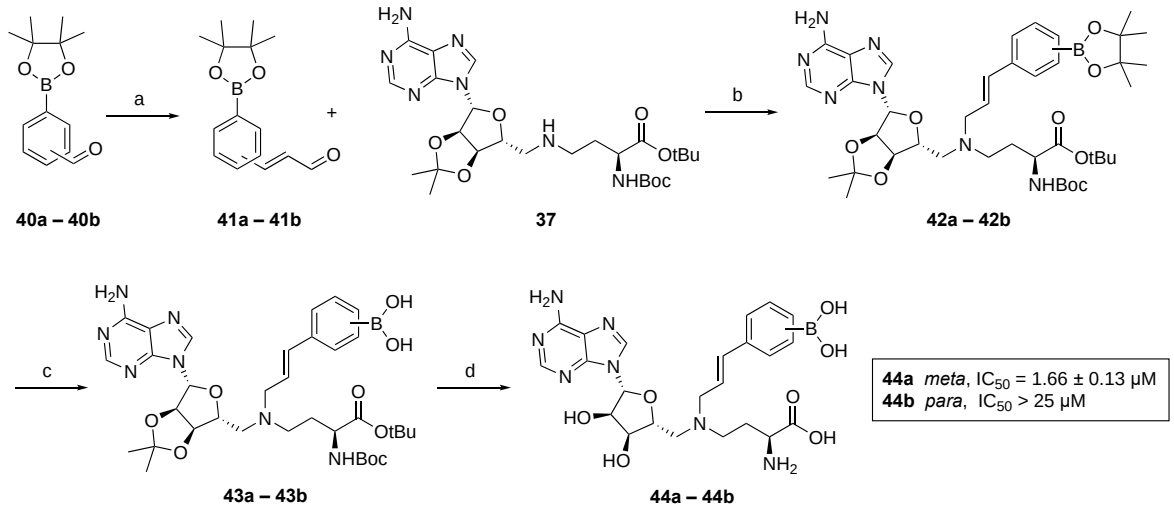

Scheme 7. Synthetic route for compounds **44a – 44b.** Reagent and conditions: (a) PPh_3=CHCHO, THF, 50 °C, overnight (15 – 36%); (b) $NaBH(OAc)_3$, DCE, AcOH (37 – 44%) ; (c) $NaIO_4$, 0.2 M HCl(aq), THF, 2h ; (d) TFA, DCM, H_2O, rt, 2h (17 – 38%, over two steps).

The analysis of boronic acid substituted compounds **44a-b** revealed a steep SAR with no appreciable inhibition observed for para-substituted boronic acid **44b**, but low micromolar inhibition seen for meta-substituted boronic acid **44a (**IC_{50} value of 1.66 ± 0.13 µM). This is the same trend as observed for the amide substituted compounds (**chapter 3**), which could suggest that the boronic acids are mimicking the amide functional group, only less efficiently. To evaluate

the mode of action of the boronic acid analogues, the compounds will be evaluated in biochemical assays using the serine-to-alanine mutants of NNMT as described above.

Modelling Studies

To further explore how the inhibitors described in this chapter might bind within the NNMT active site, docking studies were carried out using Autodock Vina[30]. Using available crystal structures of NNMT bound to previously reported bisubstrate inhibitor LL320 (PDB ID: 6PVS),[31] compounds **17b**, **39a-b**, and **44a-b** were docked in the NNMT active site. Overlaying compound **17b** with the ligand LL320 show good overlay, but no hydrogen bonding interactions are predicted for the chloroacetamide moiety binding in the amino acid pocket. In addition, it seems that the covalent warhead of compound **17b** does not have the correct spacing and orientation to engage with cysteine residues C159 or C165 in the NNMT active site. The distance between the α-carbon of the chloroacetamide and the sulphur atom of C165 is around 8.2 Å in the overlay and cysteine C159 is located even further away. These distances would be too large to be able to form a covalent interaction (Figure 4). Nevertheless, compound **17b** still shows good NNMT inhibition, which indicates that the chloroacetamide warhead is well accommodated in the active site, e.g. through hydrophobic interactions.

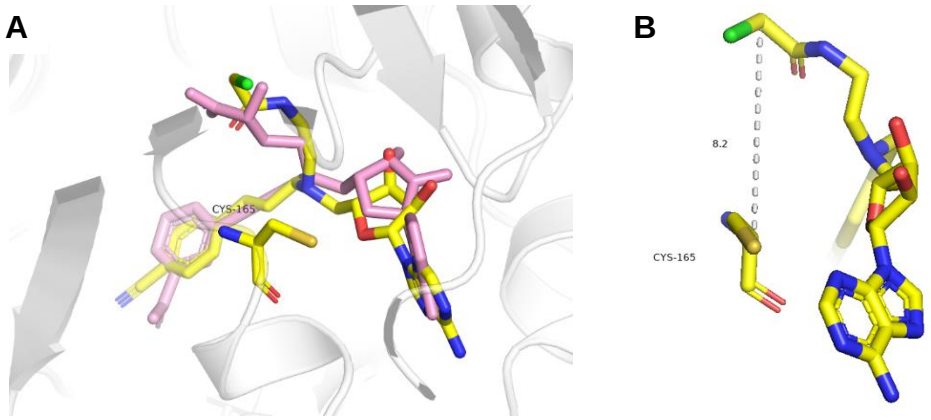

Figure 4. (A) Overlay of the docking model of compound **17b** with the crystal structure of compound LL320 (pink) bound to hNNMT (gray), and (B) the distance between the α-carbon of the chloroacetamide in **17b** to the sulphur atom of cysteine residue C165 is around 8.2 Å, which would be too far to form a covalent interaction.

Compounds **39a**, **39b**, **44a**, and **44b** were designed to covalently target serine residues S201 or S213. Therefore, the focus of modelling these compounds was on the interactions of the

sulfonyl fluoride and boronic acid substitutions with the serine residues in the nicotinamide pocket of NNMT. When docking compounds **39a-b** in the NNMT active site (PDB ID: 6PVS), good overlay with compound LL320 was found (Figure 5A) and both the *meta*- and *para*-substituted sulfonyl fluorides appear to be close enough to serine residues S201 and S213 to possible engage in covalent interactions with predicted distances of 2.9 and 3.4 Å respectively (Figure 6A and 6B). The docking of both *meta*- and *para*-substituted boronic acid compounds **44a-b** revealed a slight difference in overlay with compound LL320 for para-substituted boronic acid compound **44b** while the *meta*-substituted boronic acid compound **44a** showed a similar orientation of the boronic acid motif with the amide moiety of LL320 (Figure 5B). This may explain the difference in activity observed for **44a** and **44b**. However, from the modelling data of compounds **44a** and **44b**, no clear explanation for the difference in activity can be found as in both cases the boronic acid seems to be in close proximity with both targeted serine residues (Figure 6C and 6D).

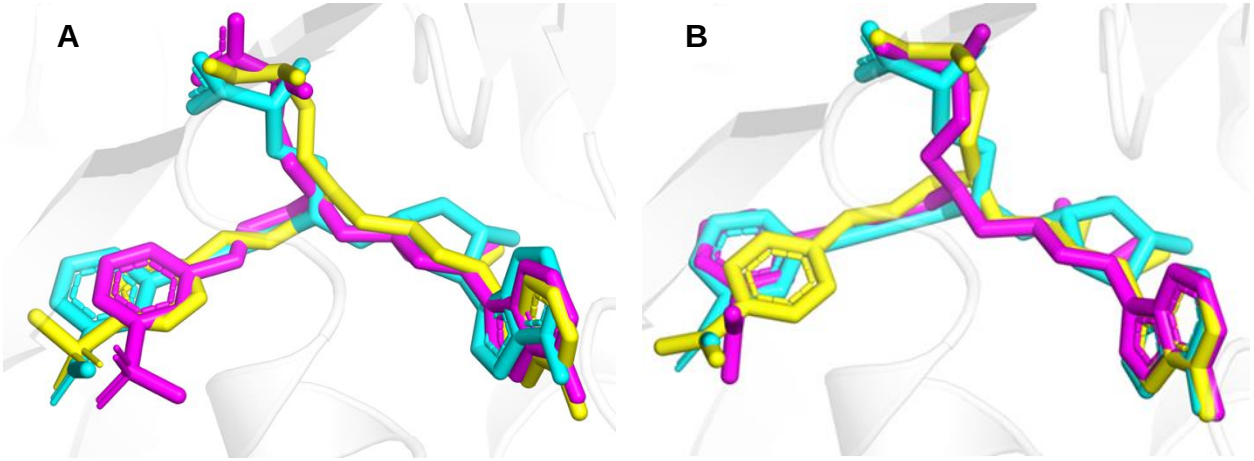

Figure 5. A) Overlay of the docking models of compounds **39a** (pink) and **39b** (yellow) with the hNNMT (gray)–LL320 (cyan) complex (PDB 6PVS), (B) Overlay of the docking models of compounds **44a** (pink) and **44b** (yellow) with the hNNMT (gray)–LL320 (cyan) complex (PDB 6PVS).

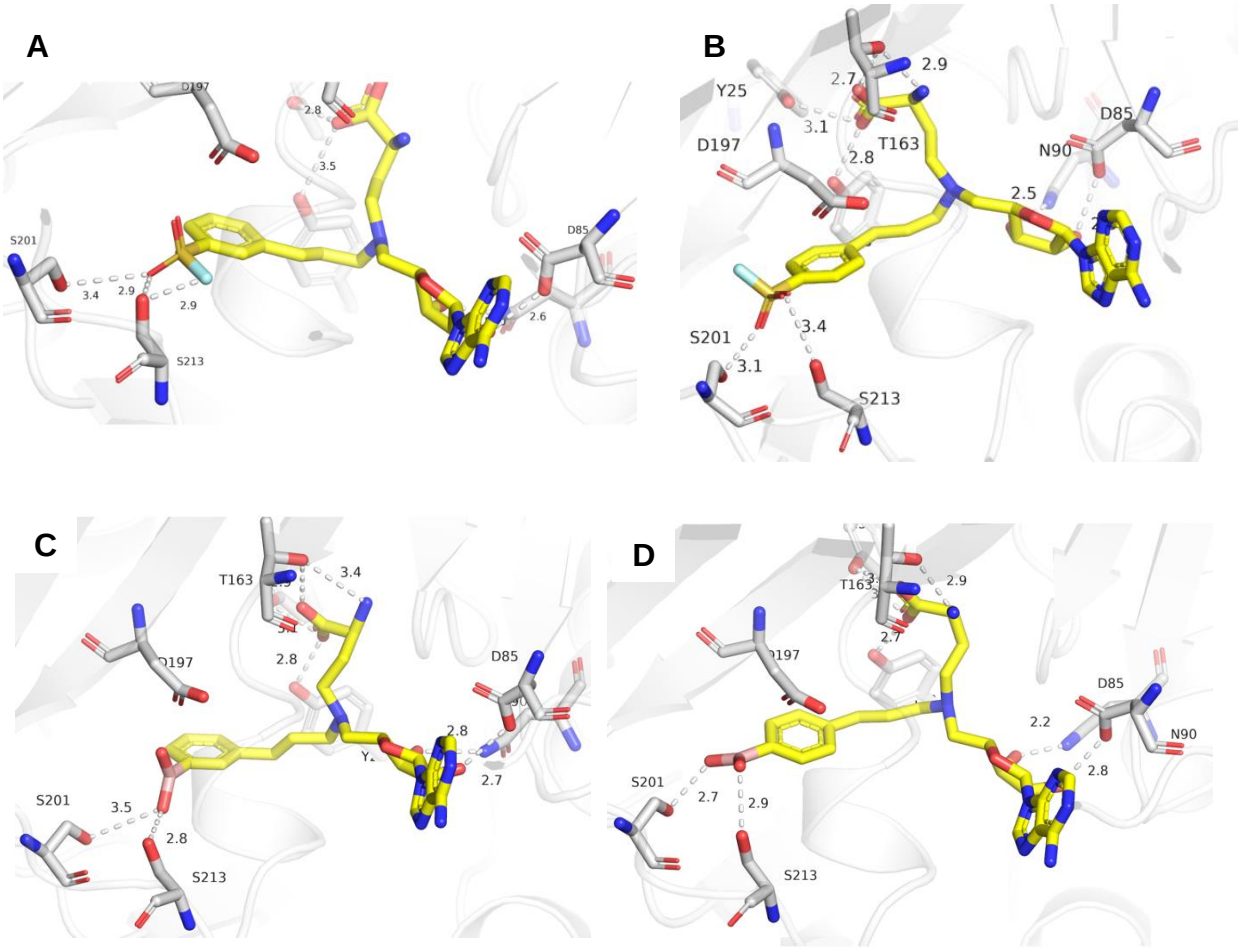

Figure 6. Docking analysis of compounds **39a** (A), **39b** (B), **44a** (C) and **44b** (D) in the binding sites of hNNMT (gray) structure (PDB ID: 6PVS). Hydrogen bonding interactions are shown in gray dotted lines with calculated distances in Angstrom.

Conclusions

Building on the structure of the potent bisubstrate NNMT inhibitors **17u** and **17v**, described in **chapter 3**, we designed and synthesized a focused library of novel inhibitors containing different warheads designed to target cysteine or serine residues in the NNMT active site. To this end, the amino acid functionality was replaced by acrylamides and chloroacetamides with different linkers and evaluated for their inhibitory activity of NNMT with the aim of interacting with cysteine residues C159 or C165, previously targeted by covalent inhibitors of NNMT. In addition, serine residues S201 and S213, involved in binding to the amide moiety of NA pocket, were targeted using sulfonyl fluoride and boronic acid groups. By probing the NNMT binding pockets with different linkers and covalent warheads, we found that linker length is crucial for activity. Among the Michael-acceptor compounds prepared, compound **17b** showed the most potent activity with

an IC_{50} value of 400 nM. It is noteworthy to mention, that this is the first example of a bisubstrate inhibitor of NNMT in which the amino acid functionality is replaced whilst partially retaining its activity. Whether or not the interaction of compound **17b** with the NNMT active site is covalent is still under investigation.

In pursuit of targeting the serine residues in the nicotinamide pocket of NNMT, sulfonyl fluoride analogues **39a** and **39b** showed very promising activity with both compounds exhibiting nanomolar activity. As described in **chapter 3**, we previously found that the orientation of electron withdrawing functional groups at the aromatic ring generally have a preference for the *para*-position and only the amide functionality was found to be most active in the *meta*-position. In the case of the sulfonyl fluoride motif, both orientations work equally well. Modelling of compounds **39a-b** indicate that the sulfonyl fluoride moiety in both compounds is in close proximity to serine residues S201 and S213, potentially allowing for a covalent interaction. For the boronic acid derivatives, only *meta*-orientated boronic acid compound **44a** showed activity, albeit with a moderate IC_{50} value of 1.6 μM. Compound **44b**, which has its boronic acid motif in the *para*-position, did not show any activity. No clear explanations can be provided for the potencies of compounds **44a-b** based on the modelling data obtained. The role of the serine residues is currently under investigation involving the use serine-to-alanine mutants of NNMT.

Experimental Procedures

General Procedures

All reagents employed were of American Chemical Society grade or finer and were used without further purification unless otherwise stated. For compound characterization, ^{1}H NMR spectra were recorded at 400 MHz or 500MHz with chemical shifts reported in parts per million downfield relative to tetramethylsilane, H_2O (δ 4.79), $CHCl_3$ (7.26), or methanol (δ 3.31). ^{1}H NMR data are reported in the following order: multiplicity (s, singlet; d, doublet; t, triplet; q, quartet; and m, multiplet), coupling constant (*J*) in hertz (Hz) and the number of protons. Where appropriate, the multiplicity is preceded by br, indicating that the signal was broad. ^{13}C NMR spectra were recorded at 101 MHz with chemical shifts reported relative to $CDCl_3$ (δ 77.16), methanol (δ 49.00), or DMSO (δ 39.52). The ^{13}C NMR spectra of the compounds recorded in D_2O could not be referenced. High-resolution mass spectrometry (HRMS) analysis was performed using a Q-TOF instrument. Compounds **1b**, **4a**,[32] **4b**,[33] **4c**,[34] **34a**,[35] **34b**[36] and **37**, were prepared as previously described and had NMR spectra and mass spectra consistent with the assigned structures.

N-(((3a*R*,4*R*,6*R*,6a*R*)-6-(6-amino-9*H*-purin-9-yl)-2,2-dimethyltetrahydrofuro[3,4-d][1,3]dioxol-4-yl)methyl)acrylamide (11a). To a solution of 9-((3a*R*,4*R*,6*R*,6a*R*)-6-(aminomethyl)-2-methyltetrahydrofuro[3,4-d][1,3]dioxol-4-yl)-9H-purin-6-amine **10a** (10 mg, 0.033 mmol) in 5 mL DMF were added 0.1 mL DIPEA and 0.1 mL acryloyl chloride under ice bath. After the addition, the ice bah was removed the mixture stirred at rt 2 hours, then removed the solvent under reduced pressure and the residue (yellow oil) **11a** was not purified for next step.

N-(((3a*R*,4*R*,6*R*,6a*R*)-6-(6-amino-9H-purin-9-yl)-2,2-dimethyltetrahydrofuro[3,4-d][1,3]dioxol-4-yl)methyl)-2-chloroacetamide (11b) Following the procedure described for compound **11a**, coupling **10a** (10 mg, 0.033 mmol) and 2-chloroacetyl chloride (0.1 mL) afforded compound **11b** as yellow oil without purification for next step.

N-(((3a*R*,4*R*,6*R*,6a*R*)-6-(6-amino-9H-purin-9-yl)-2,2-dimethyltetrahydrofuro[3,4-d][1,3]dioxol-4-yl)methyl)-*N*-((*E*)-3-(4-cyanophenyl)allyl)acrylamide (11c). Following the procedure described for compound **11a**, coupling 4-((*E*)-3-((((3a*R*,4*R*,6*R*,6a*R*)-6-(6-amino-9*H*-purin-9-yl)-2,2-dimethyltetrahydrofuro[3,4-d][1,3]dioxol-4-yl)methyl)amino)prop-1-en-1-yl)benzonitrile **10b** (15 mg, 0.033 mmol) and acryloyl chloride (0.1 mL) afforded compound **11c** as yellow oil without purification for next step.

N-(((3a*R*,4*R*,6*R*,6a*R*)-6-(6-amino-9*H*-purin-9-yl)-2,2-dimethyltetrahydrofuro[3,4-d][1,3]dioxol-4-yl)methyl)-2-chloro-*N*-((*E*)-3-(4-cyanophenyl)allyl)acetamide (11d). Following the procedure described for compound **11a**, compound **10b** (15 mg, 0.033 mmol) and 2-chloroacetyl chloride (0.1 mL) afforded compound **11d** as yellow oil without purification for next step.

N-(((2*R*,3*S*,4*R*,5*R*)-5-(6-amino-9*H*-purin-9-yl)-3,4-dihydroxytetrahydrofuran-2-yl)methyl)acrylamide (12a). To a solution of compound **11a** (14mg, crude) in 1 mL of CH_2Cl_2 has added a mixture of 9 mL TFA and 1 mL H_2O, and the solution was stirred for 2 h at room temperature. The mixture was concentrated, and the crude product was purified by preparative HPLC, affording compound **12a** as a yellow oil (4 mg, 38% yield over two steps, >70 % pure), LRMS (ESI): calculated for $C_{13}H_{17}N_6O_4$ $[M+H]^+$ 321.13, found 321.16.

***N*-(((2*R*,3*S*,4*R*,5*R*)-5-(6-amino-9*H*-purin-9-yl)-3,4-dihydroxytetrahydrofuran-2-yl)methyl)-2-chloroacetamide (12b).** Following the procedure described for compound **12a**, compound **11b** (16mg, crude) was deprotected and purified, affording compound **8** as a yellow powder (3 mg, 27% yield over two steps, > 70% pure). LRMS (ESI): calculated for $C_{12}H_{16}ClN_6O_4$ $[M+H]^+$ 343.09, found 349.11.

***N*-(((2*R*,3*S*,4*R*,5*R*)-5-(6-amino-9*H*-purin-9-yl)-3,4-dihydroxytetrahydrofuran-2-yl)methyl)-N-((*E*)-3-(4-cyanophenyl)allyl)acrylamide (12c).** Following the procedure described for compound **12a**, compound **11c** (21mg, crude) was deprotected and purified, affording compound **12c** as a white powder (5 mg, 32% yield over two steps, > 70% pure). LRMS (ESI): calculated for $C_{23}H_{24}N_7O_4$ $[M+H]^+$ 462.1890, found 462.1892.

***N*-(((2*R*,3*S*,4*R*,5*R*)-5-(6-amino-9*H*-purin-9-yl)-3,4-dihydroxytetrahydrofuran-2-yl)methyl)-2-chloro-N-((*E*)-3-(4-cyanophenyl)allyl)acetamide (12d).** Following the procedure described for compound **12a**, compound **11d** (25mg, crude) was deprotected and purified, affording compound **12d** as a yellow powder (3 mg, 18% yield over two steps, 70% pure). LRMS (ESI): calculated for $C_{22}H_{23}ClN_7O_4$ $[M+H]^+$ 484.15, found 484.19.

***tert*-butyl (2-((((3a*R*,4*R*,6*R*,6a*R*)-6-(6-amino-9*H*-purin-9-yl)-2,2-dimethyltetrahydrofuro[3,4-d][1,3]dioxol-4-yl)methyl)((*E*)-3-(4-cyanophenyl)allyl)amino)ethyl)carbamate (14a).** Amine **10b** (840 mg, 1.89 mmol), *tert*-butyl (2-oxoethyl)carbamate **13a** (360 mg, 2.26mmol), $NaBH(OAc)_3$ (600 g, 2.83 mmol) and AcOH (1 drop) were added to 1,2-dichloroethane (DCE, 50 mL) in a 250 mL round-bottom flask (RBF) and the mixture was stirred at room temperature under N_2 atmosphere overnight. The reaction was quenched by adding 1 N NaOH (20 mL), and the product was extracted with CH_2Cl_2. The combined organic layers were washed with brine and dried over Na_2SO_4. The solvent was evaporated, and the crude product was purified by column chromatography (5% MeOH in EtOAc) to give compound **14a** as a white powder (724 mg, 65% yield). ^{1}H NMR (400 MHz, $CDCl_3$) δ 8.17 (s, 1H), 7.88 (s, 1H), 7.49 (d, *J* = 8.3 Hz, 2H), 7.27 (d, *J* = 7.2 Hz, 2H), 6.63 (s, 2H), 6.39 (br d, *J* = 15.9 Hz, 1H), 6.28 – 6.18 (m, 1H), 6.03 (d, *J* = 1.9 Hz, 1H), 5.44 – 5.33 (m, 2H), 5.04 – 4.97 (m, 1H), 4.27 (q, *J* = 6.5 Hz, 1H), 3.26 (d, *J* = 6.0 Hz, 2H), 3.21 – 3.01 (m, 2H), 2.76 (d, *J* = 6.2 Hz, 2H), 2.59 (d, *J* = 5.2 Hz, 2H), 1.57 (s, 3H), 1.37 (br d, *J* = 12.7 Hz, 12H). ^{13}C NMR (101 MHz, $CDCl_3$) δ 156.0, 153.0, 149.0, 141.3, 132.4, 131.1, 126.7, 120.2, 119.0, 114.6,

110.6, 90.4, 85.6, 83.9, 83.1, 56.8, 55.9, 53.7, 38.3, 28.5, 27.2, 25.5. HRMS (ESI): calculated for $C_{30}H_{39}N_8O_5$ $[M+H]^+$ 590.3043, found 590.3045.

tert-butyl 3-((((3a*R*,4*R*,6*R*,6a*R*)-6-(6-amino-9*H*-purin-9-yl)-2,2-dimethyltetrahydrofuro[3,4-d][1,3]dioxol-4-yl)methyl)((E)-3-(4-cyanophenyl)allyl)amino)pyrrolidine-1-carboxylate (14b). Following the procedure described for compound **14a**, compound **10b** (210 mg, 0.47 mmol) coupled with (9*H*-fluoren-9-yl)methyl (3-oxopropyl)carbamate **13b** (121 mg, 0.70 mmol) afforded compound **14b** as yellow powder (204 mg, 72% yield). ^{1}H NMR (400 MHz, $CDCl_3$) δ 8.16 (s, 1H), 7.93 (s, 1H), 7.46 (d, *J* = 8.3 Hz, 2H), 7.23 (d, *J* = 8.3 Hz, 2H), 6.76 (s, 2H), 6.35 (br d, *J* = 16.0 Hz, 1H), 6.27 – 6.16 (m, 1H), 6.08 – 6.02 (m, 1H), 5.52 – 5.36 (m, 2H), 4.99 (dd, *J* = 5.6, 3.3 Hz, 1H), 4.36 – 4.32 (m, 1H), 3.25 – 3.00 (m, 4H), 2.68 (d, *J* = 6.8 Hz, 2H), 2.49 (t, *J* = 6.4 Hz, 2H), 1.56 (s, 3H), 1.35 (d, *J* = 7.2 Hz, 12H). ^{13}C NMR (101 MHz, $CDCl_3$) δ 156.0, 153.0, 149.0, 141.3, 139.5, 132.3, 131.2, 130.8, 126.6, 120.2, 119.0, 114.3, 110.4, 90.7, 85.8, 84.0, 83.3, 56.4, 51.8, 38.7, 28.5, 27.1, 25.4. HRMS (ESI): calculated for $C_{31}H_{41}N_8O_5$ $[M+H]^+$ 605.3200, found 605.3201.

tert-butyl (4-((((3a*R*,4*R*,6*R*,6a*R*)-6-(6-amino-9*H*-purin-9-yl)-2,2-dimethyltetrahydrofuro[3,4-d][1,3]dioxol-4-yl)methyl)((*E*)-3-(4-cyanophenyl)allyl)amino)butyl)carbamate (14c). Following the procedure described for compound **14a**, compound **10b** (210 mg, 0.47 mmol) coupled with *tert*-butyl (4-oxobutyl)carbamate **14** (130 mg, 0.70 mmol) afforded compound **5c** as yellow powder (200 mg, 69% yield). ^{1}H NMR (400 MHz, $CDCl_3$) δ 8.22 (s, 1H), 7.95 (s, 1H), 7.50 (d, *J* = 8.3 Hz, 2H), 7.28 (d, *J* = 9.3 Hz, 2H), 6.53 (s, 2H), 6.38 (br d, *J* = 16.0 Hz, 1H), 6.31 – 6.22 (m, 1H), 6.06 (s, 1H), 5.49 – 5.43 (m, 1H), 4.97 (dd, *J* = 6.0, 3.3 Hz, 2H), 4.36 (s, 1H), 3.58 (s, 1H), 3.30 – 3.20 (m, 2H), 3.11 – 2.95 (m, 2H), 2.72 (d, *J* = 6.5 Hz, 2H), 2.48 (s, 2H), 1.57 (s, 3H), 1.38 (d, *J* = 13.7 Hz, 17). ^{13}C NMR (101 MHz, $CDCl_3$) δ 155.8, 153.0, 149.1, 141.3, 140.2, 132.4, 131.33, 130.9, 126.7, 120.2, 119.1, 114.3, 110.5, 90.9, 85.8, 83.9, 83.3, 56.8, 56.0, 54.3, 28.5, 27.8, 27.1, 25.4, 24.3. HRMS (ESI): calculated for $C_{32}H_{43}N_8O_5$ $[M+H]^+$ 619.3356, found 619.3358.

4-((*E*)-3-((((3a*R*,4*R*,6*R*,6a*R*)-6-(6-amino-9*H*-purin-9-yl)-2,2-dimethyltetrahydrofuro[3,4-d][1,3]dioxol-4-yl)methyl)(2-aminoethyl)amino)prop-1-en-1-yl)benzonitrile (15a). To a solution of **14a** (118 mg, 0.2 mmol) in CH_2Cl_2 (9mL) was added TFA (1 mL), after 1 hour, solvent and TFA were removed under reduced pressure, the crude yellow oil was used for next step directly

without purification (assumed quantitive yield). LRMS (ESI): calculated for $C_{25}H_{31}N_8O_3$ $[M+H]^+$ 491.25, found 491.27.

4-((*E*)-3-((((3a*R*,4*R*,6*R*,6a*R*)-6-(6-amino-9*H*-purin-9-yl)-2,2-dimethyltetrahydrofuro[3,4-d][1,3]dioxol-4-yl)methyl)(3-aminopropyl)amino)prop-1-en-1-yl)benzonitrile (15b). Following the procedure described for compound **15a**, compound **14b** was selectively deprotected, the cude compound **6b** was used for next step directly without purification (assumed quantitive yield). LRMS (ESI): calculated for $C_{26}H_{33}N_8O_3$ $[M+H]^+$ 505.26, found 505.31.

4-((*E*)-3-((((3a*R*,4*R*,6*R*,6a*R*)-6-(6-amino-9*H*-purin-9-yl)-2,2-dimethyltetrahydrofuro[3,4-d][1,3]dioxol-4-yl)methyl)(3-aminopropyl)amino)prop-1-en-1-yl)benzonitrile (15c). Following the procedure described for compound **15a**, compound **14c** was selectively deprotected, the cude compound **6c** was used for next step directly without purification (assumed quantitive yield). LRMS (ESI): calculated for $C_{27}H_{35}N_8O_3$ $[M+H]^+$ 519.28, found 519.33.

***N*-(2-((((3a*R*,4*R*,6*R*,6a*R*)-6-(6-amino-9*H*-purin-9-yl)-2,2-dimethyltetrahydrofuro[3,4-d][1,3]dioxol-4-yl)methyl)((*E*)-3-(4-cyanophenyl)allyl)amino)ethyl)acrylamide (16a).** Following the procedure described for compound **11a**, compound **15a** (25 mg, 0.05 mmol) and acryloyl chloride (0.05 mL) afforded compound **7a** as yellow oil without purification for next step.

***N*-(2-((((3a*R*,4*R*,6*R*,6a*R*)-6-(6-amino-9*H*-purin-9-yl)-2,2-dimethyltetrahydrofuro[3,4-d][1,3]dioxol-4-yl)methyl)((*E*)-3-(4-cyanophenyl)allyl)amino)ethyl)-2-chloroacetamide (16b).** Following the procedure described for compound **11a**, compound **15a** (25 mg, 0.05 mmol) and 2-chloroacetyl chloride (0.05 mL) afforded compound **16b** as yellow oil without purification for next step.

***N*-(3-((((3a*R*,4*R*,6*R*,6a*R*)-6-(6-amino-9*H*-purin-9-yl)-2,2-dimethyltetrahydrofuro[3,4-d][1,3]dioxol-4-yl)methyl)((*E*)-3-(4-cyanophenyl)allyl)amino)propyl)acrylamide. (16c)** Following the procedure described for compound **11a**, compound **15b** (25 mg, 0.05 mmol) and acryloyl chloride (0.05 mL) afforded compound **16c** as yellow oil without purification for next step.

***N*-(3-((((3a*R*,4*R*,6*R*,6a*R*)-6-(6-amino-9*H*-purin-9-yl)-2,2-dimethyltetrahydrofuro[3,4-d][1,3]dioxol-4-yl)methyl)((*E*)-3-(4-cyanophenyl)allyl)amino)propyl)-2-chloroacetamide (16d).**

Following the procedure described for compound **11a**, compound **15b** (25 mg, 0.05 mmol) and 2-chloroacetyl chloride (0.05 mL) afforded compound **16d** as yellow oil without purification for next step.

***N*-(4-((((3a*R*,4*R*,6*R*,6a*R*)-6-(6-amino-9*H*-purin-9-yl)-2,2-dimethyltetrahydrofuro[3,4-d][1,3]dioxol-4-yl)methyl)((*E*)-3-(4-cyanophenyl)allyl)amino)butyl)acrylamide (16e).** Following the procedure described for compound **11a**, compound **15c** (26 mg, 0.05 mmol) and acryloyl chloride (0.05 mL) afforded compound **16e** as yellow oil without purification for next step.

***N*-(4-((((3a*R*,4*R*,6*R*,6a*R*)-6-(6-amino-9*H*-purin-9-yl)-2,2-dimethyltetrahydrofuro[3,4-d][1,3]dioxol-4-yl)methyl)((*E*)-3-(4-cyanophenyl)allyl)amino)butyl)-2-chloroacetamide (16f).** Following the procedure described for compound **11a**, compound **15c** (26 mg, 0.05 mmol) and 2-chloroacetyl chloride (0.05 mL) afforded compound **16f** as yellow oil without purification for next step.

***N*-(2-((((2*R*,3*S*,4*R*,5*R*)-5-(6-amino-9*H*-purin-9-yl)-3,4-dihydroxytetrahydrofuran-2-yl)methyl)((*E*)-3-(4-cyanophenyl)allyl)amino)ethyl)acrylamide (17a).** Following the procedure described for compound **12a**, compound **16a** was deprotected and purified, affording compound **17a** as a yellow powder (3 mg, 18% yield over two steps). ^{1}H NMR (500 MHz, CD_3OD) δ 8.39 (s, 1H), 8.30 (s, 1H), 7.72 (d, *J* = 8.4 Hz, 2H), 7.56 (d, *J* = 8.3 Hz, 2H), 6.93 (br d, *J* = 15.8 Hz, 1H), 6.54 – 6.45 (m, 1H), 6.16 – 6.03 (m, 3H), 5.65 (dd, *J* = 9.6, 2.2 Hz, 1H), 4.80 (d, *J* = 3.7 Hz, 1H), 4.56 (d, *J* = 10.5 Hz, 1H), 4.49 (t, *J* = 4.9 Hz, 1H), 4.23 (d, *J* = 7.2 Hz, 2H), 3.96 – 3.87 (m, 1H), 3.73 (d, *J* = 3.9 Hz, 1H), 3.70 (d, *J* = 2.3 Hz, 1H), 3.67 (d, *J* = 9.4 Hz, 1H), 3.55 – 3.44 (m, 2H). ^{13}C NMR (126 MHz, CD_3OD) δ 168.6, 139.7, 139.1, 132.4, 129.3, 127.4, 126.8, 119.7, 118.1, 112.0, 90.9, 78.7, 73.8, 73.2, 55.1, 34.9, HRMS (ESI): calculated for $C_{25}H_{29}N_8O_4$ $[M+H]^+$ 505.2312, found 505.2218.

***N*-(2-((((2*R*,3*S*,4*R*,5*R*)-5-(6-amino-9*H*-purin-9-yl)-3,4-dihydroxytetrahydrofuran-2-yl)methyl)((*E*)-3-(4-cyanophenyl)allyl)amino)ethyl)-2-chloroacetamide (17b).** Following the procedure described for compound **12a**, compound **16b** was deprotected and purified, affording compound **17b** as a yellow powder (12 mg, 38% yield over two steps). ^{1}H NMR (500 MHz, CD_3OD) δ 8.49 (s, 1H), 8.36 (s, 1H), 7.68 (d, *J* = 8.4 Hz, 2H), 7.52 (d, *J* = 8.3 Hz, 2H), 6.86 (d, *J* = 15.8 Hz, 1H), 6.50 (dd, *J* = 15.4, 7.9 Hz, 1H), 6.17 (d, *J* = 3.8 Hz, 1H), 4.74 – 4.70 (m, 1H), 4.59 – 4.52 (m, 2H), 4.06 (s, 2H), 3.90 (dd, *J* = 13.9, 9.9 Hz, 1H), 3.76 (dd, *J* = 13.9, 1.6 Hz, 1H), 3.69 (t, *J* = 6.1 Hz, 2H), 3.51 (t, *J* = 6.1 Hz, 2H). ^{13}C NMR (126 MHz, CD_3OD) δ 169.5,

151.1, 148.2, 139.8, 138.9, 132.4, 127.3, 120.0, 119.9, 118.2, 111.9, 91.1, 78.7, 73.5, 72.3, 55.6, 54.94, 54.9, 52.9, 41.7, 34.8, HRMS (ESI): calculated for $C_{24}H_{27}ClN_8O_4$ $[M+H]^+$ 527.1922, found 527.1925.

***N*-(3-((((2*R*,3*S*,4*R*,5*R*)-5-(6-amino-9*H*-purin-9-yl)-3,4-dihydroxytetrahydrofuran-2-yl)methyl)((*E*)-3-(4-cyanophenyl)allyl)amino)propyl)acrylamide (17c).** Following the procedure described for compound **12a**, compound **16c** was deprotected and purified, affording compound **17c** as a yellow powder (14mg, 44% yield over two steps, > 70% pure). LRMS (ESI): calculated for $C_{26}H_{31}N_8O_4$ $[M+H]^+$ 519.24, found 519.29.

***N*-(3-((((2*R*,3*S*,4*R*,5*R*)-5-(6-amino-9*H*-purin-9-yl)-3,4-dihydroxytetrahydrofuran-2-yl)methyl)((E)-3-(4-cyanophenyl)allyl)amino)propyl)-2-chloroacetamide (17d).** Following the procedure described for compound **12a**, compound **16d** was deprotected and purified, affording compound **17d** as a yellow powder (14 mg, 42% yield over two steps). ^{1}H NMR (500 MHz, CD_3OD) δ 8.48 (s, 1H), 8.35 (s, 1H), 7.68 (d, *J* = 8.2 Hz, 2H), 7.52 (d, *J* = 7.0 Hz, 2H), 6.87 – 6.80 (m, 1H), 6.48 – 6.42 (m, 1H), 6.17 (d, *J* = 3.4 Hz, 1H), 4.68 (s, 1H), 4.56 – 4.51 (m, 2H), 4.12 (d, *J* = 7.3 Hz, 2H), 4.02 (s, 2H), 3.86 – 3.81 (m, 1H), 3.68 (br d, *J* = 13.6 Hz, 1H), 3.38 – 3.33 (m, 2H), 2.06 – 2.01 (m, 2H). ^{13}C NMR (126 MHz, CD_3OD) δ 168.7, 161.3, 161.0, 151.1, 148.2, 139.7, 138.6, 132.4, 127.3, 120.0, 119.8, 118.1, 111.9, 90.5, 55.27, 73.5, 72.3, 55.3, 51.3, 41.8, 36.3, 23.9, HRMS (ESI): calculated for $C_{25}H_{30}ClN_8O_4$ $[M+H]^+$ 541.2079, found 541.2083.

***N*-(4-((((2*R*,3*S*,4*R*,5*R*)-5-(6-amino-9*H*-purin-9-yl)-3,4-dihydroxytetrahydrofuran-2-yl)methyl)((*E*)-3-(4-cyanophenyl)allyl)amino)butyl)acrylamide (17e).** Following the procedure described for compound **12a**, compound **16e** was deprotected and purified, affording compound **17e** as a yellow powder (12mg, 36% yield over two steps, >70% pure). LRMS (ESI): calculated for C27H33ClN8O4 [M+H]+ 533.26, found 533.30.

***N*-(4-((((2*R*,3*S*,4*R*,5*R*)-5-(6-amino-9*H*-purin-9-yl)-3,4-dihydroxytetrahydrofuran-2-yl)methyl)((*E*)-3-(4-cyanophenyl)allyl)amino)butyl)-2-chloroacetamide (17f).** Following the procedure described for compound **12f**, compound **16f** was deprotected and purified, affording compound **17f** as a yellow powder (16 mg, 47% yield over two steps). ^{1}H NMR (500 MHz, CD_3OD) δ 8.47 (s, 1H), 8.34 (s, 1H), 7.68 (d, *J* = 8.0 Hz, 2H), 7.49 (s, 2H), 6.81 (br d, *J* = 15.8 Hz, 1H), 6.48 – 6.42 (m, 1H), 6.17 (d, *J* = 3.3 Hz, 1H), 4.68 (s, 1H), 4.56 – 4.50 (m, 2H), 4.10

(d, *J* = 7.3 Hz, 2H), 4.06 (s, 2H), 3.84 – 3.79 (m, 1H), 3.66 (br d, *J* = 13.4 Hz, 1H), 3.39 – 3.33 (m, 2H), 3.27 (t, *J* = 6.5 Hz, 2H), 1.89 – 1.75 (m, 2H), 1.65 – 1.56 (m, 2H). ^{13}C NMR (126 MHz, CD_3OD) δ 168.3, 161.1, 151.3, 148.11, 139.7, 138.6, 132.4, 119.8, 118.1, 111.9, 91.2, 73.5, 72.3, 53.4, 41.9, 38.2, 26.1, 20.9, HRMS (ESI): calculated for $C_{26}H_{32}ClN_8O_4$ $[M+H]^+$ 555.2235, found 555.2238.

tert-butyl 3-((((3a*R*,4*R*,6*R*,6a*R*)-6-(6-amino-9*H*-purin-9-yl)-2,2-dimethyltetrahydrofuro[3,4-d][1,3]dioxol-4-yl)methyl)((*E*)-3-(4-cyanophenyl)allyl)amino)azetidine-1-carboxylate (19a). Following the procedure described for compound **14a**, compound **1b** (40 mg, 0.090 mmol) coupled with *tert*-butyl 3-oxoazetidine-1-carboxylate **18a** (19 mg, 0.11 mmol) afforded compound **19a** as yellow powder (10 mg 19% yiled over two steps, > 70% pure). LRMS (ESI): calculated for $C_{31}H_{39}N_8O_5$ $[M+H]^+$ 603.30, found 603.31.

tert-butyl 3-((((3a*R*,4*R*,6*R*,6a*R*)-6-(6-amino-9*H*-purin-9-yl)-2,2-dimethyltetrahydrofuro[3,4-d][1,3]dioxol-4-yl)methyl)((*E*)-3-(4-cyanophenyl)allyl)amino)pyrrolidine-1-carboxylate (19b). Following the procedure described for compound **14a**, compound **1b** (200 mg, 0.45 mmol) coupled with *tert*-butyl 3-oxoazetidine-1-carboxylate **18b** (92 mg, 0.54 mmol) afforded compound **19b** as yellow powder (174 mg, 63 yield). ^{1}H NMR (400 MHz, $CDCl_3$) δ 8.25 (br d, *J* = 34.0 Hz, 1H), 7.87 (s, 1H), 7.51 – 7.43 (m, 2H), 7.22 (br d, *J* = 19.8 Hz, 2H), 6.78 – 6.67 (m, 2H), 6.42 – 6.32 (m, 1H), 6.29 – 6.18 (m, 1H), 6.03 (d, *J* = 2.0 Hz, 1H), 5.43 – 5.39 (m, 1H), 5.05 – 4.96 (m, 1H), 4.38 – 4.26 (m, 1H), 3.67 – 2.99 (m, 7H), 2.93 – 2.73 (m, 2H), 1.98 – 1.86 (m, 1H), 1.78 – 1.63 (m, 1H), 1.54 (s, 3H), 1.39 (d, *J* = 5.5 Hz, 9H), 1.34 (s, 3H). ^{13}C NMR (101 MHz, $CDCl_3$) δ 155.9, 154.5, 153.0, 149.0, 140.2, 140.2, 132.4, 130.8, 126.6, 120.3, 119.0, 114.4, 110.6, 90.7, 86.2, 84.0, 83.1, 79.4, 61.9, 60.8, 54.7, 44.7, 44.3, 29.7, 28.5, 27.2, 25.5. HRMS (ESI): calculated for $C_{32}H_{41}ClN_8O_5$ $[M+H]^+$ 617.3200, found 617.3201.

tert-butyl 4-((((3a*R*,4*R*,6*R*,6a*R*)-6-(6-amino-9*H*-purin-9-yl)-2,2-dimethyltetrahydrofuro[3,4-d][1,3]dioxol-4-yl)methyl)((*E*)-3-(4-cyanophenyl)allyl)amino)piperidine-1-carboxylate (19c). Following the procedure described for compound **14a**, compound **1b** (40 mg, 0.090 mmol) coupled with *tert*-butyl 3-oxoazetidine-1-carboxylate**18c** (22 mg, 0.11 mmol) afforded compound **19c** as yellow powder (13mg, 23% yield). LRMS (ESI): calculated for $C_{33}H_{41}N_8O_5$ $[M+H]^+$ 631.33, found 631.35.

4-((*E*)-3-((1-acryloylazetidin-3-yl)(((2*R*,3*S*,4*R*,5*R*)-5-(6-amino-9*H*-purin-9-yl)-3,4-dihydroxytetrahydrofuran-2-yl)methyl)amino)prop-1-en-1-yl)benzonitrile (22a). To a solution of compound **19a** (30 mg, 0.05 mmol) in CH_2Cl_2 (9 mL) was added TFA (1 mL), after 30 mins, solvent was removed under reduced pressure, the crude oil was redissolved in CH_2Cl_2 (10 mL), DIPEA (0.1 mL) added and acryloyl chloride (0.05 mL) was added under 0 ℃. After 2 hours, solvent was removed under reduced pressure. A mix ture of TFA/CH_2Cl_2/H_2O (9mL/1mL/1ml) was added to the crude oil, after 2 hours, solvent was removed and the crude compound was purifiifed by prep-HPLC to offer compound **22a** as yellow powder, (9 mg, 29% yield over 3 steps, >70% pure). LRMS (ESI): calculated for $C_{26}H_{29}N_8O_4$ $[M+H]^+$ 517.23, found 517.29.

4-((*E*)-3-((((2*R*,3*S*,4*R*,5*R*)-5-(6-amino-9*H*-purin-9-yl)-3,4-dihydroxytetrahydrofuran-2-yl)methyl)(1-(2-chloroacetyl)azetidin-3-yl)amino)prop-1-en-1-yl)benzonitrile (22b). Following the procedure described for compound **22a**, compound **22b** was obtained as a white powder (11 mg, 35% yield over 3 steps). ^{1}H NMR (300 MHz, CD_3OD) δ 8.46 (s, 1H), 8.34 (s, 1H), 7.69 (d, *J* = 8.4 Hz, 2H), 7.51 (d, *J* = 8.2 Hz, 2H), 6.88 – 6.73 (m, 1H), 6.51 – 6.41 (m, 1H), 6.14 (d, *J* = 3.5 Hz, 1H), 4.75 – 4.65 (m, 2H), 4.61 – 4.33 (m, 5H), 4.29 – 4.17 (m, 3H), 4.05 (d, *J* = 4.2 Hz, 2H), 3.93 (d, *J* = 9.9 Hz, 2H), 3.63 – 3.41 (m, 2H), 2.70 (d, *J* = 2.7 Hz, 1H). ^{13}C NMR (75 MHz, CD_3OD) δ 167.2, 146.8, 143.7, 131.6, 126.5, 117.0, 88.9, 77.7, 74.1, 71.6, 53.7, 53.5, 52.4, 51.4, 39.6, 21.8. HRMS (ESI): calculated for $C_{25}H_{28}ClN_8O_4$ $[M+H]^+$ 539.1922, found 539.1923.

4-((*E*)-3-((1-acryloylpyrrolidin-3-yl)(((2*R*,3*S*,4*R*,5*R*)-5-(6-amino-9*H*-purin-9-yl)-3,4-dihydroxytetrahydrofuran-2-yl)methyl)amino)prop-1-en-1-yl)benzonitrile (22c). Following the procedure described for compound **22a**, compound **22c** was obtained as a yellow powder (7mg, 23% yield over 3 steps, >70% pure). LRMS (ESI): calculated for $C_{27}H_{31}ClN_8O_4$ $[M+H]^+$ 531.24, found 531.26.

4-((*E*)-3-((((2*R*,3*S*,4*R*,5*R*)-5-(6-amino-9*H*-purin-9-yl)-3,4-dihydroxytetrahydrofuran-2-yl)methyl)(1-(2-chloroacetyl)pyrrolidin-3-yl)amino)prop-1-en-1-yl)benzonitrile (22d). Following the procedure described for compound **22a**, compound **22d** was obtained as a white powder (13 mg, 39% yield, over 3steps). ^{1}H NMR (300 MHz, CD_3OD) δ 8.42 (s, 1H), 8.38 – 8.26 (m, 1H), 7.70 – 7.66 (m, 2H), 7.53 – 7.39 (m, 2H), 6.91 – 6.72 (m, 1H), 6.54 – 6.40 (m, 1H), 6.21 – 6.11 (m, 1H), 4.75 – 4.47 (m, 4H), 4.29 – 4.08 (m, 5H), 4.02 – 3.55 (m, 6H), 2.70 – 2.68 (m, 1H), 2.39 – 2.33 (m, 2H). ^{13}C NMR (75 MHz, CD_3OD) δ 165.5, 150.9, 148.0, 145.1,

131.6, 125.1, 96.4, 77.5, 72.9, 69.5, 53.5, 52.4, 51.3, 39.3, 24.3, HRMS (ESI): calculated for $C_{26}H_{30}ClN_8O_4$ $[M+H]^+$ 553.2079, found 553.2081.

4-((*E*)-3-((1-acryloylpiperidin-4-yl)(((2*R*,3*S*,4*R*,5*R*)-5-(6-amino-9*H*-purin-9-yl)-3,4-dihydroxytetrahydrofuran-2-yl)methyl)amino)prop-1-en-1-yl)benzonitrile (22e). Following the procedure described for compound **22a**, compound **22e** was obtained as a white powder (9 mg, 27% yield over 3 steps). LRMS (ESI): calculated for $C_{26}H_{33}N_8O_4$ $[M+H]^+$ 545.26, found 545.31.

4-((*E*)-3-((((2*R*,3*S*,4*R*,5*R*)-5-(6-amino-9*H*-purin-9-yl)-3,4-dihydroxytetrahydrofuran-2-yl)methyl)(1-(2-chloroacetyl)piperidin-4-yl)amino)prop-1-en-1-yl)benzonitrile (22f). Following the procedure described for compound **22a**, compound **22f** was obtained as a white powder (10 mg, 30% yield over 3 steps). ^{1}H NMR (400 MHz, CD_3OD) δ 8.38 (s, 1H), 8.27 (s, 1H), 7.67 (d, *J* = 7.9 Hz, 2H), 7.44 (s, 2H), 6.83 (br d, *J* = 15.7 Hz, 1H), 6.49 – 6.40 (m, 1H), 6.14 (d, *J* = 2.4 Hz, 1H), 4.74 – 4.57 (m, 3H), 4.47 (t, *J* = 7.4 Hz, 1H), 4.38 – 4.34 (m, 1H), 4.30 – 4.25 (m, 1H), 4.16 (d, *J* = 7.2 Hz, 3H), 3.90 – 3.72 (m, 3H), 3.30 – 3.15 (m, 1H), 2.82 – 2.72 (m, 1H), 2.23 (d, *J* = 26.9 Hz, 2H), 1.99 – 1.72 (m, 2H). ^{13}C NMR (101 MHz, CD_3OD) δ 166.1, 148.2, 139.6, 138.0, 131.5, 127.1, 120.9, 119.7, 118.1, 111.9, 91.2, 73.5, 72.2, 52.2, 44.2, 40.6, 29.8. HRMS (ESI): calculated for $C_{27}H_{32}ClN_8O_4$ $[M+H]^+$ 567.2235, found 567.2241.

***tert*-butyl 3-(((((3a*R*,4*R*,6*R*,6a*R*)-6-(6-amino-9*H*-purin-9-yl)-2,2-dimethyltetrahydrofuro[3,4-d][1,3]dioxol-4-yl)methyl)((*E*)-3-(4-cyanophenyl)allyl)amino)methyl)azetidine-1-carboxylate (24).** Following the procedure described for compound **14a**, compound **1b** (40 mg, 0.090 mmol) coupled with *tert*-butyl 3-formylazetidine-1-carboxylate **23** (19 mg, 0.11 mmol) afforded compound **24** as yellow powder (35 mg, 63% yield). LRMS (ESI): calculated for $C_{32}H_{41}N_8O_5$ $[M+H]^+$ 617.32, found 617.33.

4-((*E*)-3-(((1-acryloylazetidin-3-yl)methyl)(((2*R*,3*S*,4*R*,5*R*)-5-(6-amino-9*H*-purin-9-yl)-3,4-dihydroxytetrahydrofuran-2-yl)methyl)amino)prop-1-en-1-yl)benzonitrile (27a). Following the procedure described for compound **22a**, compound **27a** was obtained as a yellow powder (6 mg, 20% yield over three steps). LRMS (ESI): calculated for $C_{27}H_{31}N_8O_4$ $[M+H]^+$ 531.24, found 531.28.

4-((*E*)-3-((((2*R*,3*S*,4*R*,5*R*)-5-(6-amino-9*H*-purin-9-yl)-3,4-dihydroxytetrahydrofuran-2-yl)methyl)((1-(2-chloroacetyl)azetidin-3-yl)methyl)amino)prop-1-en-1-yl)benzonitrile (27b). Following the procedure described for compound **27a**, compound **27b** was obtained as a white powder (9 mg, 28% yield over three steps). ^{1}H NMR (400 MHz, CD_3OD) δ 8.47 (s, 1H), 8.33 (s, 1H), 7.69 (d, *J* = 8.4 Hz, 2H), 7.48 (d, *J* = 8.2 Hz, 2H), 6.82 (d, *J* = 15.8 Hz, 1H), 6.51 – 6.44 (m, 1H), 6.18 (d, *J* = 3.2 Hz, 1H), 4.70 – 4.64 (m, 1H), 4.62 – 4.43 (m, 4H), 4.12 (d, *J* = 7.4 Hz, 3H), 4.03 (d, *J* = 6.7 Hz, 2H), 3.91 – 3.77 (m, 2H), 3.74 – 3.67 (m, 3H), 3.31 (d, *J* = 6.8 Hz, 1H). ^{13}C NMR (101 MHz, CD_3OD) δ 167.3, 161.6, 151.7, 148.1, 142.9, 139.7, 138.7, 132.3, 127.2, 120.0, 118.1, 111.9, 91.2, 78.5, 73.5, 72.3, 55.8, 54.2, 52.0, 38.8, 29.8, 24.7, HRMS (ESI): calculated for $C_{26}H_{30}ClN_8O_4$ $[M+H]^+$ 553.2079, found 553.2082.

***tert*-butyl (2-(((((3a*R*,4*R*,6*R*,6a*R*)-6-(6-amino-9*H*-purin-9-yl)-2,2-dimethyltetrahydrofuro[3,4-d][1,3]dioxol-4-yl)methyl)((*E*)-3-(4-cyanophenyl)allyl)amino)methyl)phenyl)carbamate** (**29a**). Following the procedure described for compound **14a**, compound **1b** (200 mg, 0.45 mmol) coupled with *tert*-butyl (2-formylphenyl)carbamate **28a** (24 mg, 0.11 mmol) afforded compound **29a** as yellow powder (61 mg, 21% yield). LRMS (ESI): calculated for $C_{35}H_{41}N_8O_5$ $[M+H]^+$ 653.32, found 653.35.

***tert*-butyl (3-(((((3a*R*,4*R*,6*R*,6a*R*)-6-(6-amino-9*H*-purin-9-yl)-2,2-dimethyltetrahydrofuro[3,4-d][1,3]dioxol-4-yl)methyl)((*E*)-3-(4-cyanophenyl)allyl)amino)methyl)phenyl)carbamate (29b).** Following the procedure described for compound **14a**, compound **1b** (200 mg, 0.45 mmol) coupled with *tert*-butyl (3-formylphenyl)carbamate **28b** (150 mg, 0.67 mmol) afforded compound **29b** as yellow powder (110 mg, 38% yield). ^{1}H NMR (400 MHz, $CDCl_3$) δ 8.18 (s, 1H), 7.92 (s, 1H), 7.47 (d, *J* = 8.3 Hz, 3H), 7.28 (d, *J* = 8.3 Hz, 2H), 7.22 – 7.09 (m, 2H), 6.90 (d, *J* = 7.4 Hz, 1H), 6.75 (s, 2H), 6.43 (br d, *J* = 15.9 Hz, 1H), 6.34 – 6.25 (m, 1H), 6.07 (d, *J* = 2.2 Hz, 1H), 5.38 (dd, *J* = 6.4, 1.9 Hz, 1H), 4.96 (dd, *J* = 6.3, 3.2 Hz, 1H), 4.43 – 4.39 (m, 1H), 3.58 (br d, *J* = 15.1 Hz, 2H), 3.31 – 3.21 (m, 2H), 2.76 (d, *J* = 6.2 Hz, 2H), 1.56 (s, 3H), 1.47 (s, 9H), 1.35 (s, 3H). ^{13}C NMR (101 MHz, $CDCl_3$) δ 156.0, 153.0, 149.1, 141.4, 139.8, 139.7, 138.8, 132.3, 131.5, 131.0, 126.7, 123.43, 123.4, 120.1, 119.1, 114.3, 90.7, 85.6, 83.9, 83.2, 59.0, 56.5, 55.6, 28.4, 27.2, 25.4. HRMS (ESI): calculated for $C_{35}H_{41}N_8O_5$ $[M+H]^+$ 653.3200, found 653.3202.

***tert*-butyl (4-(((((3a*R*,4*R*,6*R*,6a*R*)-6-(6-amino-9*H*-purin-9-yl)-2,2-dimethyltetrahydrofuro[3,4-d][1,3]dioxol-4-yl)methyl)((*E*)-3-(4-**

cyanophenyl)allyl)amino)methyl)phenyl)carbamate (29c). Following the procedure described for compound **1a**, compound **1b** (200 mg, 0.45 mmol) coupled with *tert*-butyl (4-formylphenyl)carbamate **28c** (150 mg, 0.68 mmol) afforded compound **29c** as yellow powder (165 mg, 56% yield). ^{1}H NMR (400 MHz, $CDCl_3$) δ 8.16 (s, 1H), 7.88 (s, 1H), 7.50 (d, *J* = 8.3 Hz, 2H), 7.31 – 7.23 (m, 4H), 7.18 (d, *J* = 8.5 Hz, 2H), 6.59 (s, 2H), 6.40 (br d, *J* = 15.9 Hz, 1H), 6.31 – 6.24 (m, 1H), 6.06 (d, *J* = 1.9 Hz, 1H), 5.38 (dd, *J* = 6.4, 1.9 Hz, 1H), 4.93 (dd, *J* = 6.3, 3.4 Hz, 1H), 4.45 – 4.39 (m, 1H), 3.58 (d, *J* = 4.4 Hz, 2H), 3.34 – 3.17 (m, 2H), 2.76 (d, *J* = 6.5 Hz, 2H), 1.58 (s, 3H), 1.49 (s, 9H), 1.36 (s, 3H). LRMS (ESI): calculated for $C_{35}H_{41}ClN_8O_5$ $[M+H]^+$ 653.32, found 653.35.

***N*-(2-(((((2*R*,3*S*,4*R*,5*R*)-5-(6-amino-9*H*-purin-9-yl)-3,4-dihydroxytetrahydrofuran-2-yl)methyl)((*E*)-3-(4-cyanophenyl)allyl)amino)methyl)phenyl)acrylamide (31a).** Following the procedure described for compound **27a**, compound **31a** was obtained as a yellow powder (7 mg, 22% yield over three steps, > 70% pure). LRMS (ESI): calculated for $C_{30}H_{11}N_8O_4$ $[M+H]^+$ 567.24, found 567.29.

***N*-(2-(((((2*R*,3*S*,4*R*,5*R*)-5-(6-amino-9*H*-purin-9-yl)-3,4-dihydroxytetrahydrofuran-2-yl)methyl)((*E*)-3-(4-cyanophenyl)allyl)amino)methyl)phenyl)-2-chloroacetamide (31b).** Following the procedure described for compound **27a**, compound **31b** was deprotected and purified, affording compound **31b** as a yellow powder (9 mg, 26% yield over three steps). ^{1}H NMR (400 MHz, CD_3OD) δ 8.42 (s, 1H), 8.23 (s, 1H), 7.96 (br d, *J* = 19.4 Hz, 1H), 7.70 (d, *J* = 8.1 Hz, 2H), 7.58 – 7.39 (m, 4H), 7.32 (d, *J* = 7.1 Hz, 1H), 6.87 (br d, *J* = 15.7 Hz, 1H), 6.55 – 6.48 (m, 1H), 6.18 (d, *J* = 2.1 Hz, 1H), 4.62 – 4.51 (m, 5H), 4.22 (s, 2H), 4.16 (d, *J* = 5.8 Hz, 2H), 3.80 (d, *J* = 5.9 Hz, 1H), 3.68 (br d, *J* = 13.7 Hz, 1H), 2.79 – 2.68 (m, 1H). ^{13}C NMR (101 MHz, CD_3OD) δ 172.7, 166.3, 151.3, 148.0, 139.7, 130.1, 119.8, 118.1, 111.9, 92.8, 81.2, 73.7, 72.3, 57.6, 55.2, 54.1, 42.6, HRMS (ESI): calculated for $C_{29}H_{30}ClN_8O_4$ $[M+H]^+$ 589.2079, found 589.2086.

***N*-(3-(((((2*R*,3*S*,4*R*,5*R*)-5-(6-amino-9*H*-purin-9-yl)-3,4-dihydroxytetrahydrofuran-2-yl)methyl)((*E*)-3-(4-cyanophenyl)allyl)amino)methyl)phenyl)acrylamide (31c).** Following the procedure described for compound **27a**, compound **31c** was obtained as a yellow powder (11 mg, 33% yield over three steps). LRMS (ESI): calculated for $C_{30}H_{11}ClN_8O_4$ $[M+H]^+$ 567.24, found 567.25.

***N*-(3-(((((2*R*,3*S*,4*R*,5*R*)-5-(6-amino-9*H*-purin-9-yl)-3,4-dihydroxytetrahydrofuran-2-yl)methyl)((*E*)-3-(4-cyanophenyl)allyl)amino)methyl)phenyl)-2-chloroacetamide (31d).** Following the procedure described for compound **27a**, compound **30d** was deprotected and purified, affording compound **32d** as a white powder (13 mg, 38% yield over three steps). ^{1}H NMR (400 MHz, CD_3OD) δ 8.42 (s, 1H), 8.23 (s, 1H), 7.96 (br d, 1H), 7.70 (d, *J* = 8.1 Hz, 2H), 7.58 – 7.39 (m, 4H), 7.32 (d, *J* = 7.1 Hz, 1H), 6.87 (br d, *J* = 15.7 Hz, 1H), 6.55 – 6.48 (m 1H), 6.18 (d, *J* = 2.1 Hz, 1H), 4.62 – 4.51 (m, 5H), 4.22 (s, 2H), 4.16 (d, *J* = 5.8 Hz, 2H), 3.80 (d, *J* = 5.9 Hz, 1H), 3.68 (br d, *J* = 13.7 Hz, 1H), 2.79 – 2.68 (m, 1H). ^{13}C NMR (101 MHz, CD_3OD) δ 172.7, 166.3, 151.3, 148.0, 145.0, 143.1, 139.7, 138.8, 130.07, 132.3, 130.9, 130.1, 119.8, 118.1, 111.9, 91.4, 78.5, 73.7, 72.3, 57.6, 55.2, 54.1, 42.6, 22.9, HRMS (ESI): calculated for $C_{29}H_{30}ClN_8O_4$ $[M+H]^+$ 589.2079, found 589.2088.

***N*-(3-(((((2*R*,3*S*,4*R*,5*R*)-5-(6-amino-9*H*-purin-9-yl)-3,4-dihydroxytetrahydrofuran-2-yl)methyl)((*E*)-3-(4-cyanophenyl)allyl)amino)methyl)phenyl)acrylamide (32e).** Following the procedure described for compound **27a**, compound **32e** was obtained as a yellow powder (14 mg, 41% yield over three steps, > 70% pure). LRMS (ESI): calculated for $C_{30}H_{11}N_8O_4$ $[M+H]^+$ 567.24, found 567.24.

***N*-(3-(((((2*R*,3*S*,4*R*,5*R*)-5-(6-amino-9*H*-purin-9-yl)-3,4-dihydroxytetrahydrofuran-2-yl)methyl)((*E*)-3-(4-cyanophenyl)allyl)amino)methyl)phenyl)-2-chloroacetamide (32f).** Following the procedure described for compound **27a**, compound **30f** was deprotected and purified, affording compound **32f** as a yellow powder (13 mg, 37% yield over three steps). ^{1}H NMR (400 MHz, CD_3OD) δ 8.40 (s, 1H), 8.22 (s, 1H), 7.69 (t, *J* = 8.9 Hz, 4H), 7.50 (t, *J* = 8.3 Hz, 4H), 6.81 (br d, *J* = 15.7 Hz, 1H), 6.51 – 6.45 (m, 1H), 6.16 (s, 1H), 4.55 (br d, *J* = 26.4 Hz, 5H), 4.23 (s, 2H), 4.14 (d, *J* = 13.7 Hz, 2H), 3.86 – 3.73 (m, 1H), 3.65 (br d, *J* = 13.9 Hz, 1H). ^{13}C NMR (101 MHz, CD_3OD) δ 166.3, 148.0, 139.9, 139.7, 125.0, 119.8, 118.1, 111.9, 91.5, 73.6, 72.3, 57.4, 55.3, 42.7. HRMS (ESI): calculated for $C_{29}H_{30}ClN_8O_4$ $[M+H]^+$ 589.2079, found 589.2085.

(*E*)-3-(3-oxoprop-1-en-1-yl)benzenesulfonyl fluoride (36a). To a solution of 3-formylbenzenesulfonyl fluoride **35a** (18 mg, 0.1 mmol), in toluene (10 mL) was added (triphenylphosphoranylidene)acetaldehyde (45 mg, 0.15 mmol), the resulting mixture refluxed overnight. The solvent was removed under reduced pressure, the residue was purified by FCC to give 36a as yellow powder (9 mg, 44% yield). ^{1}H NMR (400 MHz, $CDCl_3$) δ 9.73 (d, *J* = 7.5 Hz,

1H), 7.78 (s, 1H), 7.74 (d, *J* = 7.8 Hz, 1H), 7.67 (d, *J* = 7.6 Hz, 1H), 7.56 (t, *J* = 7.8 Hz, 1H), 7.49 (br d, *J* = 16.0 Hz, 1H), 6.75 (dd, *J* = 16.0, 7.5 Hz, 1H).

(*E*)-4-(3-oxoprop-1-en-1-yl)benzenesulfonyl fluoride (36b). Following the procedure described for compound **36a** , 4-formylbenzenesulfonyl fluoride **35b** (250 mg, 1.3 mmol) coupled with (triphenylphosphoranylidene)acetaldehyde (525 mg, 1.73 mmol), compound **36b** was obtained as yellow powder (190 mg, 67% yield). ^{1}H NMR (500 MHz, $CDCl_3$) δ 9.81 (s, 1H), 8.12 – 8.05 (m, 2H), 7.82 (d, *J* = 9.1 Hz, 2H), 7.55 (br d, *J* = 16.1 Hz, 1H), 6.89 – 6.81 (m, 1H).

***tert*-butyl (*S*)-4-((((3a*R*,4*R*,6*R*,6a*R*)-6-(6-amino-9*H*-purin-9-yl)-2,2-dimethyltetrahydrofuro[3,4-d][1,3]dioxol-4-yl)methyl)((*E*)-3-(3-(fluorosulfonyl)phenyl)allyl)amino)-2-((*tert*-butoxycarbonyl)amino)butanoate (38a).** Following the procedure described for compound **5a**, compound **36a** (13 mg, 0.06 mmol) coupled with *tert*-butyl (*S*)-4-((((3a*R*,4*R*,6*R*,6a*R*)-6-(6-amino-9*H*-purin-9-yl)-2,2-dimethyltetrahydrofuro[3,4-d][1,3]dioxol-4-yl)methyl)amino)-2-((*tert*-butoxycarbonyl)amino)butanoate **37** (28 mg, 0.05 mmol) afforded compound **38a** as white powder (25 mg, 67% yield). ^{1}H NMR (500 MHz, $CDCl_3$) δ 8.25 (s, 1H), 7.90 (s, 1H), 7.53 (s, 1H), 7.44 (d, *J* = 7.7 Hz, 2H), 7.39 – 7.35 (m, 1H), 6.42 (d, *J* = 15.9 Hz, 1H), 6.28 – 6.21 (m, 1H), 6.06 (br d, *J* = 24.3 Hz, 2H), 5.61 (d, *J* = 8.0 Hz, 1H), 5.44 (d, *J* = 5.5 Hz, 1H), 4.98 (s, 1H), 4.37 (s, 1H), 4.23 – 4.16 (m, 1H), 3.33 – 3.30 (m, 1H), 3.27 – 3.18 (m, 1H), 2.84 – 2.81 (m, 1H), 2.67 – 2.62 (m, 2H), 2.56 – 2.51 (m, 1H), 2.01 – 1.94 (m, 1H), 1.79 – 1.74 (m, 1H), 1.59 (s, 3H), 1.45 – 1.32 (m, 21H). ^{13}C NMR (125 MHz, $CDCl_3$) δ 171.7, 155.7, 155.5, 153.1, 149.2, 140.0, 131.4, 131.0, 130.8, 129.4, 129.0, 125.0, 124.0, 122.9, 120.3, 114.5, 90.7, 85.6, 83.9, 83.3, 81.7, 56.9, 56.0, 52.8, 50.7, 29.6, 28.3, 27.9, 27.2, 25.4, HRMS (ESI): calculated for $C_{35}H_{49}FN_7O_9S$ $[M+H]^+$ 762.3297, found 762.3301.

***tert*-butyl (*S*)-4-((((3a*R*,4*R*,6*R*,6a*R*)-6-(6-amino-9*H*-purin-9-yl)-2,2-dimethyltetrahydrofuro[3,4-d][1,3]dioxol-4-yl)methyl)((*E*)-3-(4-(fluorosulfonyl)phenyl)allyl)amino)-2-((*tert*-butoxycarbonyl)amino)butanoate (38b).** Following the procedure described for compound **5a**, compound **36b** (24 mg, 0.12 mmol) **37** (56 mg, 0.1 mmol) afforded compound **38b** as white powder (27 mg, 71%). ^{1}H NMR (400 MHz, $CDCl_3$) δ 8.24 (s, 1H), 7.89 (d, *J* = 1.8 Hz, 1H), 7.59 (d, *J* = 8.3 Hz, 2H), 7.43 (d, *J* = 8.4 Hz, 2H), 6.74 (br d, *J* = 16.0 Hz, 1H), 6.62 – 6.56 (m, 1H), 6.48 – 6.32 (m, 2H), 6.13 (br s, 2H), 6.07 (s, 1H), 5.59 (d, *J* = 8.2 Hz, 1H), 5.47 – 5.43 (m, 1H), 5.02 – 5.00 (m, 1H), 4.42 (dd, *J* = 4.8, 1.7 Hz, 2H), 4.26 – 4.21(m, 1H), 3.37 – 3.25 (m, 2H), 2.87 – 2.80 (m, 2H), 2.71 – 2.52 (m, 3H), 2.07

– 1.90 (m, 1H), 1.81 – 1.76 (m, 1H), 1.62 (s, 3H), 1.48 – 1.32 (m, 21H). ^{13}C NMR (101 MHz, $CDCl_3$) δ 171.7, 155.6, 153.0149.1, 144.4, 140.1, 134.7, 128.9, 127.7, 127.04, 90.8, 85.7, 84.0, 83.3, 56.2, 52.8, 28.4, 25.5, HRMS (ESI): calculated for $C_{35}H_{49}FN_7O_9S$ $[M+H]^+$ 762.3297, found 762.3303.

(*S*)-2-amino-4-((((2*R*,3*S*,4*R*,5*R*)-5-(6-amino-9*H*-purin-9-yl)-3,4-dihydroxytetrahydrofuran-2-yl)methyl)((*E*)-3-(3-(fluorosulfonyl)phenyl)allyl)amino)butanoic acid (39a). Following the procedure described for compound **3a**, compound **38a** (10 mg, 0.013 mmol) was deprotected and purified, affording compound **39a** as a white powder (7 mg, 83%). ^{1}H NMR (400 MHz, CD_3OD) δ 8.50 (s, 1H), 8.29 (s, 1H), 7.68 (s, 1H), 7.64 – 7.60 (m, 2H), 7.53 (t, *J* = 7.7 Hz, 1H), 6.90 (br d, *J* = 15.8 Hz, 1H), 6.49 – 6.42 (m, 1H), 6.17 (d, *J* = 4.0 Hz, 1H), 4.71 – 4.67 (m, 1H), 4.61 – 4.55 (m, 1H), 4.49 (t, *J* = 5.4 Hz, 1H), 4.14 – 4.09 (m, 3H), 3.87 – 3.80 (m, 1H), 3.71 (br d, *J* = 13.8 Hz, 1H), 3.64 – 3.55 (m, 2H), 2.54 – 2.48 (m, 1H), 2.36 – 2.26 (m, 1H). ^{13}C NMR (101 MHz, CD_3OD) δ 170.6, 161.7, 161.3, 161.0, 151.2, 144.9, 143.0, 139.2, 136.3, 131.0, 130.7, 129.4, 125.1, 119.5, 118.0, 115.1, 90.6, 78.9, 73.6, 72.2, 54.8, 51.2, 50.9, 24.9, HRMS (ESI): calculated for $C_{23}H_{29}FN_7O_7S$ $[M+H]^+$ 566.1833, found 566.1837.

(*S*)-2-amino-4-((((2*R*,3*S*,4*R*,5*R*)-5-(6-amino-9*H*-purin-9-yl)-3,4-dihydroxytetrahydrofuran-2-yl)methyl)((*E*)-3-(4-(fluorosulfonyl)phenyl)allyl)amino)butanoic acid (39b). Following the procedure described for compound **3a**, compound **38b** (10 mg, 0.013 mmol) was deprotected and purified, affording compound **39b** as a white powder (6 mg, 72%). ^{1}H NMR (500 MHz, CD_3OD) δ 8.47 (s, 1H), 8.34 (s, 1H), 8.01 (d, *J* = 8.6 Hz, 2H), 7.70 (d, *J* = 8.5 Hz, 2H), 6.93 (br d, *J* = 15.8 Hz, 1H), 6.65 – 6.56 (m, 1H), 6.17 (d, *J* = 3.8 Hz, 1H), 4.70 – (m, 1H), 4.59 – 4.54 (m, 1H), 4.53 – 4.50 (m, 1H), 4.15 (h, *J* = 7.6 Hz, 2H), 4.08 (dd, *J* = 8.5, 4.6 Hz, 1H), 3.85 – 3.80 (m, 1H), 3.71 (dd, *J* = 13.9, 1.7 Hz, 1H), 3.66 – 3.53 (m, 2H), 2.53 – 2.46 (m, 1H), 2.31 – 2.27 (m, 1H). ^{13}C NMR (126 MHz, CD_3OD) δ 170.5, 151.6, 142.8, 137.8, 132.2, 122.1, 119.6, 117.7, 115.4, 113.1, 90.8, 79.0, 73.5, 72.5, 55.0, 25.0, HRMS (ESI): calculated for $C_{23}H_{29}FN_7O_7S$ $[M+H]^+$ 566.1833, found 566.1835.

(*E*)-3-(3-(4,4,5,5-tetramethyl-1,3,2-dioxaborolan-2-yl)phenyl)acrylaldehyde (41a). Following the procedure described for compound **36a**, compound 3-(4,4,5,5-tetramethyl-1,3,2-dioxaborolan-2-yl)benzaldehyde **40a** (46 mg, 0.2 mmol) coupled with

(triphenylphosphoranylidene)acetaldehyde (90 mg, 0.3 mmol) to offer **41a** as yellow powder (26 mg, 50%). The compound was not stable on silica column and directly used in the next step.

(*E*)-3-(3-(4,4,5,5-tetramethyl-1,3,2-dioxaborolan-2-yl)phenyl)acrylaldehyde (41b). Following the procedure described for compound **36a**, compound 3-(4,4,5,5-tetramethyl-1,3,2-dioxaborolan-2-yl)benzaldehyde **40b** (46 mg, 0.2 mmol) coupled with (triphenylphosphoranylidene)acetaldehyde (90 mg, 0.3 mmol) to offer **41b** as yellow powder (23 mg, 45%). The compound was not stable on silica column and directly used in the next step.

***tert*-butyl (*S*)-4-((((3a*R*,4*R*,6*R*,6a*R*)-6-(6-amino-9*H*-purin-9-yl)-2,2-dimethyltetrahydrofuro[3,4-d][1,3]dioxol-4-yl)methyl)((*E*)-3-(3-(4,4,5,5-tetramethyl-1,3,2-dioxaborolan-2-yl)phenyl)allyl)amino)-2-((*tert*-butoxycarbonyl)amino)butanoate (42a).** Following the procedure described for compound **5a**, compound **37** (28 mg, 0.05 mmol) coupled with **41a** (26 mg, 0.10 mmol) afforded compound **42a** as yellow powder (16mg, 39%). The compound was not stable on silica column and directly used in the next step. LRMS (ESI): calculated for $C_{41}H_{61}BN_7O_9$ $[M+H]^+$ 806.46, found 806.50.

***tert*-butyl (*S*)-4-((((3a*R*,4*R*,6*R*,6a*R*)-6-(6-amino-9*H*-purin-9-yl)-2,2-dimethyltetrahydrofuro[3,4-d][1,3]dioxol-4-yl)methyl)((*E*)-3-(4-(4,4,5,5-tetramethyl-1,3,2-dioxaborolan-2-yl)phenyl)allyl)amino)-2-((*tert*-butoxycarbonyl)amino)butanoate (42b).** Following the procedure described for compound **5a**, compound **37** (28 mg, 0.05 mmol) coupled with **41b** (26 mg, 0.10 mmol) afforded compound **42b** as yellow powder (6 mg, 15%). The compound was not stable on silica column and directly used in the next step. LRMS (ESI): calculated for $C_{41}H_{61}BN_7O_9$ $[M+H]^+$ 806.46, found 806.53.

(*S*)-2-amino-4-((((2*R*,3*S*,4*R*,5*R*)-5-(6-amino-9*H*-purin-9-yl)-3,4-dihydroxytetrahydrofuran-2-yl)methyl)((*E*)-3-(3-boronophenyl)allyl)amino)butanoic acid (44a). To a solution of **42a** (40 mg, 0.05mmol) in THF/H_2O = 6 mL/2mL added $NaIO_4$ (31 mg, 0.15 mmol). The resulting mixture stirred at r.t 30 mins. 0.5 mL 1 M HCl(aq) was added to the solution and stirred 30 mins. The solvent was removed, a mixture of TFA/CH_2Cl_2/H_2O = 9 mL/1mL/1mL was added to the residue, the solution stirred at rt 2h, the solvent was removed, and the crude compound was purified by prep-HPLC to offer final compound **44a** as white powder (12 mg, 38% yield over two steps). ^{1}H NMR (500 MHz, CD_3OD) δ 8.40 (br, d, *J* = 11.0 Hz, 1H), 8.24 (d, *J* = 7.8 Hz, 1H), 7.70 (br d, *J* = 18.1 Hz, 2H), 7.42 – 7.25 (m, 2H), 6.78 (d, *J* =

16.1 Hz, 1H), 6.31 – 6.25 (m, 1H), 6.14 (d, *J* = 3.7 Hz, 1H), 4.69 (t, *J* = 4.2 Hz, 1H), 4.53 (d, *J* = 2.6 Hz, 2H), 4.14 – 4.00 (m, 2H), 3.99 – 3.94 (m, 1H), 3.86 – 3.76 (m, 1H), 3.70 – 3.48 (m, 4H), 2.49 – 2.39 (m, 1H), 2.20 (d, *J* = 6.3 Hz, 1H). ^{13}C NMR (126 MHz, CD_3OD) δ 170.8, 141.0, 134.4, 132.0, 127.7, 91.4, 79.1, 73.4, 71.9, 25.2, HRMS (ESI): calculated for $C_{23}H_{31}BN_7O_7$ $[M+H]^+$ 528.2378, found 528.2378.

(*S*)-2-amino-4-((((2*R*,3*S*,4*R*,5*R*)-5-(6-amino-9*H*-purin-9-yl)-3,4-dihydroxytetrahydrofuran-2-yl)methyl)((*E*)-3-(4-boronophenyl)allyl)amino)butanoic acid (44b). Following the procedure described for compound **42a**, compound **42b** (40mg, 0.05 mmol) was deprotected and purified, affording compound **44b** as a white powder (5 mg, 17% yield over two steps). ^{1}H NMR (500 MHz, CD_3OD) δ 8.43 (s, 1H), 8.26 (s, 1H), 7.69 (s, 2H), 7.30 (d, *J* = 7.7 Hz, 2H), 6.77 (br d, *J* = 15.8 Hz, 1H), 6.35 – 6.29 (m, 1H), 6.15 (d, *J* = 3.6 Hz, 1H), 4.70 (t, *J* = 4.0 Hz, 1H), 4.54 (d, *J* = 6.2 Hz, 2H), 4.13 – 3.97 (m, 3H), 3.84 – 3.79 (dd, *J* = 13.8, 9.9 Hz, 1H), 3.69 – 3.49 (m, 3H), 2.50 – 2.42 (m, 1H), 2.28 – 2.18 (m, 1H). ^{13}C NMR (126 MHz, CD_3OD) δ 148.3, 140.7, 133.9, 125.6, 119.8, 91.0, 79.1, 73.4, 72.4, 54.6, 51.9, 25.1, HRMS (ESI): calculated for $C_{23}H_{31}BN_7O_7$ $[M+H]^+$ 528.2378, found 528.2380.

Modeling protocol by AutoDock Vina

The crystal structure of the human NNMT (6PVS) was retrieved from the Protein Data Bank.[31] Polar hydrogen atoms were added using AutoDockTools (ADT).[30] United atom Kollman charges were assigned for the protein. The 3D structures of the ligands used for the docking studies were constructed using ChemDraw and Chem3D. These ligands were energetically minimized by using Chem3D. The AutoDock vina[37] molecular docking program was employed, using a genetic algorithm with local search (GALS). The pose with the highest docking score was exported and analysed by PyMOL 2.4.

References

1. Thomas MG, Sartini D, Emanuelli M, van Haren MJ, Martin NI, Mountford DM, et al. Nicotinamide N-methyltransferase catalyses the N-methylation of the endogenous -carboline norharman: evidence for a novel detoxification pathway. *Biochem J*. 2016;473(19):3253-67.
2. Alston TA, Abeles RH. Substrate specificity of nicotinamide methyltransferase isolated from porcine liver. *Arch Biochem Biophys*. 1988;260(2):601-8.
3. van Haren MJ, Sastre Toraño J, Sartini D, Emanuelli M, Parsons RB, Martin NI. A Rapid and Efficient Assay for the Characterization of Substrates and Inhibitors of Nicotinamide N -Methyltransferase. *Biochemistry*. 2016;55(37):5307-15.
4. Pissios P. Nicotinamide N -Methyltransferase: More Than a Vitamin B3 Clearance Enzyme. *Trends Endocrinol Metab*. 2017;28(5):340-53.
5. Khalil EM, Mackie BD, Mao Y. Methyltransferases: Key Regulators in Cardiovascular Development and Disease. *Ann Vasc Med Res*. 2016;3(2):1032-9.
6. Fedorowicz A, Mateuszuk Ł, Kopec G, Skórka T, Kutryb-Zając B, Zakrzewska A, et al. Activation of the nicotinamide N-methyltransferase (NNMT)-1-methylnicotinamide (MNA) pathway in pulmonary hypertension. *Respir Res*. 2016;17(1):108.
7. Jung J, Kim LJY, Wang X, Wu Q, Sanvoranart T, Hubert CG, et al. Nicotinamide metabolism regulates glioblastoma stem cell maintenance. *JCI Insight*. 2017;2(10):1-23.
8. Kraus D, Yang Q, Kong D, Banks AS, Zhang L, Rodgers JT, et al. Nicotinamide N-methyltransferase knockdown protects against diet-induced obesity. *Nature*. 2014;508(7495):258-62.
9. ten Klooster JP, Sotiriou A, Boeren S, Vaessen S, Vervoort J, Pieters R. Type 2 diabetes-related proteins derived from an in vitro model of inflamed fat tissue. *Arch Biochem Biophys*. 2018;644(February):81-92.
10. Parsons RB, Smith SW, Waring RH, Williams AC, Ramsden DB. High expression of nicotinamide N -methyltransferase in patients with idiopathic Parkinson ' s disease. *Neurosci Lett*. 2003;342(1–2):13-6.
11. Parsons RB, Smith M-L, Williams AC, Waring RH, Ramsden DB. Expression of Nicotinamide N-Methyltransferase (E.C. 2.1.1.1) in the Parkinsonian Brain. *J Neuropathol Exp Neurol*. 2002;61(2):111-24.
12. Sartini D, Santarelli A, Rossi V, Goteri G, Rubini C, Ciavarella D, et al. Nicotinamide N-Methyltransferase Upregulation Inversely Correlates with Lymph Node Metastasis in Oral Squamous Cell Carcinoma. *Mol Med*. 2007;13(7-8):415-21.

13. Sartini D, Muzzonigro G, Milanese G, Pierella F, Rossi V, Emanuelli M. Identification of Nicotinamide N-Methyltransferase as a Novel Tumor Marker for Renal Clear Cell Carcinoma. *J Urol*. 2006;176(5):2248-54.
14. Zhang J, Wang Y, Li G, Yu H, Xie X. Down-Regulation of Nicotinamide N-methyltransferase Induces Apoptosis in Human Breast Cancer Cells via the Mitochondria-Mediated Pathway. Filleur S, ed. *PLoS One*. 2014;9(2):e89202.
15. Palanichamy K, Kanji S, Gordon N, Thirumoorthy K, Jacob JR, Litzenberg KT, et al. NNMT Silencing Activates Tumor Suppressor PP2A , Inactivates Oncogenic STKs , and Inhibits Tumor Forming Ability. *Cancer Ther Preclin*. 2016;23(9):1-11.
16. Ulanovskaya OA, Zuhl AM, Cravatt BF. NNMT promotes epigenetic remodeling in cancer by creating a metabolic methylation sink. *Nat Chem Biol*. 2013;9(5):300-6.
17. Lim BH, Cho BI, Yu NK, Jae WK, Park ST, Lee CW. Overexpression of nicotinamide N-methyltransferase in gastric cancer tissues and its potential post-translational modification. *Exp Mol Med*. 2006;38(5):455-65.
18. Nemmara V V., Tilvawala R, Salinger AJ, Miller L, Nguyen SH, Weerapana E, et al. Citrullination Inactivates Nicotinamide-N-methyltransferase. *ACS Chem Biol*. 2018;13(9):2663-72.
19. Gao Y, Martin NI, van Haren MJ. Nicotinamide N-methyl transferase (NNMT): An emerging therapeutic target. *Drug Discov Today*. 2021;xxx(xx):1-8.
20. Singh J, Petter RC, Baillie TA, Whitty A. The resurgence of covalent drugs. *Nat Rev Drug Discov*. 2011;10(4):307-17.
21. Peng Y, Sartini D, Pozzi V, Wilk D, Emanuelli M, Yee VC. Structural Basis of Substrate Recognition in Human Nicotinamide N -Methyltransferase. *Biochemistry*. 2011;50(36):7800-8.
22. Horning BD, Suciu RM, Ghadiri DA, Ulanovskaya OA, Matthews ML, Lum KM, et al. Chemical Proteomic Profiling of Human Methyltransferases. *J Am Chem Soc*. 2016;138(40):13335-43.
23. Sen S, Mondal S, Zheng L, Salinger AJ, Fast W, Weerapana E, et al. Development of a Suicide Inhibition-Based Protein Labeling Strategy for Nicotinamide N-Methyltransferase. *ACS Chem Biol*. 2019;14(4):613-8.
24. Lee H-Y, Suciu RM, Horning BD, Vinogradova E V., Ulanovskaya OA, Cravatt BF. Covalent inhibitors of nicotinamide N-methyltransferase (NNMT) provide evidence for target engagement challenges in situ. *Bioorg Med Chem Lett*. 2018;28(16):2682-7.

25. Resnick E, Bradley A, Gan J, Douangamath A, Krojer T, Sethi R, et al. Rapid Covalent-Probe Discovery by Electrophile-Fragment Screening. *J Am Chem Soc*. 2019;141(22):8951-68.
26. Martin JS, MacKenzie CJ, Fletcher D, Gilbert IH. Characterising covalent warhead reactivity. *Bioorg Med Chem*. 2019;27(10):2066-74.
27. Plescia J, Moitessier N. Design and discovery of boronic acid drugs. *Eur J Med Chem*. 2020;195:112270.
28. DAVID E. FAHRN AMG. Sulfonyl Fluorides as Inhibitors of Esterases. I . Rates of Reaction with Acetylcholinesterase,α-Chymo trypsin, and Trypsin. *J Am Chem Soc*. 1963;2016(85):997-1000.
29. Narayanan A, Jones LH. Sulfonyl fluorides as privileged warheads in chemical biology. *Chem Sci*. 2015;6(5):2650-9.
30. Morris GM, Huey R, Lindstrom W, Sanner MF, Belew RK, Goodsell DS, et al. AutoDock4 and AutoDockTools4: Automated docking with selective receptor flexibility. *J Comput Chem*. 2009;30(16):2785-91.
31. Chen D, Li L, Diaz K, Iyamu ID, Yadav R, Noinaj N, et al. Novel Propargyl-Linked Bisubstrate Analogues as Tight-Binding Inhibitors for Nicotinamide N-Methyltransferase. *J Med Chem*. 2019;62(23):10783-97.
32. Dose C, Seitz O. Single nucleotide specific detection of DNA by native chemical ligation of fluorescence labeled PNA-probes. *Bioorganic Med Chem*. 2008;16(1):65-77.
33. Freeman NS, Hurevich M, Gilon C. Synthesis of N-substituted Ddz-protected hydrazines and their application in solid phase synthesis of aza-peptides. *Tetrahedron*. 2009;65(8):1737-45.
34. Zhao T, Kurpiewska K, Kalinowska-Tłus¨cik J, Herdtweck E, Dömling A. α-Amino Acid-Isosteric α-Amino Tetrazoles. *Chem - A Eur J*. 2016;22(9):3009-18.
35. Han LC, Stanley PA, Wood PJ, Sharma P, Kuruppu AI, Bradshaw TD, et al. Horner-Wadsworth-Emmons approach to piperlongumine analogues with potent anti-cancer activity. *Org Biomol Chem*. 2016;14(31):7585-93.
36. Van Der Zouwen AJ, Lohse J, Wieske LHE, Hohmann KF, Van Der Vlag R, Witte MD. An in situ combinatorial methodology to synthesize and screen chemical probes. *Chem Commun*. 2019;55(14):2050-3.
37. Oleg Trott AJO. Software News and Updates Gabedit — A Graphical User Interface for Computational Chemistry Softwares. *J Comput Chem*. 2010;31(2):455-61.

Chapter 6

Summary

SUMMARY

The function of NNMT in healthy and disease states has gained increased attention in recent years. Overexpressed levels of NNMT have been observed in various cancers, and increased NNMT expression has been related to tumour progression, metastasis, and worse clinical outcomes. NNMT is considered to be a new potential pharmacological target in the treatment of a variety of cancers, metabolic disease and other pathologies. The growing number of publications elucidating the role of NNMT in disease has in turn spurred the development of potent and selective inhibitors of NNMT with an increasing number of compounds being disclosed in the past five years.

Chapter 1 provides a comprehensive review of the current status of NNMT inhibitor development, relevant *in vitro* and *in vivo* studies, and a discussion of the challenges faced in the development of NNMT inhibitors. Although the search for effective NNMT inhibitors is still in its infancy, substantial achievements have been made in identifying potent and selective small-molecule inhibitors of NNMT. That said, the limited cellular and *in vivo* activity of these compounds speak to the need to develop more drug-like inhibitors. The clinical importance of NNMT in various diseases, including cancer and metabolic disorders, support it as a promising therapeutic target. However, there are many limitations in the currently available set of NNMT inhibitors. The adenosine and amino acid moieties of the SAM mimetics are considered critical moieties in NNMT inhibitors. While these features are crucial for activity, they also negatively affect cell permeability. To assess the therapeutic viability of NNMT inhibition in more detail, the current set of NNMT inhibitors available needs to be expanded to be provide more drug-like molecules.

In **chapter 2**, a diverse library of inhibitors was prepared to probe the different regions of NNMT's binding site. To this end, various structural motifs were explored for their ability to improved potency and binding within the NNMT binding pocket. Among the bisubstrate analogues prepared, the most potent NNMT inhibitor was found to be naphthalene-containing compound **78**, displaying an IC_{50} value of 1.41 μM, >10-fold better than its parent compound MvH45 (compound **1** in **chapter 2**). From modelling studies, the improved activity of compound **78** can be rationalized by the apparent presence of an intramolecular hydrogen bonding interaction predisposing the compound to an active conformation with lower entropic cost. In addition, the modelling indicates

that the naphthalene group in **78** is appropriately oriented to benefit from additional π–π stacking interactions with several tyrosine residues in the nicotinamide binding pocket of NNMT. (Figure 1). The cellular data obtained for compound **78** show a dose-dependent effect on cell proliferation in HSC-2 oral cancer cells.

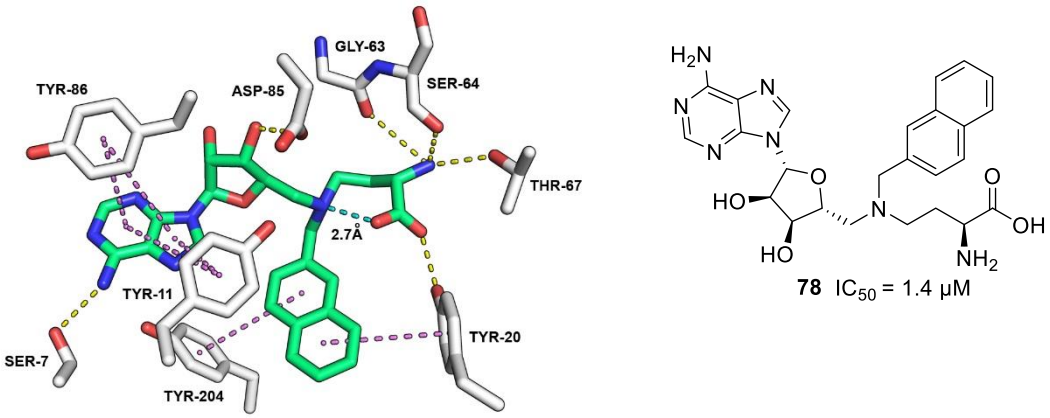

Figure 1. Modelling results for compound **78** in the NNMT active site (PDB ID: 3ROD). Molecular dynamics simulation indicates the presence of an intramolecular hydrogen bond (2.7Å, shown in cyan) specific to compound **78** (in green)

Chapter 3 reports a scaffold-hopping strategy to generate novel and potent bisubstrate NNMT inhibitors (**17o**, **17r**, **17u**, Figure 2). The inhibition data of the inhibitors thus prepared revealed a striking effect for electron-withdrawing groups present on the aromatic ring, predominantly when introduced at the position *para* to the alkene linker. Among these compounds, the *para*-cyano substituted styrene-based inhibitor **17u** was identified as the most potent NNMT inhibitor with an IC_{50} value of 3.7 nM. These studies demonstrated that minor changes in the amino acid side chain and adenosine moiety lead to remarkable decreases in potency. Modelling studies predict the presence of hydrogen bonding interactions between the *para*-cyano group and two active site serine residues in the nicotinamide binding pocket of NNMT, providing a possible explanation for the potency of compound **17u**. Notbaly, the potent inhibition exhibited by **17u** in biochemical assays was not observed in cell-based assays; only when tested at a very high concntraiton of 100 μM was a decline in cell viability observed for oral, lung, and bladder cancer cell lines treated with the compound.

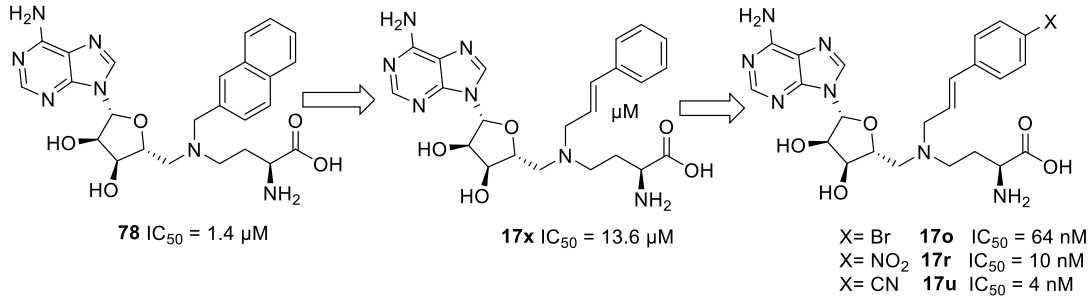

Figure 2. Scaffold-hopping strategy to generate novel and potent bisubstrate inhibitors.

In **chapter 4** a prodrug strategy is described to decrease the polarity of compound **17u** and improve its cellular activity. Specifically, the carboxylic acid on inhibitor **17u** was masked as an ester using a variety of alkyl and benzyl groups, and the amine moiety was masked using the trimethyl-lock (TML) group. The different combinations of esterase-cleavable prodrugs thus prepared lead to the selection the isopropyl prodrug **12e** and the isopropyl-TML dual-prodrug **14e** (Figure 3) as the compounds with the most promising profile in terms of stability and cellular activity. Initially, the compounds were tested in an MTT cell viability assay using three different cancer cell lines, but cellular activity was observed only at the highest concentration of 100 μM tested. Subsequently, a cellular MNA determination assay was performed, revealing a dose-dependent effect of NNMT prodrug inhibitors **12e** and **14e** on MNA levels in cells, with significant improvement over the parent compound. The data presented here demonstrate the suitability of a prodrug strategy to deliver polar NNMT inhibitors into cells.

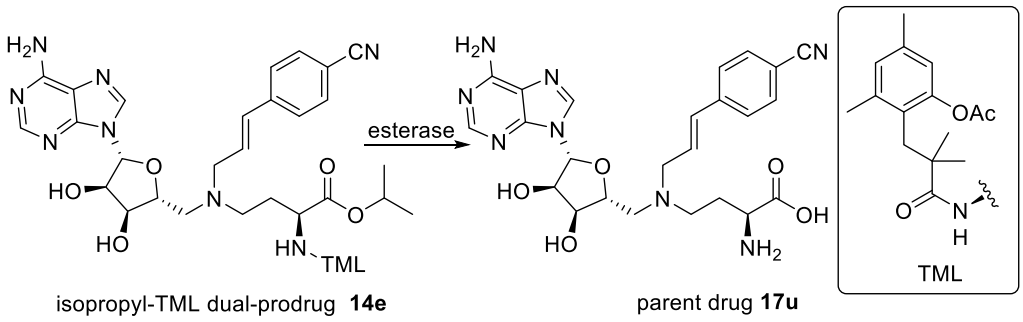

Figure 3. Prodrug **14e** hydrolysis to form parent drug **17u**.

In **chapter 5**, the design and synthesis of a library of compounds is described that aim to covalently target active site cysteine and serine residues using a variety of different

warheads. To do so, the amino acid sidechain in the potent NNMT inhibitor **17u** (identified in chapter 3) was replaced by an acrylamide or chloroacetamide warhead with different linkers to target cysteine residues C159 and C165, for which covalent inhibitors have been described previously. The most active compound (**17b**, Figure 4) thus prepared showed an IC_{50} value of 400 nM, making it the first example of a bisubstrate inhibitor in which the amino acid sidechain was successfully replaced without rendering it inactive. In another approach, the cyano group of compound **17u** was replaced by either a sulfonyl fluoride or a boronic acid moiety with the aim of targeting serine residues S201 or S213 present in the nicotinamide pocket of NNMT. These efforts lead to potent NNMT inhibition by *meta*- and *para*-sulfonyl fluoride compounds **39a** (IC_{50} = 89 nM) and **39b** (IC_{50} = 68 nM, Figure 4). Interestingly, the significant difference in activity observed for *meta*- versus *para*-substitution, discussed in **chapter 3**, was not observed for the sulfonyl fluorides. The boronic acid compounds revealed moderate activity for the *meta*-substitution with no inhibition observed for *para*-substituted boronic acid. Modelling data of compounds **39a-b** suggest that the distance of 2.9 and 3.4 Å between the sulfonyl fluoride group and the hydroxyls of serine residues S201 and S213 could allow for a covalent interaction. Studies to reveal the mechanism of action of compounds **17b**, **39a** and **39b** are ongoing.

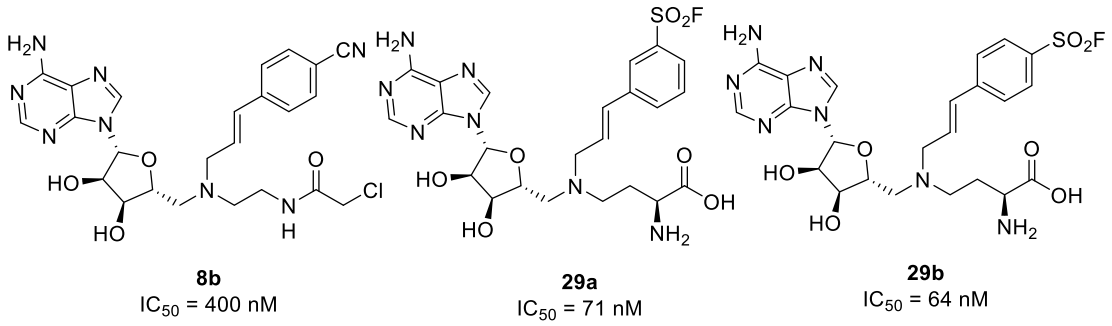

Figure 4. Structures of **17b**, **39a** and **39b.**

Addendum

List of Abbreviations

Samenvatting

Curriculum vitae

List of publications

List of Abbreviations

ABPP, activity-based protein profiling;

αCA, alpha-chloroacetamide;

Boc, *tert*-Butyloxycarbonyl;

BOP, benzotriazol-1-yloxytris(dimethylamino)phosphonium hexafluorophosphate;

BPO, benzoyl peroxide;

DCE, 1,2-dichloroethane;

DIBAL-H, diisobutylaluminium hydride;

DNMT1, DNA (cytosine-5)-*N*-methyltransferase 1;

DOT1L, disruptor of telomeric silencing 1-like;

EWG, electron- withdrawing;

FEP, free energy perturbation;

FP, fluorescence polarization;

hNNMT, human NNMT;

IC_{50}, half-maximal inhibitory concentration;

ITC, isothermal titration calorimetry;

K*d*, dissociation constant;

MLL1, mixed-lineage leukemia 1;

MNA, 1-methyl-nicotinamide;

NA, nicotinamide;

NMO, *N*-Methylmorpholine *N*-oxide;

NNMT, nicotinamide *N*-methyltransferase;

NNMTwt, wild-type NNMT;

PAMPA, parallel artificial membrane permeability assay;

PDC, pyridinium dichromate;

PNMT, phenylethanolamine *N*-methyltransferase;

PRMT, protein arginine *N*-methyltransferase ;

RBF, round-bottom flask;

SAH, S-adenosyl-L-homocysteine;

SAM, S-adenosyl-L-methionine;

SAR, structure–activity relationship;

SETDB1, SET domain bifurcated 1;

SETD2, SET domain-containing 2;

SMYD2, SET and MYND domain containing protein 2;

SF, sulfonyl fluoride;

Trt, triphenylmethyl (trityl);

UHP-HILIC, ultra-high-performance hydrophilic liquid interaction chromatography;

YD, Yuanhuadine;

Samenvatting

De functie van NNMT in gezonde toestand en in ziekten heeft de laatste jaren meer aandacht gekregen. Overexpressie van NNMT is waargenomen in verschillende kankers, en verhoogde NNMT expressie is gerelateerd aan tumorprogressie, metastase, en slechtere klinische resultaten. NNMT wordt beschouwd als een nieuw potentieel farmacologisch doelwit in de behandeling van een verscheidenheid van kankers, stofwisselingsziekten en andere pathologieën. Het toenemend aantal publicaties waarin de rol van NNMT bij ziekten wordt opgehelderd, heeft op zijn beurt de ontwikkeling van krachtige en selectieve remmers van NNMT gestimuleerd, waarbij in de afgelopen vijf jaar een toenemend aantal verbindingen is onthuld.

Hoofdstuk 1 geeft een uitgebreid overzicht van de huidige status van de ontwikkeling van NNMT remmers, relevante *in vitro* en *in vivo* studies, en een bespreking van de uitdagingen waar men bij de ontwikkeling van NNMT remmers voor staat. Hoewel de zoektocht naar effectieve NNMT-remmers nog in de kinderschoenen staat, zijn er belangrijke successen geboekt bij het identificeren van krachtige en selectieve kleine molecuul remmers van NNMT. De beperkte cellulaire en *in vivo* activiteit van deze verbindingen wijst echter op de noodzaak om meer geneesmiddel-achtige remmers te ontwikkelen. Het klinisch belang van NNMT bij verschillende ziekten, waaronder kanker en stofwisselingsstoornissen, ondersteunt het als een veelbelovend therapeutisch doelwit. De momenteel beschikbare reeks NNMT-remmers kent echter vele beperkingen. De adenosine- en aminozuurgroepen van de SAM-mimetica worden beschouwd als kritische groepen in NNMT-remmers. Hoewel deze eigenschappen cruciaal zijn voor de activiteit, hebben zij ook een negatieve invloed op cel-permeabiliteit. Om de therapeutische levensvatbaarheid van NNMT-remming beter te kunnen beoordelen, moet de huidige reeks beschikbare NNMT-remmers worden uitgebreid om meer geneesmiddel-achtige moleculen te kunnen leveren.

In **hoofdstuk 2** werd een gevarieerde bibliotheek van remmers geprepareerd om de verschillende gebieden van de NNMT bindingsplaats te onderzoeken. Daartoe werden verschillende structurele motieven onderzocht op hun vermogen om de potentie en binding binnen de NNMT bindingsplaats te verbeteren. Van de bereide bisubstraat-analogen bleek naftaleen-verbinding **78** de krachtigste NNMT-remmer te zijn, met een IC_{50}-waarde van 1,41 μM, >10 maal beter dan voorloper **MvH45** (verbinding **1** in **hoofdstuk 2**). Uit modeleerstudies blijkt dat de verbeterde activiteit van verbinding **78** beredeneerd kan

worden door de schijnbare aanwezigheid van een intramoleculaire waterstofbruginteractie die de verbinding voorbestemt tot een actieve conformatie met lagere entropische kosten. Bovendien blijkt uit de modellering dat de naftaleengroep in **78** correct georiënteerd is om te profiteren van extra π-π stacking interacties met verschillende tyrosineresiduen in de nicotinamidebindingsplaats in NNMT (**Figuur 1**). De cellulaire gegevens die zijn verkregen voor verbinding **78** laten een dosis-afhankelijk effect zien op de celproliferatie in HSC-2 mondkankercellen.

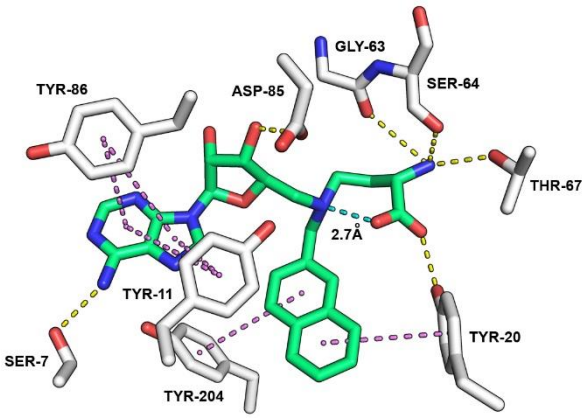

Figuur 1. Modelleringsresultaten voor verbinding **78** in de actieve site van NNMT (PDB ID: 3ROD). Moleculaire dynamica simulatie toont de aanwezigheid van een intramoleculaire waterstofbrug (2.7Å, aangegeven in cyaan) specifiek voor verbinding **78** (in groen)

In **hoofdstuk 3** wordt verslag gedaan van een scaffold-hopping strategie om nieuwe en krachtige bisubstraat NNMT remmers te genereren (**17o**, **17r**, **17u**, **figuur 2**). De inhibitiegegevens van de aldus bereide remmers onthulden een opvallend effect voor elektron-onttrekkende groepen aanwezig op de aromatische ring, voornamelijk wanneer ze worden ingebracht op de positie *para* van de alkeenlinker. Onder deze verbindingen werd de *para*-cyano gesubstitueerde styreen-gebaseerde remmer **17u** geïdentificeerd als de meest krachtige NNMT-remmer met een IC_{50}-waarde van 3,7 nM. Deze studies toonden aan dat kleine veranderingen in de aminozuurzijketen en het adenosinegedeelte tot opmerkelijke verminderingen van de potentie leiden. Modeleerstudies voorspellen de aanwezigheid van waterstofbruginteracties tussen de para-cyanogroep en twee actieve serine residuen in de nicotinamide bindingsplaats van NNMT, wat een mogelijke verklaring biedt voor de potentie van verbinding **17u**. Opmerkelijk is dat de krachtige remming die **17u** in biochemische tests vertoonde, niet werd waargenomen in celgebaseerde testen;

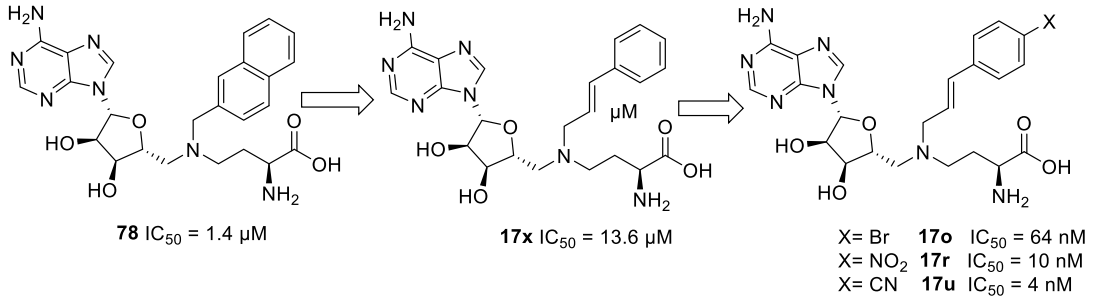

Figuur 2. Scaffold-hopping strategie om nieuwe en krachtige bisubstraatremmers te genereren.

alleen bij een zeer hoge concentratie van 100 µM werd een afname van de levensvatbaarheid van de cellen waargenomen bij cellijnen voor mond-, long- en blaaskanker die met de verbinding werden behandeld.

In **hoofdstuk 4** wordt een prodrug strategie beschreven om de polariteit van verbinding **17u** te verlagen en de cellulaire activiteit te verbeteren. Meer specifiek werd het carboxylzuur op remmer **17u** gemaskeerd als een ester met behulp van een verscheidenheid aan alkyl- en benzylgroepen, en het aminegedeelte werd gemaskeerd met behulp van de trimethyl-lock (TML) groep. De verschillende combinaties van esterase-splitsbare prodrugs die zo werden bereid leidden tot de selectie van de isopropyl prodrug **12e** en de isopropyl-TML duaal prodrug **14e** (**figuur 3**) als de verbindingen met het meest veelbelovende profiel wat betreft stabiliteit en cellulaire activiteit. Aanvankelijk werden de verbindingen getest in een MTT-cellevensvatbaarheidstest met drie verschillende kankercellijnen, maar de cellulaire activiteit werd alleen waargenomen bij de hoogst geteste concentratie van 100 µM. Vervolgens werd een cellulaire MNA bepalingstest uitgevoerd, waarbij een dosisafhankelijk effect van de NNMT prodrug remmers **12e** en **14e** op de hoeveelheid MNA in de cellen werd aangetoond, met een significante verbetering ten opzichte van de hoofdverbinding. De hier gepresenteerde gegevens tonen de geschiktheid aan van een prodrugstrategie om polaire NNMT-remmers in cellen af te leveren.

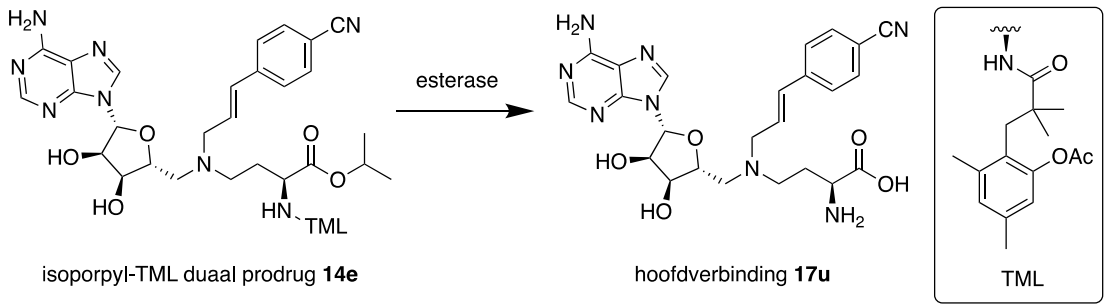

Figuur 3. Hydrolyse van prodrug **14e** om hoofdverbinding **17u** te vormen.

In **hoofdstuk 5** wordt het ontwerp en de synthese beschreven van een bibliotheek van verbindingen die zich richten op de covalente interactie met actieve site cysteïne en serine residuen met behulp van verschillende functionele groepen. Hiertoe werd de aminozuurzijketen in de krachtige NNMT-remmer **17u** (geïdentificeerd in **hoofdstuk 3**) vervangen door een acrylamide of chlooracetamide fragment met verschillende linkers om cysteïneresiduen C159 en C165 aan te pakken, waarvoor covalente remmers al eerder zijn beschreven. De meest actieve verbinding (**17b**, **figuur 4**) die aldus werd bereid, vertoonde een IC_{50}-waarde van 400 nM, waardoor dit het eerste voorbeeld is van een bisubstraatremmer waarin de aminozuurzijketen met succes werd vervangen zonder dat het inactief werd. In een andere benadering werd de cyanogroep van verbinding **17u** vervangen door hetzij een sulfonylfluoride, hetzij een boronzuurgroep, met als doel de serineresiduen S201 of S213, die aanwezig zijn in de nicotinamide bindingsplaats van NNMT, aan te pakken. Deze inspanningen leidden tot een krachtige remming van NNMT door de *meta*- en *para*-sulfonylfluorideverbindingen **39a** (IC_{50} = 89 nM) en **39b** (IC_{50} = 68 nM, **figuur 4**). Interessant is dat het significante verschil in activiteit dat werd waargenomen voor *meta*- versus *para*-substitutie, besproken in **hoofdstuk 3**, niet werd waargenomen voor de sulfonylfluoriden. De boronzuurverbindingen vertoonden een matige activiteit voor de *meta*-substitutie, terwijl geen remming werd waargenomen voor *para*-gesubstitueerd boronzuur. Modelleringsgegevens van verbindingen **39a-b** suggereren dat de afstand van 2.9 en 3.4 Å tussen de sulfonylfluoride groep en de hydroxylen van serine residuen S201 en S213 een covalente interactie mogelijk zou kunnen maken. Studies om het werkingsmechanisme van verbindingen **17b**, **39a** en **39b** te onthullen zijn aan de gang.

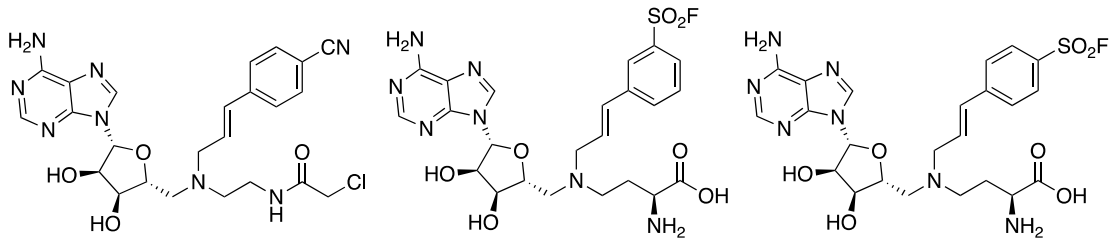

Figuur 4. Chemische structure van verbindingen **17b**, **39a** en **39b**.

Curriculum vitae

Yongzhi Gao was born on October 14th, 1995, in Xishui, a tiny town in central China. He studied pharmaceutic science at Wuhan University and graduated with a bachelor's degree in 2009. After spending three years in a pharma company as a progress chemist, he returned to Wuhan University to chase his master's degree, where he conducted his research under Prof. Haibing Zhou and Prof. Chune Dong. In 2015, he was granted a fellowship from China Scholar Council (CSC) to perform his PhD research in the Netherlands under the supervision of Prof. dr. Nathaniel I. Martin and Dr. Matthijs J. van Haren. In the Martin lab, his research has been focused on the development of inhibitors of NNMT. As a PhD candidate, he was trained to be an organic/ medicinal chemist in the Netherlands. He is married and has a daughter.

List of publications

Publications from doctoroal research period

(1) **Gao, Y.**; Martin, N.I., van Haren, M.J. (2021). Nicotinamide *N*-methyl transferase (NNMT): an emerging therapeutic target. *Drug Discov Today*. In press. DOI: 10.1016/j.drudis.2021.05.011

(2) **Gao, Y.**; van Haren, M. J.; Moret, E. E.; Rood, J. J. M.; Sartini, D.; Salvucci, A.; Emanuelli, M.; Craveur, P.; Babault, N.; Jin, J.; Martin, N. I . (2019): Bisubstrate Inhibitors of Nicotinamide *N*-Methyltransferase (NNMT) with Enhanced Activity. *J. Med. Chem*. 62, 6597−6614.

(3) **Gao, Y.**; van Haren, M.J.; Buijs, N.; Innocenti, P.; Zhang, Y.; Sartini, D. Campagna, R.; Emanuelli, M.; Parsons, R.B.; Jespers, W.; Gutiérrez-de-Terán, H.; van Westen, G.; Martin, N.I.; (2021) Potent Inhibition of Nicotinamide *N*-Methyltransferase by Alkene-Linked Bisubstrate Mimics Bearing Electron Deficient Aromatics. *J. Med. Chem*. In press. DOI:10.1021/acs.jmedchem.1c01094

(4) van Haren, M. J.; **Gao, Y.** (co-first author); Buijs, N.; Campagna, R.; Sartini, D.; Emanuelli, M.; Mateuszuk, L.; Kij, A.; Chlopicki, S.; Escudé, P.; Castilla, M. De; Schiffelers, R. Esterase-Sensitive Prodrugs of a Potent Bisubstrate NNMT Inhibitor Display Cellular Activity. *Manuscript under review*.

Patent from doctoral research period

Netherlands Priority Patent Application No. N2027866; Title: Inhibitors of Nicotinamide NMethyl Transferase (NNMT) Inventors: Martin, N.I., **Gao, Y.**, van Haren, M.J., Buijs, N., Parsons, R.B., Emanuelli, M., Sartini, D. Priority date: March 30, 2021.